TRACTION OF COPPER AND ZINC IONS
WITH POLYMETHACRYLIC ACID (PMA)

Dissertation

presented to

The Ahmadu Bello University

for the degree of

DOCTOR OF PHILOSOPHY

in the

Faculty of Science

BY

EMMANUEL GBADEBO KOLAWOLE

Department of Chemistry

Ahmadu Bello University

Zaria.

April, 1974.

A C K N O W L E D G E M E N T S

It is my greatest pleasure to express my thanks to Dr. S. M. Mathieson who initiated and supervised this project. Gratefully I acknowledge her assistance, kindness, untiring encouragement and useful suggestions throughout the course of this project. I would like to thank her for being kind enough in reading through the draft and pointing out some errors, omissions and obscurities.

I sincerely thank Prof. A. R. Mathieson, Head of Chemistry Department and Deputy Vice-Chancellor for his keen interest in this research programme. I thank him for his assistance and for making available to me all the facilities of the chemical laboratories.

I thank the technical and stores staff for their patience and co-operation.

My thanks go to Mr. J. O. Aina of Chemistry Department for typing this thesis so admirably.

I particularly thank my friend and colleague Dr. J. Y. Olayemi for his assistance, constructive and useful suggestions throughout this project.

I thank my children, Bukola and Dele for their co-operation and most especially, my wife, Modupe, for being a continual source of inspiration, encouragement, devotion and understanding in all matters.

Finally, I thank the Ahmadu Bello University for providing the grant for this reseach work.

April, 1974. E. G. Kolawole.

ABSTRACT

The interaction between polymethacrylic acid (PMA) and divalent metal ions has been studied at 25 °C and. varying conditions of ionic strength, polymer concentration, cation concentration and degree of ionization by different experimental techniques. The experimental techniques used were conductance measurements, viscometric titration, spectrophotometric titration, dialysis equilibrium, potentiometric titration and light scattering.

Data from different experimental methods reveal that both copper and zinc interact quite strongly with preionized PMA to form complexes. Copper has been found to he a stronger hinder than zinc.

Copper ions bind PMA to form complexes involving four, two and one carboxylate groups per copper ion while zinc forms complexes involving two and one carhoxylate groups per zinc ion.

FMA molecules exist in tightly coiled state when unneutralized or at low degrees of ionization ($0.1>\alpha$). The ionized molecules undergo a configurations! transition in the range $0.1 < \alpha < 0.27$. The transition is completed at a = 0.27. Maximum chain extension has been achieved at 70% neutralization. The uncoiling of the polymer molecule has been attributed to strong electrostatic repulsive forces between the charged carboxylate groups along the polymer backbone. The uncoiling of the compact PMA molecules is a single-step process.

It has been established that some experimental techniques used were more sensitive than others. With conductance measurements, spectrophotometry and potentiometric titrations it is quite possible to detect almost all types of complex species present in M^{2+}-PMA systems with their corresponding co-ordination numbers, while viscometric titrations and dialysis equilibrium will only detect the most stable complex formed and the corresponding co-ordination number.

The results presented in chapter 4 for spectrophotometries titrations show that Cu^{2+}-FMA complexes are charge-transfer complexes.

In chapter 5, equations were derived for M^{2+} PMA

systems to enable the author to calculate the stability constants and the co-ordination numbers of complexes formed. These equations were tested graphically and there was satisfactory agreement between theory and experiment. It was found that, on the average, each cation formed complexes involving two carboxylate groups per metal ion and that the mode of binding could be either intramolecularly or intramolecularly depending on the ionic strength and degree of ionization (a).

It has been shown convincingly in chapter 6 that the acid dissociation constant K_a is not a constant but a function of a. Potentiometric behaviour of PMA in the absence and in the presence of divalent cations has been discussed in light of double layer effect and also in light of the empirical equations developed for calculating $[coo^-]$bound and $[M^{2+}]$bound.

Light scattering studies confirm that at low degrees of ionization a dimer is formed in the presence of Cu^{2+} and Zn^{2+} ions because the molecular weight is approximately doubled. This suggests that the most likely mode of binding is intermolecularly. Light scattering studies also confirm that partially ionized PMA molecules exist in random coils.

Finally in chapter 8, the results obtained from different chapters are compared and the interpretation and deductions made are found to corroborate. Cumulative constants β have been calculated for the various complex species in the reaction mixture.

C O N T E N T S

CHAPTER		Page
1	Introduction, Previous work and General Theory of Binding	1
2	Conductance Studies	48
3	Viscosity	69
4	Spectrophotometric Titrations	110
5	Dialysis Equilibrium	141
6	Potentiometric Titrations	180
7	Light Scattering Studies of the binding of Potassium, Zinc and Copper to PMA	229
8	Comparison of Data and Conclusions	267
	A p p e n d i x	

Chapter 1

INTRODUCTION, PREVIOUS WORK AND GENERAL THEORY OF BINDING

C O N T E N T S

		Page
1.1.	Introduction	1
1.2.	Previous work on Polymethacrylic acid ..	9
1.2.1.	On the structural conformations of PMA in solutions	9
1.2.2.	On Ion-binding by PMA	21
1.3.	General Theory of Binding	27
1.3.1.	Multiple Equilibria	27
1.3.2.	Binding by identical and completely independent sites - Single Association	30
1.3.3.	Cases where more than one ligand per metal ion is bound	32
1.3.4.	Identical sites with Electrostatic Interaction between them	36
1.3.5.	Electrostatic Interaction and Free Energy of Polyelectrolytes	38
1.4.	R e f e r e n c e s	45

Chapter 1

1.1 I N T R O D U C T I O N

Polyelectrolytes are polymeric substances which incorporate ionic substituents in their polymer chains. Chemically, these substances constitute an extremely heterogenous group, whose various structures and functions endow them with a broad spectrum of physical properties.

Polyelectrolytes can be divided broadly into two categories: naturally occuring macromolecules and synthetic macromolecules. Much of the stimulation for the study of linear synthetic macromolecules has been derived from the fact that proteins and nucleic acids which are occuring naturally and are so indispensable to life, fall into the category of polyelectrolytes. It has been pointed out by Staudinger[1a] that both synthetic and natural polyelectrolytes present characteristically similar problems. The natural polyelectrolytes are complex materials and have complex chemistries which make interpretation of derived data difficult.

It has therefore been suggested that in order to understand fully the chemistry of these complex materials, appropriate studies should be carried out on synthetic polyelectrolytes containing a single type of repeating unit along the polymer chain.

Electrochemically, the polyelectrolytes comprise polyacids and polybases with a single or several types of ionizable groups, and polyampholytes with both acidic and basic groups. Some typical examples of polyacids are polyacrylic acid, polymethacrylic acid, alginic acid and polygalacturonic acid. In these materials the ionizable groups are weakly acidic so that the charge density along the molecular chain can be varied at will by varying the degree of neutralization. Strongly ionizing polymers are available in poly(vinyl-sulphonic) acid and poly(styrene sulphonic) acid. Weakly basic polymers are available in polyvinylamine and poly(4-vinyl pyridine) which may be converted to a strong base by quanternization. Amphoteric poly-electrolytes are obtained in two naturally occuring forms - the proteins and nucleic acids as well as synthetic copolymers.

Polyelectrolytes are usually studied in aqueous solutions. The properties of such solutions are strongly affected by such factors as molecular weight and molecular weight distribution, the extent of chain branching, rigidity of the molecules and addition of simple electrolytes. Another feature of such solutions may be that a molecule of polyelectrolyte dissociates into numerous counterions and a polyion and hence the thermodynamic properties of polyelectrolyte solutions such as the second virial coefficient are highly affected by the properties of the counterions. Because of the combination of these various features, the physical behaviour of polyelectrolyte solution is quite complicated.

To understand the solution properties of polyelectrolytes, it is imperative that appropriate means to elucidate the structure of the molecule being studied are found, and suitable relationships must be established to express the dependence of chemical, physical and electrochemical properties on the structure so evaluated. It is well known that solutions of linear polyelectrolyte show various characteristic physical properties among the most important of which is the high expansion of the polyion coil. This high expansion is

brought about for charged polymers, by the charges along the polymer chain. If a molecule which has a coiled structure is converted by titration or chemical modification to a chain carrying a large number of ionizable groups, the mutual repulsional forces between adjacent ionized groups along the molecular chain will lead to chain expansion and the coiled structure opens to a rod-like one as the chain stiffens. The radius of gyration of a polyion in solution is not only much more increased than that of a corresponding non-ionic polymer but also changes more markedly with the experimental conditions. The ionic charges attached to the polymer chain do not affect only the conformation of a molecule, they also create a high local charge density which must affect very strongly the properties of simple ions in the solution.

It has long been known that certain naturally occuring substances like proteins and nucleic acids which fall into the category of polyeldctrolytes form stable complexes with ions of heavy metals. And although the metals in these complexes no longer behave as simple inorganic ions, the complexes are in equilibrium with a proportion of inorganic ions from

which they are formed. It is also known that other biologically important substances have a similar affinity for metallic ions. Hence it may be profitable to think of cells and tissues of all kinds as areas in which traces of metallic ions are competed for by various complex-forming agents present. However, the complex chemistry of these natural materials makes interpretation of derived data extremely complicated. It is the hope of the author that studies on simpler polyelectrolytes would serve as a useful guide and the behaviour of these complex, naturally occuring systems can be explained by modifying data derived from studies on simple synthetic polyelectrolytes.

So that in understanding this work, the author is concerned with various phenomena. It is intended to investigate to what extent the polymer chain will be expanded as a result of mutual repulsion of the fixed charges and how this expansion will affect the properties of the polyelectroltye solution. The author also wishes to know how the electrochemistry of the solution is modified by the presence of the simple ions. It is intended to study quantitatively

(i) affinity of the polyelectrolyte for the ions of various metals

(ii) to establish if those complex-forming metals affect the stability of the structure and if they have any influence on the properties of ionizable polyelectrolyte.

It is quite clear that the objectives outlined above can not be strictly separated. The interaction of simple divalent cations with polyions will lead to a distribution of the ions which modifies the repulsion of the polyions. Conversely, not only the charge but also the shape of the polyion will determine its interaction with the metal ions. It is this interdependence coupled with the objectives outlined above which is responsible for the complexities and the fascination of this field of study for the author.

There exists a wealth of data on the expansion of linear polyelectrolytes, notably polymethacrylic acid and polyacrylic acid but there is comparatively little information about the binding of heavy metal ions to polymethacrylic acid. No investigator has yet presented a detailed study on stoichiometry, mechanism and extent of binding of these ions to polymethacrylic acid. Many investigators feel confortable by presenting their experimental results only without making any

critical analysis of the derived data. Many have studied the solution properties of polyelectrolytes either from a theoretical or experimental points of view, but many problems such as the relation between the expansion coefficient and ionic strength or limiting viscosity number, the possible dimerization of polymer molecules in the presence of divalent cations have been left unsolved.

Attempts have been made by the author to solve some of these problems. A detailed study has been made on conventional polymethacrylic acid using potentiometric titration techniques. Also, dialysis equilibrium and light scattering techniques have been used.

Light scattering constitutes a particularly powerful means of studying the complicated physical behaviour of polyelectrolytes since it is the best means of determining the radius of gyration and molecular weight without ambiguity and also provides reliable data on the second virial coefficient.

Using combined viscometric and spectrophotometric titration techniques, attempts have been made to determine the molecular weight of the polymer and also the shape and configuration of the polymer in solution.

Similar studies have been carried out on polymethacrylic acid using dialysis equilibrium and conductance methods. These studies provide means of evaluating the stoichiometry and extent of binding. Attempts have been made to obtain values for the binding constant.

Interactions between polymethacrylic acid and divalent cations have been studied in great detail by potentiometric and viscometric titration techniques. These have been carried out with a view to finding out to what extent the chain has expanded as a result of the repulsion of the fixed charges and how this expansion has affected the properties of the polyelectrolyte solutions, especially the electrostatic interaction between the charged sites. The results and conclusion arrived at have been presented in this thesis.

1.2. PREVIOUS WORK ON POLYMETHACRYLIC ACID (PMA)

1.2.1 On the structural conformations of PMA in solutions:

Polymethacrylic acid (PMA) is one of the vinyl polyelectrolytes whose physicochemical properties have been studied in great detail. Particular interest in PMA has arisen because the solution properties of PMA exhibit deviations from the expected behaviour of synthetic polyelectrolytes as found in other polyvinilic compounds[1-7]. PMA represents the first dear example of synthetic vinyl polyelectrolyte whose chain can undergo in aqueous solution a pH - induced conformational transition of distinctly co-operative character. Furthermore, to the author's knowledge, polymethacrylic acid is the only vinyl polyelectrolyte available in samples with a different degree and type of stereoregularity. Such samples have been prepared and examined in considerable detail by various workers[1-10].

The author will now briefly review the available experimental evidence on the basis of which occurence of a conformational transition of PMA chains has been advanced to account for the peculiar behaviour of PMA in aqueous solution. Where-ever possible, comparisons will be made between solution properties of isotactic, syndiotactic and conventional PMA.

Various authors have used the potentiometric method to investigate the structural changes of PMA in solution. Mandel and Leyte[7] first recognised the existence of two conformations of PMA and said that this was responsible for its abnormal titration behaviour. Crescenzi[8] showed that in the potentiometric titration of syndiotactic and isotactic PMA, the isotactic PMA is seen to behave as a weaker acid over the whole range of degree of neutralisation, α.

Similar results on potentiometric titration of conventional, isotactic and syndiotactic PMA were obtained by Nagasawa and co-workers[9]. They found that the pK values for the isotactic form are always higher than for the syndiotactic form. The corresponding values for conventional PMA are intermediate. They accounted for the differences in the two stereoregular forms by assuming that the isotactic PMA has a locally helical structure in solution. Loebl and O'Neill[10] also reported that significant differences exist in the titration behaviour of isotactic and atactic PMA, their apparent dissociation constant differing by 0.3 pK units. In all cases, when the potentiometrically obtained pH values are plotted against α in a Henderson-Hasselbalch presentation, one finds a more or less clearly defined step between α values correxponding to values of the

degree of dissociation of about 0.1 to 0.3 which is absent in the titration curve of PAA or other vinyl polyelectrolytes so far studied. The anomalies have been attributed by Mandel and Leyte[7] to a conformational transition of co-operative character taking place in the PMA chains over this narrow range of α values. In this range, the two states exist in comparable concentrations. This anomalous behaviour of PMA samples of different types and amounts of chain stereoregularity over a narrow range of degree of neutralization has been confirmed using a number of different experimental techniques[11]. It is also well known[12,13] that the potentiometric titration curve of a polyelectrolyte is to a large extent independent of polymer molecular weight and concentration.

All the different techniques employed to monitor the transition consistently indicate that this occurs over a narrow range of α roughly 0.1 to 0.3. Mandel and Leyte[6] also showed from their spectroscopic studies that at $\alpha = 0.17$ the two states are present in equal concentrations. While a coiled form predominates at small degrees of ionization ($\alpha < 0.1$), PMA at larger values of α ($\alpha > 0.3$) exists mainly in an open stretched out form. The stretching out of the hitherto compact

molecules during the course of titration is the result of increasing electrostatic repulsion between each individual chain segment[3,6,7,14]. Schaffa and Hansjurgen[15] confirmed the observation of Mandel and Leyte[7] and also recognised that the range of conformational transition depends on the concentration of PMA. They also concluded that the stability of the compact state with respect to the extended state at zero degree of neutralisation decreases with increasing temperature.

The transport properties of PMA have been used by a number of investigators[11,15-21] as a means of studying the structural properties of PMA. These studies have been extremly valuable as a means of determining the structure and size of the polyion in solution.

Katchalsky and Lifson[23] calculated the electrostatic free energy of rodlike, partially ionized PMA molecules. Calculated osmotic coefficients were close to the experimental osmotic coefficients determined by Kern[13], at high degree of neutralization and dilute concentrations. From these theoretical studies, it is concluded that the shape of the macromolecular ion (polyion) is between that of a coiled chain and a rodlike structure

depending upon the degree of neutralization and concentration of polyelectrolyte solution.

From the peculiar trend of PMA viscosity against the degree of neutralization it was first argued[7] that the conformational transition of PMA may be visualised as an unwinding of a thightly coiled undissociated polymeric acid, impermeable to flow of solvent, stable at low degrees of neutralization. On ionization, the chain opens in favour of a highly solvated conformation[2] at high degrees of ionization. This observation is linked with the revelation in potentiometric plots i.e. a fraction of the carboxyl groups would not be accessible in the compact PMA structure stable at low pH values, as these become titratable only above the transition.

Overbeck and co-worker[1] observed the peculiar shape of the plots of the viscosity and pK against α where $pK = pH - \log \frac{\alpha}{1-\alpha}$ and α = degree of neutralization. Similarly, this was found by Arnold[4] in his plots of pK against α. He observed, however, that the peculiarity is absent in the plots of PAA which was confirmed by Mandel[8]. The sigmoid shape of the viscosity curve was also observed by Gregor, Gold and Frederic[5].

From the work of Arnold and Overbeck[1] it may be seen that specific viscosity of 10^{-2} eq./litre PMA in the presence of 10^{-3}M KCl increases moderately during the first 10% dissociation, then increases greatly and levels at about 30% dissociation. The apparent pK as derived from potentiometric titrations exhibits a dependence on α and that may be correlated with observed changes in viscosity. In the first region of viscosity increase, the apparent pK is seen to increase greatly. The region of large viscosity increase coincides with nearly constant pK. In the last region both pK and viscosity increase moderately. Katchalsky[3] and Arnold[4] relate these phenomena qualitatively to conformational changes of the polymer chain as a result of the repulsion of the identical charges that are fixed on the chain.

Light scattering and viscosity data by Oth and Doty[15], indicate that the expansion of the polyion is about seven fold when the degree of neutralization (α) of PMA was increased from 0 to 70%. It has also been concluded from light scattering that entropy and heat of dilution of PMA are negative[16]. The expansion of the molecule of PMA, according to Oth and Doty[15] is to

approximately one half of the contour length of the polyion. These conclusions were confirmed by the results of the diffusion properties of PMA by Kedem and Katchalsky[17]. They showed that the polyion is completely extended at 70% neutralization. These authors also show that uncoiling is a one step process occuring between 15-25% degree of neutralization. They derived an equation for the diffusion of polyelectrolytes as a function of the hydrodynamic resistance, the number of counterions and the osmotic pressure.

$$D = \frac{kT}{PV\left[\phi + \partial\phi/(\partial \ln \eta)\right]} \quad \ldots\ldots\ldots \quad (1-1)$$

where D is the diffusion coefficient, P is the hydrodynamic resistance, V is the number of ionized groups, ϕ is the osmotic coefficient, n is the number of moles of solutes per millilitre, k is the Boltzman constant, and T is the absolute temperature and η is the viscosity of the solution. From equation (1 - 1) above, one can see that D is inversely proportional to the size of the polyion due to the hydrodynamic resistance and directly proportional to the number of ionized groups. Because of the mobility of the counterions, a Nearst potential is developed, which

effectively increases the diffusion coefficient of the polyelectrolyte as the degree of neutralization is increased. Thus, diffusion measurements can be used to study both the size and the degree of ionization of the polyion.

An independent means of determining the size and shape of the polyion, is by the measurement of the electrical anisotropy effect by a Coutte apparatus described by several workers in the field of colloid science[24-26]. The measurement of the electrical anisotropy effect allows estimation of the rotational diffusion constant, which is related approximately to the length of the charged particle by the equation[18]

$$L_{cm} \simeq (8kT/\Pi\eta_o D_r)^{\frac{1}{2}} \quad \text{.....(1 - 2)}$$

where L is the length, η_o is the viscosity of the solvent and D_r is the rotational diffusion constant.

Recently Kern and Anderson[18] reported the use of diffusion properties and anisotropic electrical conductivity of PMA to determine the structure of PMA at varying degrees of neutralization and at different concentrations. They concluded in both kinds of measurements that the polyion chain goes from a coiled

to an extended configuration as the chain is ionized. Their diffusion data showed that at 0-10% neutralization, the molecules of PMA are in a hypercoiled state. At 10-25% neutralization, the macromolecules open to an extended configuration. In addition, it was found that at low concentrations, the opening of the chain is a two-step process, whereas at higher concentration, the mechanism involves a single step. Their viscosity plots also show an irregular shape in the range of α between 10% and 25% presumably by the effect mentioned above.

The question of what factors are responsible for the stabilization of the coiled form has been the subject of several investigations, but it is not yet unambiguously answered. Several peculiar properties associated with the tightly coiled state of PMA chains at low degrees of neutralization in dilute aqueous solutions have been found from studying the binding of acridine orange onto PMA[27] and in particular, the solubility of aliphatic[28] and aromatic[28] hydrocarbons in PMA solutions. The data showed that the extinction coefficient of monomeric acridine orange bound to PMA is higher than that exhibited by the dye bound to PAA for $\alpha < 0.2$ but rapidly decreases at higher degrees of

neutralization. The solubility of hydrocarbons in unneutralized PMA solutions which is some 25 (hexane) or 8 (pentane) times the solubility in pure water drops to very low values when α exceeds about 0.15. The same phenomenon has been observed in the case of some aromatic hydrocarbons[28,29].

This evidence as well as that presented by other workers led Liquori and collaborators[11] to conclude that in the tightly coiled random chains of PMA most of the methyl groups have been conceived of as being in the interior of the coils together with a fraction of the carboxyl groups, compatible with the obvious work of steric restrictions controlling the local conformation of the chain. According to this picture, the randomly coiled chains of unneutralized PMA provide non-polar cores, stabilized by hydrophobic interactions in which insertion of polar molecules of some hydrocarbons would occur with an overall free energy variation more favourable than that accompanying the dissolution of the same hydrocarbon in bulk water. Hydrophobic interaction would also produce the effect observed with acridine[27]. Beyond the critical value of the degree of neutralization which makes the onset of PMA

conformation transition, the tight coils rapidly expand into more solvated conformations and the polyelectrolyte loses its solubilizing power.

However, the view that hydrophobic forces are responsible for the compact structure of PMA at low degrees of neutralization which was also held by the Russian workers[30] has been severely critisized by Mandel and Leyte[31] and Kern and Anderson[18]. Mandel and Leyte[31] draw on spectroscopic and potentiometric measurements carried out on convention PMA in water and in water-methanol (40%) mixture. According to them, the stability of the compact state with respect to the extended state of PMA, at zero degree of neutralization, decreases with increasing temperature and also in the mixed solvent the conformational transition of PMA still occurs at about the same region of α as in water. Mandel and Leyte[31] concluded that the stabilization of the compact state of PMA is not primarily due to hydrophobic binding but should be ascribed to a direct stabilization of certain chain conformations by Van der Waals interactions between the methyl side chains. Kern and Anderson[18] on the other hand attributed the compact state of PMA to hydrogen bonding at low degrees of neutralization.

Crescenzi[8] has noted that the conclusions reached by Mandel and Leyte[7] appears rather misleading and if generalized could lead to erroneous predictions of "stable" conformation of polymers in the dissolved state. Discussion of factors controlling chain conformations considering side chain interactions which is the case in PMA and many other water soluble polymers and polyelectrolytes should take into account the effect of solvent - water - on the polymer.

In this case, therefore, the data presented by Liquori[11] and his collaborators seems fairly conclusive. It will be recalled that it has been stated earlier on that the heat and entropy of dilution of PMA are negative[16]. This evidence led Silberberg, Eliassaf and Katchalsky[16] to assume that there is a "particularly marked build-up of structure (of the solvent) in the solutions of PMA", in other words, hydrophobic bonding would greatly impose on the physico-chemical properties of this polyacid in dilute aqueous solutions. Therefore it could be concluded that in the case of PMA specific solvent effects thus appear to be extremely relevant.

At the 1965 International Union of Pure and Applied Chemistry Symposium of Macromolecular Chemistry in Prague,

the compact state of PMA was simultaneously discussed in two papers which both concluded that the uncharged molecule in water is essentially stabilized by bydrophobic interactions in analogy with some theories about globular proteins.

1.2.2. On Ion-Binding by PMA:

The author is now passing to a brief examination of some of the properties of PMA apart from conformational transition, the interesting point of how stereoregularity influences physico-chemical properties of PMA solutions.

The interaction of polyions with monovalent counterions has been thoroughly investigated and some interesting results have been obtained. Counterion binding of alkali cations has been demonstrated by dilatometric measurements[32]. The current-carry properties of polyelectrolytes as related to ion binding phenomenon has been investigated by Fouss and Edelson[33]. These two authors showed that even when those polyelectrolytes in which the monomeric components are completely ionized show the conductometric behaviour of weak electrolytes. Oth and Doty[15] studied the behaviour of PMA neutralized with sodium hydroxide using the

the techniques of light scattering, viscosity, potentiometric titration and conductance. The calculated root mean square extension of the polymer from viscosity and titration data were in agreement. The increases in reduced viscosity with increasing counterion size undoubtedly reflects the uncoiling of the polymer chain as a result of its increased charge[34].

The association of divalent cations with polyelectrolytes to form chelate complexes has been investigated in a number of laboratories. The various systems which were investigated include those containing zinc, maggnesium, cadmium and copper ions with partially ionized PMA[20,21,36-38]. The divalent cations form more stable complexes with polyanions than the monovalent cations. Of the cations studied so far, copper (II) in partially ionized PMA has received greater attention. Its interpretation has been somewhat difficult. In the PMA-Cu^{2+} system the ligand groups are evenly spaced along the polyion and the cation is capable of forming complexes with up to four carboxylate groups.

A measure of copper binding to PMA has been obtained by Kotlair and Morawetz[20] from equilibrium

dialysis measurements. Such measurements of copper binding by PMA were carried out using large polymeric acid/copper ratios in the presence of high concentration of potassium nitrate to swamp the Donnan effect and minimize electrical free energy of complexation. It was also found that the affinity of Cu(II) decreases with increasing polymer concentration which seems to indicate a competition of polymer-polymer association with ion binding. Such data gave no information about the nature of the complex.

Various authors[20,21,36-38], have used the potentiometric titration technique to demonstrate the formation of a complex between PMA and copper and zinc. They obtained pronounced shifts to lower pH values in the titration curves and they ascribed this to complex formation. Similar concentrations of alkaline earth ions produce no shift in the titration curves of PMA in strong salt solution. The data obtained have been interpreted to indicate the presence of chelates with two carboxylate groups bound to a cupric ion.

The results of spectroscopic studies of PMA-Cu(II) systems in acetate buffer both in the visible and uv regions by Kotlair and Morawetz[20] and by Morawetz[36] pointed to the formation of a copper-tetracarboxylate

complex in the presence of PMA. This conclusion is in agreement with the results obtained by these authors[20] from dialysis equilibrium measurements. Furthermore, this finding is also in agreement with the work of Klotz and Feiss[39] who had earlier showed that the absorption maximum shift from 770 to 750 to 730mμ as copper ions bind one, two and three acetate groups. Kotlair and Morawetze[20] interpretation of UV studies met with a lot of opposition from Mandel and Leyte[37] who found that from viscometric, spectroscopic and electrophoretic measurements two carboxylate groups are bound to one cupric ion. Mandel and Leyte[37] have also studied the binding of zinc, magnesium, cadmium, Nickel and Colbalt by PMA using titration shift method. They showed that all ions are bound less strongly by PMA than Cu(II). It is noted that the order of binding strength is

$$Co^{2+} < Ni^{2+} < Cu^{2+} < Zn^{2+} < Cd$$

as is usual for these ions[39]. All these ions have a co-ordination number of one except copper having two. Quite recently Bolewski and Lublina[38] found a similar order $Zn^{2+} < Cd^{2+} < Cu^{2+}$ for these ions using the method of polarography.

Interesting results have been found in the properties of isotactic and syndiotactic PMA by studying their binding capacity towards various counterions. Recent electrophoretic studies[41] have shown that isotactic PMA moves slower in electric field that syndiotactic PMA. Comparative studies of Cu^{2+} and Mg^{2+} [40] with isotactic, syndiotactic and conventional PMA were carried out by dialysis equilibrium over a range of ionization of the polymeric acid. It was found that the isotactic polymer has a higher affinity for Cu^{2+}, while Mg^{2+} is bound more strongly to the syndiotactic species. Significant differences have also recently been pointed out in the extent to which Na^{+} ions bind to isotactic and syndiotactic PMA[32]. The data obtained showed that the fraction of Na^{+} ions bound to the conventional (and syndiotactic) PMA is greater than that bound to isotactic PMA. The difference extends over the whole range of α- values. In this case also, the difference in counterion binding efficiency on the stereoisomerism of PMA chains is not readily understood. The suggestion is that in the author's opinion, these findings seem to suggest that

chelate formation involves carboxylate groups which are kept at well defined spacing from one another by prefered conformation of the chain backbone. In addition, the electrostatic free energy change due to the bringing together of negatively charged COO^- groups caused by metal complex formation may be more favourable in one case than in the other.

1.3. GENERAL THEORY OF BINDING

Practically all polyelectrolyte interactions with cations produce complexes with the components present in molecular quantities other than in a simple ratio of one to one. This feature of these interactions must be kept in mind in the interpretation of the derived data, as well as in designing experimental procedures. A full appreciation of the characteristics of multiple equilibria is, therefore desirable as a prelude to a discussion of the significance of the experimental findings.

1.3.1 Multiple Equilibria:[44-46]

Any treatment of ion or molecule binding by macromolecule must take into account the fact that it is possible for more than one ion or molecule to be bound by a macromolecule which may have a large number of combining sites. Before going to treatments for simple cases, it is profitable to think of equations

resulting from multiple equilibria. The following equations describe the resulting equilibria.

$$\left.\begin{array}{lcll} P+M & = PM & k_1 & = \left[PM\right]/\left(\left[P\right]\left[M\right]\right) \\ PM+M & = PM_2 & k_2 & = \left[PM_2\right]/\left(\left[PM\right]\left[M\right]\right) \\ \vdots & \vdots & \vdots & \vdots \\ PM_{n-1}+M & = PM_n & k_n & = \left[PM_n\right]/\left(\left[PM_{n-1}\right]\left[M\right]\right) \end{array}\right\} \quad (1\text{-}3)$$

In the above equations P is the free polymer, M is the free metal and n is the maximum number of metal ions which can be bound. The concentrations of the individual species $\left[P\right]$, $\left[PM\right]$, $\ldots\ldots\left[PM_n\right]$ are not usually experimentally determinable. Instead in a study of the interaction of a macromolecule with a smaller ion the experimental quantity which is most useful in describing metal-macromolecule interaction is r, the average number of moles of M bound per mole of P. This quantity is measured as

$$r = \frac{\text{Moles of M bound}}{\text{Total moles of P present}} \qquad \ldots\ldots\ldots(1\text{-}4)$$

The various methods available for determining r have been described in appropriate sections in this thesis.

It is possible to express r in terms of the association constants using equation (1-3)

$$\left.\begin{aligned}
\left[PM\right] &= k_1\left[M\right]\left[P\right] \\
\left[PM_2\right] &= k_2\left[PM\right]\left[M\right] = k_1k_2\left[P\right]\left[M\right]^2 \\
&\vdots \\
\left[PM_n\right] &= k_n\left[PM_{n-1}\right]\left[M\right] = k_1k_2\ldots k_n\left[P\right]\left[M\right]^n
\end{aligned}\right\} \quad \ldots\ldots(1\text{-}5)$$

So that the equation for r becomes

$$r = \frac{\left[PM\right] + 2\left[PM\right] + \ldots\ldots n\left[PM_n\right]}{\left[P\right] + \left[PM\right] + \ldots\ldots \left[PM_n\right]} \quad \ldots\ldots\ldots(1\text{-}6)$$

Substituting from expression in equation (1-3) for the concentrations of each species of complex in equation (1-6) in terms of the free metal, free polymer and equilibrium constants,

$$r = \frac{k_1\left[M\right] + 2k_1k_2\left[M\right]^2 + \ldots\ldots nk_1k_2\ldots k_n\left[M\right]^n}{1 + k_1\left[M\right] + k_1k_2\left[M\right]^2 + \ldots\ldots k_1k_2\ldots k_n\left[M\right]^n} \quad \ldots(1\text{-}7)$$

Equation (1-7) is perfectly general, and involves only the assumption that the interaction is reversible and that the polymer has a fixed number of sites for binding the metal.

1.3.2 Binding by identical and completely independent sites - Single Association:[44-46]

Let P be a large polymeric molcule having n sites capable of binding ligand M. Assume that the interacting sites are structurally and electrically identical and devoid of electrostatic or steric interactions between them. Consider, first the simplest situation in which the polymeric molecule P combines with only one molecule of ligand M to form a single complex PM so that

$$P + M = PM \quad \ldots\ldots\ldots\ldots (1\text{-}8)$$

and the association constant k is defined by the following equation

$$k = [PM] / ([P][M]) \quad \ldots\ldots\ldots (1\text{-}9)$$

in which the square brackets represent the concentrations of the respective species. It follows readily from equation (1-9) that

$$[PM] = k[P][M] \quad \ldots\ldots\ldots\ldots (1\text{-}10)$$

In addition, it will be useful to make a substitution for $[P]$ in equation (1-10) by means of the relation

$$[P_t] = [PM] + [P] \quad \ldots\ldots\ldots\ldots (1\text{-}11)$$

where P_t represents the total polymer concentration. By combining equations (1-10) and (1-11) it follows that

$$[PM] = k\{[P_t] - [PM]\}[M] \quad \text{.....(1-12)}$$

and by rearrangement $[PM] + k[M][PM] = k[M][P_t]$ ...(1-13)

or $$\frac{[PM]}{[P_t]} = \frac{k[M]}{1+k[M]} \quad \text{.....(1-14)}$$

The ratio $\frac{[PM]}{[P_t]}$ is evidently the number of moles of bound M per mole of total polymer. Thus

$$r = \frac{k[M]}{1 + k[M]} \quad \text{.....(1-15)}$$

Equation (1-15) is essentially the same as that derived by Langmuir to describe certain adsorption isotherm. Several alternative forms of equation (1-15) are particularly useful in connection with fitting of equations to data. For such purposes a linear equivalent is especially desirable. On rearrangement, equation (1-15) transforms to $\frac{[M]}{r} = \frac{1}{k} + M$ .....(1-16)

and another equivalent form of equation (1-16) is

$$\frac{1}{r} = \frac{1}{k} \cdot \frac{1}{M} + 1 \quad \text{.....(1-17)}$$

and a third form is given by

$$1 - r = \frac{1 - k[M]}{1 + k[M]} = \frac{1}{1 + k[M]} \quad \text{.....(1-18)}$$

Hence from equation (1 - 18) it follows that

$$\frac{r}{1-r} = k[M] \quad \text{.....(1-19)}$$

and finally a simple linear relationship is obtained by transposition to the form

$$\frac{r}{[M]} = k - k\,r$$
$$= k(1 - r) \quad \text{.....(1-20)}$$

Expressing equation (1 - 20) in logarithmic form, it gives $\log k = \log \frac{r}{1-r} - \log[M]$ .....(1-21)

1.3.3. Cases where more than one ligand per metal ion is bound[44-46]

Now let there be n combining sites which are identical and have no effects upon one another whatsoever. The n association constants can all be related to a single associaition constant k. Suppose that the n identical sites of a macromolecule P could be labeled in some way, so that they could all be distinguished. There would then be n different forms the species PM, n(n-1)| 2! of the species PM_2 and in general n!| i! (n-i)! forms of the species PM_i. The forms P and PM_n would be unique. If PM* represent a particular species of PM, i.e. a species with M attached

to a particular site, then the association constant $\left[PM^*\right] \mid \left[P\right]\left[M\right]$ would, for identical sites, have the same value of k for every possible species. There being n equally probable forms of PM and only one form of P. The first association constant $\left[PM\right] \mid \left[P\right]\left[M\right]$, which is the sum of all the possible $\left[PM^*\right] \mid \left[P\right]\left[M\right]$, would be equal to nk. There being $n(n-1) \mid 2!$ forms of PA_2, $k_1k_2 = \left[PM_2\right] \mid \left[P\right]\left[M^2\right]$ would similarly be equal to $n(n-1)k^2 \mid 2!$; i.e. k_2 would be equal to $\frac{1}{2}(n-1)k$. Therefore, from the above considerations a general expression for k_i will be $k_i = k \frac{n-i+1}{i}$ .....(1-22) and if this is substituted in equation (1-7) we get

$$r = \frac{\sum_{i=1}^{n} i\left\{\prod_{j=1}^{i} \frac{(n-j+1)}{j}\right\}k^i\left[M^i\right]}{1 + \sum_{i=1}^{n}\left\{\prod_{j=1}^{i} \frac{(n-j+1)}{j}\right\}k^i\left[M^i\right]} \qquad .....(1-23)$$

The product appearing in equation (1 - 23) is simplified thus

$$\prod_{j=1}^{i} \frac{(n-j+1)}{j} = \frac{n!}{(n-i)!\,i!} \qquad .....(1-24)$$

So that equation (1 - 23) becomes

$$r = \frac{\sum_{i=1}^{n} i \;\frac{n1}{(n-1)!\,i!}(k\left[M\right])^i}{1 + \sum_{i=1}^{n} \frac{n!}{(n-1)!\,i!}(k\left[M\right]^i} \qquad .....(1-25)$$

but $(1 + k[M])^n = 1 + \sum_{i=1}^{n} \frac{n!}{(n-1)!i!}(k[M])^i$ .....(1-26)

and differenting equation (1 - 26) with respect to $k[M]$ leads to

$$k[M]\frac{d(1 + k[M])^n}{d(k[M])} = k[M]n(1 + k[M])^{n-1}$$

$$= \sum_{i=1}^{n} i \frac{n!}{(n-1)!i!}(k[M])^i \quad \ldots(1\text{-}27)$$

A close look at equation (1 - 26) and (1 - 27) reveals that they are the same with the denominator and numerator, respectively, of equation (1 - 25) so that the latter becomes

$$r = \frac{k[M]n(1 + k[M])^{n-1}}{(1 + k[M])^n} = \frac{nk[M]}{1 + k[M]} \quad \ldots.(1\text{-}28)$$

and rearranging equation (1 - 28) we get

$$\frac{r}{n-r} = k[M] \quad \ldots\ldots\ldots\ldots(1\text{-}29)$$

Both equations (1 - 19) and (1 - 29) are identical. A plot of $\frac{1}{r}$ against $\frac{1}{[M]}$ should be linear with the slope of $\frac{1}{nk}$ and the intercept on the ordinate is $1/n$.

The constant k appearing in equation (1 - 29) can be redefined as the equilibrium constant for the

reaction at a single site. Now let the state of equilibrium at any such site be represented by its degree of association θ. $\theta = \frac{r}{n}$ represents the fraction of such sites (on different molecules) which are combined with M. The uncombined fraction is then $1-\theta$ and the equilibrium condition becomes

$$\frac{\theta}{1-\theta} = K_{eq}[M] \quad \text{.....(1-30).}$$

A treatment similar to that applied above for the association may be applied to equilibria viewed in terms of dissociation. If α is the degree of dissociation at any site and k is the dissociation constant for the reverse of the following equation

Free site + M $\rightleftharpoons$ combined site ..... (1-31) then one may write $\frac{\alpha}{1-\alpha} = \frac{r}{n-r} = \frac{K_{eq}}{[M]}$ .....(1-32)

The advantage of equations (1 - 19) and (1 - 30) is that they represent polyequilibria by a single constant rather than n separate constants. The assumption made in their derivations is not of course generally applicable i.e. these equations rarely, if ever, fit experimental curves. In light of these, it is necessary to mention briefly the chief factors responsible for the observed deviations and also methods which take into account these deviations.

1.3.4 Identical Sites with Electrostatic Interaction between them:[45]

Suppose a macromolecule has n identical electrostatiscally charged sites which interact with one another in such a way that the binding at any site affects the binding affinity at other sites. For example, consider the aliphatic dibasic acid, it can be seen that $\bar{O}OC-(CH_2)_n-COO^-$ species should have a greater affinity for H^+ ion than does the $HOOC-(CH_2)_n-COO^-$ species because of the added electrostatic attraction due to the second COO^- group in the former. This electrostatic attraction tends to make k_1, the first association constant greater than k_2 - the second association constant. If n is large, however, k_1 and k_2 approach each other. It is possible to allow for the former effect without in any way altering equation (1-19) simply by allowing k and ΔF^o (standard free energy charge of complexation) to vary as $\bar{r}$ varies. Now, the intrinsic association constant K_{int} defined as the limiting value of k_{ass} when r = 0 i.e. before any interaction due to binding occurs. Corresponding to K_{int} there is the intrinsic standard free energy change when electrostatic factors are taken into account is given by $\Delta F^o = \Delta F^o_{int} + RT\,\phi(\bar{r})$ .....(1-33).

Expression(1-26) can be expressed in terms of the association constants i.e.

$$K_{ass} = K_{int} e^{-\phi(\bar{r})} \quad \ldots\ldots\ldots(1\text{-}34)$$

Where $\phi(\bar{r})$ is some function of r such that $\phi(\bar{r}) = 0$ when $\bar{r} = 0$ and $\phi(\bar{r})$ is a completely unrestricted function

Now, if $\phi(\bar{r})$ is an increasing function of $\bar{r}$, binding at some sites makes binding at other sites difficult, but if $\phi(\bar{r})$ is a decreasing function of $\bar{r}$, there is co-operative interaction between sites i.e. occupation of some sites facilitates binding at other sites.

It should be clearly stated at this stage, that interacting identical sites do not remain identical when binding takes place; sites located nearest the occupied site will be subjected to a stronger interaction than those farther away. Here ΔF^{o} and $\phi(\bar{r})$ represents average properties, averaged over all sites and all configuration at any value of $\bar{r}$.

By combining equations (1-23) and (1-27) we get

$$\frac{\bar{r}}{n-\bar{r}} = \frac{\theta}{1-\theta} = K_{ass}\left[M\right] = K_{int} e^{-\phi(\bar{r})}\left[M\right] \quad \ldots(1\text{-}35)$$

which when re-expressed gives

$$\log \frac{\bar{r}}{n-\bar{r}} = \log[M] + \log K_{ass} = \log K_{int} - 0.434\,\phi(\bar{r}) \quad ..(1\text{-}36)$$

Equation (1-36) above can be used with great advantage if the reacting sites are identical and the number n is known, then it could be applied directly to determine the qualitative nature of the interaction between the sites. If calculations of the electrostatic term are made, and the necessary corrections to equation (1-36) are made, ideal behaviour of polyelectrolytes in solution will be obtained. Since there is very great difficulty in attempting to calculate $\phi(\bar{r})$ and therefore most workers are satisfied with approximate treatment of experimental data.

1.3.5 Electrostatic Interaction and Free Energy of Polyelectrolytes:[45]

The predominant form of interaction between polyelectrolytes and the simple ions is electrostatic in nature i.e. $\phi(\bar{r})$ is directly related to the effect of charged sites on the chemical potential of the reacting species. Electrostatic forces are non-specific in nature, and it is therefore necessary to modify the preceeding treatment so as to allow for interaction

between all charged sites i.e. not only the charges resulting from $\bar{r}$ bound ions but also those which may be present elsewhere in the molecule. In the light of the anticipated modification in the interaction taking place, the intrinsic properties of a site are redefined as those which it would have in the absence of any charges, rather than when $\bar{r} = 0$. The majority of equilibrium studies have involved polyampholytes - these are macromolecules which possess no form devoid of charges. For these molecules, the intrinsic properties are defined as those which such a molecule would possess in a hypothetical discharged state. In this state of affairs, it is assumed that all electrostatic interactions vanish when the average net charge per molecule $\bar{Z}$ is equal to zero, and thus the intrinsic properties of a site are defined as those it possesses when $\bar{Z} = 0$. For a macromolecule which can possess charges of only one kind, e.g. poly(methacrylic) acid, the state $\bar{Z} = 0$ is infact the discharged state. If both negative and positive charges are present, the interaction between them does not vanish at $\bar{Z} = 0$, and the intrinsic properties defined here then differ from those of a completely discharged state. At this stage,

an equation similar to equation (1-36) can be written in terms of the number of charges being carried by the polyion:

$$\Delta F^{o} = \Delta F^{o}_{int} + RT\, \Theta(\bar{Z}) \quad \ldots\ldots\ldots (1\text{-}37)$$

where ΔF^{o} and ΔF^{o}_{int} have the usual meanings. Here, $\Theta(\bar{Z})$ will be a positive function of $\bar{Z}$ for combination with a positive ion and a negative function for combination with a negative ion i.e. a net positive charge will always tend to repel a positive ion and attract a negative one and vice versa. Similarly, an analogous equation to equation (1 - 35) is

$$\frac{\bar{r}}{n-\bar{r}} = \frac{\theta}{1-\theta} = k\left[M\right] = k_{int}\, e^{-\Phi(\bar{Z})}\left[M\right] \quad \ldots\ldots (1\text{-}38)$$

$\Phi(\bar{Z})$ is related to the electrostatic free energy W_{el} of a macromolecule. To show this relationship, a simple approximation has to be made i.e. the average free energy of complexation per molecule in a solution is replaced by the free energy of complexation of the average molecule.

Now, consider the process of adding on the average $d\bar{r}$ ions of charge z_i to a macromolecule which already

has an average $\bar{Z}$ so that on the average $\frac{d\bar{r}}{n}$ ions will be added to each of the n identical sites for binding. Hence the resultant free energy change per mole of sites is given by

$$dF = \left[\Delta F^{o} + RT\ln \frac{\theta}{(1-\theta)M}\right]\frac{d\bar{r}}{n} \quad \ldots\ldots\ldots(1\text{-}39)$$

Now let us consider the process of discharging a macromolecule with charge $\bar{Z}$. The resulting free energy change per mole of macromolecule will be $- NW_{el}(\bar{Z})$ where W_{el} is the electrostatic energy of a single macroion and N is the Avogadros number. The corresponding free energy change per mole of sites will be $- NW_{el}(\bar{Z})|n$. Per mole of sites $\frac{d\bar{r}}{n}$ moles of small ions are being added, and they are also discharged with free energy change $- NW_i d\bar{r}|n$ where W_i is the work of charging a single ion of charge z_i.

We next combine the sites on the discharged macromolecule with the discharged ions. Since the dependence of ΔF on θ and on C is entirely independent of whether the combining species are charged, the result will again be $d\bar{r}|n$ times the value of ΔF giving the following equation

$$\Delta F = \Delta F^{*}\frac{d\bar{r}}{n} + RT\left(\frac{dr}{n}\right)\ln\frac{\theta}{(1-\theta)M} \quad \ldots\ldots\ldots(1\text{-}40)$$

where ΔF^* represents the standard free energy.

Finally let the charge previously removed be restored and assume all of it goes onto the macro ion, which now has a charge of $(\bar{Z} + z_i d\bar{r})$. The free energy change per mole of sites is $+ NW_{el}(\bar{Z} + zid\bar{r})$ or $NW_{el}(\bar{Z})|n + N.(\frac{\partial W_{el}}{\partial Z})zi\ \frac{d\bar{r}}{n}$ where N is the Avogadros number. The overall free energy change is obtained by adding all these contributions. Hence

$$dW = \left[\Delta F^* - NW_i + z_i N(\frac{\partial W_{el}}{\partial Z}) RT\ln \frac{\theta}{(1-\theta)M}\right]\frac{\partial r}{n} \quad \ldots\ldots\ldots(1-41)$$

Equation(1-41) is identical with equation (1-31) and follows that

$$\Delta F^o = \Delta F^* - NW_i + z_i N(\frac{\partial W_{el}}{\partial \bar{Z}}) \quad \ldots\ldots\ldots(1-42)$$

But $W_{el} = A(\bar{Z})^2 \quad \ldots\ldots\ldots(1-43)$

Differentiation of equation(1-43), to get $(\frac{\partial W_{el}}{\partial \bar{Z}})$, gives

$$\Delta F^o = \Delta F^* - NW_i + 2ANz_i\bar{Z} \quad \ldots\ldots\ldots(1-44)$$

But $\Delta F^o = \Delta F_{int}$ when $\bar{Z} = 0$.

Thus $\Delta F^* - RT\nu_i = \Delta F'_{int}$, hence

$$\Delta F^{\circ} = \Delta F^{\circ}_{int} + 2ANz_i Z^- \ldots\ldots\ldots (1-45)$$

By comparing equation (1-45) with equation (1-41)

one gets $$\theta(\bar{Z}) = 2ANz_i Z/RT = 2wz_i \bar{Z} \ldots\ldots\ldots (1-46)$$

where $$w = A\bar{e}/RT \ldots\ldots\ldots (1-47)$$

is constant independent of z_i and Z. Thus equation (1-46) gives the electrostatic contribution of the fixed charges on a polyelectrolyte. If calculations of $\dot{\phi}(\bar{Z})$ are made, and the necessary corrections made to equation (1-46) for example, ideal behaviour of polyelectrolytes in solution will be obtained. But all other constants appearing in equation (1-46) and the preceding ones have values of $\dot{\phi}(\bar{Z})$ obtained is to have any reasonable meaning. It normally presents extreemly great difficulty in attempting to calculate $\dot{\phi}(\bar{Z})$ or $\dot{\phi}(r)$ and consequently, most workers are satisfied with an approximate treatment of experimental data.

The value of w appearing in equation (1-47) depends on the model chosen to represent the macromolecule i.e. on which particular equation is used, for W_{el} and on the parameters occuring in these equations such as radius or length, ionic strength or temperature, w is independent of the combining site. Various equations have been proposed to calculate W_{el}

For a flexible linear polyelectrolyte[45]

$$W_{el} = \frac{3Z^2e^2}{2DR_e}\left\{ \frac{1}{K^2R_e^2} - \frac{3}{2K^5R_e^5}\left[K^2R_e^2 - 1 + (1 + KR_e)^2 \cdot e^{-2KR_e}\right]\right\} \quad \ldots\ldots\ldots(1\text{-}48)$$

Where R_e is the radius of sphere equivalent to the polyelectrolyte ion. D is the dielectric constant. Hill[42] has also computed W_{el} for long cylindrical ions. In his derivation, he assumed that a cylindrical ion of length L can be considered to have the same electrostatic free energy as a section of length L of an infinite cylinder i.e. he neglected the fact that the electrostatic field at the ends of real cylinders must be somewhat different from that nearer the middle. His results could be represented in the following equation

$$W_{el} = \frac{Z^2e^2}{DL}\left[\frac{K_o(K_a)}{K_aK_1(K_a)} + \text{In}\ \frac{9}{R}\right] \quad \ldots\ldots1\text{-}49$$

where R is the radius of the cylinder, a is the radius of exclusion, Z is uniform charge spread over the surface and K_o and K_1 represent modified Bessel functions of the second kind[43].

1.4 REFERENCES

Staudinger, H., Die Hochmolecularen Organ'schen Verbindungen, Springer, Berlin Page 39, (1932).

1. Arnold, R. and Overbeek, J. Th. G., Rev. Trav. Chim. 69, 162, (1950).

2. Katchalsky, A. and Eisenberg, H., J. Poly. Sc. 6, 145, (1951).

3. Katchalsky, A., J. Poly. Sc. 7, 393, (1951).

4. Arnold, R., J. Colloid Sci. 13, 549, (1957)

5. Gregor, H. P., Gold, D. H. and Federick, M., J. Poly. Sc. 23, 467, (1957).

6. Mandel, M. and Leyte, J. C., J. Poly, Sc. 56, 525, (1962).

7. Mandel, M. and Leyte, J. C. J. Poly. Sc. A2, 1879, (1964).

8. Crescenzi, V., Adv. Poly. Sc. 5, 358, (1968).

9. Nagasawa, M., Murase, T., and Konds, K., J. Phys. Chem. 69, 4005, (1965).

10. Loebl, E. M. and O'Neill, J. J., J. Poly Sc. 45, 538, (1960).

11. Liquori, A. M., Barone, B., Crescenzi, V., Quadrifoglio, F. and Vitagliano, V., J. Macromol. Chem. 1, 291, (1966).

12. Arnold, A. and Overbeck J. Th. G., Rev. Trav. Chim. 68, 879, (1949)

13. Kern, W., Z. Physik. Chem. (Lopzig), A181, 249,(1938).

14. Schaffa, V. O. and Hansjurgen, H., Bun. Der Bussengesselschaft Fur. Phys. Chem. 73, 94, (1969).

15. Oth, A. and Doty, P., J. Phys. Chem. 56, 43, (1952)

16. Silberberg, A. Elissaf, J. and Katchalsky, A., J. Poly. Sc. 23, 259, (1957)

17. Koden, O. and Katchalsky, A., J. Poly. Sc. 15, 43, (1954).

18. Kern, L. E. and Anderson, D.K., J. Poly Sc. A1, 2765, (1968).

19. Strauss, U. P. and Leung, Y. P., J An. Chem. Soc. 87, 1476, (1965).

20. Kotliar, M. and Morawetz, H., J. Am. Chem. Soc. 77, 3692, (1955).

21. Gregor, H. P., Luttinger, B. and Loebl, E.M., J. Phys. Chem. 59, 34, (1955).

22. Irving, H. M. H., London Chem, Soc. Special Publication, 13, 1959.

23. Katchalsky, A. and Lifson, S., J. Poly. Sc. 13, 43, (1952).

24. Schwarz, G., Z. Physik, 145, 563, (1956).

25. Gotz, K. G., J. Colloid Sc. 20, 289, (1955).

26. Hockman, K., Z. Physik, Chem. (Frankfurt) 9, 318, (1956).

27. Barone, G. Crescenzi, V., Quadrifoglio, F. and Vitagliano, V., Ric. Sc. 36, 503, (1966).

28. Barone, G., Crescenzi, V., Pispisa, B. and Quadrifoglio, F. J. Macromol. Chem. 1, 761, (1966).

29. Barone, G., Crescenzi, V. and Quadrifoglio, F., J. Phys. Chem. 71, 2341, (1967).

30. Brishtein, T. M., Anufrieva, E.V., Nakrasova, I.N., Dtitsyn, O.B. and Sheveleva, T.V., Vysokomolecul. Soedin 7, 372, (1965).

31. Mandel, M., Leyte, J.C. and Stadhouder, M. C., J. Phys. Chem. 73, 603, (1967).

32. Constantino, L., Crescenzi, V., Quadrifoglio, F. and Vitagliano, V., J. Poly. Sc. A2, 771, (1967).

33. Edelson, D. and Fouss, R.M., J. Am. Chem. Soc. 72, 306, (1950).

34. Kagawa, I. and Gregor, H.P., J. Poly. Sc. 23, 472, (1957).

35. Wall, F. T. and Gill, S.J., J. Phys. Chem. 58, 1128, (1954).

36. Morawetz, H., J. Poly. Sc. 17, 442, (1955).

37. Mandel, M. and Leyte, J.C., J. Poly. Sc. A2, 2883, 3771, (1964).

38. Bolewski, K. and Lubina, M. Roc. Chem. Ann. Soc. Chim. 44, 647, (1970).

39. Klotz, I.M. and Feiss, A.F., J. Phys. Colloid. Chem. 54, 18, (1950).

40. O'Neil, J.J., Loebl, E.M. Kadania, A.Y. and Morawetz, H., J. Poly. Sc. 3, 4201, (1965)

41. Anzuino, G. Constantino, L., Gallo, R. and Vitagliano, V., J. Poly. Sc. B4, 459, (1966).

42. Hill, T. L., Arch. Biochem, Biophys. 57, 229, (1955).

43. Watson, G. N., Bessel Functions, Cambridge University Press, Page 79, (1922).

General References:

44. Rossenber, R. M. and Klotz, I. M., in Laboratory Mannual of Analytical Methods in Protein Chem.

45. Tanford, C., Physical Chem. of Macromolecules.

46. Klotz, I. M., Proteins Interaction in The Proteins, Vol. I Part B.

Chapter 2

CONDUCTANCE STUDIES

C O N T E N T S

		Page
2.1.	Theoretical	48
2.2.	Experimental Details	52
2.3.	Results and Discussion	55
2.3.1.	Results	55
2.3.2.	Discussion	60
2.3.2.1.	Effect of Conductance Curve on Configuration of Polymethacrylic acid	66
2.4.	R e f e r e n c e s	68

Chapter 2

CONDUCTANCE STUDIES

2.1 Theoretical:

The conductance of solutions containing polyelectrolytes as well as simple electrolytes may be considered as the sum of the contributions made by the small ions and the polyions. It is usually assumed that the mobility of the small ions is the same in a polyelectrolyte solution as in a simple salt solution of the same ionic strength. This assumption has been critically examined by Fujita and Hermans[1] who found that it applies rigorously in all cases where the electrophoretic behaviour of the polyion is that expected of a free draining coil. This means that at all salt concentrations the Debye-Huckel shielding length $^{1}/k$ should be small compared with the hydrodynamic shielding length of the polymer coil.

A quantity commonly used in describing conductance changes in a solution is the molar conductance λ_m. This can not be easily measured directly but can be

computed from specific conductance L which can be measured easily and the concentration of solute expressed in moles per litre. λ_m is given by

$$\lambda_m = \frac{1000L}{C} \quad \ldots\ldots(2\text{-}1)$$

If it is assumed that all mobile ions in a system, in which the molar concentration of the charges carried by polyion is m_f and the concentration of a uni-univalent electrolyte is m_s, contributing independently to the conductance, then it is not difficult to obtain an expression for L. Assuming also that only a fraction α_d of the polyion charges are dissociated from their counterions then the specific conductance L is given by

$$L = \left[\left(\frac{F}{1000}\right)\left\{m_f\alpha_d\bar{\mu}_p + m_s\bar{\mu}_b + (m_s + m_f\alpha_d)\bar{\mu}_c\right\}\right] \ldots(2\text{-}2)$$

where F is the Faradays constant, $\bar{\mu}_p$, $\bar{\mu}_b$ and $\bar{\mu}_c$ are the mobilities of the polyion, byion and counterions respectively. Husenga *et al*[2] were the first to apply equation 2-2 to calculate α_d for salt-free polyacrylic acid, partially neutralized with sodium hydroxide. Their results predicted that ion binding is extensive at high charge densities.

It is also appropriate at this stage to consider how the degree of counterion dissociation α_d depends on the counterion concentration. Mock et al[3] found that with polysulphonic acids α_d is independent of polymeric concentration of the polyions which would not be expected to form specific complexes with their counterions. It has been severally observed that with sodium salts of polymeric acids molar conductance of the polyelectrolyte decreases slowly with increasing sodium ions concentration[2, 3, 4], reflecting apparently on increasing tendency towards specific complex formation.

The conductance of long chain polyelectrolytes is independent of the chain length of the polyion, but a chain length dependence should be observed at relatively low degrees of polymerization. Schindewoolf[5] found that the equivalent conductance of polyelectrolyte first increases with the degree of polymerization and later decreases to approach an asymptotic value. This behaviour reflects the superposition of two effects. Firstly, the ratio of the charge of the polyion to its frictional coefficient tends to increase with increasing chain length. Secondly counterion binding increases as the polyion chain increases in length.

When polyions exist in a highly extended form, their mobilities become significantly larger in the direction of maximum chain extension than in other directions. Thus, if the polyions are induced to assume a prefered spatial orientation, the electrical conductivity of the solution becomes dependent on the direction in which it is being measured. This interesting effect has been observed in solutions of polyelectrolytes oriented by high shear gradients[5, 6].

In conductometric titrations, practically all ions contribute to the conductance so that the pattern of variation in conductance will reveal any specific changes taking place in the solution, such changes can modify the structures of the molecule and thereby affect the macromolecular parameters. Conductance measurements will be expected, therefore, to reveal any changes in stoichiometry, nature of complex formed and effect of the complex formation in modifying the macromolecular structure, also small ion concentration variations.

Volumetric analyses are classified under the headings of neutralization, oxidation reduction, precipitation etc. During the progress of each of these

types of reaction, there is, in general some change of electrical conductivity. This change of conductance is useful to follow the progress of a reaction and particularly to decide when it has reached completion. The equivalence point is ususally denoted by a specific change in the slope of the conductance/concentration plot. The change in slope is indicated by discontinuities in the straight lines which result from the plot. There may be one or more equivalence points and each corresponds to a specific degree of co-ordination. When all the charged sites have been occupied, the conductance increases since the divalent ions are free to move and carry electricity.

2.2 Experimental Details:

A highly sensitive Wayne Kerr Universal Conductivity Bridge Model B221 was used for conductance measurements. The measurements were made at 220V and 50 c/sec. The voltage was stabilized by an 'advanced adjustable stabilizer' across the conductivity bridge. The conductivity cell used was of the dipping type with platinum electrodes, coated with platinum black. The cell constant was 1.07 cm^{-1}. The experimental solutions were contained in a glass container capable of holding 50 ml of solution.

All conductance measurements were made at 25±0.1 °C. Conductivity water obtained by passing double glass distilled water through a resin was used for all solution preparations and for rinsing of the cell and cell holder. Conductometric titrations were carried out in .01M KNO_3 and at various degrees of neutralization of polymethacrylic acid.

The general procedure in a typical experiment was as follows:-

Before titrations of the pre-ionised PMA with divalent cations were carried out, the reproducibility of the measurements was tested with the conductance bridge. This was done by measuring the specific conductance of increasing concentrations of added zinc nitrate or copper nitrate. In order to achieve this, 25.0 mls of .01M KNO_3 were placed in the glass cell holder and 0.10 ml aliquots of the stock solutions of $Zn(NO_3)_2$ or $Cu(NO_3)_2$ were added. The corresponding conductance of the solution was read after each addition and after shaking for about three minutes to ensure thorough mixing and attainment of thermal equilibrium. Generally low concentrations of the cations were used - of the order of 10^{-4}M. A graph of specific concductance

against concentration of added cation was plotted. A straight line was obtained showing that each mobile ion present in the solution contributed independently to the overall conductance. The procedure was repeated after one week and the two results were found to be in good agreement.

Generally, conductometric titrations with divalent metal ions in the presence of polymer were carried out with polymer solutions pretitrated to varying degrees of neutralisation using KOH solution. Four different degrees of neutralisation (α=0.3 to α=0.7) were used. For each solution at a particular degree of neutralization, a reference titration was always carried out. For each titration 25.0 ml of the polyelectroltye (2.5×10^{-3}M) in 10^{-3}M KNO_3 was always used. In each case, a total of 3.5 ml of the stock solution of $Zn(NO_3)_2$ or $Cu(NO_3)_2$ was added in 0.10 ml aliquots. Correction was made for dilution effects after each addition and plots of specific conductance against concentration of added cations were made.

2.3. RESULTS AND DISCUSSION

The conductance study of the binding of divalent cations to partially ionized PMA has attracted very little attention. This is probably because information which one would seek from such studies is obtainable from simpler methods and also interpretation of derived data is extremely difficult and entirely qualitative in nature. In the present work, the author has drawn attention to the stoichiometry of the complex formed between PMA and divalent cations and also to obtain information about posibility of molecular aggregation.

2.3.1 Results:

Figures 2.1-12 represent the plot of change in specific conductance against concentration of added cation for various solutions. Conductance titrations were obtained for solutions of KNO_3 - water and various concentrations of aqueous copper or zinc nitrate. Similarly, data were obtained for PMA - KNO_3 and various concentrations of copper or zinc nitrate added. Each of the graphs in Figures 2.1-3 and Figures 2.7-9 was obtained by subtracting the initial conductance reading i.e. contribution by water-KNO_3 or water-PMA (at $[M^{2+}]_{added} = 0$) from any other subsequent values of

conductance for the different concentration of the divalent cation. In these figures, the graph for KNO_3 - M^{2+} is above that of KNO_3 - PMA - M^{2+} owing to the subtraction of the initial conductance (i.e. conductance at M^{2+} = 0) values which was greater for KNO_3 - PMA - M^{2+} system. To obtain the graphs in Figures 2.4-6 and Figures 2.10-12, the conductance values for the PMA - M^{2+} - KNO_3 were subtracted from the values for KNO_3 - M^{2+} systems. The resulting contributions were plotted against the concentration of the cation. Most of the points fall on straight lines intersecting at equivalent points. The lines are in different segments having different slopes, indicating that conductance of PMA is highly affected by the presence of divalent cations.

The end-points of Titrations:

Three end points were observed in Figures 2.1-6 for copper and these end-points are manifested by the appearance of discontinuity in the straight lines. In the case of zinc nitrate i.e. Figures 2.7-12, two end-points have been observed. If the concentration

of the divalent metal ions are known one could calculate the ratio of original number carboxylate groups $\bar{n}$ bound per metal ion present.

$$(\bar{n} = \left[COO^-\right]_{bound} / \left[M^{2+}\right]_{total})$$

where the concentration of the carboxylate is expressed in monomeric units per litre. These have been calculated in Tables 2-I and 2-II. In calculating $\bar{n}$, the assumption is made that nearly all metal ion added and all COO^- groups are bound.

Tables 2-I and 2-II below show a summary of results obtained from conductance titrations showing the concentration of metal ion at the equivalent points and the number of carboxylate groups binding per metal ion at various degree of ionization of PMA in .01M KNO_3.

Table 2-I

α	$[Cu^{2+}] \times 10^4$ at equivalent point	No. of carboxylate groups per Cu^{2+} ion
0.3	1.95	3.85
	3.70	2.03
	7.45	1.00
0.5	3.00	4.17
	6.40	1.95
	12.50	1.00
0.7	4.30	4.07
	8.20	2.13
	17.50	1.00

Table 2-II.

α	$[Zn^{2+}] \times 10^4$ at equivalent point	No. of Carboxylate groups binding per Zn^{2+} ion
0.5	6.25	2.00
	12.45	1.00
0.6	7.55	1.99
	15.00	1.00
0.7	8.70	2.01
	17.40	1.01

2.3.2.Discussion:

Conductance measurements have been carried out in .01M KNO_3. KNO_3 does not bind appreciably with PMA but its presence in solution helps to reduce the electrostatic energy. The conductance of solutions containing PMA as well as added simple electrolyte KNO_3, may be considered as the sum of the contributions made by the small ions and the polyions. It is assumed that the mobility of the small ions is the same in polyelectrolyte solution as in a simple salt of the same ionic strength. This assumption is doubtful but it is the only assumption that can be made. Since it is only the concentration of the divalent cation and their anions, that are effectively changing, then one attribute the variation in conductance of the system, to the variation of concentration of these small ions. Therefore, it can be assumed that any major changes in the pattern of conductance may be attributed to changes in the concentration of divalent cations which bind the PMA.

It is evident from the blank titrations shown in Figures 2.1-3 and Figures 2.7-9 that all mobile ions contribute linearly to the overall conductance of the solution. In each of these figures, it can be seen that

the graphsfor KNO_3 - M^{2+} systems are above that of PMA - M^{2+} - KNO_3 system. This observation can be correlated with observations in potentiometric titrations. In potentiometric titrations, there is a shift to lower pH values as divalent cation is added and this has been interpreted as a tendency for the divalent cation towards specific complex formation. In conductometric titrations on the other hand, the conductance of the solution containing PMA - M^{2+} is found to shift to lower values of conductance when the values are compared with the corresponding KNO_3 - cation graph at the same concentration of divalent cation. This means that M^{2+} are bound to polymeric species in solution. Tranference experiments by Wall et al[9] have clearly demonstrated that the mobility of large ions is sufficiently great to make appreciable contribution to the conductance of solution; so that the reduction in conductance is the combined effect of complex formation which makes the polymer less electrically mobile and the reduction in the number of divalent cations caused by binding to PMA.

Now considering the graph for the solution, one finds that the conductance increases with increasing concentration of added divalent electrolyte. It has just been

stated that conductance of metal - PMA complex decreases with increasing binding. However, as binding takes place, H^+ are being thrown out into the solution, and nitrate ions from the copper nitrate are also increasing with increase in binding. H^+ ion has a high mobility so also does the NO_3^- ion; so that the observed increase from one end point to another is due to the contribution of H^+ ions released by bound M^{2+} and the nitrate ions.

The discontinuities in these curves and especially the dependence of these discontinuities on the concentration of M^{2+} added is a clear indication of specific binding of M^{2+} to PMA. The conductances of the complex at these end points shift with change in composition as is expected from theory. The end points are characterised by changes in slope on going from one segment to another but no definite pattern is followed. These end points have been associated with change in type of binding between the M^{2+} and COO^-. If the concentrations of the cation at these points are known, and subject to the conditions mentioned previously, it should be possible to find the stochiometry of the binding of Cu(II) and Zn(II) with PMA.

From Figures 2.1-6 i.e. in the case of copper, three equivalent points were obtained. The ratio $[COO^-]/[M^{2+}]_{added}$ at the equivalent points has been found to correspond to four, two and one carboxylate group binding per copper ion. These have been presented in Table2-I for various degrees of ionization studied. In the case of zinc i.e. from Figures 2,7-12, two end points were obtained and the ratio $[COO^-]/[M^{2+}]_{added}$ has been found to correspond to two and one carboxylate groups binding per zinc ion. These have been presented in Table 2-II.

The four fold co-ordination achieved in the case of copper and not in the case of zinc call for an explanation. Morawetz and Kotliar[7] have also obtained four-fold co-ordination for copper binding PMA by dialysis equilibrium method and also a copper-tetracarboxylate complex in acetate solutions using UV Spectroscopy[8]. The results of these authors did not give any information about the structure of the complex and the authors themselves made no attempt to explain their results. It has been suggested by the present worker in the section on viscosity (Chapter 3) that there exists a posibility of dimerization of the polymer in the

presence of copper. It is also suggested in the same section that copper forms stable square-planar complexes whereas the tetrahedral complex with zinc is unstable. There are two forces acting in the process of complexing; the electrostatic repulsive forces due to ionized groups and attractive coulombic forces between the COO^- groups and M^{2+}. The process of complexing could be pictured as a reaction between metal ions M and ligands L, so that in the presence of excess ligands one gets

$$M + L \rightarrow ML$$

In the present study, the ligands are the carboxylate groups and M are the cupric ions. Once M^{2+} ions are held in the vicinity of COO^-, the electrostatic repulsive forces are reduced and this process enhances the approach of more COO^- groups to further interact with the metal ions. In copper - PMA solutions, this could happen when cation concentration is low and the carboxylate groups concentration is high. This could lead to dimerization. It is not easy to say the actual mode of linkage i.e. whether it is intrachain or interchain linkage, in actual fact both are feasible. It has been suggested from viscometric studies that partially ionized PMA molecules exist in random coils

between $0.3 \leq \alpha \leq 0.7$. The present study has been conducted within this range. In this case, the metal ions could form a link between different segments of the same inter-winding chain in such a way that each segment would furnish the metal ion with two carboxylate groups i.e. intrachain linkage or the metal ions could form a link between two inter-winding chains to give interchain linkage. In this case each chain would supply the copper ion with two carboxylate groups.

One would not expect a four-co-ordinated Cu^{2+} - PHA complex to be of exceptional stability because of the much talked of electrostatic energy will incur some strain on the molecule. On addition of more copper ions the four-co-ordinated complex is likely to break down to a more energetically favoured 2:1 complex i.e. the ratio $[COO^-]_{bound}/[M^{2+}]_{added}$ is 2. This happens in presence of excess metal ions. On further addition of more M^{2+} ions the two co-ordinated complex further is also likely to down to a one to one co-ordination in the presence of large excess of M^{2+}. Similar observations were made for zinc.

2.3.2.1. Effect of Conductance Curve on Configuration of Polymethacrylic acid:

Molecular aggregation in the presence of Cu(II) will produce a considerable decrease in the mobility of the polyion and consequently a reduction in the conductivity. The polyion becomes less mobile as M^{2+} are bound. This is one of the reasons for the observed decrease in conductance of the solution. Figures 2.1-3 and Figures 2.7-9 show that the increase in relative specific conductance before the first end point is reached is quite small. This will be expected since the molecule will be quite large owing to four fold co-ordination and will be less mobile than one involving a co-ordination of two. The increase is greatest after the third end point is reached in the case of copper and after second end point is reached in the case of zinc. Here it is assumed that maximum binding has occured and once again the metal ions and the nitrate ions are free to move.

The graphs for difference in relative specific conductance against concentration of M^{2+} i.e. Figs. 2.4-6 and 2.10-12 do not seem to follow any particular pattern.

From these figures it would appear that the conductance of PMA is a very mild function of polymer size. The shapes of the graphs in the presence of M^{2+} are strongly influenced by the degree of ionization. It has been stated under viscosity studies that PMA molecules undergo configurational transitions between $\alpha=0.1$ and $\alpha=0.3$. Below $\alpha=0.3$ they exist in random coils and above $\alpha=0.3$ they exist in extended random coils. Maximum extension is achieved at $\alpha=0.7$. Because PMA changes configuration as α increases up to $\alpha=0.7$, one would expect each configuration to respond differently to conductance measurements. This probably explains why various types of graphs are obtained for PMA-copper complex as α varies from 0.3 to 0.7. In the case of zinc, studies have been carried out between $\alpha=0.5$ and $\alpha=0.7$. With this range of α values, PMA exist in the same form and one would not expect any abnormal behaviour, and true to expectation, figures 2,10-12 have identical shapes.

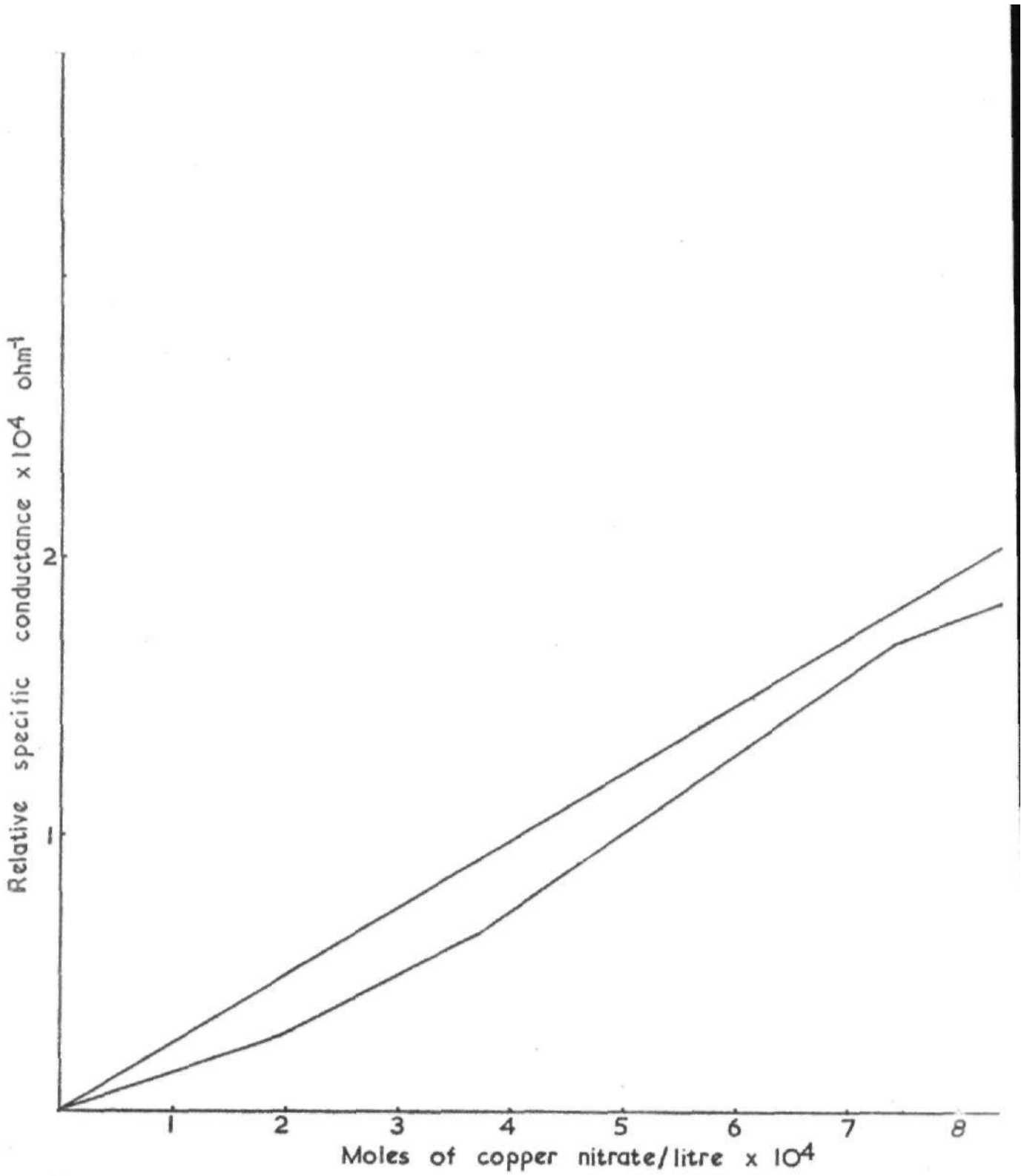


FIG 2.1 Condutivity titration of PMA in KNO_3 solution with copper nitrate at 25°C . q = 0.3 ; I = 0.1 ; [PMA] = 25×10^{-3} M

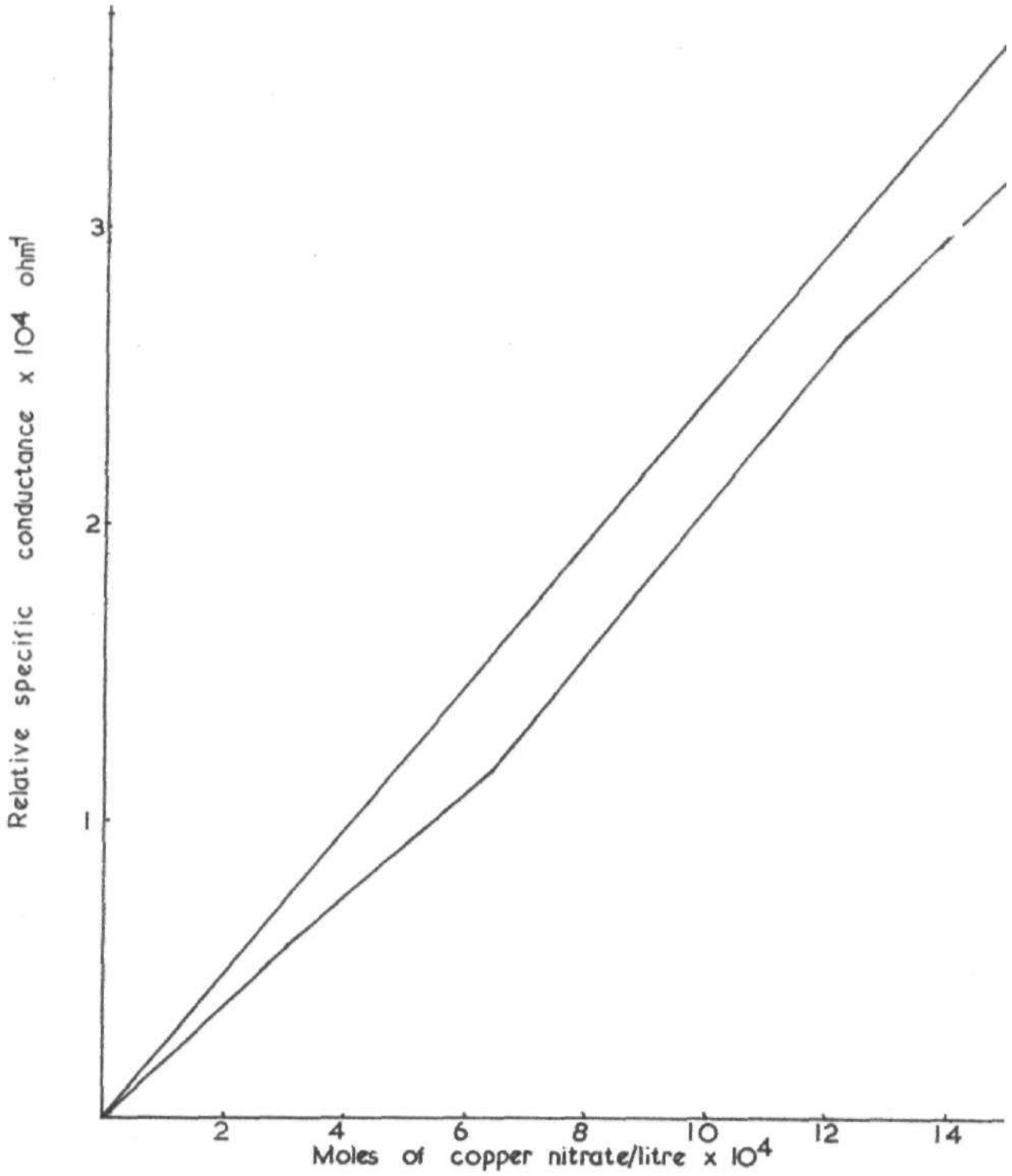


FIG 2.2 Conductance titration of PMA in KNO_3 solution with copper nitrate at 25 °C.

d = 0.5 ; I = 0.1 ; [PMA] = 2.5 X 10^{-3}M

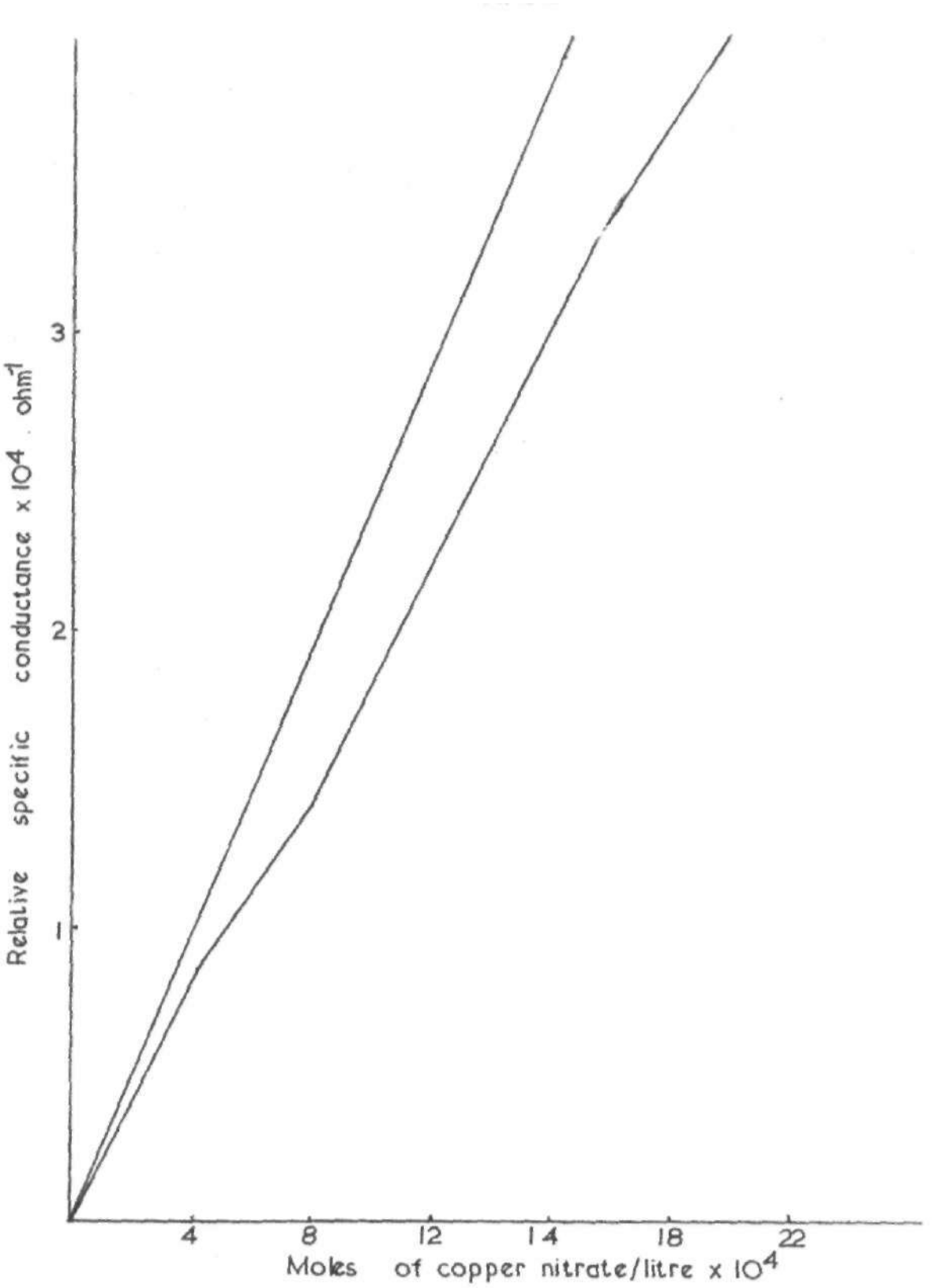


FIG 2.3 Conductivity titration of PMA in KNO_3 with copper nitrate at 25° C

$\alpha = 0.7$; $I = 0.1$; [PMA] = 2.5×10^{-3} M

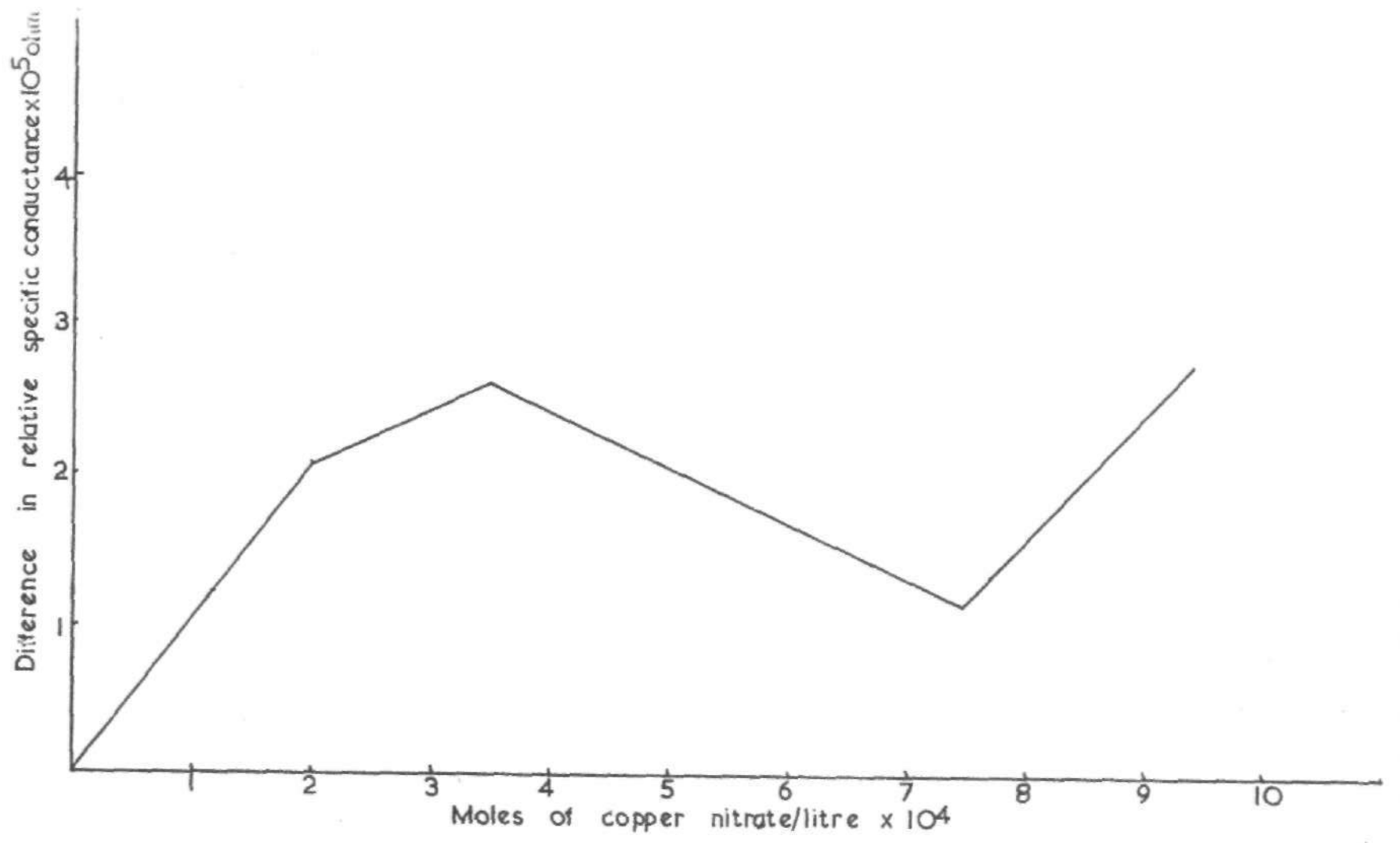


FIG 2·4 Conductivity titration of PMA in KNO_3 solution with copper nitrate at 25°C

$\alpha = 0.3$; $I = 0.1$; [PMA] = 2.5×10^{-3} M

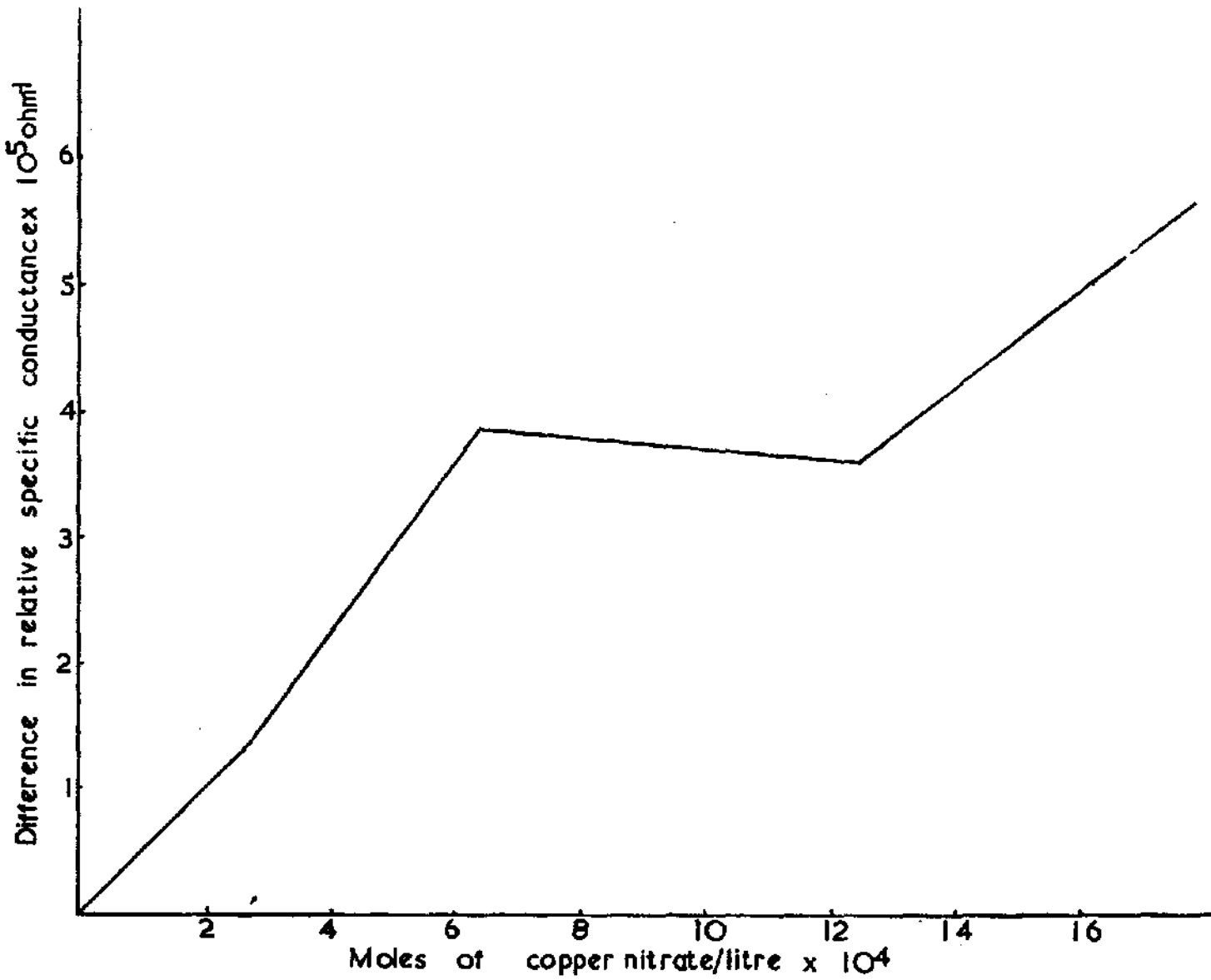


FIG 2.5 Conductivity titration of PMA in KNO_3 solution with copper nitra at 25°C $\alpha = 0.5$; $\bar{I} = 0.1$; $[PMA] = 2.5 \times 10^{-3}$

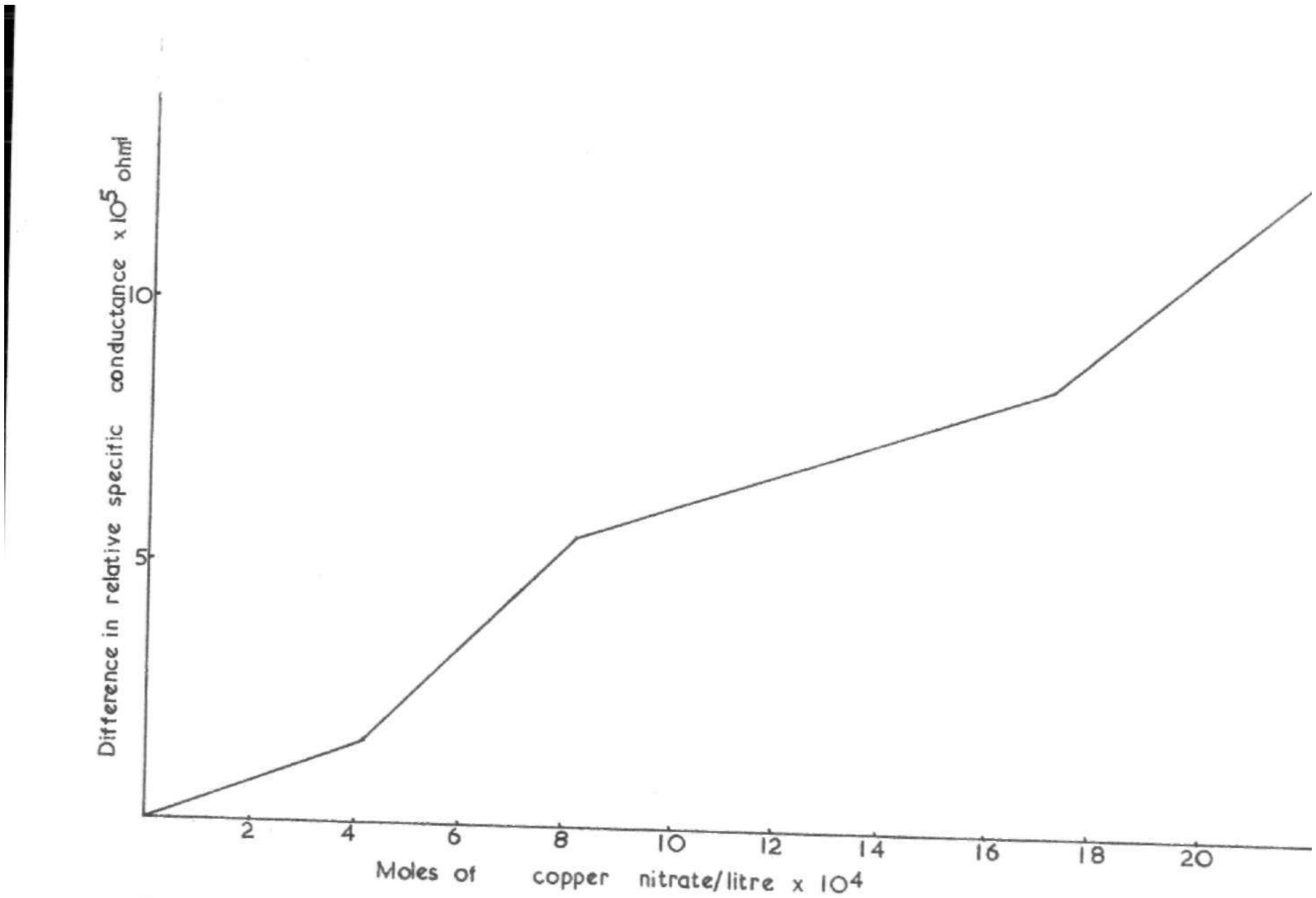


FIG 2.6 Conductivity titration of PMA in KNO_3 solution with copper nitrate at 25°C
$\alpha = 0.7$; $I = 0.1$; [PMA] = 2.5 X 10^{-3}M

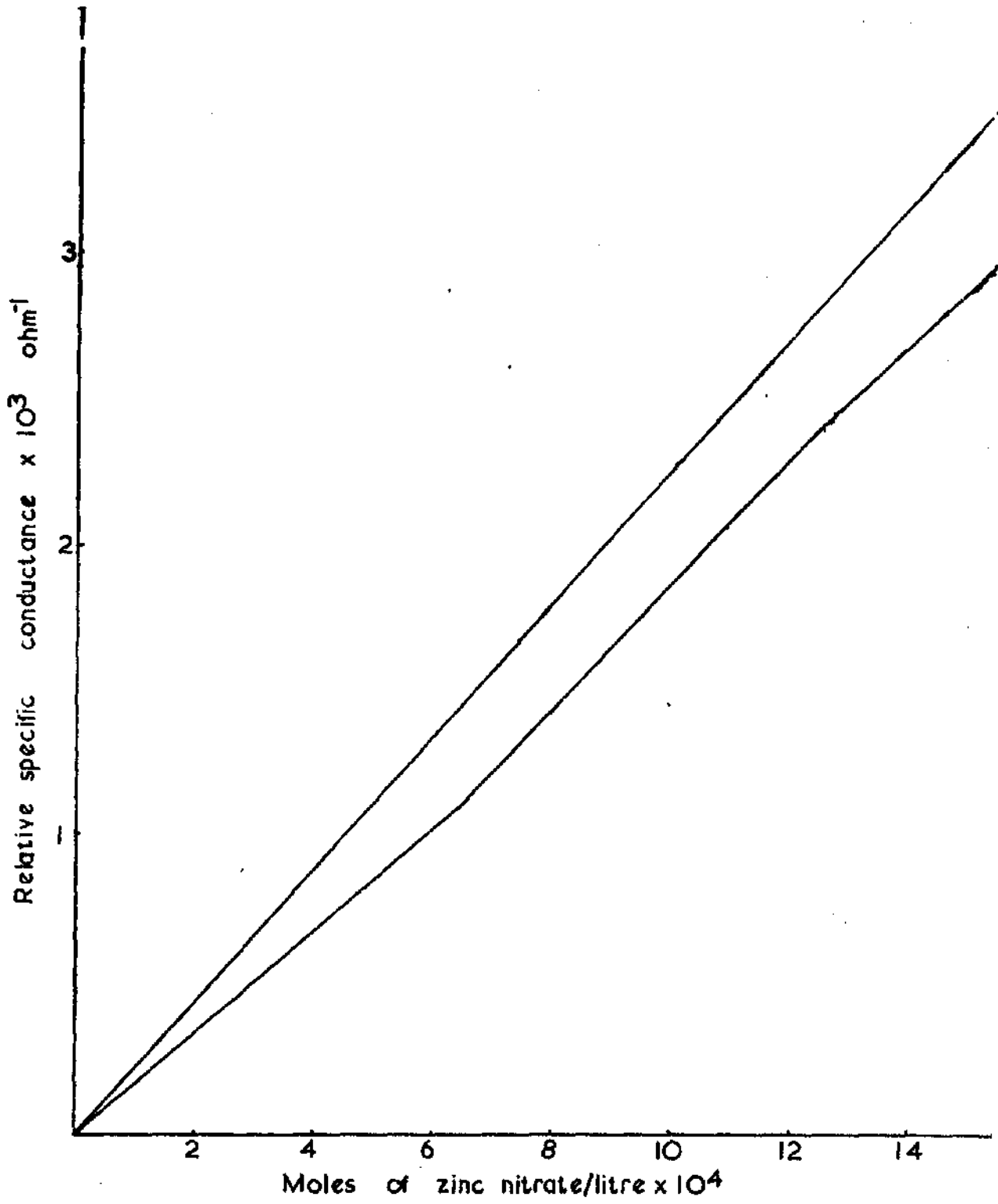


FIG 2.7 Condutivity titration of PMA in KNO_3 solution with zinc nitrate at 25°C

$\alpha = 0.5$; $I = 0.1$; $[PMA] = 2.5 \times 10^{-3}$ M

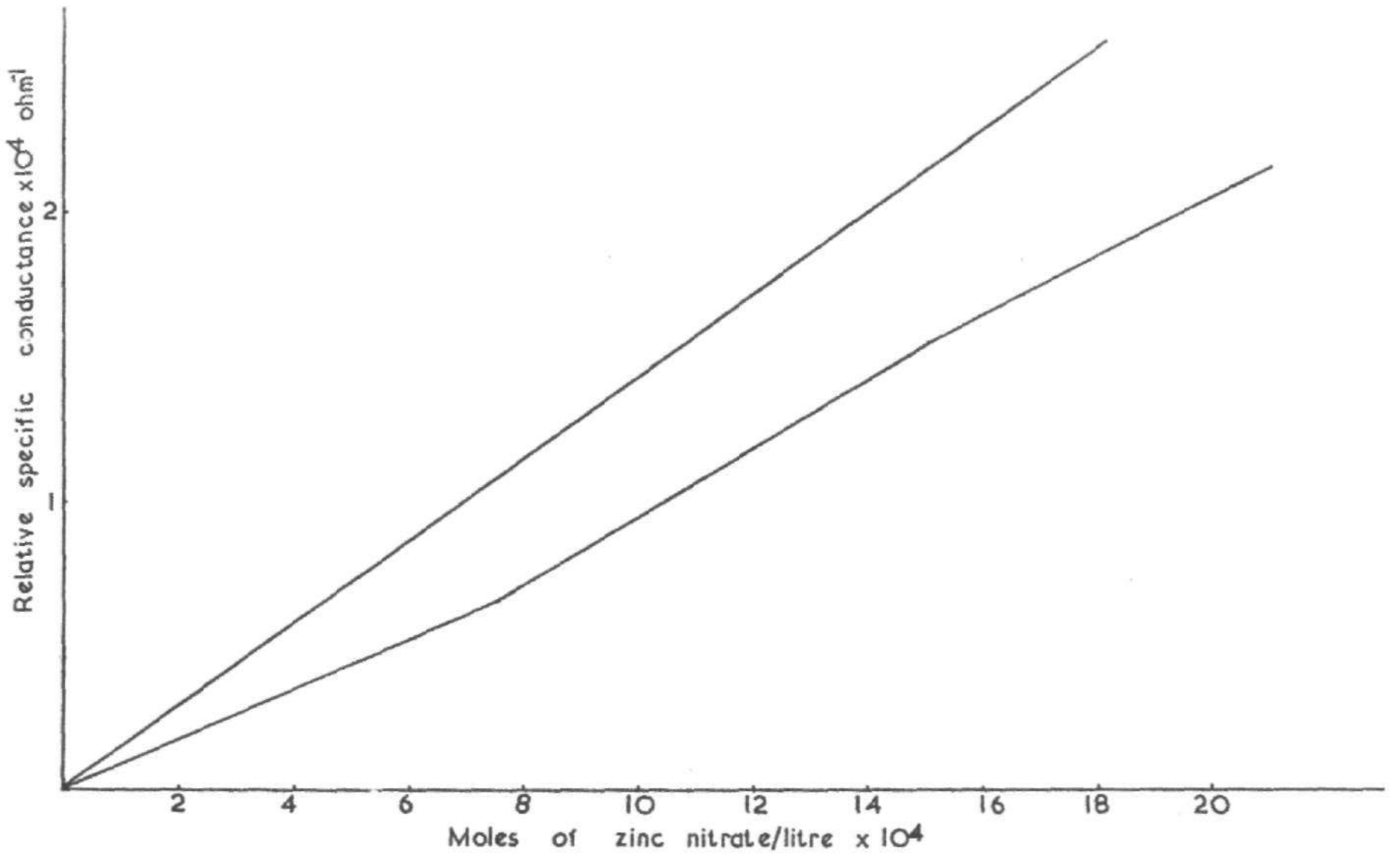


FIG 2.8 Conductivity titration of PMA in KNO with zinc nitrate at 25°C

$a = 0.6$; $I = 0.1$; [PMA] = 2.5×10^{-3}M .

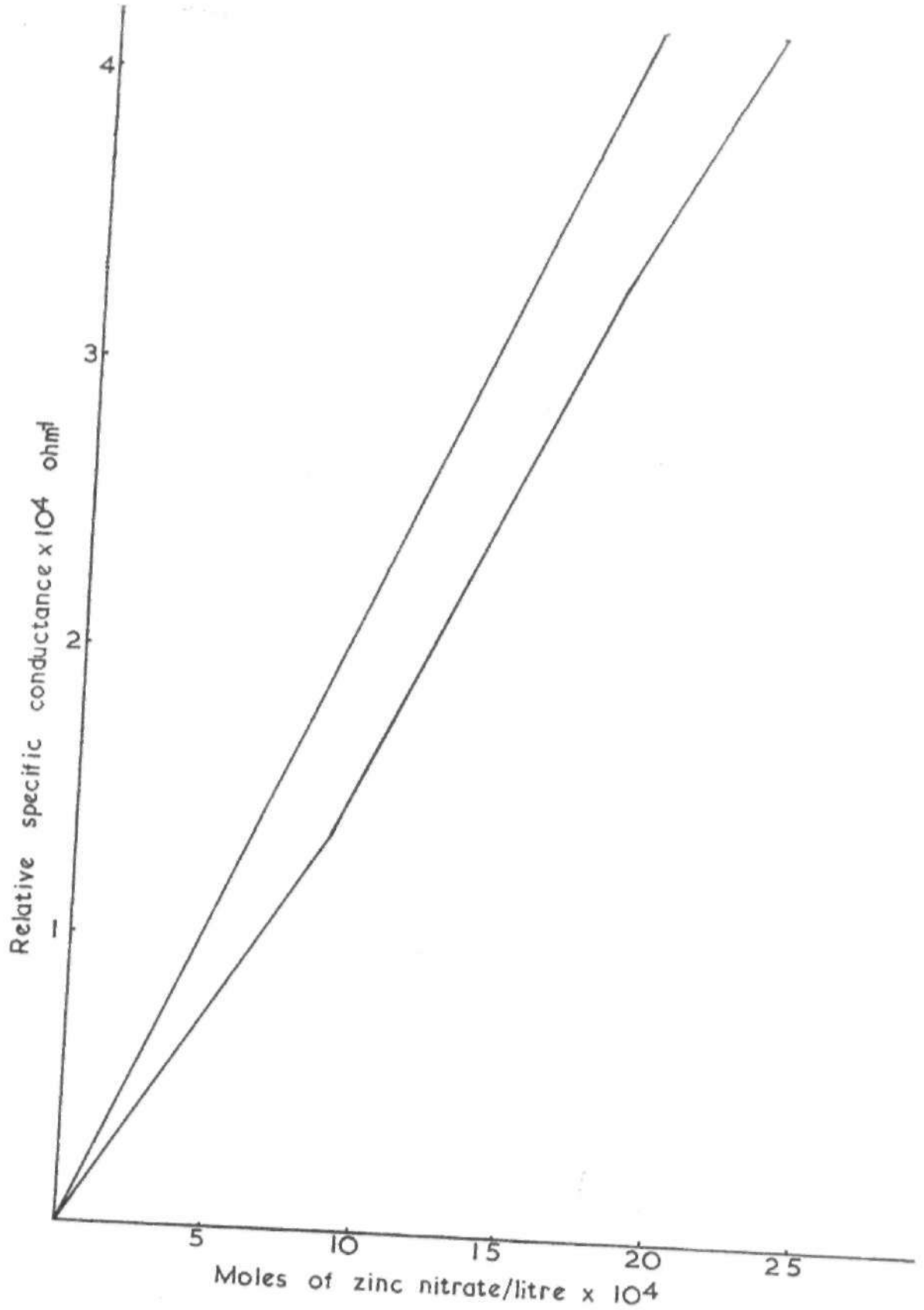


FIG 2.9 Conductivity titration of PMA in KNO_3 solution with zinc nitrate at 25°C.
$\alpha = 0.7$; $I = 0.1$; [PMA] = 2.5×10^{-3}M

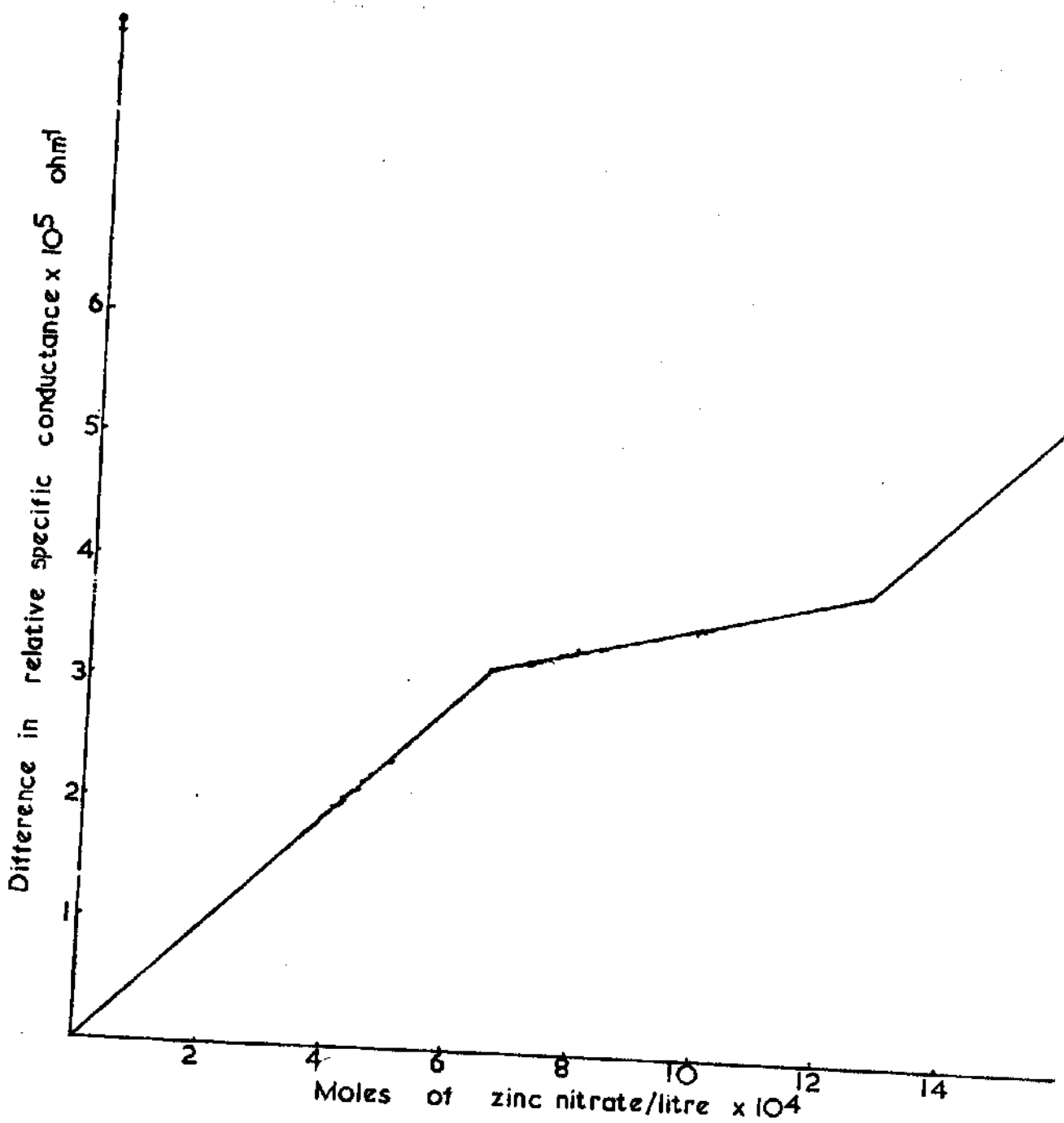


FIG 2.10 Conductance titration of PMA in KNO_3 solution with zinc nitrate at 25°C

$\alpha = 0.5$; $I = 0.1$; [PMA] = 2.5×10^{-3}

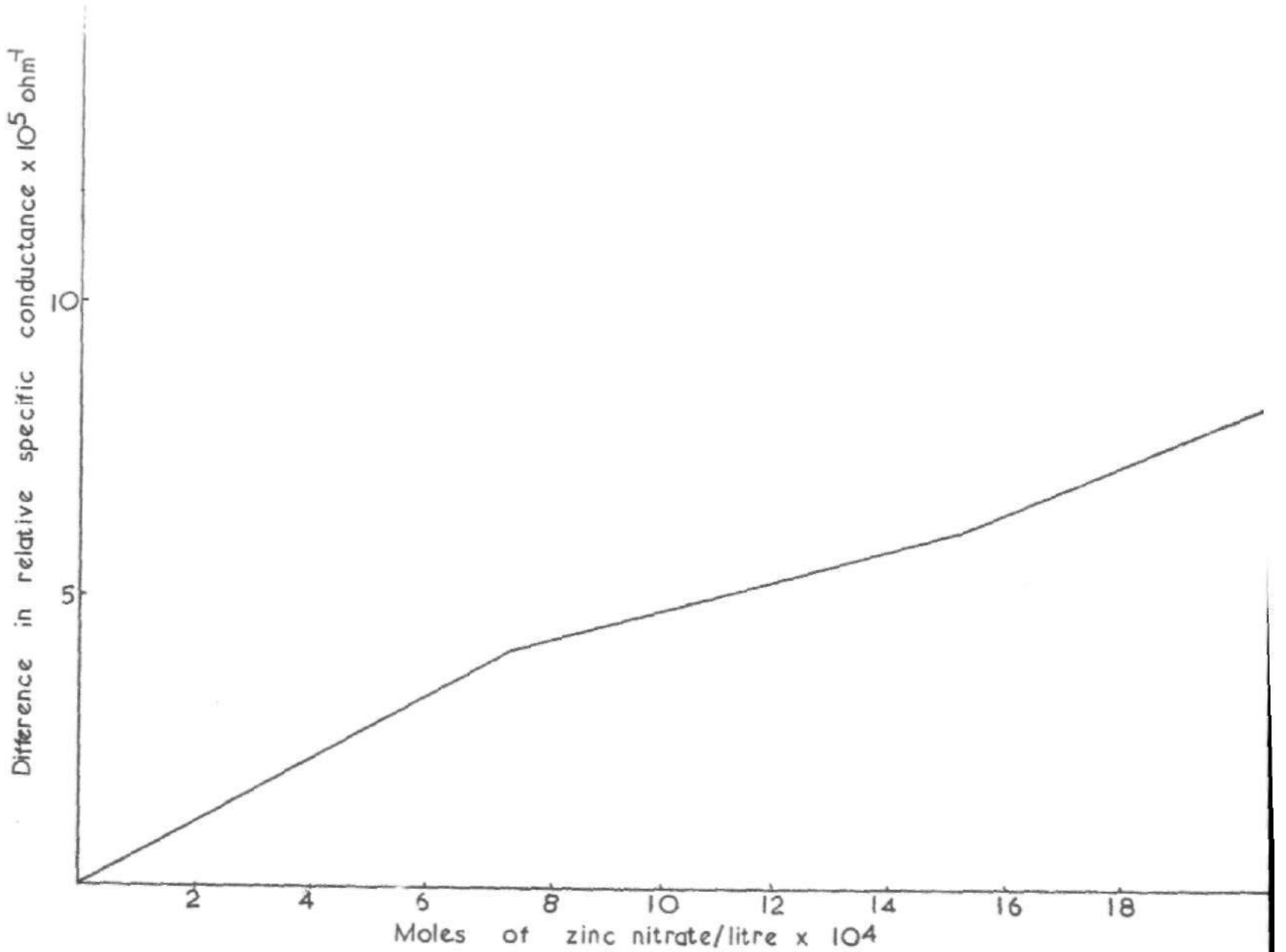


FIG 2.11 Conductivity titration of PMA in KNO_3 with zinc nitrate at 25°C
$\alpha = 0.6$; $\bar{I} = 0.1$; [PMA] = 2.5×10^{-3}M

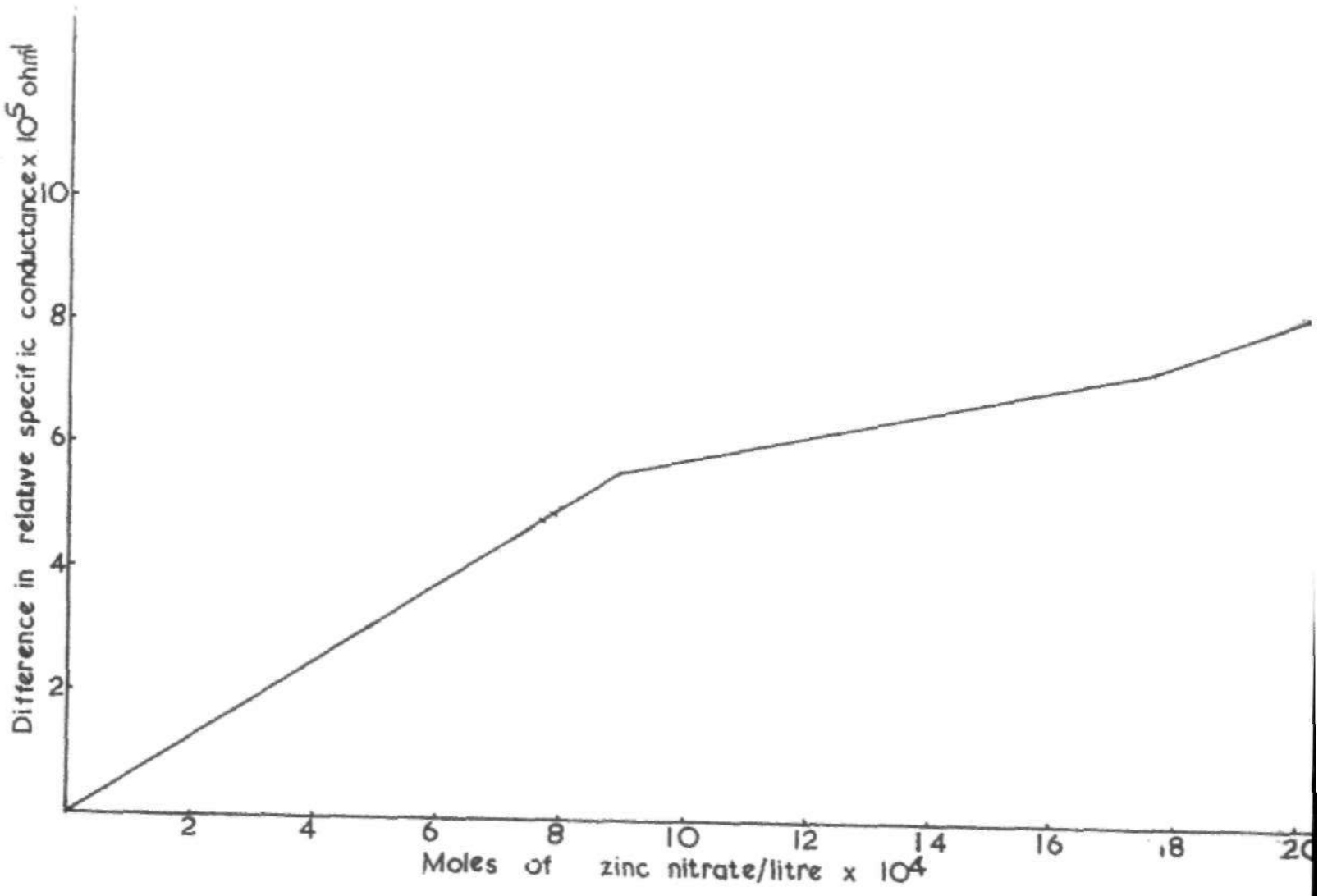


FIG 2.12 Conductivity titration of PMA in KNO_3 with zinc nitrate at 25°C

$\alpha = 0.7$; $I = 0.1$; $[PMA] = 2.5 \times 10^{-3}$ M

2.4. R E F E R E N C E S

1. Fujital H. and Hermans J. J., Proc. Roy. Netherland Acad. Sc. B58, 188, (1955)

2. Huizenga J. R., Gueger P. F. and Wall F. T., J. Am. Chem. Soc. 72, 2636, (1950).

3. Mock R. A., Marshall C. A. and Slykhouse T. E., J. Phys. Chem. 58, 498, (1954).

4. Oth A. and Doty P., J. Phys. Chem. 56, 43, (1952).

5. Jacobson B., Rev. Sci. Instr. 24, 949, (1953).

6. Schinderwold U., Z. Phyzik. Chem. (Frankfurt) 1, 129, (1954).

7. Kotliar, M. and Morawetz, H., J. Am. Chem. Soc. 77, 3692, (1955).

8. Morawetz, H., J. Poly. Sc. 17, 442, (1955)

9. Wall, F. T. and Gill, S. J., J. Phys. Chem 58, 1128, (1954).

Chaper 3

V I S C O S I T Y

C O N T E N T S

		Page
3.1.	Introduction	69
3.2.	Development of general equations and general considerations of polymer viscosity	70
3.3.	Methods of Measuring Viscosity	82
3.3.1.	Capillary Flow Method	84
3.4	Viscometric Titrations	85
3.4.1	Procedure	85
3.4.1.1.	Preparation of Solution	85
3.4.1.2.	Cleaning of Viscometer	86
3.4.1.3.	Viscosity Measurement	87
3.5.	Results and Discussion	88
3.6.	R e f e r e n c e s	107

V I S C O S I T Y

3.1. Introduction:

In the laboratory, and especially in industrial work, the viscosity of dilute solutions of polymers is very often used as a quick measure of molecular weights and other macromolecular parameters[1,2,3].

Staudinger[4] first noticed the dependence of the viscosity of dilute polymer solutions on their molecular weights and attempted to express it quantitatively. However, subsequent investigations[5,6] did not confirm the simple relationship between molecular weight and viscosity ($[\eta] = kM$) proposed by Staudinger. The viscosity of polymer solutions depends in the first place on the factors which determine the volume occupied by the macromolecule in solution, i.e. molecular weight, interaction of the solvent with the polymer, chemical structure of the polymer and the concentration of the solution. The effects of these factors have been the subject of numerous studies.

However, despite the abundance of experimental data, it is not yet possible to give a complete quantitative description of the effects of these factors on the viscous properties of solutions. Hence viscosity can not be used as an absolute method of molecular weight determination. To find molecular weight from viscosity data, it is necessary to use empirical equations which give viscosity as a function of molecular weight. Nevertheless, measurement of the viscosity of dilute solutions, provides one of the simplest methods of obtaining information about the size and shape of the molecules. The information is however not very direct and interpretation of viscosity results in terms of molecular structure and ion binding, must be accepted with caution, since they involve a number of assumptions.

3.2 Development of general equations and general considerations of polymer viscosity:

The limiting viscosity number $[\eta]$ is the most frequently used parameter in the characterisation of the molecular weight of flexible chain polymers. It is also frequently employed for the estimation of the dimensions of the molecular coil. The empirical dependence established for a polymer of a specified chemical

structure is only valid for a given solvent and temperature. Viscosities of polymer solutions are usually higher than those of pure solvents. The relative increment in the viscosity of the solvent in the viscosity of the solvent caused by the dissolved substance is called the specific viscosity (η_{sp})

$$\eta_{sp} = \frac{\eta - \eta_o}{\eta_o} = \eta_{rel} - 1. \quad .....(3-1)$$

where η is the viscosity of the solution and η_o is the viscosity of the solvent. The relative increment in viscosity may be found for example from the ratio between the eflux times of the solvent t_o and the solution t.

$$\eta_{sp} = \frac{t}{t_o} - 1 = \eta_{rel} - 1 \quad .....(3-2)$$

Provided $\frac{t}{t_o}$ is not too close to unity and $\frac{t}{t_o} < 2$. The specific viscosity increases with the increase in the concentration of the polymer solution. The concentration dependence of the viscosity of the polymer solutions is dealt with by extrapolation of the measured values of the reduced viscosity η_{sp}/c or the logarithm of the reduced relative viscosity $\frac{\ln \eta_{rel}}{c}$ to infinite dilution. It is this extrapolated value that is called the limiting viscosity number. For uncharged polymers, a plot of

η_{sp}/c against c (where c is the concentration) usually gives a straight line over a short range of c, or a gentle curve which is easy to extrapolate.

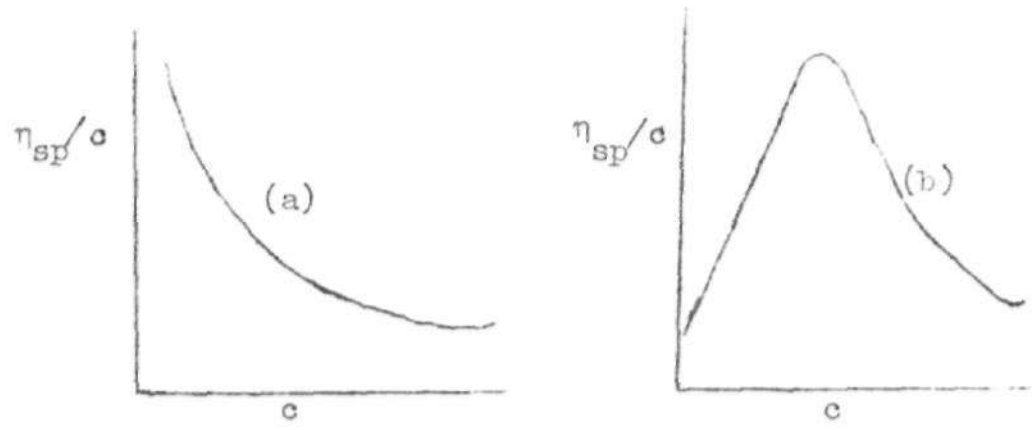
In polyelectrolytes the situation is quite different. If the viscosity of polyelectrolyte solutions containing no added salt is to be investigated, the data can not be interpreted in terms of polyion expansion, since consequences of the mutual interaction of the polyions can not be properly taken into account. With uncharged chain molecules, effects of particle interaction are eliminated by extrapolation of η_{sp}/c to zero solute concentration, but this extrapolation is possible only because the shape of the individual polymer coil depends only slightly on solution concentration. The situation is very different in polyelectrolyte solutions: here an increasing dilution provides increasing volume for the counterions, which will then tend to distribute themselves at larger distances from the polyion. As a consequence, the shielding of the fixed charges will be reduced, their mutual repulsion will increase, and the polyion will tend to expand. It is then not suprising to find that reduced viscosities of polyelectrolytes will typically increase sharply on dilution.

Plots of η_{sp}/c against c are frequently curved making an extrapolation impossible. A suggestion for the treatment of such data was provided by Fouss[8a] who suggested a relation of the type

$$\eta_{sp}/c = \frac{A}{1 + B\sqrt{c}} \quad \text{.....(3 - 2a)}$$

which predicts $(\eta_{sp}/c)^{-1}$ to be linear with $\sqrt{c}$. While this relation seems satisfactory in many cases, it has been shown to be inadequate if the polyion is very long[9]. It has just been stated that there is a marked increase in η_{sp}/c as the polyelectrolyte is diluted. It will also be seen later that the variation of reduced viscosity depends largely on the extent to which the polyion interacts. One would expect the size of the polyion to affect the shape of the η_{sp}/c against c curve. With majority of low and moderate molecular weights polymer the general shape of the η_{sp}/c against c plot is usually concave upwards. This has been observed for a number of polyelectrolytes; polymethacrylic acid[5,6], sodium polyacrylate[7] and some polyampholytes. All these give curves similar to type (a). With the majority of the high molecular weight polyelectrolytes, the concave upwards was not observed. For example a

maximum (type b) was obtained for PMA having a molecular weight of two million[9] and also for high molecular weight PMA[6].



The explanation for such behaviour as put forward by various people is summarised below.

(i) The Electroviscous Effect: The charges on the polyelectrolyte induce opposite charges in the surrounding solution thereby forming an electric double layer. This electric double layer is carried with the charged groups when the molecules move with the result friction is increased. This effect varies with pH and this affects the degree of ionization of the molecules and hence their charge. It also varies with the ionic strength of the solution.

(ii) A second cause for increased reduced viscosity is the size of the polyion which expands on dilution

due to decreased binding of the gegeions. As the size increases, any interaction due to the size will increase and as the molecule extends, the viscosity of the solution will increase.

(iii) Thirdly, the polyion may interact with the environment and this effect decreases as the concentration of the polyion decreases.

(iv) There is also a fourth effect, which is that due to the shear gradient which can affect the molecular volume. In this case, zero shear viscometers should be used unless molecular weights are not very large. However, for PMA at high salt concentration it is probably not necessary.

When neutral salt is added to a polyelectrolyte solution, the reduced viscosity undergoes a change. The shape of the curve obtained depends on the concentration of the salt, molecular weight and concentration of the polyelectrolyte. At salt concentrations below 10^{-4}M and for low molecular weight polyelectrolytes, a sharp maximum is obtained. As the salt concentration is increased, the maximum flattens out until a linear plot is finally obtained. In medium ionic strengths, the plot of η_{sp}/c against c approaches a straight line

just as is found for uncharged polymers. On going to high ionic strengths, the limiting viscosity number falls below the value expected from the same molecule in a discharged state[8]. This is as a result of the charge being reduced to zero and the coil shrinking as a result of intra-molecular attraction of the sort which stabilized the ionic lactice.

For polyampholytes, when both positive and negative charges are present, the molecule is fully contracted at the isoelectric point, where the charges balance and there is a minimum in the viscosity. A change of pH in either direction alters the ionization of the charged groups and increases the preponderance of either negative or positive charges. The mutual repulsion of like charges extends the molecule and leads to an increase in viscosity. Similarly, the viscosity of a weak polymeric acid increases as the ionization increases indicating an expansion of the coil due to electrostatic repulsion.

Mark[10] and Houwink[11] made a study of extensive experimental material and found the most general equation expressing the dependence of the limiting viscosity number on the molecular weight

$$[\eta] = kM^{\alpha} \quad \text{.....(3 - 3).}$$

Equation (3 - 3) contains two empirical coefficients k and α, which are constant for a given polymer in a given solvent over a broad range of molecular weights. Thus the logarithm of the limiting viscosity number is a linear function of the logarithm of the molecular weight:

$$\log [\eta] = \log k + \alpha \log [M] \quad .....(3 - 4)$$

The theory of solutions of macromolecules is extraordinarilly complicated and can be rigorously developed only for simple models. It is believed at present that most dissolved macromolecules can be represented as random coil which moves through the solution while occluding a certain amount of the solvent.

Hermans[12] and Kuhn and Kuhn[13] have carried out searching analyses of the limiting viscosity number to be expected of a free-draining coil. Their results predicted that coils with very high internal viscosities should be oriented to some extent in the direction of flow lines leading to a decrease in $[\eta]$ with increasing shear gradient. They also said that coils with zero internal viscosity which are expanded and compressed in phase with the alternating hydrodynamic stresses during each revolution of the coil, should have limiting

viscosity number independent of velocity gradient. Kirkwood and Riseman[14] and Debye and Bueche[15] proposed a theory according to which the solution viscosity changes with the permeability of the coil. They introduced the concept of the screening factor and computed the dependence of α on the screening factor. In other words, they took into account the hydrodynamic interaction between the monomer units and the disturbed flow of solvent through the coil. The results of the Kirkwood-Riseman theory may be written in the form

$$[\eta] = \frac{4}{3}\pi R_\eta^3 \left(\frac{N}{M}\right) F'|\equiv| \quad \text{.....(3 - 5)}$$

where $\frac{4}{3}\pi R_\eta^3$ is the volume of the rigid sphere which has the same limiting viscosity number as an impermeable Gaussian coil and $F'|\equiv|$ is the function describing the hydrodynamic permeability parameter. The Kirkwood-Riseman theory is more rigorous and represents a more complete description of the state of things. For $|\equiv| \to \infty$, $F'|\equiv| \to 1$ if $R_\eta = 0.94\ (S^2)^{\frac{1}{2}}$. Later it was found that the Kirkwood-Riseman theory contained errors which led to an over-estimation of R_η. According to Aller and Gardner[16] $R_\eta = 0.87 \langle S^2 \rangle^{\frac{1}{2}}$ and an almost identical result was obtained by Zimm[17] by a different method. Equation (3 - 5) predicts that $[\eta]$ is proportional to the volume occupied by the sphere i.e. $(\frac{4}{3})\ \pi R_\eta^3$.

In practice, the interpretation of limiting viscosity number data is greatly simplified by the fact that coils formed by flexible chain molecules closely approximate the behaviour expected for the limiting case of complete impermeability, even if the chain backbone contains only a few hundred atoms. This generalization proposed by Flory[18] has proved extremely successful in interpreting a wide variety of experimental data. Flory's theory predicts then that the limiting viscosity number is related to the mean square radius of gyration by

$$[\eta] = \Phi^1 \langle S^2 \rangle^{\frac{3}{2}} / M \quad \ldots\ldots\ldots\ldots (3-6)$$

where $\Phi^1 = \frac{4}{3}\pi N \left[R / \langle S^2 \rangle^{\frac{1}{2}} \right]^{\frac{1}{3}}$ which should be a universal constant independent of the nature of the macromolecule (provided only that the macromolecular chain is sufficiently flexible) and independent of the solvent medium. Usually Φ is defined by

$$[\eta] = \Phi \langle h^2 \rangle^{\frac{3}{2}} / M \quad \ldots\ldots\ldots\ldots (3-7)$$

where $[\eta]$ is in decilitres per gram as originally used by Flory. The formulation in equation (3 - 6) has the advantage that $\langle S^2 \rangle$ is an experimentally measured quantity. If the chains are linear flexible chains then

$$\left.\begin{aligned} (h^2) &= 6\,(s^2) \\ \text{and}\quad \Phi' &= 1006^{3/2}\,\Psi \end{aligned}\right\} \cdots\cdots\cdots (3-8)$$

is a constant and is equal to 2.1×10^{21} and using the results of Auer and Gardner[16] or of Zimm[17] the constant Φ' has a value of 4.2×10^{24}.

The effect of concentration on the viscosity of uncharged polymer solutions have been treated theoretically by Huggins[19] and for dilute solutions, the following equation has been obtained.

$$\eta_{sp}/c = [\eta] + k'[\eta]^2 c \cdots\cdots\cdots (3-9)$$

The coefficient k' varies from system to system, but is approximately constant for a given polymer, solvent and temperature.

Many other equations[20-22] have been arrived at empirically and found to agree reasonably well with experimental data for a given system or class of related systems. Most of them, however, seem to be less generally applicable than equation (3 - 9). This is probably not true, however, of a relationship proposed by Martin[23,24] which may be written in the form

$$\log_{10}(\eta_{sp}/c) = \log_{10}[\eta] + \frac{k'[\eta]c}{2.303} \cdots\cdots (3-10)$$

For solid uncharged spheres, k' should be a constant

approximately equal to 2.0. This has been found to be true both in theory[25] and in practice[26]. For flexible polymer molecules, in a good solvent, k' is always about 0.35 and in a poor solvent k' is always higher[19]. Weisberg et al[27] have pointed out that molecular particles may form short-lived doublets, with an assymmetry smaller or larger than the isolated solute molecules and since the concentration of such doublets in dilute systems would be proportional to the square of the concentration, the hydrohynamic consequences of such association may lead to an increase or reduction in k'. It has also been shown in a number of cases[28,29] that the constant k' in Huggins equation $\eta_{sp}/c = [\eta] + k'[\eta]^2 c$ is independent of molecular weight for linear polymers. It has however been found recently that polystyrene solutions may show an increase in k' with increase in molecular weight when the latter becomes very high[30,31]. The reverse behaviour i.e. decrease in k' with increasing in molecular weight has been reported by Leach[31].

Usually, all viscosity results involving polyelectrolytes are extrapolated to zero solute concentration in order to apply the theoretical equations. In salt solutions, polyelectrolytes behave more like Newtonian

liquids since the molecules are more symmetric. For highly charged polyions at low salt concentrations, the macromolecular coil is much more assymmetric than the coil formed by an uncharged chain, moreover it can no longer be considered to be hydrodynamically impermeable. Under such conditions the application of the Flory-Fox theory to the interpretation of limiting viscosity numbers in terms of chain expansion (see equation (6 - 8) is no longer justified.

In the present study, the author has carried out all viscosity measurements in a 0.02M KNO_3 and at this salt concentration all the theoretical equations stated above can adequately describe the configuration, interaction and expansion of the molecule.

3.3. Methods of Measuring Viscosity:

Among the many methods of measuring viscosity, the three that have most commonly been used, owing to the combination of a sound theoretical basis and reasonable ease of measurement, are known as the falling sphere, concentric cylinder and capillary methods. Falling spheres viscometers are used only for very viscous liquids. Falling spheres viscometers are not required for work on dilute polyelectrolyte solutions

and are not described further here.

In the concentric cylinder method, a solution is placed in the space between two concetric cylinders and one of them is rotated at a constant speed while the other is held by a torsion wire, the viscous drag will exert a turning moment on the suspended cylinder which will be balanced by the torque in the wire. By measuring the torque with the aid of a mirror and scale, the viscosity of the liquid can be obtained from a calibration of the torsion wire. The main advantage of this method is that the whole liquid is sheared at a nearby uniform rate and the rate of shear, which can be varied over a wide range, can be determined accurately. The method is, however, limited in its uses since the construction and operation of concentric cylinder or Coutte viscometers capable of giving accurate results for the difference between solution and solvent viscosities for dilute solutions, are too complex for normal use. The accuracy is in any case considerably less than obtainable with a capillary viscometer. The difficulties are due to the fact that with liquids of low viscosity it is necessary to measure very small tosional effects or to use a very narrow gap between the cylinders. The width of the latter is

limited by the practical difficulties of maintaining a narrow uniform separation between cylinders when one of them is turning. The use of concentric cylinder viscometers is not considered further here.

3.3.1. Capillary Flow Method:

In the capillary flow method, the flow of a solution through a suitable tube is timed. If the total volume of liquid passing through two fixed marks on a tube of radius a and lenth l (where $l >> a$) is V and the flow times for solution of viscosity η_1 and solvent of viscosity η_2 are t_1 and t_2 respectively, then

$$\frac{V_1}{t_1} = \frac{\pi P_1 a^4}{8\eta_1 \lambda} \quad \ldots\ldots\ldots\ldots\ldots\ldots(3\text{-}9)$$

$$\frac{V}{t_2} = \frac{\pi P_2 a^4}{8\eta_2 \lambda} \quad \ldots\ldots\ldots\ldots\ldots\ldots(3\text{-}10)$$

where P_1 and P_2 are the respective pressure heads for the solution and solvent.

Hence $$\frac{\eta_1}{\eta_2} = \frac{t_1 P_1}{t_2 P_1} \quad \ldots\ldots\ldots\ldots\ldots\ldots(3\text{-}11)$$

If the same average height h is present in each case, so that the two pressures are in the ratio of the densities of solution and solvent P_1 and P_2 then

$$\frac{\eta_1}{\eta_2} = \frac{t_1 \; h \; P_1 g}{t_2 \; h \; P_2 g} = \frac{t_1 P_1}{t_2 P_2} \quad \ldots\ldots\ldots\ldots\ldots\ldots(3\text{-}12)$$

But for dilute solutions, P_1 and P_2 are practically identical and hence without commiting very serious errors

$$\frac{\eta_1}{\eta_2} = \frac{t_1}{t_2} \qquad \text{.....(3-13)}$$

where $\frac{\eta_1}{\eta_2} = \eta_{rel}$ (relative viscosity)

Hence $\eta_{rel} = \frac{t_1}{t_2}$

3.4. Viscometric Titrations:

The Viscometric titrations were carried out by measuring the solution viscosity as a function of degree of neutralization both in the presence and absence of divalent cations notably zinc and copper. The viscometer used was the Ubbelohde 'suspendend type' dilution viscometer. This means that the head of liquid when the flow time was being measured was independent of the amount of solution in the viscometer. These viscometers also have incoporated in them sintered funnels.

3.4.1. Procedure:

3.4.1.1. Preparation of solution:

A stock solution of 0.05 base molar PMA was prepared. Enough of the stock solution was pipetted

into each of the eleven 10 ml Volumetric flasks to give the required concentration of PMA. (Concentrations ranging from 0.005 - 0.01M were used). Enough KNO_3 was added to give the required concentration of 0.02M. Varying quantities of 25.0×10^{-3}M KOH were added to each of the flasks in turn to give a degree of neutralization ranging from α=0 to α=1.0. The flasks were made up to the mark with distilled water.

In the case of the experiments involving the metal ions, the solutions were prepared as above except that zinc nitrate solutions were added to the preionized polymer in KNO_3 before making up to the mark. Similarly, in the case of copper, copper nitrate solutions were added to the preionized polymer solution. In all cases, five metal ion concentrations were used (0.00M, 0.0005, 0.001, 0.0015, and 0.002M).

3.4.1.2. Cleaning of Viscometer:

The viscometer was filled with chromic acid and allowed to stand for 24 hours after when it was emptied. The viscometer was then washed with distilled water several times. Finally, the viscometer was flushed with acetone and then sucked dry. This procedure gave a clean dry viscometer.

3.4.13.Viscosity Measurement:

The viscometer was placed suitably in the thermostat kept at 25±0.1°C. All solutions used were filtered through the incorporated sintered filter, since dust can cause serious errors in the very fine capillaries. The flow times were measured on a stop watch reading to 0.010 sec. The flow time for the pure solvent was also measured.

3.5. RESULTS AND DISCUSSION

The viscometric behaviour of polymethacrylic acid solution has been investigated in several laboratories over the past several years[32-36]. These authors have vested their interests on the effect of ionization on the structure of the polymer chain. All the previous results have pointed to the fact that the polymethacrylic acid molecule tends to be a coiled-coil in the unneutralized state and also at low degrees of neutralization ($\alpha < 10\%$). Interpretations of the derived data with respect to the mechanism of uncoiling have been rather ambigous. There have been very little said about the influence of heavy metal ions on the ionized polymer particularly their stoichiometries and effects on chain conformation.

In the present study, the author has focused attention on the extension of the molecule brought about by the ionization of the carboxyl groups along the polymer chain, and the interaction and influence of Cu(II) and Zn(II) ions on the preionized chain.

Figure 34 shows the viscometric titrations of PMA carried out by measuring the solution viscosity as a function of the degree of ionization at two polymer concentrations and in 0.02M KNO_3. One notable feature of this graph is the increased reduced viscosity above that of the solvent (reduced viscosity has been obtained from relative viscosity). This figure shows in each of the polymer concentrations, a rise in the measured viscosity up to a maximum and then a levelling off. On analysis of the curves, three distinct regions can be observed; a first region where the reduced viscosity increases very slowly i.e. at $0 < \alpha < 0.1$; a second region of large viscosity increase $0.1 < \alpha < 0.4$ and a third region of moderate viscosity increase which finally levels off at $\alpha = 0.70$.

There is a wealth of data which shows very convincingly that the PMA molecule is a tight coil when unneutralized. Liquori and his collaborators[36] have said that the compact structure of PMA is due to hydrophobic bonding of the methyl groups. This view is also held by the Russian workers[37]. Mandel and Leyte[38] have attributed the compact structure to the Vander Waal's forces. Kern and Anderson[32] attributed

such a compact structure to hydrogen bonding. The foregoing conclusions can be used as a basis for an explanation of the observed viscosity changes while strongly believing that extension of the chain is brought about by ionization of the molecule.

In the region of slow viscosity increase, the OH^- groups from alkali solution added to ionize the -COOH groups on the molecule, find it very difficult to penetrate the coiled - coil and ionize the buried -COOH. Only ionization of the few -COOH groups scattered outside the coil can take place, hence the small viscosity obtained. As the titration proceeds, the hitherto compact structure co-operatively opens up in favour of an extended structure because the existing coiled - soil below 10% dissociation can no longer withstand the great accumulation of electrostatic energy. In this region the chain is stretching out to a rod-like form. The expansion of the molecular chain occurs because of the strong repulsive forces among the negative charges along the chain. At higher degrees of ionization ($\alpha > 0.70$) the reduced viscosity appears to be independent of α. This seemingly suggests that at such high degrees of ionization there

is a structural limitation to the molecular extension.

Another striking feature in Fig. 3-1 is the proportionality between the reduced viscosity and the concentration of the polymer in solution. This probably suggests strong interactions in solution when $C > 0$. Butler et al[39], have proposed two possible theories.

The first is refered to as "attraction theory" and briefly is as follows. The interactions between charged polymer particles and their counterions can arise from the interionic forces of the type taken account of in the Debye-Huckel theory of simple dispersed electrolytes. In such case, the counterions will endeavour to complete their ionic atmospheres and in the absence of other salts, can only do so by interacting with parts of two or more polymer chains. Owing to steric factors, this will be possible only to a limited extent, but it may be sufficient to give rise to a considerable molecular interactions in polyelectrolyte solutions. However, as soon as an added simple electrlyte containing both charges is present, it will be possible for the counterions to complete their ionic atmosphere and this will greatly

diminish the tendency to attract the polyelectrolyte molecules. This attractive force between elements of two chains is a function of the distance between them and the position of the counterions.

The second theory is known as the "Repulsion Theory".

Consider a system of polyelectrolyte particles repelling each other; in such a system, the particles will take up positions as far as possible from one another. When each particle is surrounded by a diffuse double layer its hydrodynamic cross-section will be much greater than its actual cross section. If the double layers repel each other there will be in fact a restriction on the relative motions of the particles, which will increase with their concentration. Since increase of added counterion diminishes the thickness of the double layer and may also affect the size of the particle, it will decrease their range of interactions.

Now considering the above theories from point of view of experimental results then one of them can be used to explain the derived data. Butler[41] has successfully used the attraction theory to formulate

an equation which accounts for most of the observed facts in Fig.3.1. According to the equation, the increase of the reduced viscosity η_{sp}/c is proportional to the solute concentration. Measurement with partly ionized PMA shown in Figure 3.1 shows an increase in reduced viscosity with increasing concentration, in fact the reduced viscosity is doubled when the concentration is doubled. It is difficult to explain these facts on any other grounds than interaction and the theories mentioned above are quite applicable.

Figure 3.2 is obtained from a plot of change in reduced viscosity with the corresponding change in α against α, i.e. $d(\eta_{sp}/c)/d_\alpha$ against α. The purpose of such a plot is to determine the degree of ionization over which configurational transition takes place and also the number of steps through which the polymer uncoils. From the figure it can be seen that, for both figures $d(\eta_{sp}/c)/d_\alpha$ increases gradually between $0 < \alpha < 0.1$ then increases smoothly and rapidly between $0.1 < \alpha < 0.27$. Maximum value is obtained at $\alpha = 0.27$ and beyond this crictical value the direction of the curves change decreasing smoothly down to $\alpha = 0.70$.

After $\alpha = 0.70$, the curves level off. Mandel and Leyte[38] have suggested that configurational transition takes place between $\alpha = 0.10$ and $\alpha = 0.30$ and that in this region two states of PMA exist. In the present study the point of maximum change in $d(\eta_{sp}/c)/d_{\alpha}$ is associated with the point where configurational transition is completed. Below $\alpha = 0.1$ the molecules exist predominantly as coiled - coils, while, at $\alpha < 0.27$ they exist as random coils stretching out to a rod-like chain and reaching maximum extension at about $\alpha = 0.70$. Between $\alpha = 0.1$ and $\alpha = 0.27$, the two forms of PMA mentioned above exist in comparable concentrations. The magnitudes of the slopes of the curves at any point depend on the final viscosity and this may reflect the rate of accumulation of electrostatic energy by the polyion as dissociation proceeds i.e. the rate at which structures are built up in solution.

Recently Kern and Anderson[32] showed from their anisotropic electrical conductivity data that at low concentrations (e.g. 0.0058 moles per litre) the opening of the PMA molecules is a two-step process while at high concentration (such as 0.0291 moles per litre) the mechanism is a single step process.

According to the figure presented in this thesis, the author has found from viscosity measurements that transition from one state to another is a single-step process occuring between 10 - 27% dissociation. The figure also shows that the region in which the transition takes place is independent of polymer concentration in the same ionic strength.

The interaction of PMA with divalent cations notably Cu(II) and Zn(II) has also been investigated. Figures 3.(3-6) show various plots obtained from viscometric titrations of PMA solution in the absence and presence of Cu(II) and Zn(II) ions. It is easily seen from figures 3.3 and 3.4 that the reduced viscosity first decreases to a minimum at about 10% neutralization when the metal ion present is 5.0×10^{-4} M and to a minimum at about 20% neutralization when the solution contained 10.0×10^{-4} M metal ion concentration. Beyond the minimum, the viscosity increases. At the minimum viscosity, a balance exists between the charged carboxylate groups and the bound metal ions and the molecule is fully contracted just in the same way a polyampholyte at the isoionic point exhibits minimum viscosity. The minimum viscosity is associated with

the point of equivalence of metal and base i.e. the minimum point on the curve represents a point where an amount of COO^- groups equal to the cation present is bound to the divalent metal ions. At this point the net charge on the molecule is zero. The divalent metal ions present in the solution of partially ionized PAA causes electrostatic screening of the COO^- groups by interacting with them and this in turn causes a large reduction in the electrostatic repulsion between the charged groups resulting in the contraction of this molecule and this is made manifest in the observed decrease in reduced viscosity. It is found that from fig. 3-3 the ratio of $\left[COO^-\right]/\left[Cu^{2+}\right]_{total}$ is 2:1 and also from fig. 3-4 the ratio of $\left[COO^-\right]/\left[Zn^{2+}\right]_{total}$ at the minimum viscosity is 2:1. This could mean that both copper and zinc form chelate complexes involving two carboxylates groups to one metal ion provided the binding constant is high enough. These findings are in agreement with those of Mandel and Leyte[40] but are in contradiction with those of Kotliar and Morawetz[41] and Morawetz[42] who, using the technique of spectrophotometry and equilibrium dialysis, found that each copper ion binds four carboxylate groups. It has been

stated earlier that the solution viscosity of a partially ionized weak polymeric acid increases as the ionization increases because of the strong forces of repulsion between the negative charges on the chain. The increase in reduced viscosity after the minimum means expansion of the PMA molecule due to electrostatic repulsion aforementioned.

Figs. 3.5 and 3.6 show a plot of $d(\eta_{sp}/c)/d_\alpha$ against α. Certain interesting features of these graphs deserve comment.

(i) For solutions containing no metal ions, minimum viscosity is obtained at zero degree of ionization and this probably means the molecule is most compact in a state of very low ionization.

(ii) For solutions containing 5.0×10^{-4}M and 10.0×10^{-4}M metal ion concentration, the value of $d(\eta_{sp}/c)/d_\alpha$ is zero at $\alpha = 0.1$ and $\alpha = 0.2$ respectively. This again confirms that the most compact structure of the molecule is achieved at these respective degrees of neutralization. Below these α values, $d(\eta_{sp}/c)/d_\alpha$ is negative and above these α values $d(\eta_{sp}/c)/d_\alpha$ is positive. This implies that in the former case, contraction of the molecule takes place, while in the

latter case expansion of the molecule takes place.

(iii) A maximum value of $d(\eta_{sp}/c)/d_\alpha$ is obtained in each case and this signifies completion of configurational transition.

(iv) The region of transition shifts to higher α values as the concentration of the metal ion increases, the shift being proportional to the amount of metal ion present.

(v) η_{sp} for zinc tends to the same value at high α, but not so in the case of copper.

Figs. 3.7 and 3.8 are further plots to monitor configuration transition. These are plots of end-to-end dimension (obtained by extrapolating concentration to zero) against α for four different metal ion concentrations. Here also minima are obtained for each metal ion and as in previous figs. 3.3 and 3.4 these are obtained when the reduction in the electrostatic potential caused by binding with metal ion is enough to balance the potential by the charged groups. This again is another evidence that the most compact structure is achieved when the net charge on the molecule is zero.

Electrostatic consideration requires a decrease in the reduced viscosity and consequently in the en-to-end

distance as the concentration of the added divalent cation increases and if the structure of PMA - Cu(II) complex is to be more compact than that of the PMA - Zn(II) complex, then the reduction in the reduced viscosity for corresponding concentrations should be greater for copper. Fig. 3-9 which compares the plot for copper and zinc bears this out convincingly. The shape of each curve remains essentially the same, the shift to lower viscosity being proportional to the amount of cation added.

Marked differences exist between the shapes of the curves for solutions containing Cu(II) ions and those of solutions containing Zn(II) ions. In figs. 3-3 and 3-8 the highest reduced viscosity reached and the maximum end-to-end distances respectively depend on the degree of neutralization and independent of the amount of cation present. These figures predict that complex formation does not impose structural restrictions on the expansion of the molecule i.e. the extension of the molecule is in no way hindered by the configuration of the complex. In figs. 3-4 and 3-7 the highest viscosity reached depends largely on the concentration of Cu(II) ions present. After maximum extension at $\alpha = 0.70$, the shape is independent of α. In this case,

the structure of the complex formed hinders further expansion of the molecule.

The difference in the shapes of the curves for copper nitrate titrations and zinc nitrate titrations call for an explanation. The fact that the specific viscosity in the presence of Cu^{2+} reaches a constant value at $\alpha = 0.7$ and that the curves for Zn(II) continue to rise even above $\alpha = 0.7$ to attain the same value for a metal free PMA solution implies Cu PMA complex may be more stable than Zn - PMA complex or it may be that the observed differences in the shapes of the curves may just be due to structural configuration. The binding of Cu(II) to PMA restricts further expansion of the polymer beyond that obtainable in salt solution where as the binding of Zn(II) seems to have no effect on the expansion of the chain. It has been shown that the binding strength of Cu(II) Zn(II)[42-46]. The binding strengths for copper and the binding strengths for zinc are proportional to their various effective free energy changes. Two types of free energy changes are encountered in this respect:

(a) ΔG_{Chem} = ΔG for M^{2+} + COO^- i.e.
(i) the free energy change due to the binding of metal ion to the monomer or (ii) ΔG for M^{2+} + $\begin{bmatrix} COO^- \\ COO^- \end{bmatrix}$ i.e. free energy change due to chelation.

(b) $\Delta G_{elec.}$ this is the electrostatic free energy change which could be favourable or unfavourable as far as metal binding is concerned. ΔG_{elec} is favourable under the following condition.

When α increases, the concentration of COO^- increases and this means increased attraction of metal ions to the vicinity of the charged molecule and this will usually enhance binding. ΔG_{elec} could be unfavourable where α is sufficiently high for the molecule to extend to a configuration which may be unfavourable for either (i) chelation which will require folding i.e. the bringing together of many carboxylate groups to bind on metal ion will be difficult owing to strong electrostatic repulsion which will exist between the charged groups, or (ii) dimerization which requires alignment of two highly charged molecules - again because of high repulsive forces existing between the

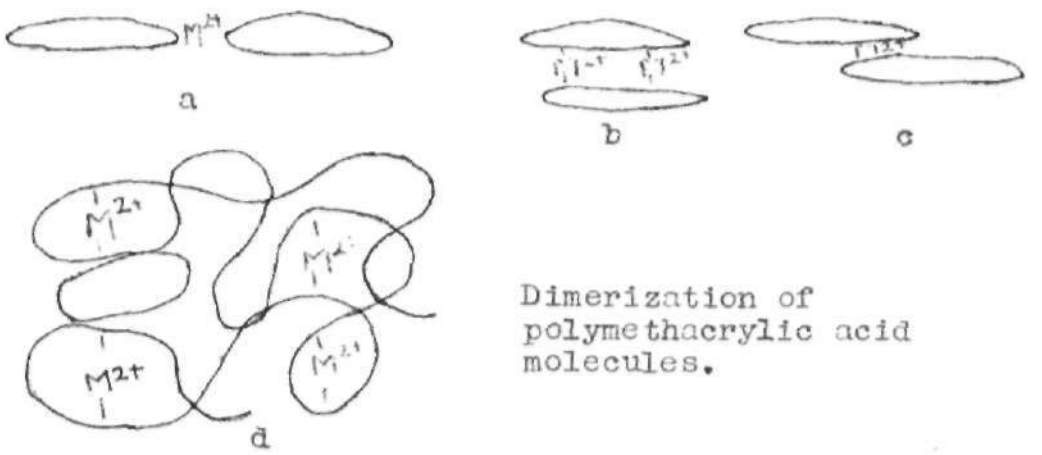
charged sites. It is seen that the two conditions under which ΔG_{elec} operate just stated above act opposite each other. It is the effective ΔG_{elec} acting in conjunction with ΔG_{Chem} which determines the free energy of complexation of the systems. The smaller this quantity the more stable the complex obtained. From figs. 3.3, 3.4 and 3.9, the viscosity reached at any corresponding α and concentration of $Cu(NO_3)_2$ and $Zn(NO_3)_2$ is always lower for the copper nitrate than for the zinc nitrate i.e. when the curves for $Cu(NO_3)_2$ and $Zn(NO_3)_2$ are compared for the same metal ion concentration the ones for copper are always displaced to lower viscosity than the ones for zinc. It is most probable that ΔG_{Chem} will play a more dominant role than the ΔG_{elec}. It is therefore concluded that the free energy change due to bringing together of COO^- groups caused by metal binding PMA appears to be less unfavourable in the case of copper than in the case of zinc.

It should be realised that such stable Cu - PMA complex is not difficult to obtain on remembering the Irving - Williams[45] series of metals:

$$Cr^{2+} < Mg^{2+} < Fe^{2+} < Co^{2+} < Ni^{2+} < Cu^{2+} > Zn^{2+}$$

which predicts the stabilities of complexes of a large number of ligands and found that the maximum value is reached in copper(II). Most of the cupric carboxylates are dimeric either in crystalline state, in solution or both[47]. Each metal ion is usually surrounded in a square-planar manner or approximately, by four atoms of oxygen binding the acetate groups. If it is assumed that metal - PMA complex is four co-ordinated (as explained later) such a four co-ordinated configuration will be square planar while in Zn-PMA a four co-ordination configuration will probably be tetrahedral, since zinc prefers a tetrahedral co-ordination. The square-planar complexes of copper are more stable than the tetrahedrally co-ordinated complex and one may anticipate a break down of the zinc-PMA as the electrostatic energy increases. Also it is quite possible that the tetrahedrally co-ordinated complex would be sterically less possible. This assertion is surported by the shape of the curves. The two types of complexes would respond differently to increasing number of charged groups and this may lead to final different configuration of the complexes.

The four co-ordination just mentioned implies possible dimerization of the molecules. In this respect, it would be possible to consider molecular aggregation, the effect of limiting viscosity number $[\eta]$ (used to calculate end-to-end distance) on linking two polymer chains through a metal ion. $[\eta]$ is a function of the axial ratio of the hydrodynamically equivalent ellipsoid of revolution. If dimerization takes place, this may lead to an increase, or a decrease in the limiting viscosity number depending on whether the association occurs end-to-end or side-by-side, resulting in an increase or decrease in the assymmetry of the particle. The following modes of dimerization have been suggested.



Dimerization of polymethacrylic acid molecules.

(a) End-to-end association, may lead to an increase in $[\eta]$ hence $\bar{h}$.

(b) Side-by-side association leading to a reduction in $[\eta]$ and consequently $\bar{h}$.

(c) An intermediate type of association, may leave $[\eta]$ and consequently $\bar{h}$ unchanged.

(d) Intramolecular type of association and this may lead to a considerable decrease in $[\eta]$ and also in $\bar{h}$.

In the system under study, structure (a) above is eliminated on the ground that increased end-to-end dimenssions were not observed. Structure (b) seems to be a most appropriate model in the case of copper for dimerization to occur at any α value. In all cases, the value of the end-to-end dimenssion is reduced and the reduction is proportional to the amount of copper nitrate present. This model would also survive in the case of zinc at low and moderate degrees of ionization. However, at high α, the graphs indicate a possible break-down of the complex to a more energetically favoured one. The structure (c) is not quite visible on the ground that owing to strong repulsive forces between the charged groups such an alignment of the PEI

molecules will be difficult. The structure (d) represents the possible structure of complex in its most compact state and also at low degrees of ionization presumably at $\alpha < 0.1$. Here the cation forms a bridge between different segments of the coiled molecule. Finally it is quite feasible that in both cases of copper and zinc, dimerization may be impossible at high α. Because of the strong repulsive forces between the charged groups the sort of alignment shown in (b) may not be possible.

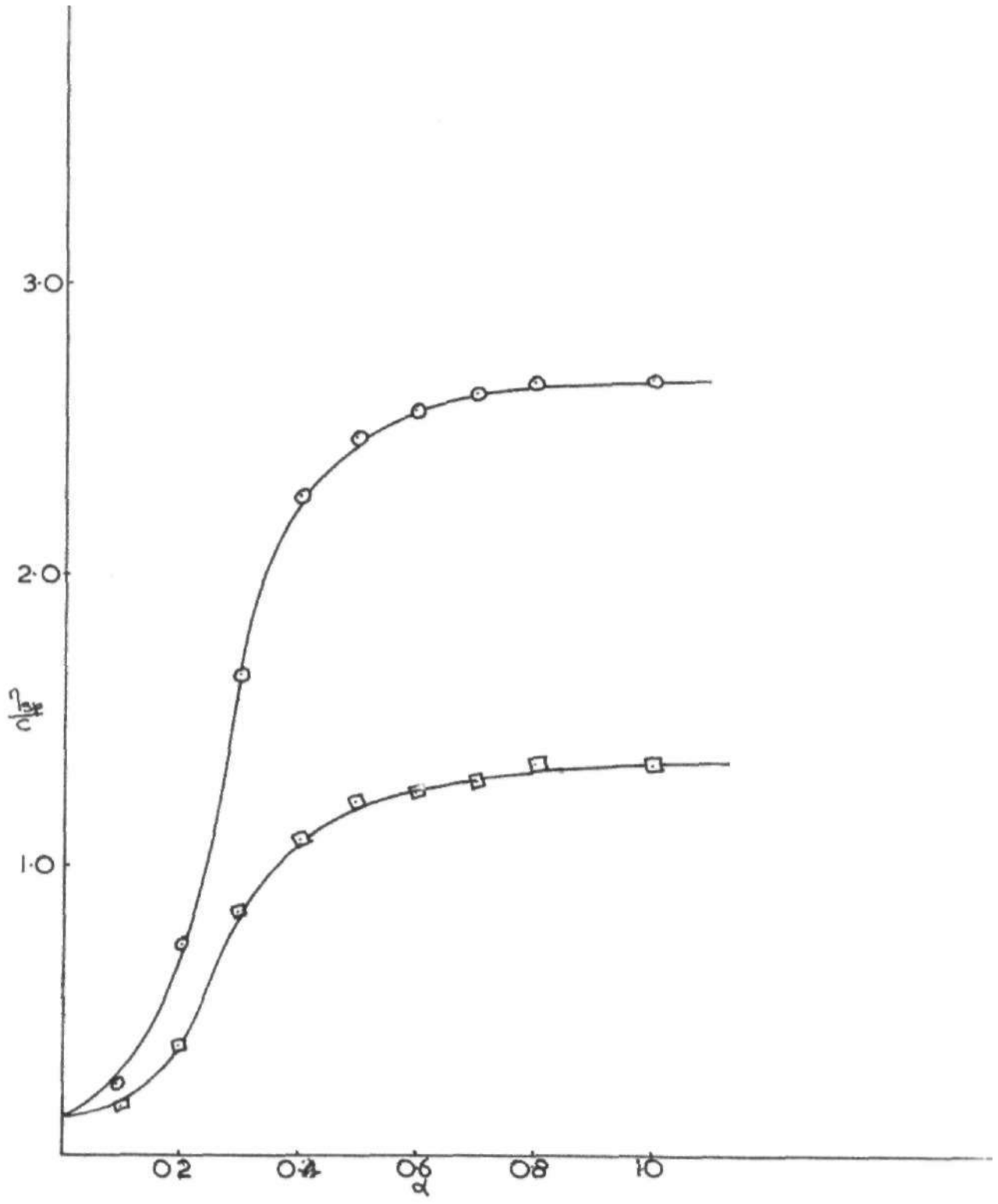


FIG: 3.1 Viscometric studies of PMA at varying concentration of PMA at 25°C
⊙-[PMA] = 0.01M ; ⊡- PMA 0.005M ; Ionic strength = 0.02

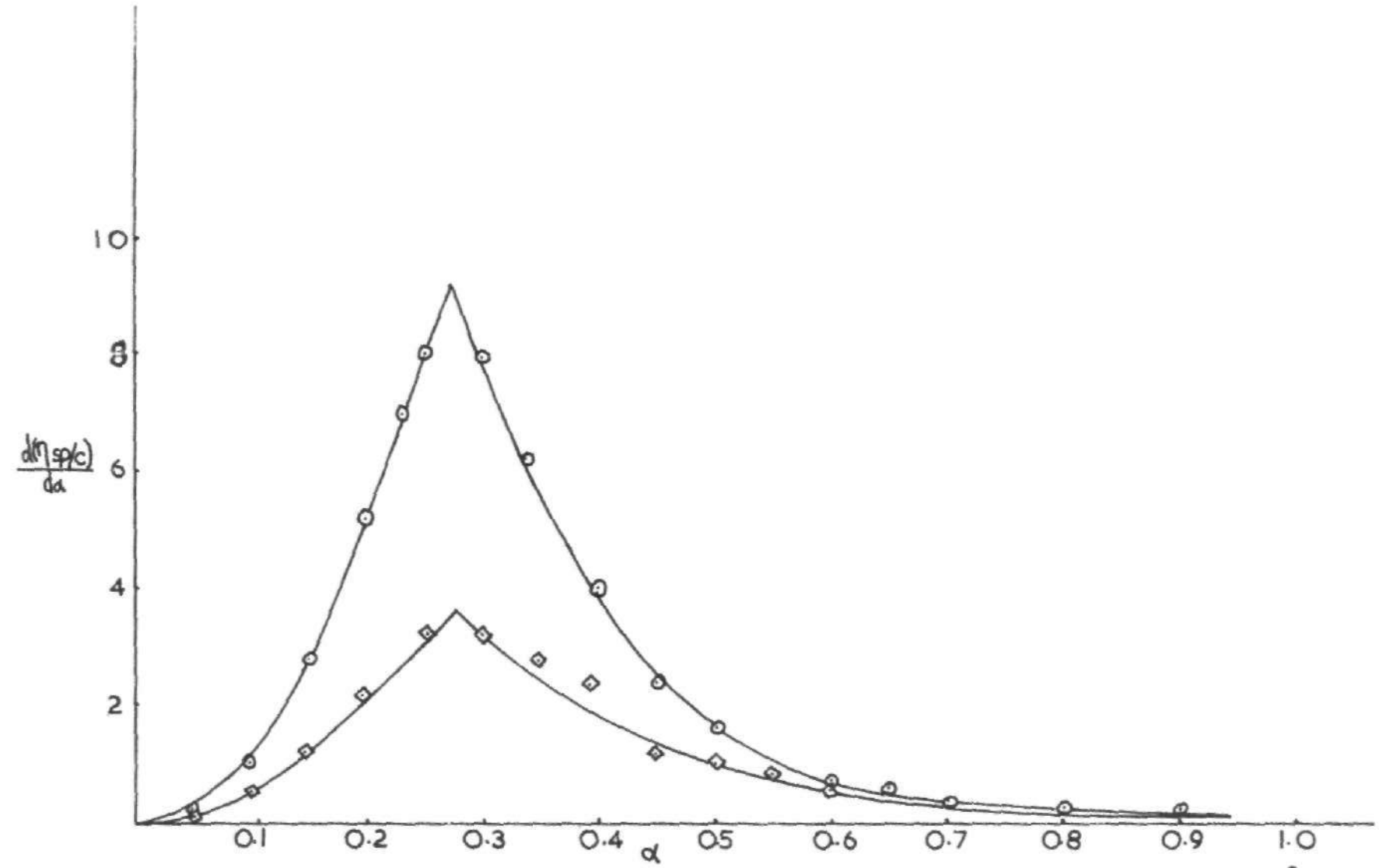


FIG 3.2 Viscometric titration of PMA at varying concentrations of PMA at 25°C

⊙— [PMA] = 0·01M ; ⊡- [PMA] = 0·005M ; I = 0·02

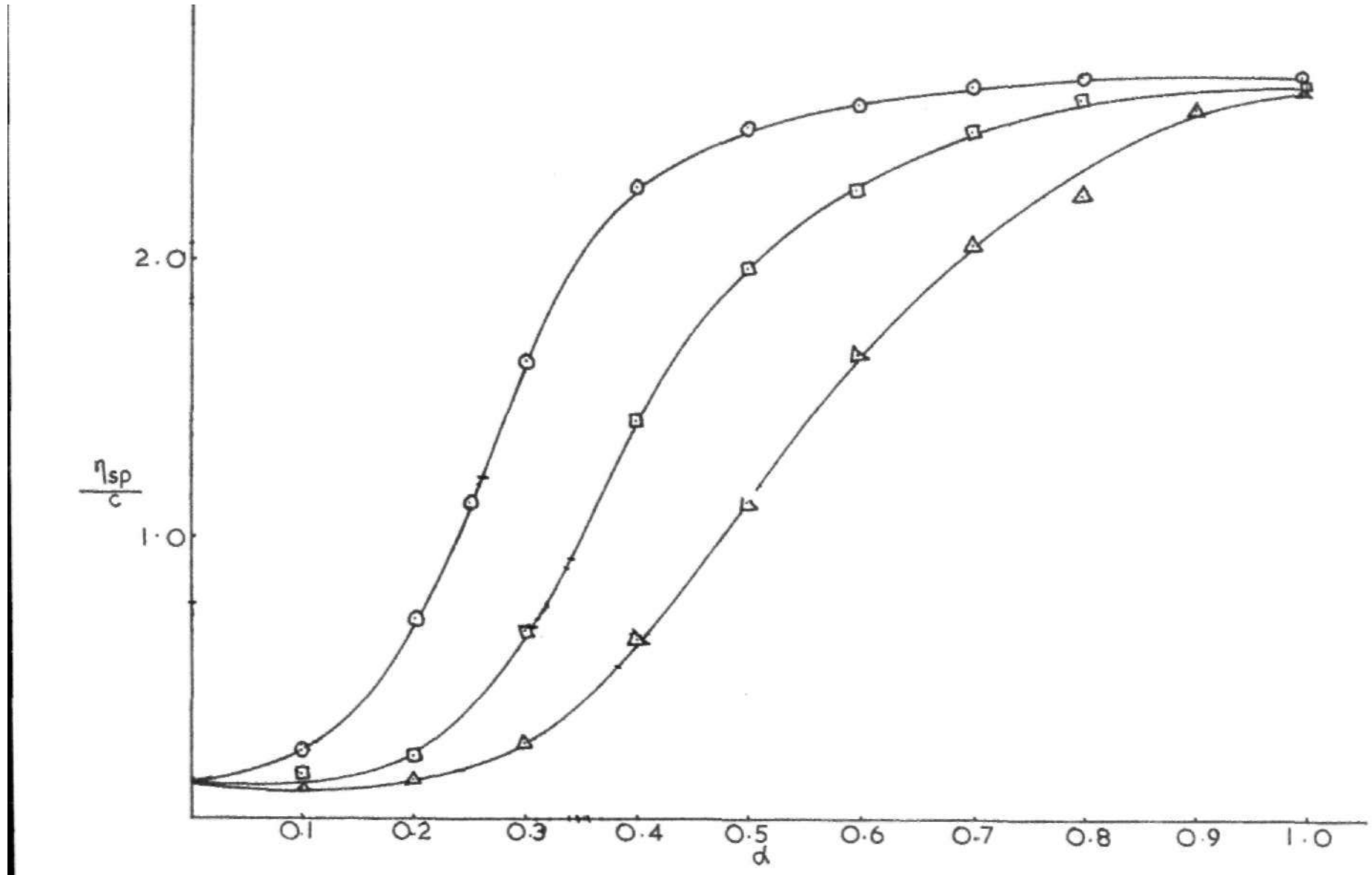


FIG 3.3 Viscometric titration of PMA at 25°C in the presence of varying concentrations of $Zn(NO_3)_2$ [PMA]=0.01M ; I = 0.02
⊙—No metal ions ; ⊡—5.0×10^{-4}M ; △—10.0×10^{-4}M ; $Zn(NO_3)_2$

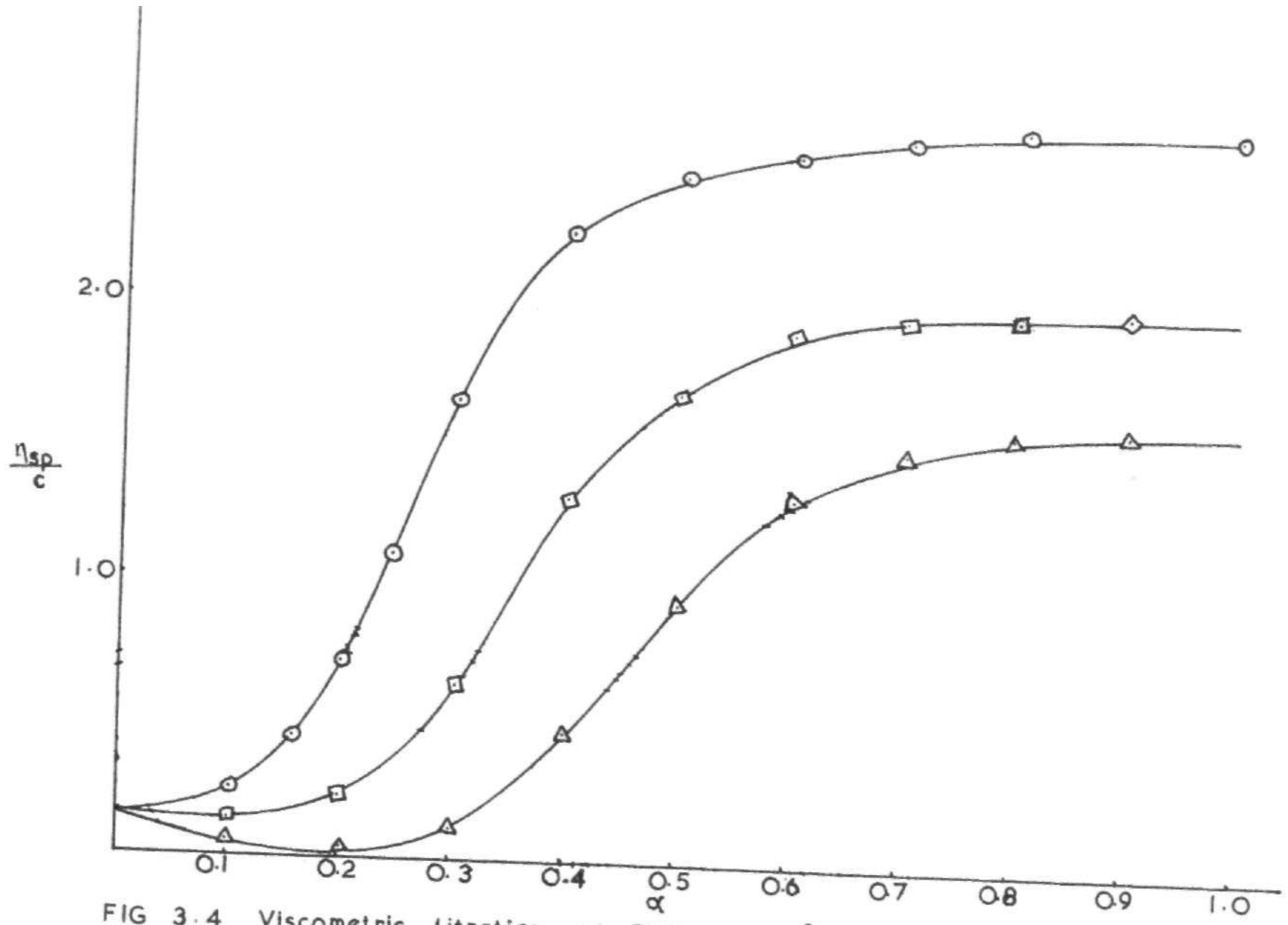


FIG 3.4 Viscometric titration of PMA at 25°C in the presence of varying concentrations of $Cu(NO_3)_2$. [PMA]=0.01M ; I=0.02
⊙—No metal ions ; ⊡—5.0×10^{-4}M ; △—10.0×10^{-4}M ; $Cu(NO_3)_2$

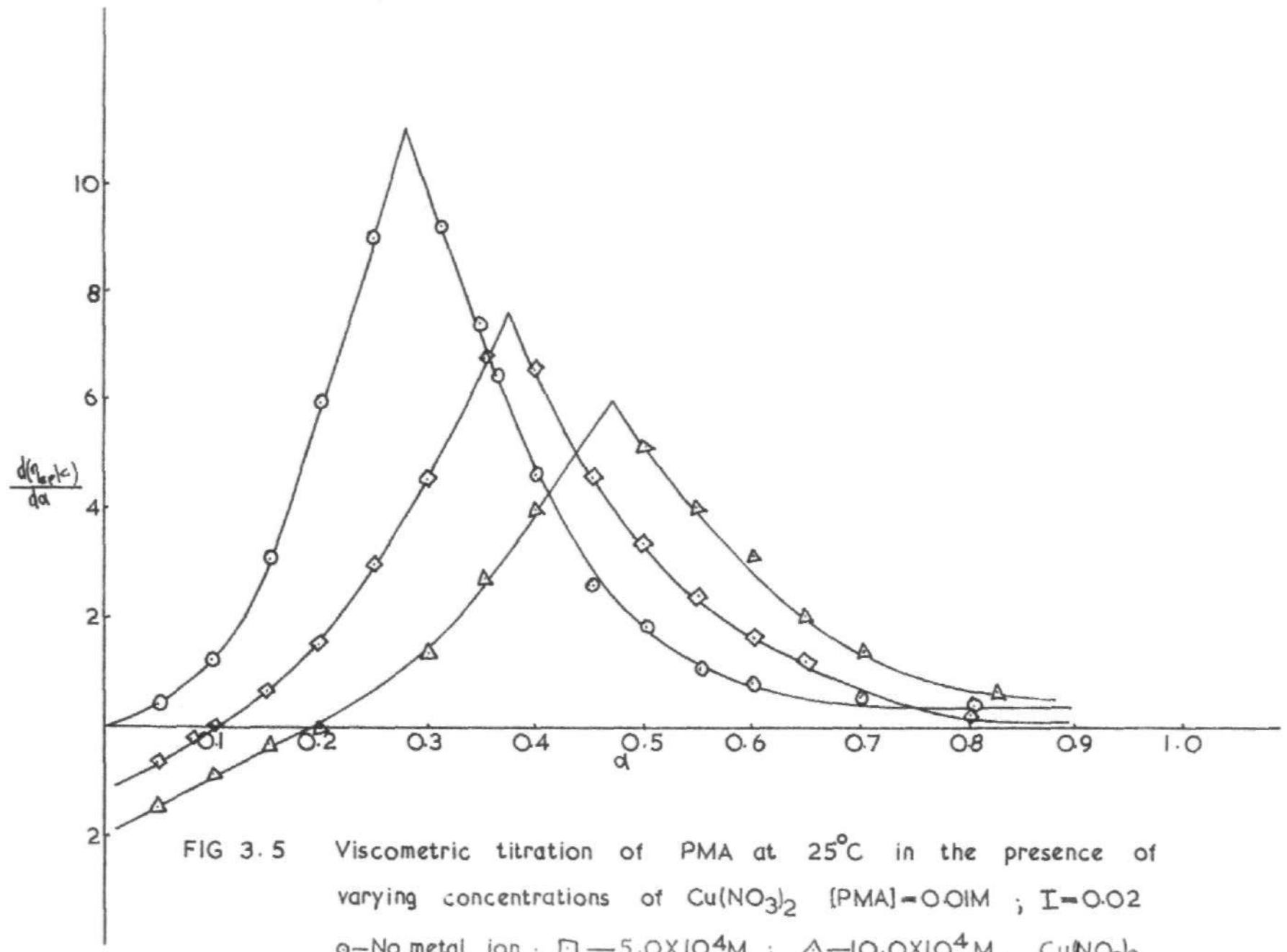


FIG 3.5 Viscometric titration of PMA at 25°C in the presence of varying concentrations of $Cu(NO_3)_2$ [PMA] = 0.01M ; I = 0.02
o—No metal ion ; □ — 5.0×10^{-4}M ; △ — 10.0×10^{-4}M , $Cu(NO_3)_2$

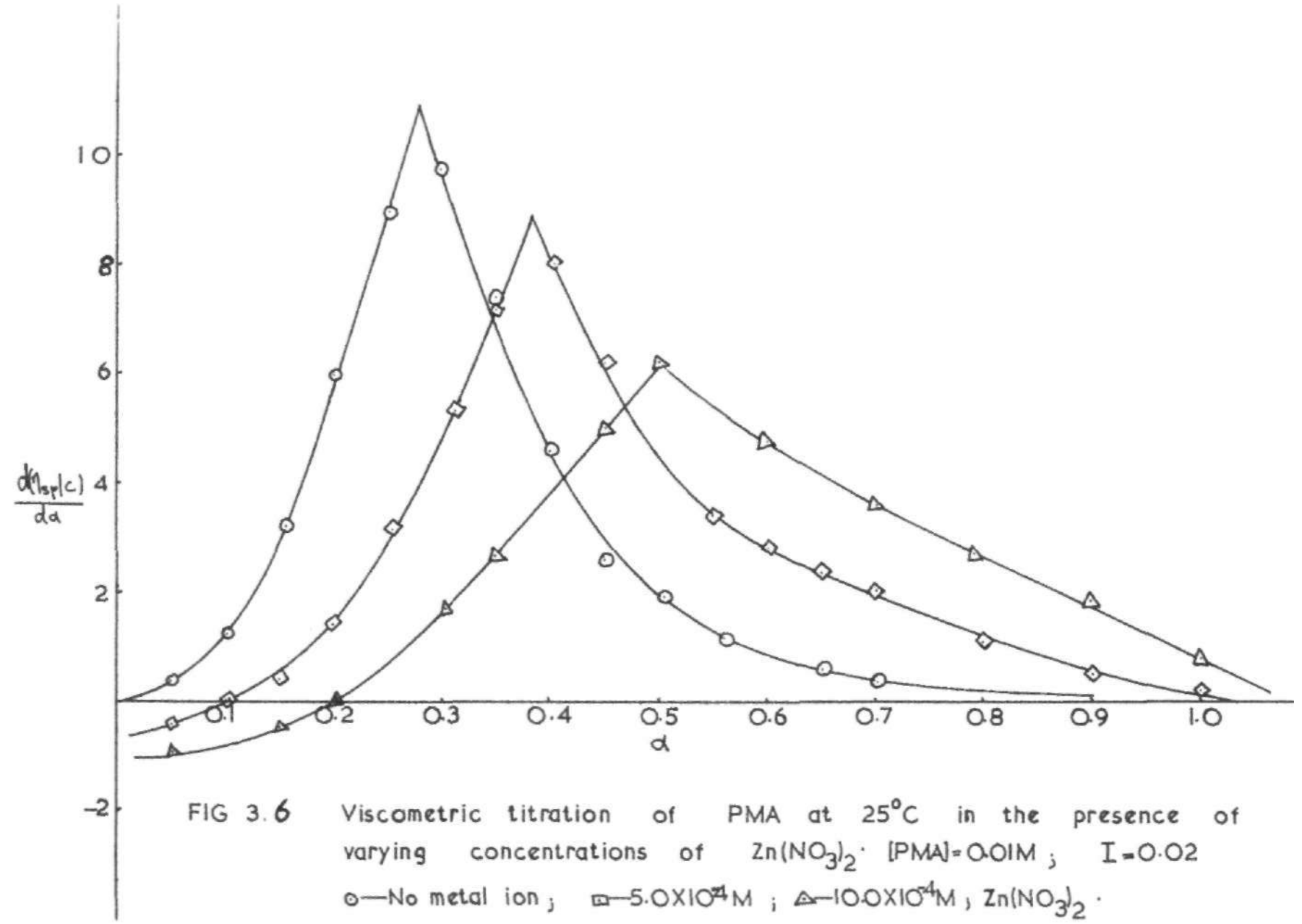


FIG 3.6 Viscometric titration of PMA at 25°C in the presence of varying concentrations of $Zn(NO_3)_2$. [PMA]=0.01M ; I=0.02
⊙—No metal ion ; □—5.0×10^{-4}M ; △—10.0×10^{-4}M , $Zn(NO_3)_2$.

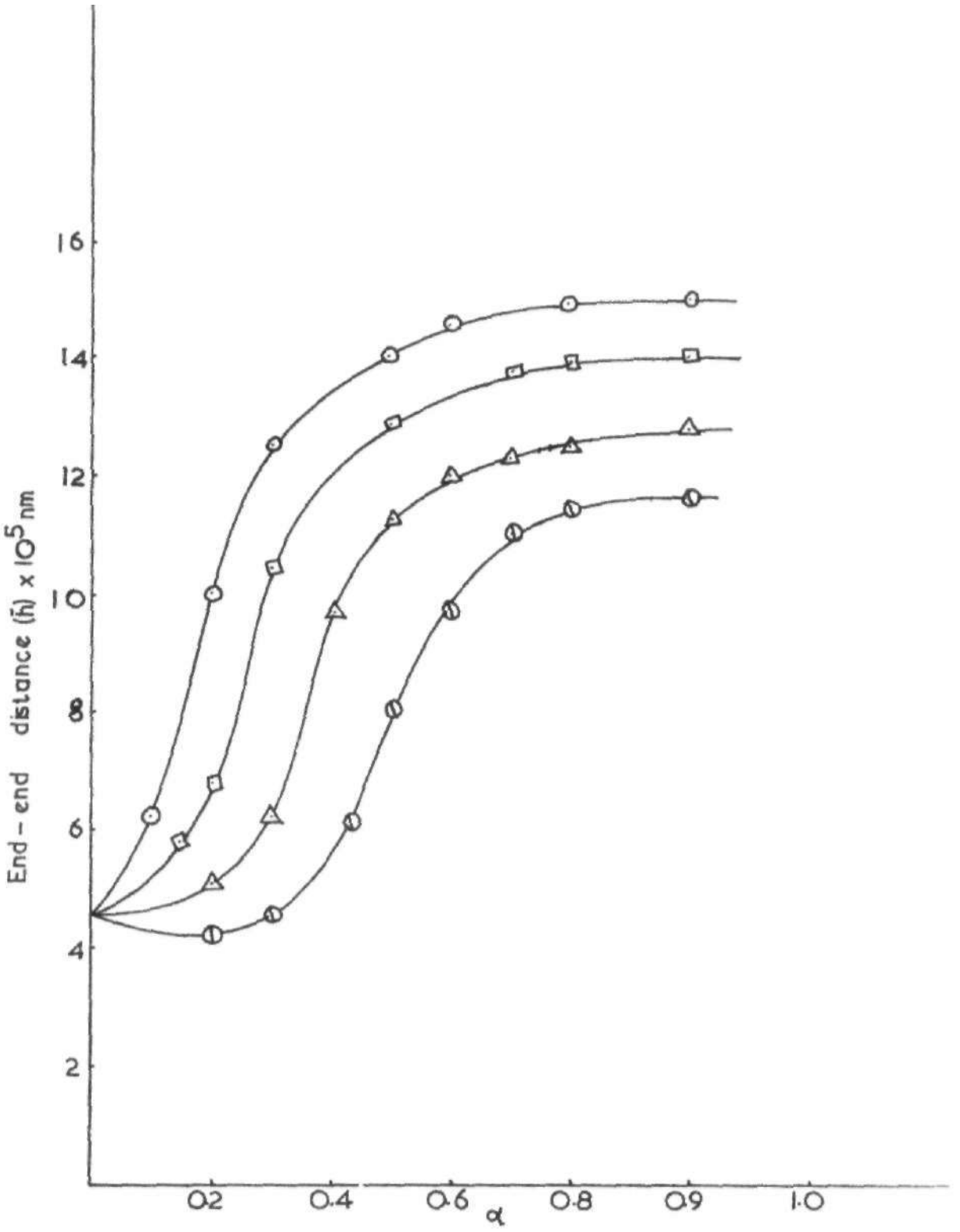


FIG. 3.7 Viscometric titrations of PMA at varying concentration of $Cu(NO_3)_2$ at 25°C
⊙-No metal ion; [PMA] = 0.01M ; $\bar{I}$ = 0.02 .
⊡-5.0X10^{-4}M; ⊿-10.0X10^{-4}M; ⊕-15.0X10^{-4}M : $Cu(NO_3)_2$

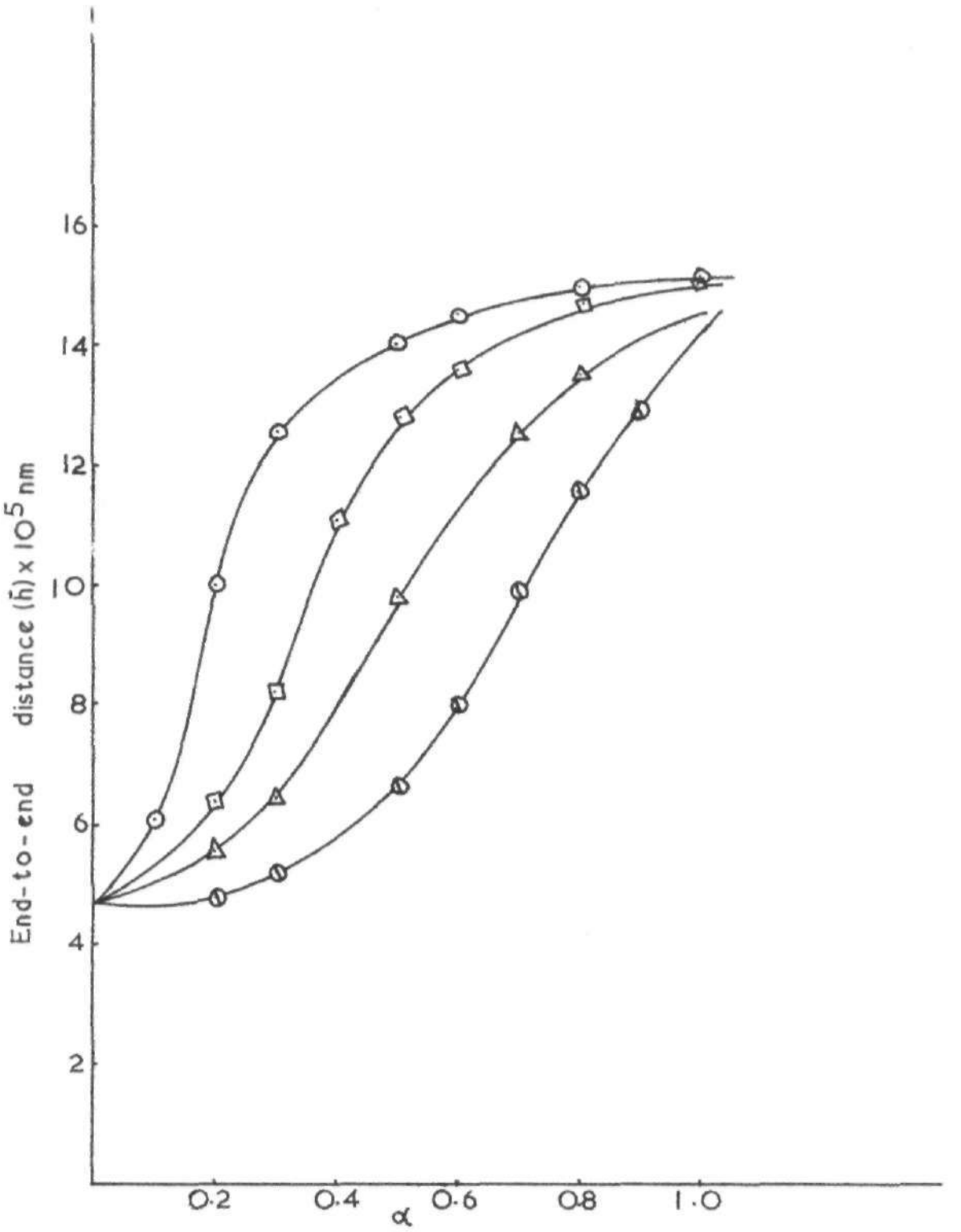


FIG 3.8 Viscometric titration of PMA at varying concentrations of $Zn(NO_3)_2$ at 25°C
[PMA]=0.01 M; I=0.02 ; ⊙ —No metal ion
□ —5.0×10^{-4}M; △ —10.0×10^{-4}M ; ◑ —15.0×10^{-4}M; $Zn(NO_3)_2$

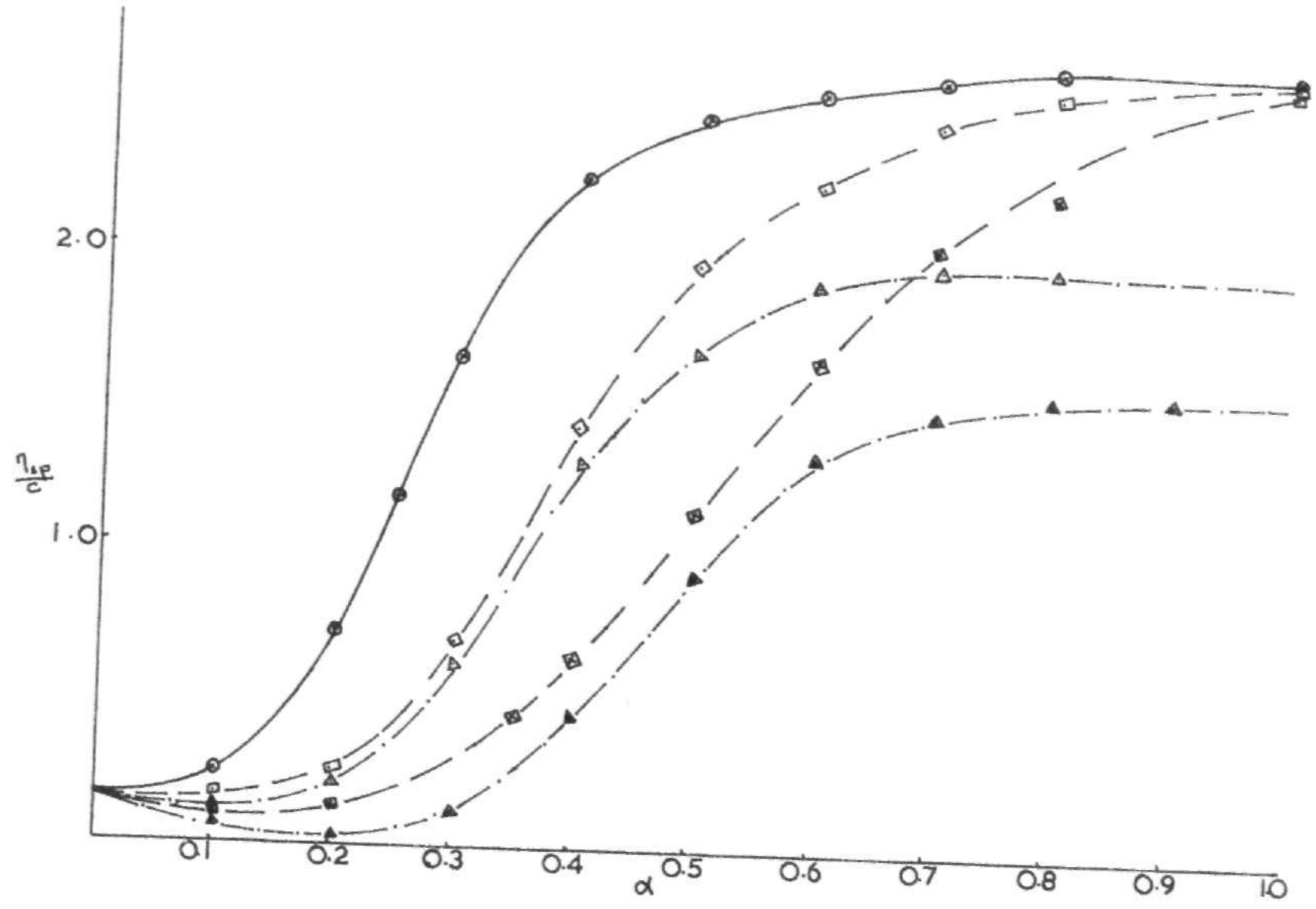


FIG 3.9 Viscometric titration of PMA at 25°C in the presence of varying concentrations of metal ios at [PMA] = 0·01M and I = 0·02
⊗—⊗, No metal ion; ⊡—⊡, $5{\cdot}0\times10^{-4}$M $Zn(NO_3)_2$; ▣ — ▣, $10{\cdot}0\times10^{-4}$M $Zn(NO_3)_2$;
△···△ $5{\cdot}0\times10^{-4}$ M $Cu(NO_3)_2$; ▲···▲ $10{\cdot}0\times10^{-4}$M $Cu(NO_3)_2$

3.6. REFERENCES

1. Eirrch, F. and Riseman, J., J. Poly. Sc. 4, 417,(1949)
2. Holl, W. H. L., Kolloid Z. 132, 35, (1953).
3. Schulz, G. V. Kolloid Z, 115, 90, (1949).
4. Staudinger, H. and Hewar, W., Ber. 63, 222, (1930).
5. Oth., A. and Doty, P., J. Phys. Chem. 56, 43, (1952)
6. Porter, M. R., Ph.D. Thesis (1956).
7. Pals, D.F.T., and Hermans, J. J., J. Poly. Sc. 3, 897, (1948)

8a. Fouss, R. M, J. Poly. Sc. 3, 603, (1948).

8. Fouss, R. M., Disc. Farad. Soc. 11, 125, (1951).
9. Alexander, P. and Hitch, S. F., Biochim Biophys. Acta. 9, 299. (1952).
10. Mark, H., J. Am. Chem. Soc. 65, 2319, (1943).
11. Houwink, R., J. Pract. Chem. 57, 15, (1940).
12. Hermans, J. J., Physica. 10, 777, (1943).
13. Kuhn, W. and Kuhn, H., Helv. Chim. Acta. 28, 1533, (1945).
14. Kirkwood, J. G., and Riseman, I.L., J. Chem. Phys. 16, 576, (1948).
15. Debye, P. and Bueche, A. M., J. Chem. Phys. 16, 576, (1948).

16. Auer, R. L. and Gardner, C. J., J. Chem. Phys. 23, 1546, (1955).

17. Zimm, H. B., J. Chem. Phys. 24, 269, (1956)

18. Flory, P. J., Principles of Polymer Chemistry, Cornel Univ. Press. Chapt. XIV Pages 610-611.

19. Huggins, M. L., J. Am. Chem. Soc. 64, 2716, (1946).

20. Heller, W., J. Colloid. Sci. 9, 574, (1954).

21. Schulz, G. V. and Blashke, F. J. Pract. Chem. 158, 130, (1941).

22. Schulz, G. V. and Sins, G., J. Prack. Chem. 161, 161, (1943).

23. Martin, A. F., Abstr. 103rd Meeting Am. Chem. Soc. Page 1, (1942).

24. Spurlin, H. M., Martin, A. F. and Tennent, H. G., J. Poly. Sc. 1, 63, (1946).

25. Simha. R., J. Applied Physics, 23, 1020, (1952).

26. Chong, P. V. and Schachman, H. K. J. Poly. Sc. 16, 19, (1955).

27. Wiesberg, S. G., Simha, R. and Rothman, S., J. Res. Natl. Bur. Std. 47, 298, (1951).

28. Brown, C. E. H., Trans. Faraday Soc. 47, 97,(1951).

29. Manson, J. A. and Cragg, L. H., Can. J. Chem. 30, 482, (1952).

30. Cragg, L. H. and Stones, R. H., J. Poly. Sc. 9, 585, (1952).

31. Leach, S. J., J. Poly. Sc. 9, 379, (1952)

32. Kern, E. E. and Anderson, D. K., J. Poly. Sc. A1, 2765, (1968).

33. Katchalsky, A. and Eisenberg, H. J. Poly. Sc. 6, 145, (1951)

34. Arnold, R. and Overbeek, J. Th. G. Rev. Trans. Chim. 69, 112, (1950)

35. Gregor, H. P., Luttinger, L. B. and Loebl, E. M., J. Phys. Chem. 69, 34, (1955).

36. Liquori, A. M., Barone, G., Crescenzi, V., Quadrifoglio, F. and Vitagliano, V., J. Macromol. Chem. 1, 291, (1966).

37. Erishtein, T. N., Anufrieva, E. V. Nakrasova, I.N., Ptitsyn, O. B., and Sheveleva, T. V., Visssokomolecul. Soedin, 7, 372, (1965).

38. Mandel, M. and Leyte, J. C., J. Poly. Sc. A2, 1879, (1964).

39. Butler, J.A.V., Conway, B.E. and James, D.W.F., Trans. Faraday. Soc. 50, 612, (1954).

40. Mandel, M. and Leyte, J.C., J. Poly. Sc. A3, 3771, (1964).

41. Kotliar, A. M. and Morawetz, H., J. Am. Chem. Soc. 77, 3692, (1955).

42. Morawetz, H., J. Poly. Sc. 17, 442, (1955).

43. Mandel, M. and Leyte, J.C.,J. Poly. Sc. A2, 2883, (1964).

44. Irving, H.M., Chem. Soc. Special Bull. (London) No.13, (1959).

45. Irving, H. M. and Williams, R. J. P., Nature, 162, 746, (1948)

46. Bolewski, K. and Lubina, M., Roc. Chem. Ann. Soc. Chem. 44, 647, (1970).

47. Kochi, J.K. and Subramian, R. V., Inorg. Chem. 4, 1527, (1965).

Chapter 4

SPECTROPHOTOMETRIC TITRATIONS

C O N T E N T S

		Page
4.1.	Theoretical	110
4.1.1.	Spectra of Transition Metal Complexes	115
4.1.1.1.	Ligand Spectra	116
4.1.1.2.	Charge-Transfer Spectra	117
4.1.1.3.	d-d Spectra	119
4.2.	Experimental	121
4.3.	Results and Discussion	123
4.3.1.	Results	123
4.3.2.	Discussion	125
4.3.2.1.	Absorption in the Ultra-Violet Region	125
4.3.2.2.	Effect of Ionic Strength	135
4.3.2.3.	Absorption in the Visible Region ..	137
4.4.	R e f e r e n c e s	140

Chapter 4

S P E C T R O P H O T O M E T R Y

4.1 Theoretical:

There are two classes of spectra, namely emission and absorption spectra. An emission spectrum is obtained by analysing the light emitted by a luminous source. An absorption spectrum is obtained by the spectroscopic analysis of the light transmitted by an absorbing medium which is placed between the light source and the spectroscope.

There are two basic laws which govern absorption intensity. These laws are well-known in their combined form as the Beer-Lambert Law of light absorption which states that the fraction of the incident light absorbed is proportional to the number of molecules in the path length. That is, if a substance is dissolved in a solvent, the absorption by the solution will be proportional to its molecular concentration, provided the solvent itself does not have any absorption in that region. This law is expressed as

$$\log_{10}\frac{I_o}{I} = \epsilon l c \quad \ldots\ldots\ldots (4\text{-}1)$$

where $\log_{10} \frac{I_o}{I}$ = optical density (O.D.) or Absorbance (A) or Extinction (E), ϵ is the absorption coefficient, c is the concentration and l is the path length. If c is measured in gram moles per litre and l in cm, then the absorption coefficient becomes molar extinction coefficient. The absorption intensity is usually expressed in terms of ϵ and the majority of the applications in spectrophotometry are based on the above mentioned equation. If the molecular weight of the substance is not known, the expression $E_{1\%}^{1cm}$ is often used. This is related to ϵ by the equation

$$E_{1\%}^{1cm} = \frac{\epsilon \times 10}{\text{Molecular Wt.}} \qquad \ldots\ldots\ldots(4\text{-}2)$$

According to Beer-Lambert law, the optical density of a solution should remain constant as long as the product of the concentration and the path length is constant. But this is not alwasys true. Quite often, the molar extinction coefficient varies appreciably with the concentration of the solute. These deviations may be due to one of many possible causes: molecular association of the solute at high concentration, ionization of the solute in the case of acids and bases, fluorescence of the solute and poor transmission of the solvent.

The absorption intensity of an electronic transition at any wavelength is governed by the probability of the transition and the size of the absorbing molecule. The absorption maximum of a band therefore corresponds to the most probable transition in that region of absorption. The extinction coefficient may be expressed as

$$\varepsilon = KPa \quad \text{.....(4-3)}$$

where K is a constant of the order of 10^{20}, P is the probability of a transition and a is the area of cross section of the molecule[1,2]. Assuming the probability of an electronic transition is unity, the maximum theoretical extinction coefficient for an average organic molecule ($a = 10\text{Å}^2$) may be calculated to be of the order of 10^5. In fact, the largest extinction coefficients experimentally observed are also of the order of 10^5.

It has been known for quite sometime that certain groups within a molecule give rise to absorption bands in definite regions of the spectrum more or less independent of the molecule. The groups containing electrons responsible for the absorption are called chromophores. There are also some groups which by themselves do not contain electrons which could give

to absorption but they could increase the intensity of absorption. Such groups are called auxochromes.

There are four basic classes of absorption bands.

(a) $\sigma \rightarrow \sigma^*$ (between σ orbitals)
(b) $\Pi \rightarrow \Pi^*$ (" Π bonds)

} From a bonding orbital in the ground state to an orbital of higher energy.

(c) $n \rightarrow \Pi^*$ (To Π orbitals)
$n \rightarrow \sigma^*$ (To σ orbitals)

} From a non-bonding atomic orbital to a high energy molecular orbital.

Generally, the position of maximum absorption band depends on the size of the chromophore and also on the extent of conjugation and substitution.

Substitution or structural changes in organic compounds result in changes in the wavelength and in the intensity of absorption bands. Wavelength changes to longer values are called bathochromic shifts and changes to shorter wavelengths are called hypsochromic shifts. An increase in the intensity of a band is called hyperchromic effect while a decrease is called hypochromic effect.

The structural character and psotion of absorption bands depends on the nature of the solvent. Generally,

poor solvents tend to shift the position of the bands and diminish the vibrational structure of the bands; particularly in hydroxylic solvents, the structure gets blurred. Non-polar solvents produce little change in the band compared with gas phase spectra. Solvent effects have been employed for the characterization of electronic transitions. Solvent and substituent effects were first employed by Burawoy[3,4] to characterise electronic transitions. His ideas have been revived by Kasha[5] and McConell[6] who have suggested that solvent effects may be of value in distinguishing between $\Pi \rightarrow \Pi^*$ and $n \rightarrow \Pi^*$ transitions. The wavelengths of the $n \rightarrow \Pi^*$ bands are generally found to decrease with increase in polarity of the solvent. The individual vibrational structure of the $n \rightarrow \Pi^*$ bands is completely blurred in polar solvents. Polar solvents generally shift the $\Pi \rightarrow \Pi^*$ transitions to longer wavelengths.

From the above considerations, a generalised statement can be made. The absorption bands of almost all organic molecules normally found in the near ultra-violet and visible regions arise from either $\Pi \rightarrow \Pi^*$ or $n \rightarrow \Pi^*$ transitions. Also the $\Pi \rightarrow \Pi^*$ transitions may be very intense (allowed) or weak (forbidden).

The n → Π* are generally forbidden and consequently of weak intensity.

4.1.1 Spectra of Transition Metal Complexes:

Because of the large number of known transition metal complexes, and the many factors which have to be taken into account, it is not possible to give a general description of the kind of spectrum these compounds exhibit which holds good in each case and every example. Commonly, the visible and the near infra-red region contains rather weak absorption bands for which ϵ_{max} values fall in the range $1 - 10^2$, and that toward the ultra-violet, much stronger absorption sets in, with ϵ now reaching 10^3 or 10^4.

There exist a number of different possible origins for the electronic absorption spectra of complexes involving transition metals. These are:

(a) Spectra associated principally with the ligand;

(b) Spectra involving electronic transition
between the metal and the ligands;
charge-transfer Spectra;

(c) Spectra associated principally with the metal, influenced by the presence of the ligands; d - d spectra.

Each of these will be treated briefly.

4.1.1.1 Ligand Spectra:

Organic molecules frequently occur as ligands in transition metal complexes, and, particularly if these molecules already contain Π - electron systems, they will themsleves possess charateristic absorption spectra which will usually be located in the ultra-violet region. These are usually intense bands due to $\Pi \rightarrow \Pi^*$ transition. Where the organic molecules are bonded to a metal in a complex ion, it generally seems that only small alterations occur in the ligand spectrum. Usually in the complexes, the intensity will be increased and the band is usually shifted to lower wave numbers. This is a common effect in all the ligand spectra and the magnitude of the shift often turns out to be a function of the oxidation state of the metal atom. In addition to organic molecules inorganic ions such as thiocyanate, nitrite and nitrate commonly possess very intense bands in the ultra-violet range as a result of internal transitions.

4.1.1.2 Charge-transfer Spectra:

Because of the loose environment of the metal atom and the ligands, and the bonding between them, the likelihood exists of new transitions occuring, these involving the transfer of an electron from the ligand to the metal or vice-versa. This type of transition is indeed known to occur and is called a Charge-transfer transition. The charge-transfer bands are often located in the ultra-violet but may partly intrude into the visible (hence the intense yellow colours of solutions of some ferric salts). Occasionally, discrete charge-transfer bands are located in the visible region such as those giving rise to intense colours of permanganate $[MnO_4^-]$ and chromate $[CrO_4^{2-}]$ ions. In both of these, the metal has formally a d° electronic configuration so that pure d-d transitions are not possible and colour can not arise in that way. Similarly, the intense colours of those metal complexes which are used as redox indicators in titrimetric analysis, originate through charge-transfer.

A charge-transfer transition must be viewed as a transition between two molecular orbitals, one of which has more ligand character than the metal, the other more

metal character than the ligand. Charge-transfer spectra are normally characterised by intense absorption. There are three general modes of charge-transfer which are known to occur.

(i) Those in which electrons from σ bonding orbitals are excited to empty Π^* or σ^* orbitals. Since the former are predominantly ligand orbitals and the latter mainly metal orbitals, these transitions transfer charge from ligand to metal.

(ii) Those in which electrons from filled Π orbitals localized mainly on the ligands are excited to the σ^* or Π^* orbitals of the metal. Again transfer of charge is from ligand to metal.

(iii) Those in which electrons from bonding orbitals are excited to vacant Π orbitals localized predominantly on the ligand. In these, the charge-transfer is modest and is from metal to ligand. Charge-transfer depends on the ease of reduction of M^{n+} to $M^{(n-1)+}$ for $L \rightarrow M$ transfer. The quantity of charge transfer is also dependent on polarity of the environment e.g. the intensity of charge transfer depends on the polarity of the medium in the vicinity of the charge.

4.1.1.3. d-d Spectra:

Whereas charge-transfer and pure ligand transitions are usually observed in the spectrum as rather intense absorption bands, quite the opposite is true for d-d spectra. Electronic transition between d-orbitals of the same quantum shell are strictly forbidden by Larporte rule, so that even allowing that no violation of the spin selection rule occurs, the resulting absorption bands, if observable at all, can only be expected to be very weak. These bands which occur principally in the visible region for transition metal complexes, originate from these d-d transitions. The fact that these transitions are not absolutely forbidden, but do have some intensity is of considerable interest in the present work and has greatly helped to clarify some doubts about the structure of the complex. There are usually several d-d absorption bands in the spectrum of a given complex, and their number and positions are strongly dependent on the metal and its oxidation state. The geometry of the complex will also have a marked effect on the spectrum, not only in respect of the

number and relative positions of the bands, but also their intensities, the position of the bands depends on the ligand field spliting energy, Δ and assymetry of the molecule.

4.2 E X P E R I M E N T A L

Various experiments were carried out under varying conditions of polymeric acid concentration, ionic strength, degree of ionization and copper(II) concentration. A typical run for a constant PMA concentration, constant ionic strength, constant copper(II) concentration and varying degrees of ionization is as follows:

0.04M stock solution of PMA was prepared. 0.50 ml of the stock solution was put into each of 11 graduated flasks, to give 2.0×10^{-3}M PMA solution. Enough KNO_3 solution was added to each flask to give the desired constant ionic strength. This was followed by enough of 25.0×10^{-3}M KOH to give the desired degree of ionization (α goes from $0 \rightarrow 1.0$).

Enough $Cu(NO_3)_2$ of 0.1M stock solution was added to give the desired metal ion concentration. Four metal ions concentrations were used (2.0, 4.0, 6.0 and 8.0×10^{-4}M). The flask was then made up to the mark

with distilled water. The spectrum of each solution was run on the same chart using the Sp.800 self recording spectrophotometer for measurements in the U.V. range. For measurements in the visible range the Hilger and Watts Spectrophotometer was used. The optical density at maximum absorption was recorded for each solution. A plot of optical density against the degree of ionization was constructed for each metal ion concentration.

In other experiments, the conditions were suitably modified in order to investigate the desired properties.

4.3 RESULTS AND DISCUSSION

The Spectrophotometric titration of polymethacrylic acid and polyacrylic acid has been studied by many investigators principally Mandel and Leyte[7], Kotliar and Morawetz[8], Morawetz[9] and Wall and Gill[10]. In all these investigations, results obtained have been very contradictory. The results obtained from viscometric studies in chapter 3 indicate a copper chelate complex involving two carboxylate groups. The results obtained from conductance studies presented in chapter 2 indicate a copper-PMA complex involving four, two and one carboxylate groups binding per metal ion. This chapter describes the titrations of PMA in the absence and in the presence of copper nitrate, under different conditions of polymeric acid concentration, ionic strength and copper(II) concentration. Unlike the previous investigators, an attempt has been made by the author to clarify the nature of the complex and propose a mechanism for the complex formation.

4.3.1. Results:

In Fig. 4-1, the Ultra-violet absorption spectra for PMA in the absence and in the presence of copper

nitrate are compared. It is seen that a new absorption peak appears in the presence of copper nitrate. The copper ions form a complex as borne out by the shift in λ_{max} (where λ_{max} is the wavelength of maximum absorption) from 213mμ for unneutralized polymer to 264 for the complex. The formation of a Cu (II)-PMA complex is also suggested by an intense blue colour which formed on addition of dilute potassium hydroxide in contrast with the usual pale blue colouration of cupric hydroxide. The intensity of the colour seemed to depend on the amount of complex formed, the most intense colour probably corresponding to maximum complex formation and such normally gave the highest optical density. The position of the absorption regions agrees with the results of previous workers[7-9]. Fig. 4.1 shows a shift to lower wavelength as the degree of polymer ionization increases.

Figure 4.2 shows a plot of O.D. against α for varying concentrations of copper nitrate at an ionic strength of 0.10. It is seen from these graphs that first, the O.D. increases linearly with increasing α after which the O.D. rises to a maximum and somewhat further the absorbance starts to decrease. This was

established for different $\left[PMA\right]/\left[Cu(NO_3)_2\right]$ ratio. Figure 4.4 is a plot of O.D. against α for four different ionic strengths at $\left[Cu(NO_3)_2\right] = 4.0 \times 10^{-4}$M.

Apart from the absorption peak found in the ultra-violet region, another absorption peak was observed in the visible range and some measurements were conducted in this region. These have been presented in figures 4.6 and 4.7. The intensity of absorption in this region is not as great as in the ultra-violet region.

4.3.2. Discussion

4.3.2.1. Absorption in the Ultra-Violet Region:

It has been stated above that absprption occurs in the U.V, region of the spectrum. The absorption in the U.V. range is quite intense and occurs at 264mμ for the Cu-PMA complex with a high extinction coefficient of the order of 10^5. These are electronic transitions and this probably suggests charge-transfer spectra. The charge-transfer is from the carboxylate ($-COO^-$) groups to the empty dx^2-y^2 orbital of the copper ions.

Fig. 4.2 shows, in each case of Cu^{2+} concentration, an initial smooth increase in absorbance which indicates

a smooth formation of Cu-PMA complex in the course of titration. This build-up of copper-PMA complex continues until all the Cu^{2+} ions are bound by COO^- groups. This is achieved at the maximum value of O.D. Within the range of concentrations of copper used, Beer-Lambert's Law was found to be valid. This means that in this region of maximum O.D., according to Beer's law, the concentration of the complex will also be maximum if a single complex existed. The configuration of the complex as a whole will be most stable in this region also. However, as the degree of ionization increases, excess COO^- are produced and the electrostatic potential of these excess COO^- groups coupled with the expansion of the molecule taking place may make the complex less stable and may cause a partial disintegration of the complex. If this happens there will be an overall reduction in the concentration of the complex. That this happens is manifested in the observed decrease in the measured otpical densities beyond maximum complex formation. Partial disintegration in favour of new form of binding must have occured. However, no new absorption region was observed. It is quite possible that the new region is masked by the existing peak.

The exact nature of the new form of binding is not clear, nevertheless, change in λ_{max} occurs.

From Fig. 4.2, it is seen that the position of the maximum O.D. depends on the Cu^{2+} concentration and on the amount of COO^- groups present for a given constant concentration of PMA. If the point of equivalence is taken as the end of the linear partion on each curve, it is found that the ratio $[COO^-]_{original}/[Cu^{2+}]_{Total} = 2$ in all copper concentrations investigated with the exception of $[Cu^{2+}] = 8.0 \times 10^{-4}M$. On the other hand, if the assumption is made that the maximum point on each curve corresponds to maximum binding capacity of Cu^{2+}, the ratio $[COO^-]_{original}/[Cu^{2+}]_{bound}$ is very nearly four for the same copper concentrations. From this observation, it is suggested that probably a copper-PMA complex involving two carboxylates groups is first formed. This is then followed by a four-fold coordination. This suggestion is in agreement with the results of Morawetz[9] who compared the spectra of Cu(II) solutions in PMA with the spectrum in 0.02M acetate in which the bulk of copper is present as $Cu(OAc)_2$.

formed. As binding takes place the amount of free carboxylate sites decreases until finally a maximum amount of complex is formed and the ratio $\left[COO\right]_{original}/\left[M^{2+}\right]_{bound}$ remains constant. At this stage all or nearly all COO^- groups must have been bound to M^{2+}. The shapes of the curves obtained at high α suggests that a new form of binding is taking place and this is bourne out by the observed decrease in the amount of the original complex formed at low metal ion concentration. This observation is similar to the one made in fig. 4.2 and various reasons have been given for this observation.

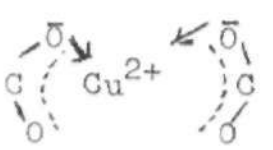
The results presented in fig. 4.3 are similar to those obtained in dialysis presented in chapter five and detailed treatment has been given in that chapter.

There are a number of reasons for the observed decrease in O.D. observed in fig. 4.2 and fig. 4.3. The viscosity studies presented in chapter three reveals that the minimum points on figure 3.4 are associated with the most stable and compact state of the complex formed. The rapid increase after the minimum point is due to rapid expansion of the molecule as it changes

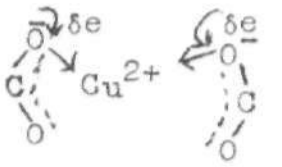
configuration from coiled state to an extended state. Generally the complex as a whole will adopt the most stable state since this would involve minimum energy of complexation. However, electrostatic consideration requires the molecule to become less stable on the whole as the degree of ionization increases i.e. as the molecule expands, probably due to excessive negative charges surrounding the bound cations. This observation is closely related to the results obtained from spectrophotometric titration where a decrease in O.D. is obtained at high α values. This can only be explained in terms of break down of the complex at high α values. The decrease in O.D. at high α values is due to the instability of the complex as more and more COO^- groups are produced i.e. as the molecule changes from coiled to extended configuration at high α values. Also, where extensive coiling has occured, copper with four co-ordinated square-planar complex may, because of its spatial orientation in the molecule cause a shielding effect on other complexed ions with the result that not all complexed ions will be exposed to radiation and this will lead to a decrease in O.D. This is known as hypochromic effect. It has earlier been suggested that

for an expanding molecule to enter into a four-co-ordinated complex with copper dimerization probably takes place. If a dimer is formed hypochromic effect will be quite considerable as observed in D.N.A[11], if two planes are lying one on top of the other so that one shields the other effectively from radiation. This means that not all the complexes formed will be exposed to radiation equally with the resultant reduction in observed O.D.

It has been stated that the value of the extinction coefficient is of the order of 10^4, which may imply a charge-transfer complex. The following is the proposed structure for a two co-ordinated (I) and four co-ordinated (II) complexes.



I



II

In each case, some contribution to the total charge transfered is made by each of the charged sites in the immediate vicinity of the copper ions. Any of the above structure can lead to dimerization depending on the degree of ionization. It is quite possible that

the charged sites are located on different chains. In the case of dimerization leading to four-fold co-ordination, a similar contribution to structure II from another chain will complete the process of dimerization. The mechanism of bonding could be explained in the following manner. First Coulumbic attraction (bonding) between Cu^{2+} and COO^- takes place. Once the Cu^{2+} ions are held in the vicinity of the COO^- groups the bonds begin to vibrate and if the period of vibration is long enough for a quantum of radiation to be absorbed, transition of charge from COO^- groups to Cu^{2+} can take place. Once the complex is formed, there will be a reduction in the excitation energy. The actual magnitude of the charge-transfer is not known but probably only partial change in the oxidation state of $Cu^{2+} \rightarrow Cu^+$ has taken place. This process may be likened to an ionic contribution which occurs at a fairly low energy. In both structures I and II, one does not know how much charge is contributed by each chain to form a dimer and the structure II in particular may be tought of as a type of resonating structures.

Now considering the above postulate from the point of view of experimental findings then one is placed in

a position to further explain the observed decrease in O.D. in figure 4.2. Yokoi and Isobe[12] have made some rather similar observations for Cu(II) complexes with uncharged molecules, ethylenediamine. They suggested that for these complexes, absorption is due to electron transfer from ligand σ-bond orbital to an antibonding orbital associated with copper. According to them, as the σ-bonding becomes more covalent the charge-transfer band shifts to longer wavelengths. However, the present study involves charged COO^- groups and Cu(II) ions. A shift to lower wavelength was obtained for the charge transfer band. As the degree of ionization increases, excess COO^- groups produced surrounding the bound cation may cause a weakening in the O-Cu bond because of the effect of repulsive electrostatic forces on the bond. This will limit the amount of charge-transfer which can take place. This may also affect the stability of the complex and will aid disintegration. In such a situation, a decrease in O.D values will be observed.

Another explanation for the decrease in amount of charge-transfer is as follows: Consider a cation surrounded by charged COO^- groups repelling each other;

in such a case, the repulsive interaction between the charged COO^- groups will force the particles to take up positions as far as possible from each other. This will lead to a situation where "no bond structure" is obtained i.e. no appreciable σ-bonding and the intensity of the charge-transfer depends on the proximity of the COO^- groups to the metal ions. Therefore at high α, the strong electrostatic repulsive forces will not allow easy approach of more than one COO^- to the metal ions thus limiting the amount of charge-transfer. This observation may also lead to a reduction in O.D.

For the U.V. region, Fig. 4.4 shows a plot of λ_{max} against the degree of ionization (α) for three different ionic strengths. One notices a shift to shorter wavelengths as α increases from C.6 - 1.0. The maximum shift of 8mμ is obtained at $\alpha = 1.0$. The shift of the charge-transfer band to lower wavelength means that the energy difference between bonding orbitals becomes larger i.e. $\epsilon = \frac{hc'}{\lambda}$, if λ is smaller then ϵ must increase since h and c' are constants and they are Plankk's constant and velocity of light in the medium respectively. The reasons for the increase in energy have been explained in the preceeding paragraphs.

It is also noted that the shift in λ_{max} always occur at about the same α i.e. it is independent of the ionic strength of the medium. It is also noted that the shift in λ_{max} does not depend on Cu^{2+} concentration for the same value of ionic strength.

4.3.2.2 Effect of Ionic Strength:

Fig. 4.5 is a plot of O.D. against α for four different ionic strengths at constant copper ion concentration and constant PMA concentration. Consider the following reaction:

$$M^{n+} + pL = M^{n+}Lp.$$

This is a reaction in which the number of free ionic charges are decreasing. In this type of reaction the effect of ionic strength will be enhanced in dilute solution and will be most marked at medium α. At low α i.e. at low concentration of the ligands L^- and sufficiently high Cu^{2+}, Cu^{2+} will be in excess and the amount of complex formed will be entirely dependent on α. This is shown in fig. 4.6 where at low α nearly equal amount of complex is formed irespective of the ionic strength. Similarly at high α, i.e. when excess of the ligands will be present, then the concentration

of the complex will depend almost entirely on concentration of M^{n+} (Cu^{2+}). This is also seen in fig. 4.5 that at high α, where irrespective of the ionic strength, equal amount of complex is formed. However, in the middle region, the concentrations of Cu^{2+} and COO^{-} are present in comparable quantities and it is in this region the equilibrium constant is a determining factor. It is also in this region where one might expect the ionic strength to be most effective. This if found to be the case in fig. 4.5. As the ionic strength increases, the amount of complex formed decreases between $\alpha = 0.3$ and $\alpha = 0.7$.

Finally fig. 4.6 shows a plot of O.D. against λ for two PMA concentrations at two different degrees of ionization. It is interesting to note from this figure that spectophtometric evidence shows that the nature of the complex is independent of dilution of PMA. This is what would be expected since the number of carboxylates with which a complex ion will associate depends only on the conditions which exists within the polymer coil to which the copper ion is bound.

4.3.2.3 Absorption in the Visible region:

In fig. 4.7 the spectra for PMA in the presence of two different concentrations of copper nitrate are presented. As in the U.V. region, first an initial smooth increase in % absorption is obtained with increasing α; this then rises to a peak and further the O.D. decreases with increasing α. The same observation is established in the two concentrations of copper nitrate used. The decrease in %A beyond the maximum is an indication that the complex formed disintegrates. In figure 4.7 the ratio of $[COO]_{original}/[Cu^{2+}]_{Total}$ at the end of the linear portion in both curves is 2 and the same ratio is 3.5 and 5.0 for the PMA containing 10.0×10^{-4}M Cu^{2+} and 5.0×10^{-4}M Cu^{2+} respectively. This is in agreement with the results obtained for the same ratio in the U.V. region.

Fig. 4.8 shows a plot of O.D. against λ for constant (PMA) and $[Cu^{2+}]$ at two degrees of ionization. Here a shift of λ_{max} to longer wavelength is obtained with increasing α.

The above observations are accounted for as follows. The absorption is probably due to a d-d transition which

as a rule is usually of weak intensity. This is so because the electron is jumping from one orbital which is centrosymmetric to another orbital which is also centrosymmetric and that all transitions of this type are normally "forbidden". Generally, the intensity and position of the transition is related to the ligand field spliting energy -Δ. In the visible region, the $Cu^{2+}(H_2O)_6$ absorption is very weak and broad but is increased by complexing with PMA (although region of absorption is roughly the same wavelength interference is quite negligible). The type of reaction one might envisage is as follows:

$$Cu(H_2O)_6^{2+} + nL \rightleftharpoons Cu^{2+}(H_2O)_{6-n}Ln + nH_2O.$$

Orgel[13] has suggested that when Cu^{2+} ions take part in complex formation the dx^2-y^2 and dz^2 orbitals are destabilized by the ligands and are infact degenate in an octrahedral environment and the usual symmetry is lost. Thus the increase in intensity in the Cu-PMA complex may be due to lack of environmental symmetry of the Cu^{2+} ion. The position of the band is typical of Cu(II) complexes and since ligand field for water and oxalate complex is similar, then one might expect absorption in similar region for $Cu(H_2O)_6^{2+}$ and Cu-PMA complex.

$Cu^{2+}(H_2O)_6$ has λ_{max} at 800mμ. Since λ_{max} at $\alpha = 0.3$ is less than λ_{max} for $Cu^{2+}(H_2O)_6$ the assumption is made that crystalfield spliting energy is greater for PMA complex or the contribution of vibrational effects increase Δ, therefore the observed increase in λ (Fig. 4.8) would tend to suggest a break down of the complex so that less COO^- groups will be attached to Cu^{2+} and the vacancies created will be replaced by H_2O i.e. the equilibrium in the above equation will be dispaced to the left.

As a result of the operation of Jahn-Teller effect, the intensity of the observed band is increased by distortion due to mixing of orbitals, therefore, the extent of distortion may decrease as the number of bound groups decreases i.e. as the complex breaks down. This will lead to decrease in observed % absorption as seen in Fig. 4.7. If this happens, this will be against the normal equilibrium where M+ nL ⇌ MLn and where L is present in excess and n is maximum co-ordination number. The configuration of the complex may be against this equilibrium and the complex will break down.

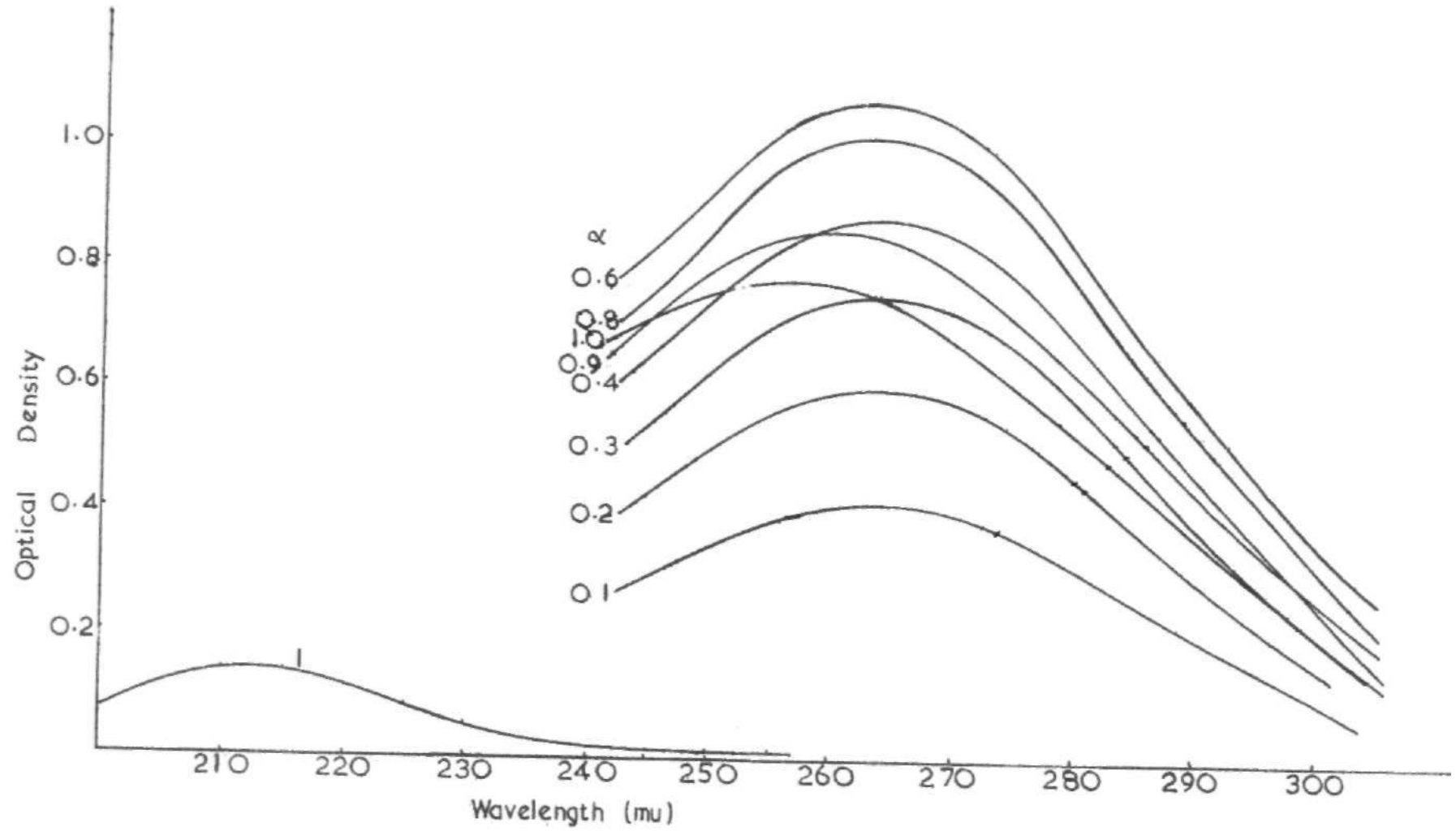


Fig 4.1 Absorption spectra of PMA and PMA—$Cu(NO_3)_2$ solution at varying α
I= 2.0×10^{-3} M PMA ; $[Cu(NO_3)_2] = 4.0 \times 10^{-4}$ M ; I-0.02

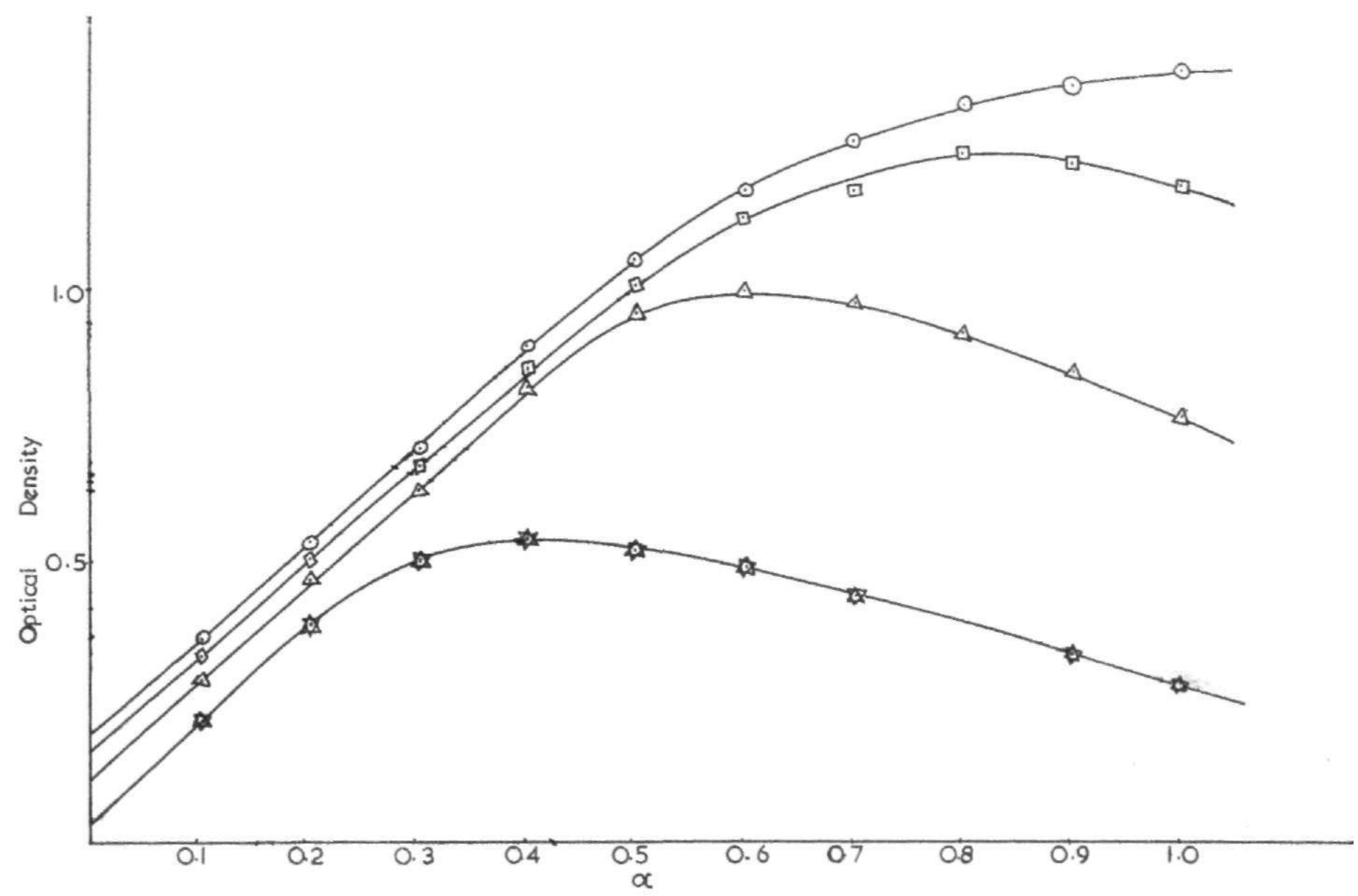


Fig 4.2 Spectrophotometric titration of PMA—$Cu(NO_3)_2$ solution with KOH
[PMA] = 2.0×10^{-3} M ; I = 0.10 ; Cell length = 5.0 mm [$Cu(NO_3)_2$] : (⊙) 8.0×10^{-4} ; (□) 6.0×10^{-4} ; (△) 4.0×10^{-4} ; (✡) 2.0×10^{-4} , M

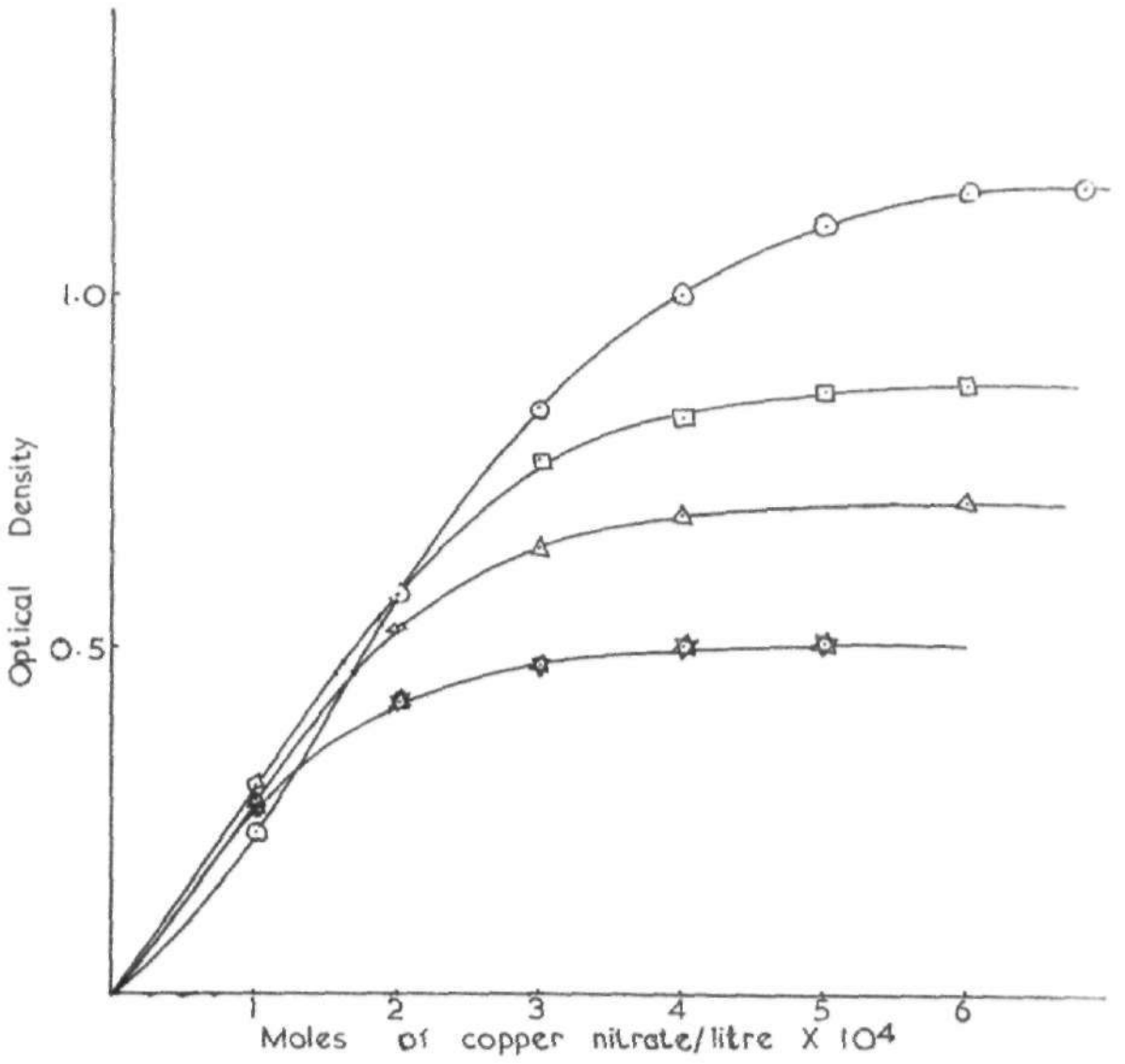


FIG 4.3 Absorption spectra of PMA—$Cu(NO_3)_2$ solutions in the presence of varying $[Cu(NO_3)_2]$
[PMA] = 2.0×10^{-3} M ; I = 0.1 ; Cell length = 5.0mm
α :- (⊙) 0.6 ; (□) 0.4 (△) 0.3 (☆) 0.2 , λ_{max} 264mu

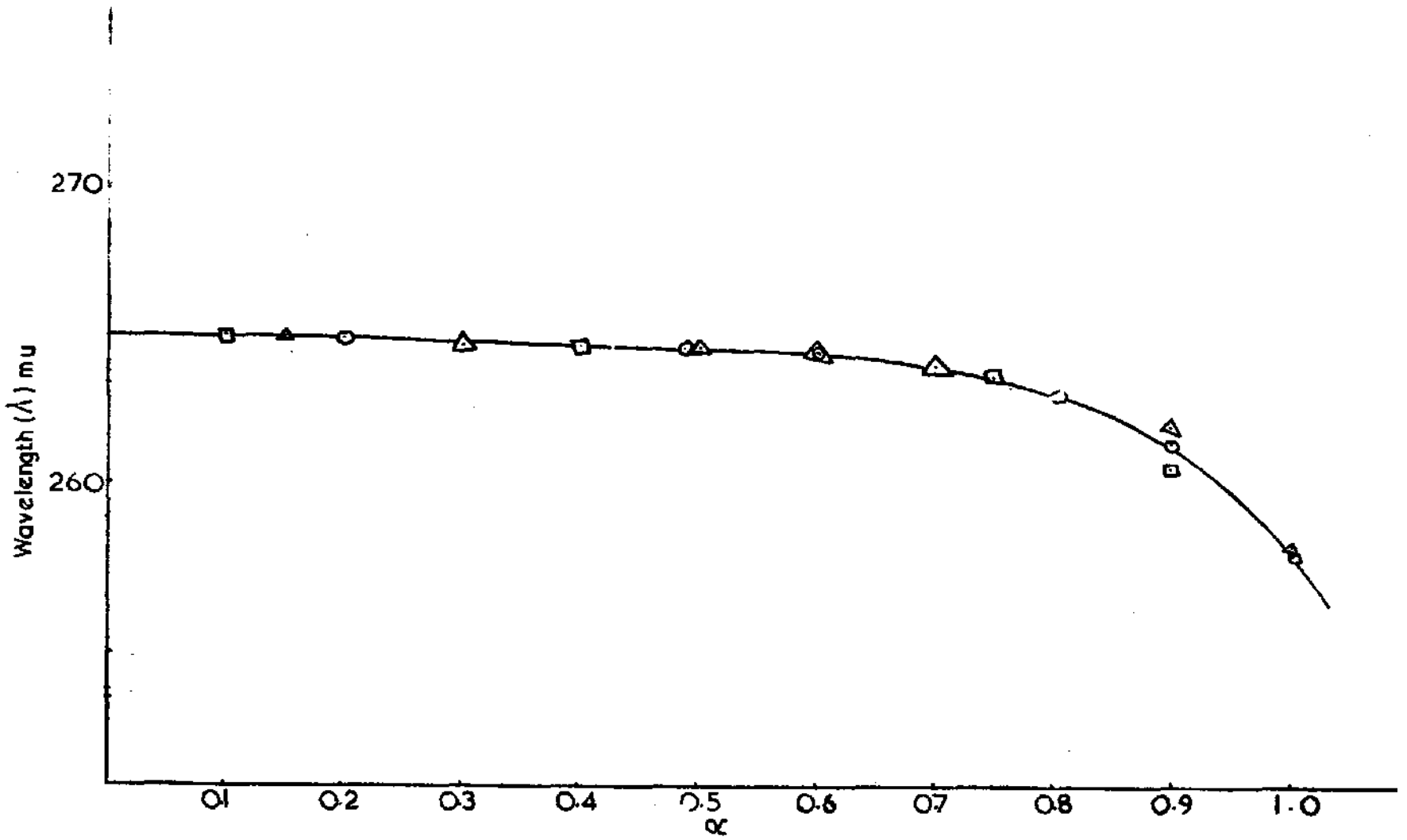


FIG 4 . 4 Spectrophotometric titration of PMA – $Cu(NO_3)_2$ solutions with KOH in the presence of varying ionic strengths

[PMA] = 2.0×10^{-3} M ; $[Cu(NO_3)_2] = 4.0 \times 10^{-4}$ M ; Cell length = 5.0 mm

I :- (□) 0.1 ; (△) 0.05 ; (○) 0.02

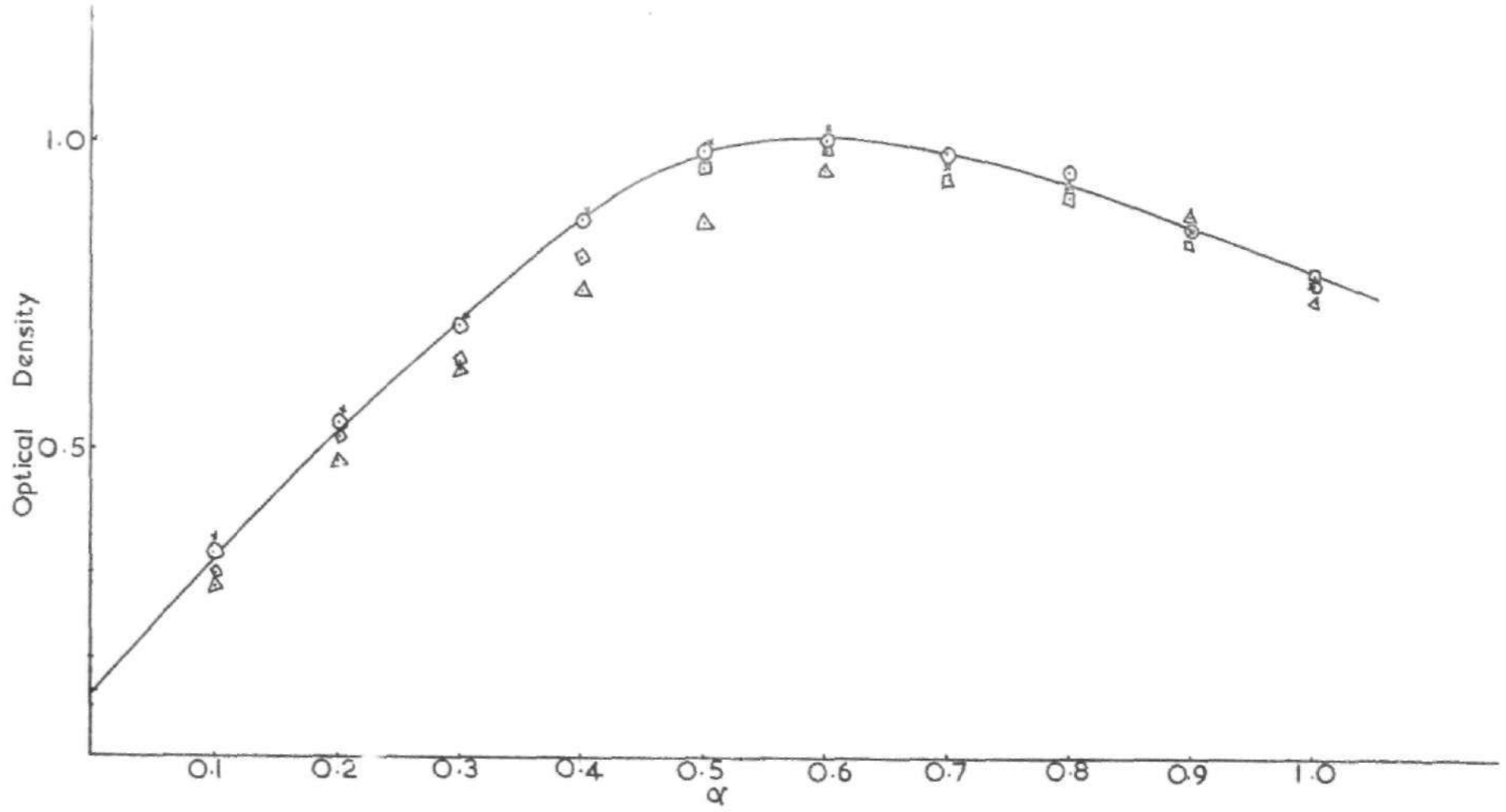


FIG 4.5 Spectrophotometric titration of PMA-$Cu(NO_3)_2$ solutions with KOH at varying ionic strengths Cell length = 5.0 mm ; λ_{max} = 264 mμ ; $Cu(NO_3)_2$ = 4.0×10^{-4} M I : (x) 0.02 ; (○) 0.05 ; (□) 0.10 ; (△) 0.50

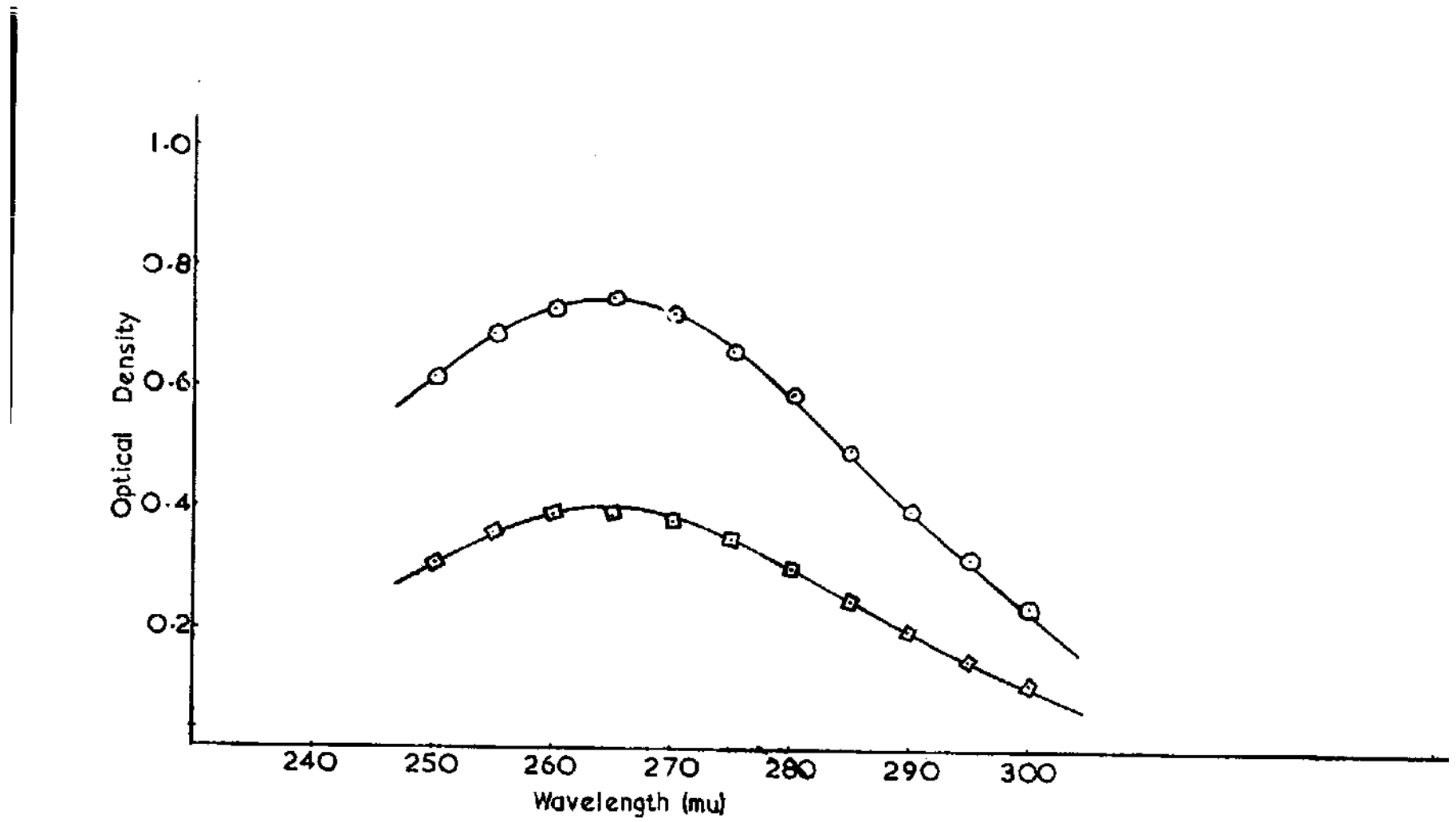


FIG 4.6 Absorption spectra of PMA– $Cu(NO_3)_2$ solutions at 60% neutralization. $Cu(NO_3)_2 = 4.0 \times 10^{-4}$ M; I = 0.1 ; (○) [PMA] = 2.0×10^{-4} M; (□) [PMA] = 1.0×10^{-4} M

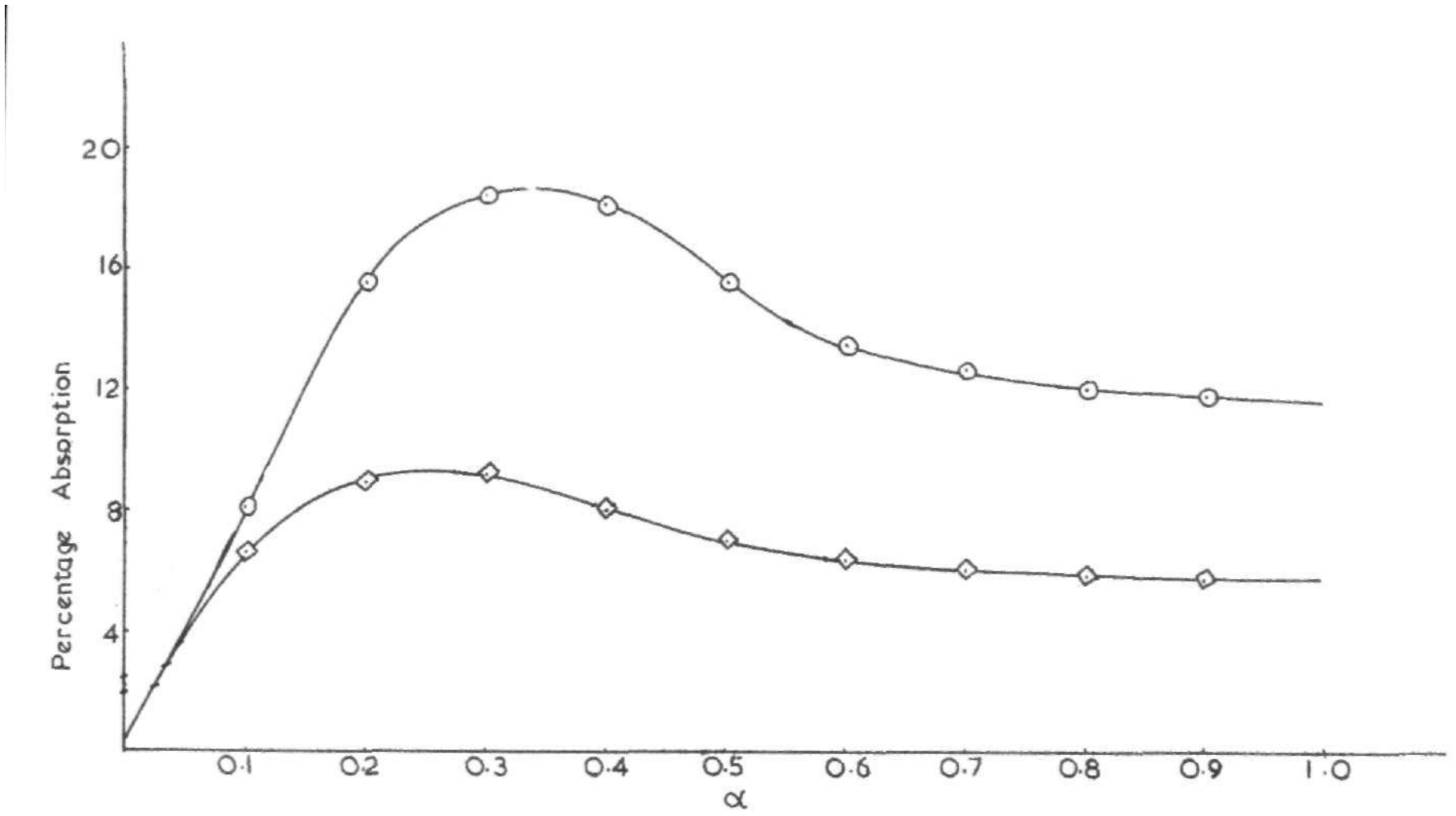


FIG 4.7 Spectrophotometric titration of PMA – $Cu(NO_3)_2$ solutions with KOH at λ = 700mu ; Cell length = 1·0 cm ; [PMA] = 0·01 M ; I = 0·02 ; $[Cu(NO_3)_2]$:- (⊙) 10.0×10^{-4} ; (□) 5.0×10^{-4} M .

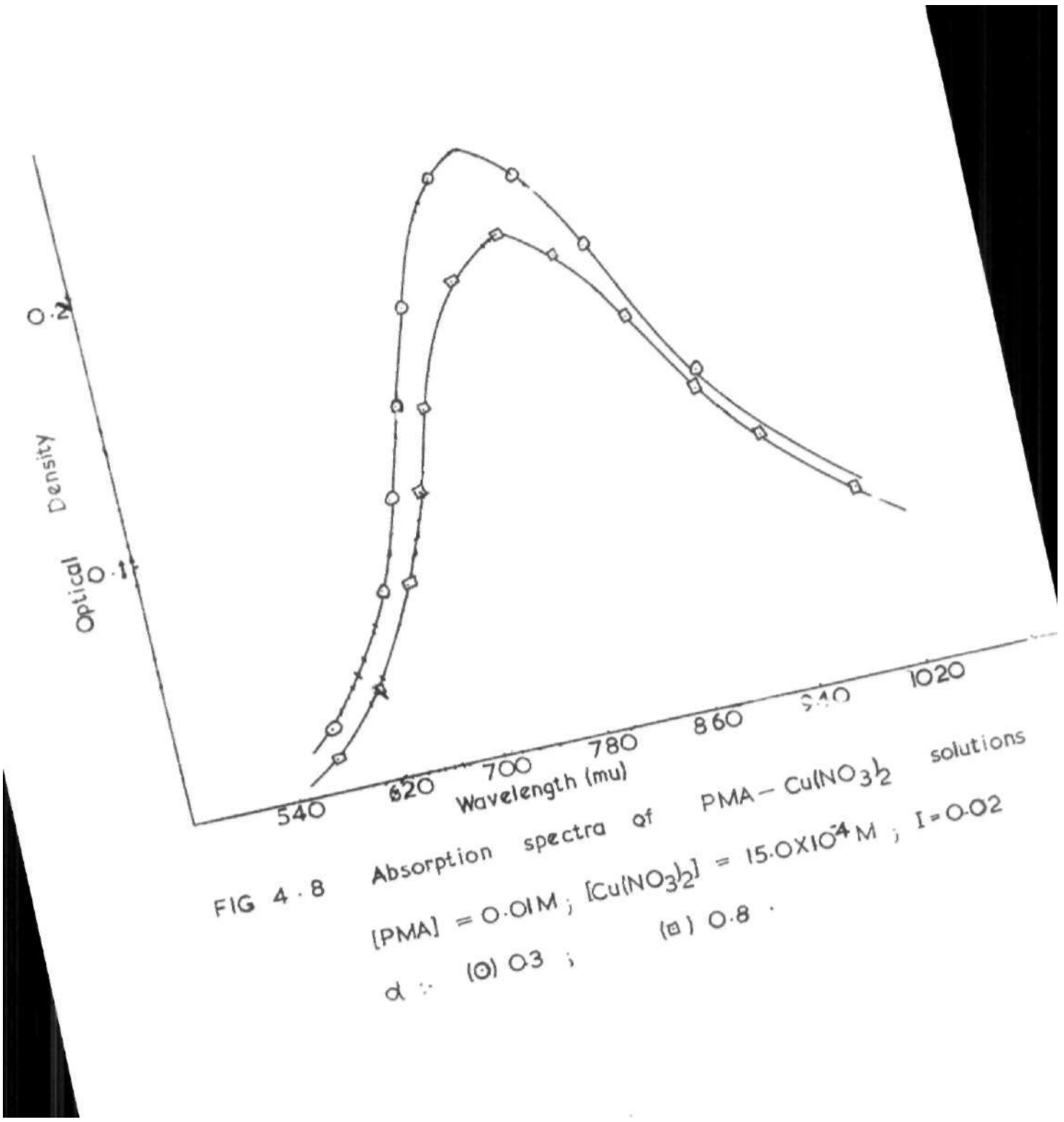


FIG 4.8 Absorption spectra of PMA – $Cu(NO_3)_2$ solutions

[PMA] = 0.01M ; $[Cu(NO_3)_2]$ = 15.0×10^{-4} M ; I = 0.02

α :- (⊙) 0.3 ; (⊡) 0.8 .

4.4 REFERENCES

1. Braude, E. A., Nature, 733, 155 (1945).
2. Braude, E. A., J. Chem. Soc. 379, (1950).
3. Burawoy, A., Ber., 63, 3155, (1963).
4. Burawoy, A., J. Chem. Soc. 1177, (1939).
5. Kasha, M., Discussion Faraday Soc. 9, 4, (1950).
6. McConnell, H., J. Chem. Phys. 20, 700, (1952).
7. Mandel, M. and Leyte, J. C., J. Poly. Sc. A2, 3771, (1964).
8. Kotliar, A. M. and Morawetz, H., J. Am. Chem. Soc. 77, 3692, (1955).
9. Morawetz, H., J. Poly. Sc. 17, 442, (1955).
10. Wall, F. T. and Gill, S. J., J. Phys. Chem. 58, 1128, (1954).
11. Olayemi, J. Y., Ph.D. Thesis.
12. Yokoi, H. and Isobe, T., Bull. Chem. Soc. Japan, 42, 2187, (1969).
13. Orgel, L. E., Introduction to Transition Metal Chemistry.

Chapter 5

DIALYSIS EQUILIBRIUM

C O N T E N T S

		Page
5.1.	Introduction	141
5.2.	The Theory of Equilibrium Dialysis ..	142
5.2.1.	Detailed treatment of Donnan's Membrane Equilibria	147
5.3.	Experimental details	154
5.3.1.	Apparatus	154
5.3.1.2.	Reagents	154
5.3.3.	Method...	155
5.3.3.1.	Preparation of Membrane	155
5.3.3.2.	Filling the dialysis Tubes	156
5.3.3.3.	Attainment of Equilibrium	157
5.4.	Analysis of solutions at Equilibrium ..	158
5.4.1.	Determination of Zinc	158
5.4.2.	Procedure	160
5.4.3.	Estimation of copper	160
5.5.	Summary of Results	162
5.6.	Results and Discussion	166

Page

5.6.1. Results 168

5.6.2. Discussion 169

5.6.2.1. Effect of binding on Polyion Configuration 171

5.6.2.2. Stability of Cu-PMA and Zn-PMA Complexes 174

5.7. Conclusion 176

5.8. R e f e r e n c e s 178

Chapter 5

DIALYSIS EQUILIBRIUM

5.1. Introduction:

The use of equilibrium dialysis technique[1] permits the gathering of precise quantitative data on polyelectrolyte - metal equilibria in solution. Since the time of development of the method many studies of polyelectrolyte-metal interaction have been carried out and a great deal of information obtained as to the molecular basis for the interaction but little has been said about the structual features required for binding. Kotliar and Morawetz[2] using the method of dialysis equilibrium obtained the amount of copper binding to PMA but their data gave no information about the nature of the complex. To contribute to the clarification of these interactions, attempts have been made to obtain, by the method of dialysis equilibrium both qualitative and quantitative information about the PMA - metal complex. In principle this technique consists of a vessel divided into two compartments by a specially

prepared membrane which is impermeable to the macromolecule but fully permeable to the small molecules and ions. If the macromolecule is confined to one compartment and if it binds some of the small ions, then at equilibrium, the total number of small ions in the macromolecule - containing chamber will exceed that in the macromolecule-free chamber. The difference between these two concentrations is a measure of the concentration of bound molecules provided the Donnan effect has been suppressed, or accounted for.

5.2. The Theory of Equilibrium Dialysis:

Attempts[3,4] have been made to explain the peculiar electrical and other effects which occur in a system in which two solutions containing electrolytes are separated by a membrane which is freely permeable to most of the ions but impermeable to one of them. A clear idea of the phenomena in question may be obtained by considering a very simple case. Suppose that a membrane M separates two solutions (1) and (2) of equal constant volume, containing initially only the salts NaA and KA, respectively, the membrane being permeable to K^+ and Na^+ ions not to the A anions. Evidently, the

cations K^+ and Na^+ can exchange places freely by means of diffusion across the membrane, but this exchange is subject to the restraint condition of equimolar quantities. The whole system is therefore subject to two conditions of restraint. At first one might be inclined to think that the interchange of sodium and potassium ions would continue until they are equally distributed throughout the whole volume of the solution. This would occur if the membrane were permeable also to the ion A^-, but that it will not generally occur in the present case can be seen readily. Assuming complete ionization, the initial and the final states are represented as follows.

	M			M	
$C_1 Na^+$		$K^+ C_2$	$C_1 - x\ Na^+$		$Na^+\ x$
			$x\ K^+$		$K^+\ C_2 - x$
$C_1 A^-$		$A^- C_2$	$C_1 A^-$		$A^- C_2$
1		2	1		2
Initial State			Equilibrium State.		

If F denotes the free energy of the system, then the equilibrium state is characterised by the condition $(dF)_{P\ T} = 0$. If the following variation is considered,

dn moles $Na^+(1) \rightarrow (2)$

dn moles $K^+(2) \rightarrow (1)$

then electrical work terms vanishe and what we get is

$$dF = RT\left\{dn\log\frac{[Na^+]_1}{[Na^+]_2} + dn\log\frac{[K^+]_2}{[K^+]_1}\right\} = 0$$

So that $$\frac{[Na^+]_1}{[K^+]_1} = \frac{[Na^+]_2}{[K^+]_2} = \frac{C_1}{C_2}$$

Thus only when $C_1 = C_2$ is it true that for equilibrium $[Na^+]_1 = [K^+]_1$ and $[Na^+]_2 = [K^+]_2$

Now let the above simple consideration be applied to a polyelectrolyte of high molecular weight separated by semi-permeable membrane from water. In this case the polyion is present only on one side of the membrane and phenomenon in question is more complex. Although the polyelectrolyte contains mobile counterions which are small enough to pass through the membrane no such passage will actually be possible, since it would involve a separation of polyions and counterions and a rapid build up of very large electrostatic charges of opposite sign in the two portions of the system. However, if a uni-univalent electrolyte such as KNO_3 is added on either side of the membrane, its cations and anions may diffuse together and the problem then

arises of how the presence of the polyion affects the equilibrium distribution of these ionic species.

This problem was solved by Donnan's[3,5] method, by imposing two conditions. The first requires the solutions on either side of the membrane to be electroneutral. Thus, if m_f is the molarity of the fixed charges in the solution containing the polyelectrolyte and m_s is the molarity of an added uni-univalent salt, the molarity of the byions will be $m_b = m_s$ and that of the counterions will be $m_c = m_f + m_s$. In the dialyzate both ions will be at the same molarity $m'_b = m'_c = m'_s$. Since the diffusible electrolyte must, at equilibrium, have the same thermodynamic activity on both sides of the dialysis membrane,

$$m_b m_c \gamma_{\pm}^2 = m'_b m'_c \gamma'^2_{\pm}$$

and $$(m_f + m_s) m_s \gamma^2_{\pm} = (m'_s)^2 (\gamma'_{\pm})^2 \quad \ldots\ldots (5\text{-}1)$$

where $\gamma^2_{\pm}$ and $\gamma'^2_{\pm}$ are the squares of the mean ionic activity coefficients in the presence and absence of polyelectrolyte respectively. Now, consider first, the result which would be obtained if the activity coefficients could be neglected. In that case equation (5-1)

gives for a relation between m_s and m'_s the following expression

$$m_s = m_f/2 + \sqrt{(m_f/2)^2 + (m'_s)^2} \quad .....(5-2)$$

If $m'_s/m_f \ll 1$, then $m_s = m'_s(m'_s/m_f)$ i.e. the added salt is largely excluded from the polyelectrolyte solution. In the other extreme case, when $m'_s/m_f \gg 1$, an expansion of equation (5-2) yields

$$m = m'_s - m_f/2 + m_f^2/8m'_s.....(5-3)$$

which leads to a difference in the total molarity of the mobile ions Δm_i on the two sides of the membrane.

$$\Delta m_i \equiv m_c + m_b - m'_c - m'_b = m_f^2/4m_s.....(5-4)$$

This difference in mobile ion concentration contributes to the osmotic pressure of the polyelectrolyte solutions. The expression in equation 5-4. shows that the effect is minimized by increasing the concentration of the added salt. In practice, large forces between polyions and their counterions will inevitably depress the ionic activity coefficient, so that $\gamma_{\pm} < \gamma'_{\pm}$. This will have the effect of increasing the difference in counterion concentration and decreasing the difference in the byion concentration on the two sides of the membrane.

If the ionic concentration is determined analytically, equation (5-1) may be used to calculate $\gamma_{\pm}$, since the activity coefficient $\gamma'_{\pm}$, corresponding to a simple salt solution may be determined by conventional methods or obtained from tabulated data.

5.2.1. Detailed treatment of Donnan's Membrane Equilibria[3,10].

Since a polyelectrolyte has a net charge (except at the isoionic point) the concentration of the free ions will not be equal on the opposite side of the membrane due to the Donnan effect. This means that the net electrostatic charge on a polyion has a profound effect upon its behaviour. When a charged particle is retained a Donnan equilibrium is set up. From thermodynamical considerations, equations have been derived to account for the Donnan equilibrium and Donnan correction.

Let us now consider two phases separated by a semipermeable membrane and containing the same solvent on either side. One phase β contains the macromolecular ionic species which can not diffuse through the membrane to the other phase α. Also present in the system are other small ions i, j, k, l ....which are readily diffusible through the mebrane.

For the solvent (designated by subscript 1)

$$\mu_1(P) = \mu_1^{o}(P) - RTg\Sigma m_i \ldots\ldots\ldots$$

$$= \mu^*_1 + PV_1 - RTg\Sigma m_i \ldots\ldots(5\text{-}5)$$

where μ is the chemical potential, $\mu_1^{o}(P)$ is the value of μ_1 (the chemical potential) for the pure solvent at the pressure P and μ_1^* is the value for the pure solvent in the limit of zero pressure, and g is the osmotic coefficient defined by

$$\ln \frac{P_i}{P_i^{o}} = -g\Sigma m_i \ldots\ldots\ldots\ldots\ldots(5\text{-}6)$$

m_i is the mole ratio of the ionic species, i, to the solvent, P_i and P_1^{o} are the vapour pressures of the solution and pure solvent respectively.

For ionic species i we can write

$$\mu_i = PV_i + ZF\Psi + RT\log \lambda^* + RT\log m_i\gamma_i$$

$\ldots\ldots(5\text{-}7)$

where λ^* is the absolute activity independent of the pressure and γ_i is the activity coefficient, Z is the valence, F, is the Faraday, Ψ is the electrostatic potential and V_i is the partial molar volume.

The condition for the membrane equilibrium can be written in general form as

$$\mu_1^{\alpha} = \mu_1^{\beta} \ldots\ldots\ldots\ldots\ldots(5\text{-}8)$$

and since the same solvent is present on either side of the membrane we have $\mu_i^\alpha = \mu_i^\beta$ .....(5-9)

Now using equation 5-5 in 5-8 and expression for the equilibrium of the pressure difference is obtained

$$P^\beta - P^\alpha = \frac{RT}{V_1}(g^\beta \Sigma_i m_i^\beta) \text{ .....(5-10)}$$

and using equation 5-7 in 5-9 one gets

$$RT \frac{m_i^\beta \gamma_i^\beta}{m_i^\alpha \gamma_i^\alpha} + ZF(\psi^\beta - \psi^\alpha) = (P^\alpha - P^\beta)V_i \text{.....(5-11)}$$

and substituting equation 5-10 into 5-11

$$\ln \frac{m_i^\beta \gamma_i^\beta}{m_i^\alpha \gamma_i^\alpha} + \frac{Z_i F}{RT}(\psi^\beta - \psi^\alpha) = \frac{V_i}{V_i}(g^\alpha \Sigma_i m_i^\alpha - g^\beta \Sigma_i m_i^\beta) \text{...(5-12)}$$

The importance of equation 5-12 lies on whether γi can be computed. If they can, then $(\psi^\beta - \psi^\alpha)$ can be computed since all other quantities in equation 5-12 are measurable. In any case, the term $(\psi^\beta - \psi^\alpha)$ can be eliminated by applying expression (5-8) to several ionic species forming an electrically neutral combination - i.e. for electrical neutrality

$$Z_i F(\psi^\beta - \psi^\alpha) = 0 \text{ .....(5-13)}$$

Thus for equilibrium distribution of the diffusible electrolyte consisting of V_i cation i and Vj anion j we obtain

$$\ln\frac{(m_i^{\beta})^{V_i}(m_j^{\beta})^{V_j}(\gamma_{ij}^{\beta})^{V_i+V_j}}{(m_i^{\alpha})^{V_i}(m_j^{\alpha})^{V_j}(\gamma_{ij}^{\alpha})^{V_i+V_j}} = \frac{v_iV_i + v_jV_j}{V_1}\left[g^{\alpha}(m_1+m_j^{\alpha}) - g^{\beta}(m_1^{\beta}+m_j^{\beta})\right] \quad \text{.....(5-14)}$$

In the case of potassium nitrate, with K^+ ions and NO_3^- ions, then they are denoted by m_i and m_j respectively.

The above treatment is now applied to the binding study between a macro-ion (PMA) and divalent electrolyte zinc and copper nitrate in the presence of potassium nitrate as the supporting electrolyte. A similar but more extended equation has been obtained. The ions encountered here are Zn^{2+} or Cu^{2+}, k^+, and NO_3^- designated by i, j, k and then equation 5-14 becomes

$$\ln\frac{(m_i^{\beta})^{V_i}(m_j^{\beta})^{V_j}(m_k^{\beta})^{V_k}(\gamma_{ij}^{\beta})^{V_i+V_j}(\gamma_{jk}^{\beta})^{(V_j+V_k)}}{(m_i^{\alpha})^{V_i}(m_j^{\alpha})^{V_j}(m_k^{\alpha})^{V_k}(\gamma_{ij}^{\alpha})^{(V_i+V_j)}(\gamma_{jk}^{\alpha})^{V_j+V_k}} =$$

$$\frac{v_iV_i + v_jV_j + v_kV_k}{V_1}\left[g^{\alpha}(m_i^{\alpha}+m_j^{\alpha}+m_k^{\alpha}) - g^{\beta}(m_i^{\beta}+m_j^{\beta}+m_k^{\beta})\right] \quad \text{.....(5-15)}$$

At high dilutions the quantity on the right hand of equation 5-15 may be so small that it comes very close

to zero (as the ions are small) and the term may be neglected and under such conditions equation 5-15 reduces to

$$(m_i^{\beta})^{V_i}(m_j^{\beta})^{V_j}(m_k^{\beta})^{V_k}(\gamma_{ij}^{\beta})^{V_i+V_j}(\gamma_{jk}^{\beta})^{V_j+V_k}$$

$$= (m_i^{\alpha})^{V_i}(m_j^{\alpha})^{V_j}(m_k^{\alpha})^{V_k}(\gamma_{ij}^{\alpha})^{V_i+V_j}(\gamma_{jk}^{\alpha})^{V_j+V_k} \quad \ldots\ldots(5\text{-}16)$$

However, this above statement is not strictly true in case of the present study and in most other dialysis studies. To make this expression applicable in the present work extrapolation to zero will be necessary but if this is done evaluation of variation of concentration with binding will not be possible. Therefore, a further assumption is made and that is that over the concentration range used in the present study, the quantity on the right hand of equation 5-15 is negligible and equation 5-16 is again obtained.

In the system studied, partially ionized PMA of concentration P on one side of the semipermeable membrane is brought to equilibrium with the cation solution of concentration N in the same solvent as is on the other side. The low molecular weight cation passes freely across the membrane such that its activity

on both sides of the membrane is the same when equilibrium is reached. The solutions on the two sides were made sufficiently similar by addition of simple electrolyte - KNO_3 so that activity coefficients should also be the same on both sides. This was necessary because both P and M are ionic and the Donnan effect must be suppressed.

The theory of dialysis equilibrium just discussed have interesting bearing on the ionic and other exchanges which take place in living cells or tissues and their circumnatant fluids. In these cases, however, the phenomena may be complicated by the variable permeability of the cell membranes and by many other factors, so that the extremely simple relationships which result from ideal membrane equilibria as presented in the foregoing sections will represent only a very small part of the associated complex of phenomena which make up the reaction of the cell towards variation of its environment. But in the phenomena of living matter, as in other branches of science, the complex can only be understood by analysing it into its simplest constituents and ascertaining, one by one, the laws which govern the operation - the

action and the equilibrium - of these constituents. Since many living cells do exhibit selective permeability as regards ions, it is possible that ionic exchanges and equilibria of the sort discussed above may occur between the cell and the external fluid[8].

5.3. EXPERIMENTAL DETAILS

5.3.1. Apparatus:

Semipermeable membrane (Viskin tubing $\frac{24}{32}$ inch) which is permeable to water and small molecules and ion and impermeable to PMA molecules, pyrex test tubes 25 x 200mm and a low temperature bath capable of keeping the temperature to within ±0.1 degree.

5.3.2. Reagents:

(a) Water:

In order to eliminate any unnecessary contamination the water used in the treatment of dialysis casings as well as in all solutions preparations was distilled water which has been redistilled in an all - glass apparatus.

(b) Buffer solution pH = 10:

Since each experiment was conducted at a particular pH and at one ionic strength, it was possible to use a single buffer. 142 ml. of concentrated ammonia solution was added to 175gm of ammonium chloride and was diluted to 250 ml of distilled water. This gave a buffer solution of pH = 10.

(c) Dye Solutions:

The Eriochrome Black T* indicator for the estimation of zinc ions was prepared by dissolving the reagent in triethanolamine and absolute alcohol. In the case of copper estimation, Fast Sulphon Black F* indicator was used. A 0.5 percent equation solution was prepared.

(d) Stock Solution of EDTA (0.10M):

37.23 gm of disodiumdihydrogen ethylene diamino tetraacetate dihydrate (analytical grade) was dissolved in distilled water and diluted to one litre in a volumetric flask with distilled water.

5.3.3. Method:

5.3.3.1. (a) Preparation of Membrane:

Lengths of Viskin tubing appropriate to the volume of acid solution (10.0 ml) to be used were put in water and heated on a steam bath for one hour. The tubings were transfered to fresh water, and the heating repeated. The tubings were next soaked at room temperature for a few hours in each of several additional portions of water. Finally the tubings were soaked in 0.1M KNO_3 for 24 hours. The pH of the solution was adjusted occassionally to the desired

value since the tubing could lower the pH of a neutral, unbuffered salt. A more rigorous treatment than the one described above may impair the properties of the dialysis tubes. Heating the tubings on a steam bath for as long as 72 hours makes the tubings permeable to molecules of molecular weight of 69,000[19].

5.3.3.2. (b) Filling the Dialysis Tubes:

A piece of dialysis tubing was removed from the potassium nitrate solution, and the excess liquid was removed. A knot was tied at one end of the tubing, 10.0 ml of solution of PMA at a particular degree of ionization and supporting electrolyte to give the desired ionic strength were added. The tube was closed and tied with a nylon string and suspended in the polymer free solution contained in the pyrex test tube. The pyrex test tube contained a total of 10.0 ml of solution made up of a varying quantities of $Zn(NO_3)_2$ and KNO_3 to give the desired equilibrium concentration and ionic strength of 0.1N. In all the experiments 2.50×10^{-3} base molar PMA solution was used and studies were carried out at varying degrees of neutralization and with varying quantities of $Zn(NO_3)_2$ i.e. for a particular degree of neutralization, varying

quantities of Zn^{2+} were used to obtained maximum binding. The same procedure was repeated in the case of the PMA -copper system.

5.3.3.3. (c) Attainment of Equilibrium:

Adequate agitation was necessary before equilibrium could be attained in the shortest possible time. To obtain the most efficient mixing, the method of Karush[•] was adopted. The dialysis bag was taut and had an airspace provided inside the bag. Equilibrium dialysis studies were carried out at 25 ± 0.1°C. For each metal ion concentration stdudied, it was necessary to determine the time required to reach dialysis equilibrium. It was also necessary to determine that an appreciable amount of polymethacrylic acid did not diffuse through the dialysis membrane in the time required for the metal ions to reach equilibrium.

The time to reach equilibrium was determined from experiments in which dialysis bags containing supporting electrolyte were immersed in the metal solution and shaken for various lengths of time. This showed on analysis of zinc solution, the time required to attain equal zinc ion concentration on both sides of the membrane and also the fraction of zinc ion bound to the

membrane. It was found that five days were required for equilibrium to be attained and that the amount of zinc or copper ions bound to the membrane was negligible.

5.4. (d) Analysis of Solutions at Equilibrium:

5.4.1, Determination of Zinc:

The anlysis of PMA.-free solution for metal ions was carried out titrimetrically. The method of analysis was with the Beckman/Spinco Model 153 Microtitrator.[9] The microtitrator does routine titrations on small volumes. The burette a small glass tubing which contains the titration solution, has a micrometer-driven displacement piston which gives remarkable reproducibility. The volume of titration solution delivered is indicated on a large dial. This can be returned to zero after each titration by pressing the zero button. A vigorous vibration stirrer is immersed in the solution during titration. There is no splashing of small drops. The position of the delivery tip and stirring tip are adjustable. This model of microtitrator has a multi-cup turntable which accommodates 10 disposable 500µl titration cups.

The method of microtitration is an adaptation of the ordinary volumetric analytical method. In principle, a highly alkaline sample of solution is titrated with EDTA in presence of Erio T in the case of sinc or Sulphon Black F in the case of copper. The metal ions present are chelated by EDTA. The absence of cations is indicated by a colour change from wine-red to blue in the case of zinc and from blue to dark green in the case of copper. The microtitration method is a particularly useful one for determining concentration of ions present in trace amounts. It also has the advantage of performing a series of determinations rapidly on small volumes - pf the order of 1 - 200µl. An estimate of about 0.005µl has been made for the accuracy of measurement with this instrument.

Preparation of Calibration Curve:

Zinc or nitrate solutions of known concentrations ranging from 0-25.0 x 10^{-4}M were prepared. 100µl of each solution was titrated with EDTA in the presence of Erio T and buffer and the volume required for complete complexation was determined. A graph of concentration of metal ions versus the corresponding volume of EDTA to completely complex 100µl was plotted to obtain the calibration curve. From the straight line graph, the unknown concentrations of any other solution was determined once the volume of EDTA needed for 100µl of the solution was known.

5.4.2. Procedure :

One hundred microlitre of zinc ion solution outside the dialysis bag was treated with one hundred microlitre of buffer pH 10 and ten microlitre of Eriochrome Black T indicator in a microtitrator cup. The solution was titrated with EDTA solution until the colour changed from wine-red to blue. The concentration of zinc ion was then obtained from a calibration curve previously prepared.

The concentration of the bound zinc ions was determined as a difference in total concentration of zinc inside and outside the bag.

The average number of zinc ions bound per base molar polymer molecule, r, is equal to the molar concentration of bound zinc ion divided by the molar concentration of the polymer present.

5.4.3. Estimation of Copper:

Various analytical methods are available for the estimation of copper. Spectroscopy offers a reliable method of estimating copper ion concentration but the results are unreliable when copper ions are present in trace or very small amounts of the order of 10^{-5}.

Titrimetric method affords a more reliable method of estimating free copper ions and especially the method of ultramicroanalytical system when the ions are present in small amounts and in small volumes.

As in the estimation of zinc, 100µl of copper solution was treated with 100µl of buffer (conc. NH_3). 10µl of Sulphon Black F indicator was added. The solution was titrated with EDTA until the colour changed from blue to deep green to give the end-point. The amount of copper ions present in the solution was obtained from a calibration curve obtained in a similar manner with that of zinc.

Summary of results obtained from dialysis equilibrium studies showing the amount of the metal ions bound and the amount of metal ions added at various degrees of ionization of PMA in 0.10 M KNO_3.

Table 5-A

α	$[Zn^{2+}]_{added} \times 10^4$	$[Zn^{2+}]_{bound} \times 10^4$
0.30	5.0	1.30
	7.5	2.35
	10.0	2.85
	15.0	3.25
	17.5	3.34
	20.0	3.40
0.45	5.0	2.13
	7.5	2.95
	10.0	3.70
	15.0	4.50
	17.5	4.55
	20.0	4.50
0.60	5.0	2.50
	7.5	3.55
	10.0	4.25
	15.0	5.50
	17.5	
	20.0	6.20
	25.0	6.70

Table 5-B

α	$[Cu^{2+}]_{added} \times 10^4$	$[Cu^{2+}]_{bound} \times 10^4$
0.30	2.50	
	3.75	1.45
	5.00	2.25
	6.50	3.00
	7.50	3.30
	10.0	3.80
	12.50	3.75
0.40	2.5	0.80
	3.75	1.80
	5.00	2.65
	6.50	3.50
	7.50	4.00
	10.00	4.70
	12.50	5.10
	15.00	5.10

Table 5-B continued

α	$[Cu^{2+}]_{added}$	$[Cu^{2+}]_{bound}$
0.50	2.5	1.0
	3.75	2.0
	5.00	2.90
	7.50	4.15
	10.0	5.60
	12.5	6.15
	15.00	6.20
0.60	2.5	-
	3.75	-
	5.00	3.10
	6.50	4.20
	7.5	4.90
	10.0	6.75
	12.50	7.20
	15.00	7.10

Tables 5-C and 5-D below show the ratio of the original carboxylate groups bound per metal ion, when maximum binding occurs at various degrees of ionization of PMA.

Table 5-C

α	$[Cu^{2+}] \times 10^4$ at binding	Ratio of original carboxylate groups to Cu^{2+} ion bound.
0.3	3.80	1.97
0.4	5.15	1.94
0.5	6.25	2.00
0.6	7.30	2.05

Table 5-D

α	$[Zn^{2+}]$ at Maximum binding	Ratio of original carboxylate groups to Zn^{2+} ion bound.
0.30	3.35	2.23
0.45	4.70	2.36
0.60	6.75	2.22

5.6. RESULTS AND DISCUSSION

It is quite difficult to find a single physical method which will offer an up-to-date and most satisfactory method for determination of stability constants of bonds between polymeric acids and divalent metallic ions. A lot of background theoretical work to determine the co-ordination numbers and stability constants of small molecules has been done by Bjerrum[12] and for large molecules by Gregor et al[13]. Other workers such as Zubay[14], Mandel and Leyte[15] have applied the same knowledge, with some modifications to study the chelate bonds between large molecules and metallic ions. Bolewski and Lublina[16] have recently applied the theory of multiple equilibria to study the interaction between Zn^{2+}, Cd^{2+} and Cu^{2+} ions and PMA using polarographic technique. Various other analytical methods such as potentiometric titrations[15], spectrophotometric methods[17] have been used to determine the co-ordination numbers and stability constants between copper(II) and PMA.

In the present study, the author has not only made use of the multiple equilibrium theory but has also

considered the type of binding taking place. Two types of reactions have been considered and equations have been obtained and tested for each type of reaction. In the first case, the reaction between M^{2+} and PMA has been considered as a straight forward chelation and secondly as chelation leading to dimerization of the molecules. In the former case the reaction

$$M + (COO^-)_2 = M(COO)_2$$

giving $K_1 = \frac{M(COO)_2}{[M][COO]_2}$ has been considered. From the relation above it can be shown that

$$\frac{1}{r} = \frac{2}{K_1[M_f]} + 2 \quad \ldots\ldots\ldots(5-17)$$

where $r = \frac{(COO)_2 \text{ Total}}{M^{2+}_{bound}}$

If $\frac{1}{r}$ is plotted against $1/M_f$ the slope is $\frac{2}{K_1}$ and an intercept of 2.

In the second case, if the co-ordination is assumed to be two i.e. n = 2, a two co-ordinated complex may be obtained or dimerization involving two separate COO^- groups i.e.

$$M^{2+} + 2COO^- = M(COO^-)_2$$

$$\text{i.e. } K_2 = \frac{M(COO^-)_2}{[M][COO^-]^2}$$

Considering the above equilibrium, it can be shown that

$$\left\{ \left\{ L^2/M_b - 4(L-M_b) \right\} = \frac{1}{K_2 M_f} \right. \quad \text{.....(5-18)}$$

where L = $[COO^-]_{original}$

M_b = Concentration in moles of the bound metal ions

M_f = Concentration in moles of free metal ions.

The above equation should also apply to the equilibrium

$$M^{2+} + 2(COO^-)_2 = M(COO^-)_4$$

where L becomes original concentration of $(COO^-)_2$ resulting in a 4-co-ordinated complex, again either within a single polymer molecule or as a consequence of dimerization.

Results:

Figs. 5.1-7 are the various plots obtained from dialysis equilibrium studies. Figs. 5.1 and 5.2 are plots of amount of divalent cation bound against total amount of divalent cation added. These figures have been obtained from data presented in Tables (5-A) and (5-B). Tables (5-C) and (5-D) show the co-ordination number $n(\cong [COO^-]/[M^{2+}]_{bound})$ i.e. maximum number of carboxylate groups bound per metal ion when maximum amount of metal ion is bound. This is based on the

assumption that nearly all COO^- groups originally present are bound and this is probably true at high metal ion concentration. These have been derived from figures 5·1 and 5·2.

5.6.2. Discussion:

In the case of Zinc-PMA complex a smooth curve which finally levels off is obtained for each degree of ionization studied. The levelling off is obtained when the ultimate binding capacity has been reached. In this case the co-ordination number has been found to be approximately equeal to two as seen from table (5-D).

A situation slightly more difficult to analyze is encountered in copper-PMA solutions. The shapes of the curves in figures 5·2 suggest two types of equilibria and probably indicating two types of complexes; one existing at high charge density and low metal ion concentration and the other at high charge density and high metal ion concentration. (A similar observation has been made in the potentiometric titrations). If the former complex exists i.e. high $[COO^-]/[M^{2+}]_{bound}$, it will probably correspond to four carboxylate groups bound per metal ion while the latter will probably give

as ratio 2:1 the quantity $[COO^-]/[M^{2+}]_{bound}$. The latter has been found to be true as recorded in table (5-C).

Figures 5-1 and 5-2 reveal that binding increases with increasing M^{2+} until the ultimate binding is reached - which probably gives a most stable complex. This means that the ratio $[COO^-]_{free}/[M^{2+}]_{bound}$ also decreases as binding takes place probably due to absence of available free COO^- groups caused by metal binding. When maximum binding has taken place, the ratio of $[COO^-]/[M^{2+}]_{bound}$ remains unchanged and this means that a stable complex has been obtained. At this stage all or nearly all charged sites must have been bound to the metal ions. Figures 5-1 and 5-2 also indicate that binding decreased with decreasing degree of ionization. This is to be expected because of changes in the net charge carboxylate sites on the polyion.

Figure 5-7 shows a plot of maximum metal binding against the degree of ionization. The figure shows that in both cases, the amount of metal bound is directly proportion to α. The figure also reveals that when the value of M^{2+} bound for zinc and copper at the same value of α are compared, more copper is bound to the polymer than zinc. These findings seemingly indicates

that the binding is dependent almost entirely on the number of charged sites available assuming exchange equilibrium existing is very small. These findings also suggest that the copper ions show a greater affinity to bind PHA than zinc.

5.6.2.1. Effect of Binding on Polyion Configuration:

At the degrees of ionization at which the present study was carried out, the molecule which would be expected to be stretching out to a rod would not be forced to do so because of the high ionic strength of the medium. The high concentration of K^+ ions would produce a considerable screening effect for the COO^- groups, consequently a large reduction in electrostatic repulsive energy and the molecule would still exist in a high degree of coiling. Under these conditions, there are two ways in which interaction can occur. These are only suggestions since the data presented here does not give a detailed picture of the structure of the complexes. Binding can take place by (i) intrachain interactions and (ii) interchain interactions.

(i) In intrachain interactions, binding of a cation to carboxylate groups on the same polymer chain

can take place. In this case two near neighbours are involved. Intrachain interactions may lead to coiling of the molecules at low degrees of ionization. Intrachain interactions involving more than two carboxylate groups would be difficult (but not impossible) on account of stereochemistry. If more than two carboxylate groups are bound, interchain interactions would probably be favoured. For polymethactylic acid, the following arrangement may be favoured in intrachain interactions.

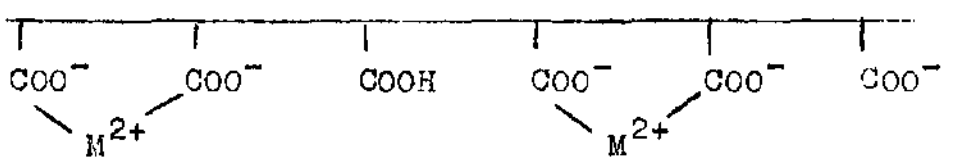


Figure (a)

(ii) Interchain interactions involves binding of a divalent metal ion to two carboxylate groups one from each PMA chain. In the present work, the ratio of the charged carboxylate groups to the bound metal ions at maximum binding capacity, has been found to be two. Bearing this in mind, interchain interactions can only be explained in terms of dimerization of the macro- molecules. This means that two chains have to align

themselves in such a way that the M^{2+} ions will form a bridge between them. Whether this will be possible or not depends on the ionic strength of the medium and the concentration of M^{2+}. At low ionic strength and low M^{2+} concentration, two highly charged macromolecules will find it difficult to approach each other because of the strong electrostatic force of repulsion. In this case, interchain linkage may not be feasible. However, at high ionic strength e.g. I = 0.1 and high M^{2+} concentration, the electrostatic force of repulsion due to the charged sites will be reduced considerably due to screening caused by K^{+} ions and binding caused by Cu^{2+} and Zn^{2+} and alignment of two polymer chains will be possible. The following type of structure will probably be favoured for interchain interaction involving two carboxylate ions binding to one divalent cation.

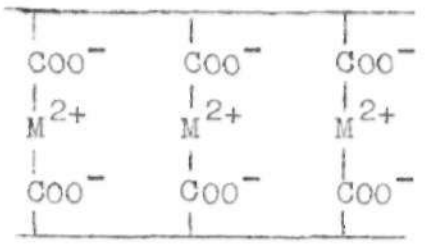


Figure (b)

Both types of complexes illustrated in figures (a) and (b) could be very stable.

Another possibility is dimerization of the macromolecule involving four carboxylate ions. In this case, each chain will supply two carboxylate groups to the M^{2+} ion.

5.6.2.2 Stability of Cu-PMA and Zn-PMA Complexes:

In an attempt to evaluate the binding constants of the complexes formed equations 5 - 17 and 5 - 18 have been obtained. Figures 5.3 and 5.4 show plots obtained from equation 5 - 17 for zinc and copper respectively. Figure 5.3 shows plots for three different degrees of ionization of the macromolecule, while figure 5.4 shows plots for four different degrees of ionization. It is evident that there are a number of differences in the shapes of the curves obtained. In the case of zinc-PMA complexes, all the points fall on a single straight line for all the degrees of ionization. This probably suggests that a single type of complex is formed. This is also indicated in Fig. 5.1. The intercept should give n which is seen to be approximately 2 and this is the value predicted by theory equation 5 - 17 . The equation also predicts a single binding constant invariant with α. This would support the reaction

$$M^{2+} + (COO^-)_2 = M(COO^-)_2.$$

The binding constant obtained is equal to 1.844×10^3.

In the case of copper i.e. figure 5.4, the plot for each degree of ionization give definite curves (concave upwards). The fact that curves and not straight lines are obtained suggests that a complex of varying stability or varying co-ordination number is formed at each stage of the reaction. In all cases, however, the graphs extrapolate to 2 which is the value predicted by equation 5 - 17.

Figures 5.5 and 5.6 show the plots derived from the expression in equation 5-18. The shapes of the curves obtained here are quite different from the previous ones i.e. figures 5.3 and 5.4. Equation 5-18 predicts that the plot should give a straight line passing through the origin. What is obtained however is quite different from that expected from theory. In both figures all the curves converge to the origin. This shows that there is deviation of experimental findings from theory. In the case of zinc, it is seen that as α increases, the plots tend to approach the theoretical prediction. In the case of copper, there is no particular order. It is here recalled that in the present work and with the new equations being tested, it is quite difficult to estimate the values of

K with absolute certainty. An attempt has been made in the case of zinc where the linear portions of the curves in figure 5·5 have been extrapolated. The following values have been obtained for the binding constant at various degrees of ionization:

$\alpha = 0.30$, $K = 8.0 \times 10^5$; $\alpha = 0.45$, $K = 10.16 \times 10^5$ and $\alpha = 0.60$, $K = 13.45 \times 10^7$.

As seen from the data presented above, binding constant increases with increasing α. These values could not be compared with those of previous workers because of the use of different expressions. Nevertheless, the author is happy to note that the value of the co-ordination number obtained is in agreement with those of Bolewski and Lublina[16] and with those of Mandel and Leyte. The present result is however in contradiction with those of Morawetz[17].

5.7. Conclusion:

1. It has been found that both copper and zinc interact quite strongly with PMA to form chelate complexes with copper interacting more strongly than zinc.

2. Expressions have been obtained to enable the author to calculate the binding constant K and the co-ordination number n.

3. Each cation form complexes involving two carboxylate groups to one metal ion and that the mode of binding could be either intramolecularly or intermolecularly depending on the cation concentration, ionic strength and the degree of ionization.

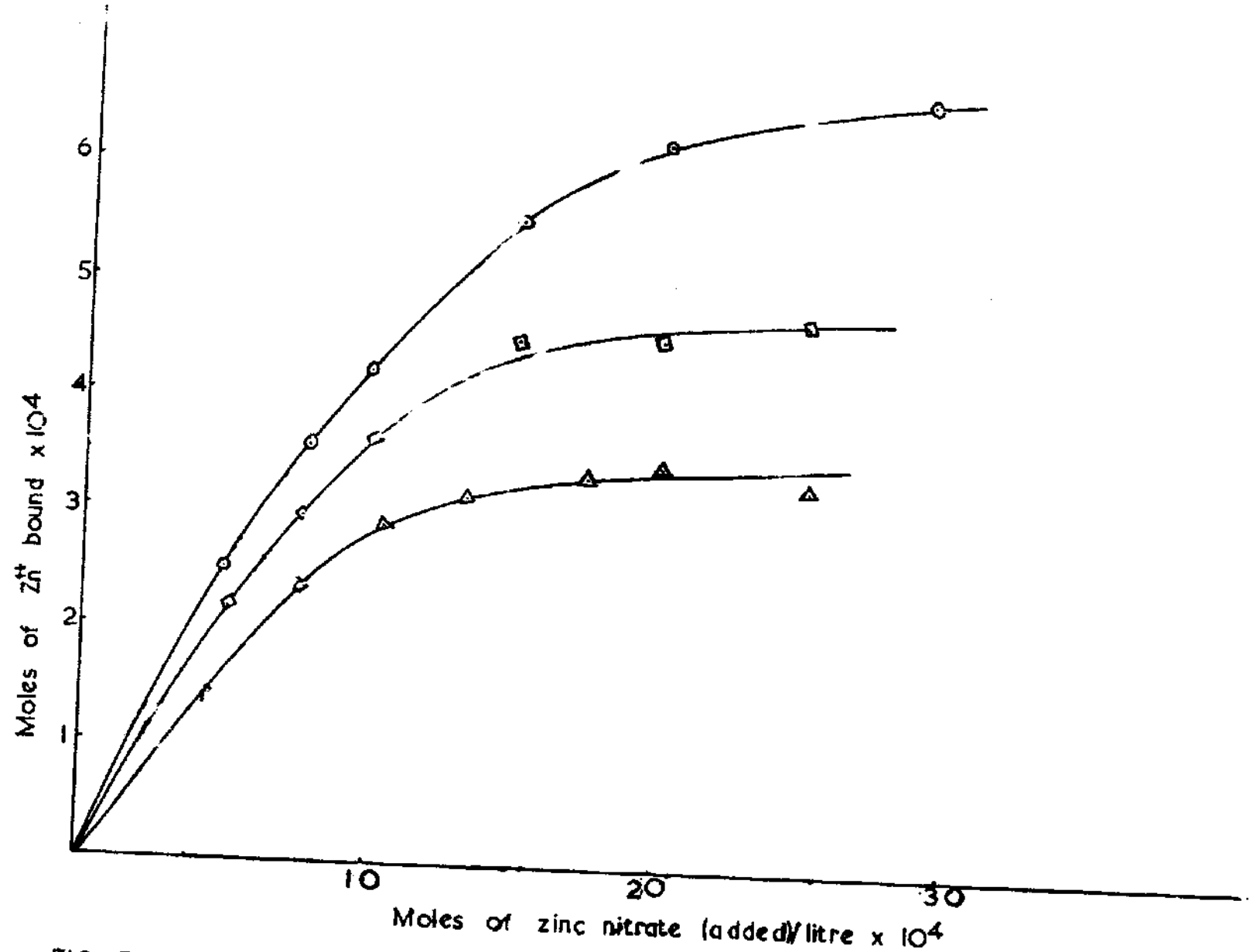


FIG 5.1 Dialysis of PMA against zinc nitrate at three degrees of ionization [PMA] = 2.5×10^{-3}M; I = 0.1; ⊙, $\alpha = 0.60$; □, $\alpha = 0.45$; △, $\alpha = 0.30$

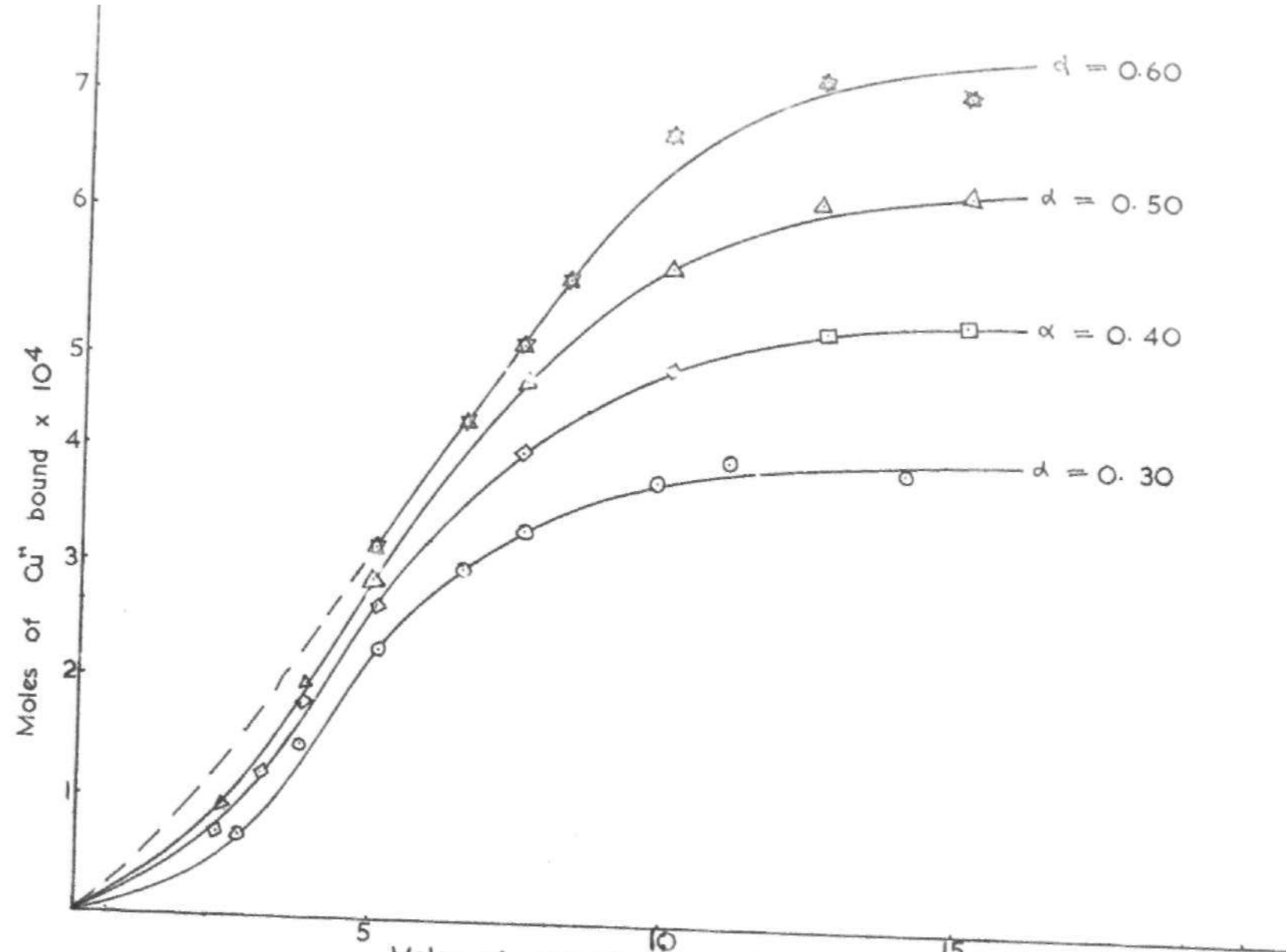


FIG 5.2 Dialysis of PMA against copper nitrate at four degrees of ionization at 25°C [PMA]=2.5 X 10^{-3}M I = 0.10

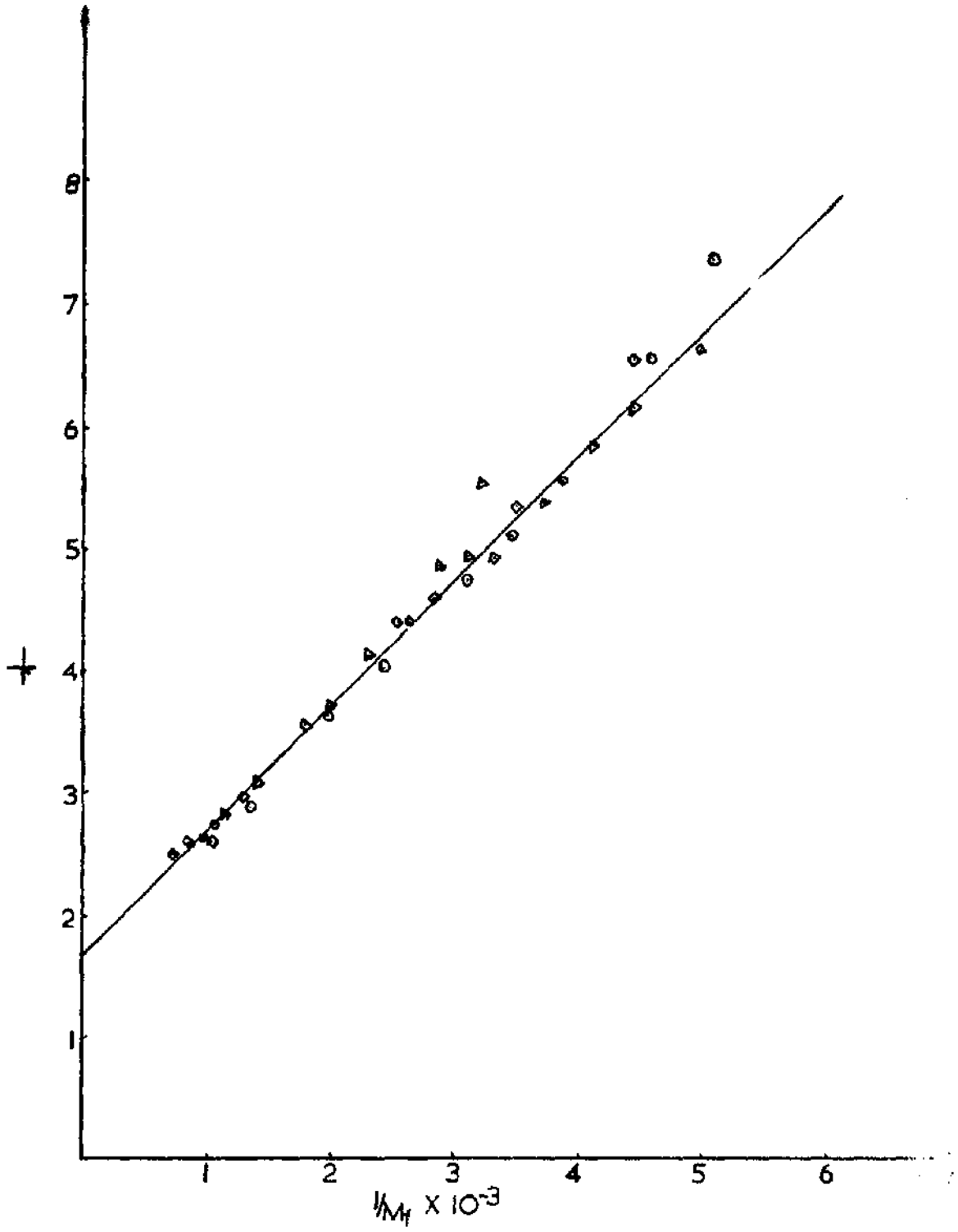


FIG 5.3 Computation of stability constants and co-ordination number of Zn–PMA complexes
[PMA] = 2.5 X 10^{-3}M ; I=0.10 .
⊙–$\bar{n}$ = 0.30; Δ–$\bar{n}$ = 0.45 ; ⊡ –$\bar{n}$ = 0.60 .

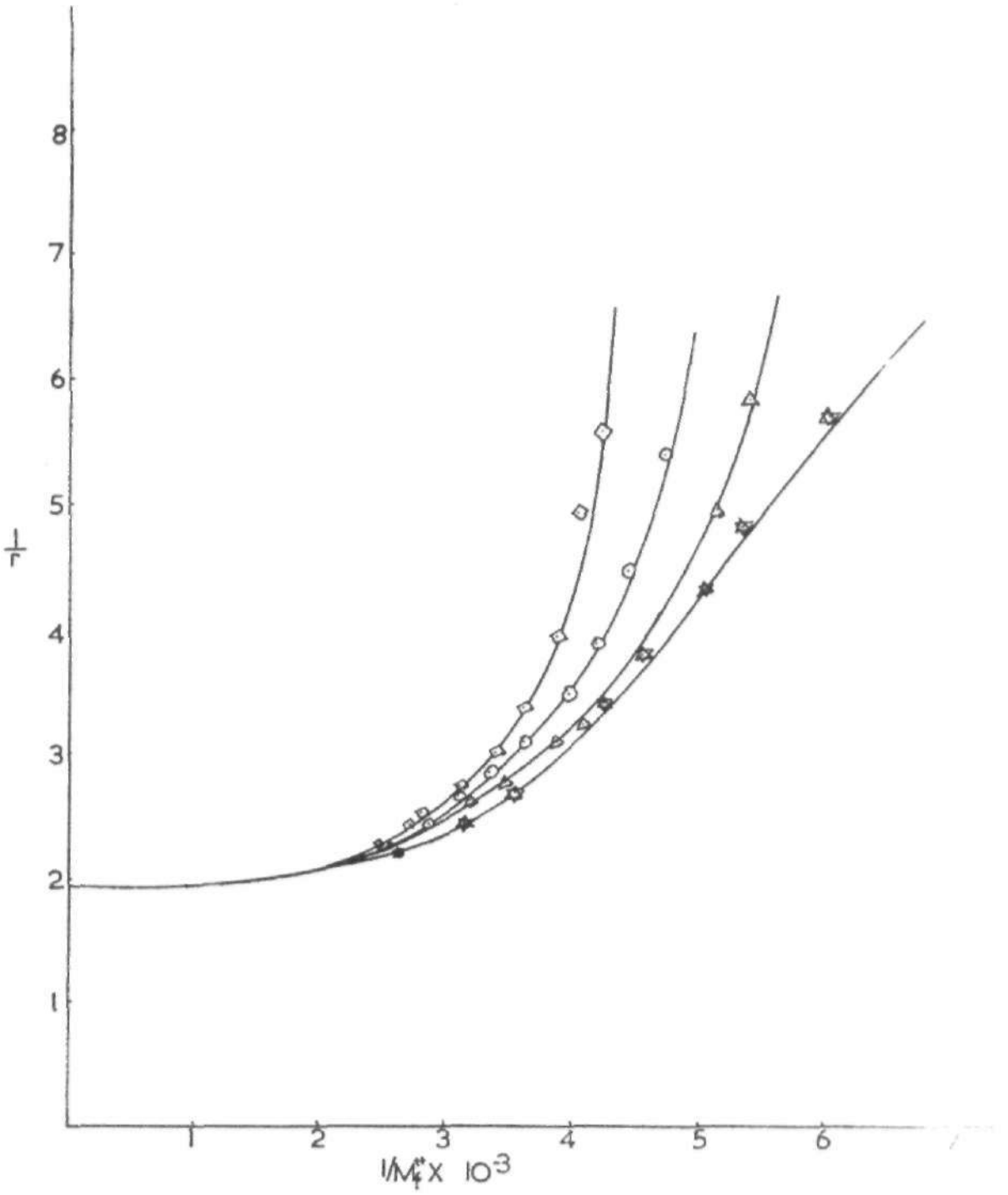


FIG 5.4 Computation of stability constants and co-ordination number of Cu—PMA complexes

[PMA] – 2.5×10^{-3}M I = 0.10

□ – α = 0.3 ; ○ – α = 0.4 ; △ – α = 0.5 ; ✲ – α = 0.6

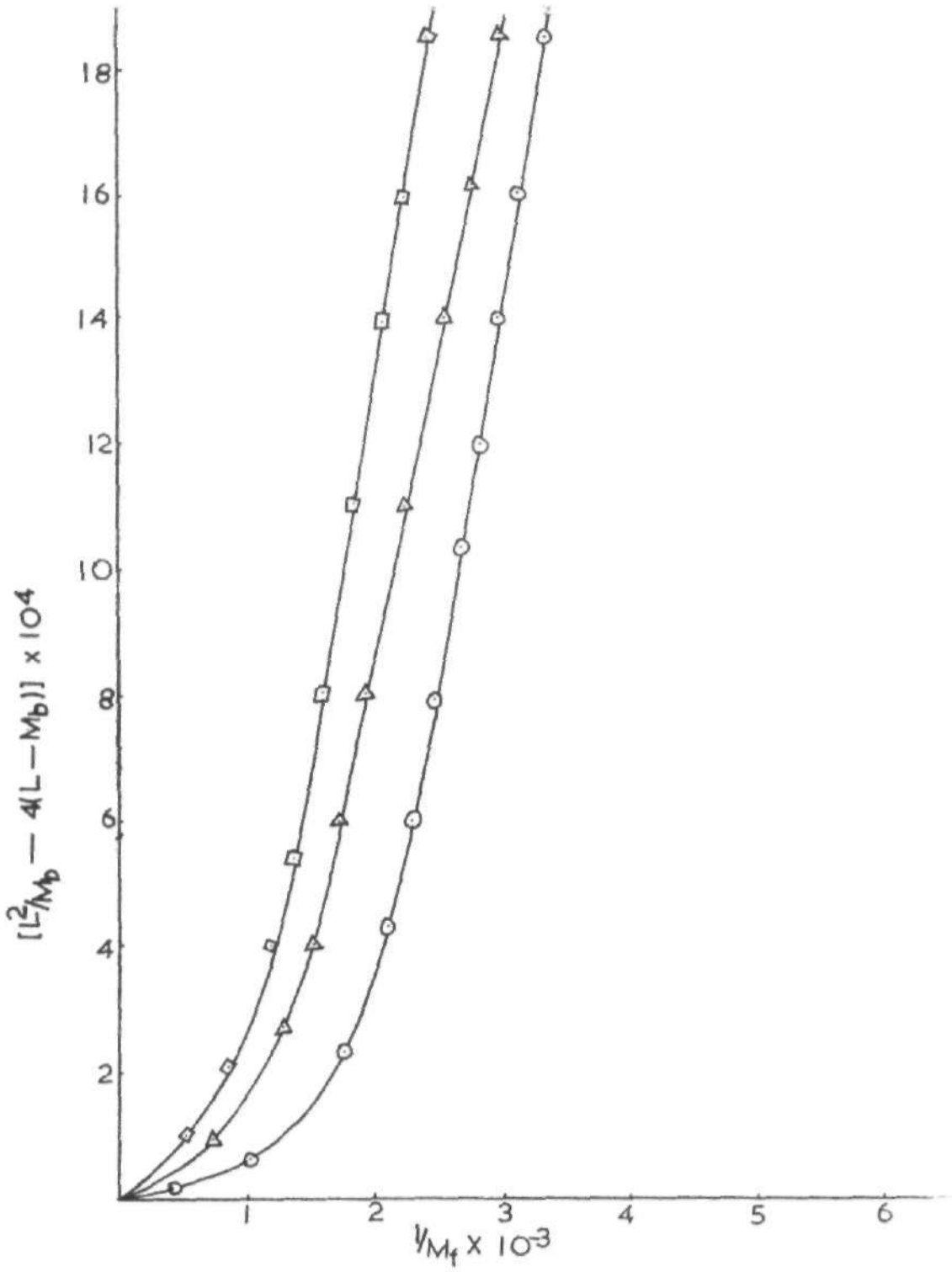


FIG 5.5 Computation of stability constants for Zn—PMA complexes at 25°C
[PMA] = 2.5×10^{-3}M ; I = 0.10 .
⊙-α = 0.30 ; ▲-α = 0.45 ; ⊡-α = 0.60 .

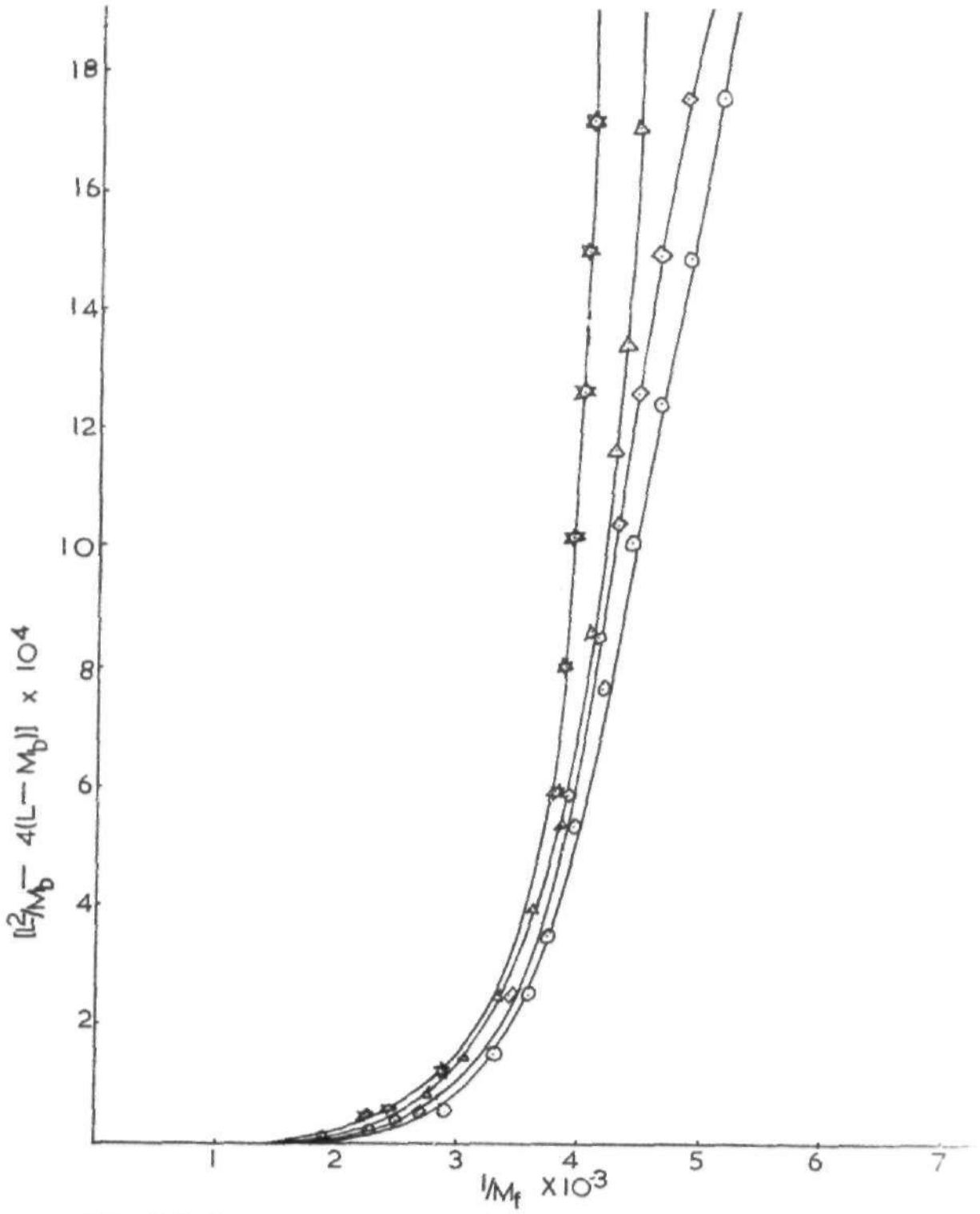


FIG 5.6 Computation of stability constants for Cu– PMA complexes at 25°C. [PMA]=2.5 X 10^{-3} M ; I= 0.10
★-α=0.30 ; △-α=0.40; ⊙-α=0.50; ⊡-α=0.60

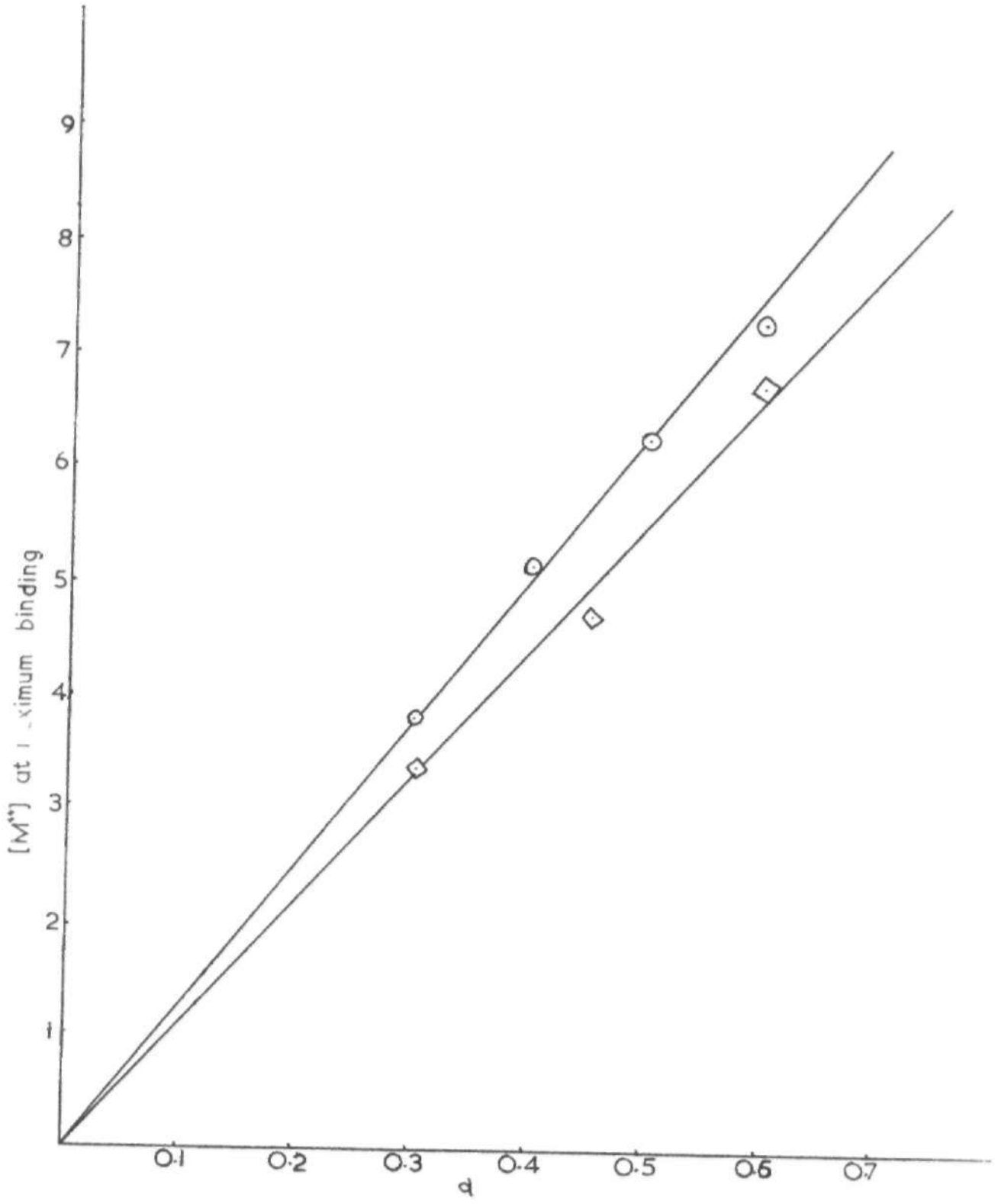


FIG 5.7 Plots for two metal ions at maximum binding
o — copper ; □ — zinc .

5.8 . REFERENCES

1. Osborn W.A., J. Physiol. 34, 84, (1906).
2. Kotliar, A. M. and Morawetz, H.; J. Am. Chem. Soc. 77, 3692, (1955).
3. Donnan, G. F.; Chemical Reviews 1, 73, (1924).
4. Ostwalt, W. Address to Sterling Chemistry Laboratory (189).
5. Donnan, G. F. and Guggenheim, E. A.; Z. Physik, Chem. (Leipzig) 162, 346, (1932).
6. Warburg, O.; Biochem. J, 16, 307, (1922).
7. Vogel, A. I., Quantitative Inorganic Chemistry. pp.433, 441.
8. Karush, F. and Sonenber, M.; J. Am. Chem. Soc. 71, 1369, (1949).
9. Beckman Instrument Inc. Technical Bulletin No. 6071C, (1960).
10. Guggenheim, E. A.; Thermodynamics, pp.337-338.
11. Horowitz, M. G.; Analytical methods of Protein Chemistry 2, 133, (1960).
12. Bjerrum, N., Z. Physik Chem, 106, 214, (1923)

13. Gregor, H. P., Luttinger, L. B. and Loebl, E. M., J. Phys. Chem. 59, 34, (1955).

14. Zubay, C., J. Phys. Chem. 61, 377, (1957).

15. Mandel, M. and Leyte, J. C., J. Poly. Sc. A2, 2883, (1964).

16. Bolewski, K. and Lublina, M., Roczniki Chemi. Ann. Soc. Chim. 44, 647, (1970).

17. Morawetz, H., J. Poly. Sc. 17, 442, (1955).

Chapter 6

POTENTIOMETRIC TITRATIONS

CONTENTS

		Page
6.1.	Theory	180
6.1.1.	Theoretical analysis of titration curves	180
6.2.	Experimental	198
6.2.1.	Potentiometric Titration of PMA ..	198
6.2.1.1.	Titration at Changing ionic Strength ..	198
6.2.1.2.	Titration at Constant ionic Strength ..	199
6.2.1.3.	Potentiometric Titration of PMA with zinc nitrate and copper nitrate solutions	200
6.3.	Results and Discussions	202
6.3.1.	Results	203
6.3.2.	Discussion	204
6.3.2.1.	Potentiometric behaviour of aqueous solution of PMA	204
6.3.2.2.	Potentiometric behaviour of PMA solutions in the presence of $Cu(NO_3)_2$ and $Zn(NO_3)_2$	209
6.3.2.3.	Transformation of titration curves to complex formation curves	217
6.3.2.4.	Effect of ionic strength	224
6.4.	R e f e r e n c e s	226

POTENTIOMETRIC TITRATIONS

6.1. Theory:

The equilibria which exist between hydrogen ions and macromolecules which are acidic, basic or amphoteric in nature have been studied more extensively than most other equilibria in polyelectrolyte systems. This is due at least in part to the fact that pH measurement provides an easy means of determining the activity of the hydrogen ions over a range from about unit activity to 10^{-14}.

6.1.1. Theoretical Analysis of Titration Curves:

Before considering the ionization equilibria of polymeric species with a large number of ionizable groups, it is necessary to deal with the titration of materials such as monocarboxylic and dicarboxylic acids.

In dilute solutions, a weak monobasic acid HA can be described by the following equations.

$$HA = H^+ + A^- \quad \ldots\ldots\ldots (6-1)$$

and the ionization constant k expressed by

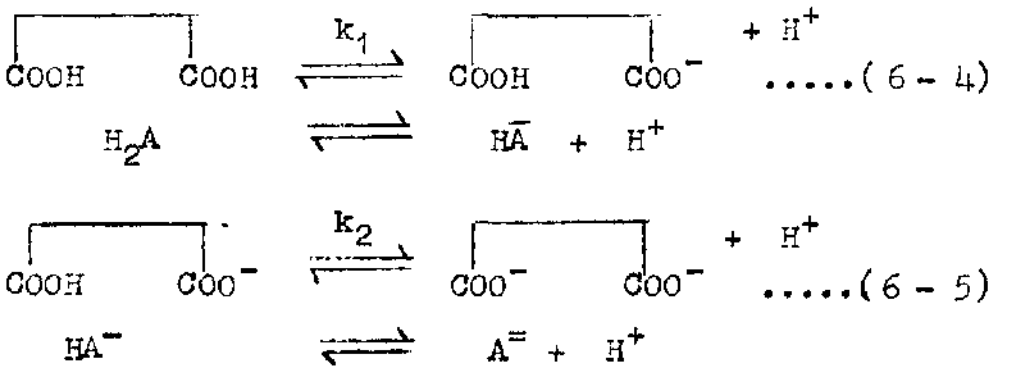
$$k = \frac{[A^-]a_{H^+}}{[HA]} = \frac{\alpha}{1-\alpha} a_{H^+} \quad \ldots\ldots\ldots (6-2)$$

where $\alpha = A^-/C_n = \frac{k}{a_{H^+}} + k \quad \ldots\ldots\ldots (6-3)$

and these expressions assume $\gamma_{A^-} = \gamma_{HA}$.

In the above equations, k is the ionization constant, α is the degree of ionization of the carboxyl groups, C_n is the concentration of the acid in equivalents (moles) per litre, a_{H^+} is the activity of hydrogen, γ_{A^-} and γ_{HA} are the activity coefficients of the species A^- and HA respectively and the bracketed quantities are the analytical quantities of the various entities. From the above relationship it can be seen that the pH at any degree of ionization can be calculated provided k is known. It can also be seen that as a consequence of equation 6-3, that pH depends on α only and not on the concentration of the acid.

The ionization equilibria in a dibasic acid may be represented schematically by



.....(6 - 4)

.....(6 - 5)

The ionization constant k_1 and k_2 are defined as

$$k_1 = \frac{[HA^-]a_{H^+}}{[H_2A]} \quad \text{.....(6 - 6)}$$

$$k_2 = \frac{[A^=]a_{H^+}}{[HA^-]} \quad \text{.....(6 - 7)}$$

and the degree of ionization α is given by

$$\alpha = \frac{[HA^-] + 2[A^-]}{C_n} = \frac{1}{2}\left[\frac{\frac{k_1}{a_H} + \frac{k_1k_2}{(a_{H^+})^2}}{1 + \frac{k_1}{a_{H^+}} + \frac{k_1k_2}{(a_{H^+})^2}}\right] \text{...(6 - 8)}$$

If the ionizable groups are far from each other, the ease of ionization of each of the carboxyl groups will be independent of the state of ionization of the other. The titration curve will then be indistinguishable from that of a monocarboxylic acid with an ionization constant k^o and a concenstration equal to the stoichiometric carboxylic concentration of the dicarboxylic acid (C_n). For any overall degree of ionization α_i, there will be a fraction $(1 - \alpha_i)^2$ of unionized, and $2\alpha_i(1 - \alpha_i)$ of singly ionized and α_i^2 of doubly ionized molecules. The identical result is obtained if to the first ionization step is assigned and equilibrium

constant $k_2 = k^o/2$, since two carboxyls may lose a proton in the first step, while a proton may attach itself to two alternative sites in the second equilibrium.

If the carboxyls are sufficiently close to one another, the removal of the proton will be impeded by the electrostatic attraction of the neighbouring carboxylate group. To overcome it, the molar free energy for the second ionization step will have to be increased by electrostatic free energy of ionization" ΔG^i_{el} given by

$$\Delta G^i_{el} = N\int_{r=r_e}^{r=\infty} \frac{e^2}{Dr^2}dr = Ne^2/Dr_e \quad \ldots\ldots\ldots\ldots (6\text{-}9)$$

D is the dielectric constant of the medium and r_e is the distance between the two ionizable groups and the ratio of the first and second ionization constants becomes then $\frac{k_1}{k_2} = \frac{1}{4} \exp(-\Delta G^i_{el}/RT)$ $\ldots\ldots\ldots (6\text{-}10)$

As a consequence of equation 6-10, if there is no interaction between the carboxyl groups, the ratio $\frac{k_2}{k_1}$ should be equal to 4^1.

If r_e is small, the proper choice of D usually presents some difficulties. Kirkwood and Westheimer[2] pointed out that it is incorrect to use the value of the dielectric constant of water (~ 80). Since most of the electrical lines of force will pass through the organic

molecule, which is charaterised by a much lower dielectric constant (~ 2). They showed that the experimental results can be accounted for by using a model in which the ionic charges are placed on an ellipsoid with the dielectric constant of an organic substance and this ellipsoid is immersed into the aqueous medium. It should be noted, however, that such agreement between predicted and experimental data presupposes a good knowledge of the conformational distribution of the dicarboxylic acid in its unionized, singly ionized and doubly ionized state. For instance, Eberson[3], reported that in the meso and the raceionic forms of α,β-dialkylsuccinic acids



the value of $\frac{k_2}{k_i}$ may differ by a factor as large as 10^4 if the R groups are sufficiently bulky.

For a polymeric acid having p monomer units per polymer molecule, the apparent stepwise dissociation constant is defined by

$$K_1 = \frac{[H_{p-1}A]a_{H^+}}{[H_pA]} \quad \text{.....(6-11)}$$

$$K_n = \frac{[H_{p-n+1}A]a_{H^+}}{[H_{p-n+1}A]} \quad \text{.....(6-12)}$$

Hence the degree of ionization α is given by

$$\alpha = \sum_{n} \frac{n\left[H_{p-n+1}A\right]}{C_n} \qquad \ldots\ldots\ldots\ldots\ldots\ldots \quad (6-13)$$

$$\text{i.e. } \alpha = \frac{\sum_{n=0}^{n=p} n (a_{H^+})^n \prod_i K_i}{\sum_{n=0}^{n=p} \frac{1}{a_{H^+}} \prod_i K_i} \qquad \ldots\ldots\ldots\ldots\ldots\ldots \quad (6-14)$$

where C_n is the concentration of the acid in equivalents (moles) per litre. In the above expressions the hydrogen ion activity has been used rather than hydrogen ion concentration, because the pH measurement, although it is not a measure of the activity of hydrogen ions as one would define it, it is closer to it than it is to a measure of hydrogen ion concentration. However, hydrogen ion activity is considered to be $pH \equiv -\log a_{H^+}$ in all the work done. The constants K_i which occur in equation 6-15 are stepwise apparent dissociation constants for a reaction such as $-COOH \rightarrow -COO^- + H^+$ at single sites. The apparent dissociation constant K_i is not a constant but is a function of the pH or degree of ionization. It is however practically impossible to determine the various K_i's for each dissociating site. However many authors have developed empirical formulae which relate the potentiometric behaviour of polymeric acids to a single dissociation constant.

It was Linderstrom - Lang[4] who first applied the theories of Bjerrum[5] and Debye to the dissociation of polyelectrolytes. He derived equations for a hypothetical polyvalent ampholyte which were particularly designed to describe the effects of ionic strength on the dissociation of proteins. Unfortunately, data adequate for a comprehensive test were not available at the time it was developed. Von Multrat[6] applied the Law of Mass Action to the polyvalent ampholyte. He pointed out that the dissociation curve of such materials can be simulated by that of an appropriate mixture of univalent acids. A number of reconstructions of proteins have been made on this principle[7,8]. There is however a considerable latitude in the choice of the number of different univalent acids which shall be employed, the proportions in which they shall be mixed, and the dissociation constants which shall be assigned to them. The choices made in a successful reconstruction, therefore, bear no necessary relation to the ionizing groups in the protein. Moreover, this method of approach affords no rational basis for a description of the important effect of the ionic strength on the shape of the curve.

Several other workers have produced empirical equations to describe the titration behaviour of polymeric

acid solutions under varying conditions. Kern[9] and Katchalsky and Spitnik[10] found that a single titration curve of polymeric acid may be described empirically by constants pK and n according to the following equations.

$$pH = pK^* + BpH \quad \text{.....(6-16)}$$

$$\text{and} \quad pH = pK_a - n \log \frac{1-\alpha}{\alpha} \quad \text{.....(6-17)}$$

Equation 6-16 was that obtained by Kern and equation 6-17 that due to Katchalsky and Spitnik. This is a modified form of the famous Henderson-Hassebalch equation:

$$pH = pK - \log \frac{1-\alpha}{\alpha} \quad \text{.....(6-18)}$$

Where pK^*, B, pK_a and n are constants for a given titration. Nagasawa and Rice[11] pointed out that equation 6-16 and 6-17 are the same if $n = 1/(1-B)$.

Katchalsky and Spitnik worked extensively on potentiometric titrations of PMA at different concentrations, different molecular weights, in the presence and absence of neutral salts as well as in dioxane-water mixtures. From their own data[10] and that of Kern[9] it was deduced that titration curves of polymeric acids of concentration C and polymerization degree P show no inflexion points and in this respect resemble the titration curves of monobasic acids of concentration PC. Katchalsky and Spitnik[10] found from their data that the pK and n are

independent of molecular weight. Both pK and n show a definite tendency to decrease with increasing concentration. This tendency was shown to be an apparent one on introducing activity corrections. This correction presuposes that the Debye-Huckel ionic atmosphere is built round each group. The equation obtained was

$$pH = pK - 2\log\frac{Pc - b}{C} - \sqrt{b} \quad .....(6-19)$$

where P is the degree of polymerization, c is the concentration of the polymer and b is the stoichometric concentration of anions. Equation 6-19 did not fit experimental data and an empirical constant λ had to be introduced.

$$pH = pK - 2\log\frac{Pc-b}{C} - \lambda\sqrt{b} \quad .....(6-20)$$

λ varies from 1 to 4 but the most frequent value is 3. The physical meaning is that the ionic atmosphere is built round more than one group but less than two on the average.

Generally, neutral salts extert a strong influence on the pH of solutions of PMA. The pH decreases in the presence of salts, the decrease in pH increasing with the salt concentration. Katchalsky and Spitnik[10] conducted a series of potentiometric titrations in the presence of different concentrations of sodium chloride.

They found that equation 6-20 accounts adequately for the decrease in pH at lower ionic strength. At higher salt concentrations, the salting out effect comes into operation and a corresponding term was added, transforming equation 6-20to

$$pH = pK - 2\log \frac{Pc-b}{C} - \lambda\sqrt{\mu} + K_s\mu \quad ..(6-21)$$

where K_s denotes the salting out constant. The validity of equation 6-21 was tested by titrations of PMA in dioxane-water mixture.

The description of titration curves of polymeric acids by an equation of the type exemplified by the following equation

$$pH = pK - n\log \frac{1-\alpha}{\alpha} \quad .....(6-18)$$

was found to suit the titration curves of certain proteins oalong the nearly linear segment of the curve[11]. Cannan[11] described the validity of equation 6-18 as being due to its approximation to a more fundamental equation based on the calculations of Linderstrom-Lang[4]. The equation used by Cannan, Kirbrick and Palmer[12] in their investigation on the titration curves of egg albumin and lactalbumin was

$$pH = pK - \log \frac{1-\alpha}{\alpha} - 0.868w(n-\alpha m)....(6-22)$$

where ω denotes $\frac{\epsilon^2}{2DkT}\left(\frac{1}{b} - \frac{\kappa}{1+\kappa a}\right)$, ϵ is the electronic charge, D is the dielectric constant, k is the Boltzman constant, b is the radius of polymeric ion, a is the radius of nearest approach of opposite ions, $\frac{1}{\kappa}$ is the thickness of the ionic atmosphere in the Debye-Huckel theory, m the number of carboxyl groups and n the number of cationic groups. In the case of PMA (or polyacids in general) it carries no cationic groups (n = o) and the number of carboxyl groups m is equal to the degree of polymerization P (m = P) then equation 6-22 transforms to

$$pH = pK + 0.868\alpha\omega p - \log\frac{1-\alpha}{\alpha} \quad \text{.....(6-23)}$$

At constant ω, this formula should yield a straight line for plot of α against $pH + \log\frac{1-\alpha}{\alpha}$. A comparison of the pH values of two curves of different ω values gives the following relation between pH and α.

$$\Delta pH = 0.868\alpha(\omega_1 - \omega_2) \quad \text{.....(6-24)}$$

Neither equation 6-23 nor 6-24 was found to hold for the titration of polymethacrylic acid. It might be expected that the spherical model underlying the calculations of Linderstrom-Lang[4] is untenable when applied to fibrillar, randomly kinked molecules.

Kagawa[13] has proposed an empirical formula for the titration of polymeric acids.

$$2pH = pK_s - \log\frac{(1-\alpha)^{m+1}}{\alpha^m} - \log C_m \quad \text{.....(6-25)}$$

where C_m denotes the polymer concentration, and pK_s and m are constants. It has been shown by Katchalsky and co-workers[14] that equation 6-25 is the same as equation 6-17 provided n is equal to $\frac{2m+1}{4}$ and pK is equal to $(pK_s + \log 2 - \log C_m)/2$. Hence the limitations on the use of empirical constants pK and n of equation 6-17 apply equally to the constants pK_s and m in equation 6-25.

Recently, Spenser[15] showed that the titration constant pK^* which appears in equation 6-16 differs from pK_a and pK_s which appear in equation 6-17 and 6-25 respectively.

$$npK^* = pK_a = pK_s \quad \text{.....(6-26)}$$

Spenser[15] showed that pK^* is a characteristic constant for a polycarboxylic acid. It is sensitive to changes in ionic strength and concentration, while pK_a and n decrease smoothly with increasing ionic strength or concentration. Spenser showed from his titration data, that pK^* is a common point in the family of curves obtained when pH is plotted against $\log \frac{1-\alpha}{\alpha}$ in equation 6-17. The plot of pH/n against $\log \frac{1-\alpha}{\alpha}$ reduces the family of curves to a single line which is independent of ionic strength.

The theory of titrations of ionizable polymeric chains under conditions where only electrical interactions

between neighbouring ionized groups need be considered has been formulated by Marcus[16]. If Fe is the free energy required to move two equivalents of isolated ionized groups to positions on the chain where they form nearest neighbour pairs, then

$$K_{app} = K_{\circ} \frac{\alpha_i(\sqrt{x+1} - 2\alpha_i+1)}{(1-\alpha_i)(\sqrt{x+1} + 2\alpha_i-1)} \quad \ldots\ldots(6\text{-}27)$$

where $x = 4\alpha_i(1-\alpha_i)\left[\exp(\Delta Fe/RT) - 1\right]$.

If $\Delta Fe = 0$, the titration behaviour of the polymer reduces to that of the monofunctional analog. On the other hand, if $\frac{\Delta Fe}{RT} \gg 1$, the ionization of the neighbouring groups becomes very difficult and alternate groups on the polymeric chain tend to be ionized first. Only when $\alpha_i > 0.5$ will it be necessary to ionize the intermidiate groups, a process which is being resisted by the electrostatic interactions of two neighbouring ionic charges. The polymer then approximates the behaviour of a dibasic acid or base whose two ionization constants differ by a factor of $\exp.\left[2\Delta Fe/RT\right]$. However, such a behaviour has never been observed with polymeric acids, although with polymeric bases nearest neighbour interactions do dominate the titration behaviour even when the concentration of simple electrolytes is relatively low[17].

Many other authors have proposed theoretical equations to analyse the potentiometric behaviour of polyelectrolytes[18,19] and their attempt may be summarised by the following equation:

$$pH = pK_o - \log \frac{1-\alpha}{\alpha} + \frac{0.4343}{kT} \left(\frac{\partial Fe}{\partial V}\right)_\kappa \quad ..(6-28)$$

where pK_o is an intrinsic dissociation constant characteristic of the ionizable group of the polymer and independent of the ionic strength, Fe is the electrostatic free energy of the ionized polyelectrolyte molecule carrying V negatively charged groups and κ is the inverse Debye radius determined by the concentration of the small ions in the solution. On the other hand, equation 6-29 describes the potentiometric behaviour of polybases

$$pH = pK'_o - \log \frac{\beta}{1-\beta} - \frac{0.4343}{kT} \left(\frac{\partial Fe}{\partial \xi}\right)_\kappa \quad ....(6-29)$$

where in this case, pK'_o represents the dissociation constant of the cationic acid conjugate to the single basic group of the polymer, β is the degree of ionization of the polybase and ξ is the number of positive ionized groups carried by the polymer.

From equations 6-28 and 6-29 one would expect the electrochemical behaviour to be charaterised by a single dissociating constant, but also to depend on the way in which the electrostatic field energy varies with the number

of charged groups and with the ionic strength of the medium.

Apart from Katchalsky et al[18], Arnold et al[19] Marcus[16] and Katchalsky[17] et al various other people[20-25] have made attempts to calculate electrostatic free energy. Katchalsky and Lifson[25] proposed the following expression for a randomly kinked polycarboxyllic acid

$$\left(\frac{\partial Fe}{\partial V}\right)_{\kappa} = \frac{2\,Ve^2}{Dh}\left[\lambda n\left(1+\frac{6h}{Kh_o^2}\right) - \frac{\alpha(S_1-S_o)}{2S}\,\frac{6h/Kh_o^2}{1+6h/Kh_o^2}\right] \quad .(6\text{-}30)$$

and a corresponding equation holds for $\left(\frac{\partial Fe}{\partial \xi}\right)_{\kappa}$ i.e. for polybases. Here h is the end to end distance of the ionized, polymolecule, stretched by the electrostatic repulsion of the V charges spread over the molecule, h_o is the end to end distance of a discharged molecule. If this equation is now introduced into equation 29 for potentiometric titrations of polymeric acid, we get,

$$pH = pK_o - \log\frac{1-\alpha}{\alpha} + \frac{2Ve^2}{DhkT}\left[\log\left(\frac{Kh_o^2+6h}{Kh_o^2}\right) - \frac{0.4343\,\alpha(S_1-S_o)\cdot}{2S}\,\frac{6h}{Kh_o^2+6h}\right] \quad .....(6\text{-}31)$$

where h = Zb and b = hydrodynamic length of the monomer and Z the degree of polymerisation. According to Kuhn[26]

$$h_o^2 = 2Sb^2 \quad .....(6\text{-}32).$$

Where S is the number of monomers per statistical element. The value of S depends on steric factors and on solute-solvent interaction. When the polyacid is highly soluble, S is independent of α. When the polyacid is only slightly soluble at low degrees of ionization and becoming highly solvated with increasing α, then S becomes markedly dependent on the degree of ionization and this dependence is represented by a linear function thus

$$S = (1 - \alpha)\, S_o + S_i \quad \ldots\ldots\ldots\ldots (6\text{-}33).$$

Equation 6-33 expresses the fact that the statistical element of the slightly solvated, undissolved polymer increases with the number of higher solvated ionized groups.

In some polyelectrolytes e.g. polyuronic acids, steric factors cause the molecules to be highly stretched already even at low degrees of ionization[27] so that h = Zb to a good approximation. Moreover, as the hydroxyl group of the polyuronic acids make the solubility largely independent of the degree of ionization, S become independent of α and $S_i - S_o = 0$. These two simplifications when applied consequently reduce the potientiometric titration expression to

$$pH = pK_o - \log \frac{1-\alpha}{\alpha} + \frac{2\alpha\epsilon^2}{DkTb_j} \log\left(1 + \frac{6}{KSb}\right) \quad \ldots(6\text{-}34)$$

Extensive potentiometric measurements were carried out in order to test the validity of the equations mentioned above for PMA. It was found by Katchalsky et al[27], and H. C. Spenser[15] that potentiometric data are independent of molecular weight. The relation between pK and pK_o and n for a stretched molecule is

$$(pK - pK_o)/(n-1) = 0.866$$

whereas for a randomly kinked molecule the relationship gives 2.66.

Recently, Letyte and Mandel[28] and Mandel et al[29] have applied a thermodynamic treatment to explain the configurational transition which occurs when PMA is titrated with a base. The transition has been described as occuring between two forms, a - dominating at low values of α and a more extended form b which is predominantly present at higher values of α. They obtained in terms of pH the enthalpy difference between the two forms a and b.

$$\int_o^{\alpha x}(pH - pH^b)d\alpha = \frac{1}{2.303ZkT}(H_o^b - H_o^a) \quad .....(6-35)$$

This expression is now transformed to a relation which is a function of pK's

$$\int_o^{\alpha x}(pK - pK^b)d\alpha = \frac{1}{2.303ZkT}(H_o^b - H_o^a) \quad ...(6-36)$$

Thus from equation 6-36 it is seen that the transition free enthalpy at α=o may be determined experimentally if pK^b is known in the region of α values below $\alpha = \alpha_\chi$. This was also established by Zimm and Rice[30] for helix - random coil transitions. To obtain pK^b, an apparent pK was introduced to extended Henderson-Hassebalch equation i.e. equation 6-17 and this gives

$$pK = pK_a - (n-1)\log \frac{1-\alpha}{\alpha} \quad \ldots\ldots(6\text{-}37)$$

Equation 6-36 on integration between α_1 and $1-\alpha_1$ shows pK_a to be equal to pK at α=0.5. Thus pK is largely dependent on α and this attributed to the increase of electrostatic free enthalpy of the ionized molecule during titration. By extrapolation of the titration plots into the transition region, it would then be possible to obtain pH^b values which may be transformed into pK^b values need to evaluate equation 6-36.

6.2. EXPERIMENTAL

6.2.1. Potentiometric Titration of Polymethacrylic Acid

Method

6.2.1.1. Titration at Changing ionic Strength:

A Beckman pH meter Model GS was used for these titrations at 24.5 ± 0.1°C. The Model GS pH meter only uses Beckman Glass Electrodes in conjuction with Beckman Reference Electrodes for pH determination and other electrochemical - potential measurements. The glass electrodes have low electrical resistance permiting the construction of thick bulbs which are nearly unbreakable and have excellent chemical durability. Accuracy and reproducibility were obtained to within 0.02 pH unit. Measurements were made inside the electrostatistically shielded compartment by using the small electrodes and sample beaker mounted on the door. A null-type meter system assured accuracy independent of the mechanical properties of a registering meter and of changes in the amplifier. Accuracy is further assured because the maximum sensitivity of the amplifier occurs at the balance point.

1.0 ml of 0.01 base molar PMA was pipetted into the titrating vessel. Enough KNO_3 was added to give the

desired concentration after the solution had been diluted to 4.0 mls. Five concentrations (1.0, 0.05, 0.025, 0.01 and 0.00)M KNO_3 were used. The solution was titrated with 25.0×10^{-3}M KOH. The results obtained have been presented in graphical form.

6.2.1.2. Titration at Constant Ionic Strength[14]

The titrations reported in the preceding section are founded on a progressive change of ionic strength. The constant ionic strength titration permitted rigorous comparison of titration curves. Two solutions were prepared, one of the free polymeric acid (A) and the other of the fully neutralised polymeric acid (B) of equal polymer concentration. Now, solution (A) was titrated with solution (B) up to α=0.50 and vice-versa and the pH values determined. By this device, practically the whole range of α from 0 to 1 was covered at constant concentration of the salt and constant PMA concentration. A series of potentiometric titrations of PMA at constant concentration (0.00, 0.01, 0.05, 0.1 and 0.05)M KNO_3 were carried out at $24.5 \pm 0.1^{\circ}C$.

6.2.1.3. Potentiometric Titration of Polymethacrylic acid with zinc nitrate and Coper Nitrate Solutions:

It has been reported by various authors that polymethacrylic acid forms stable complexes with Cu(II) ions[31-33], while Mandel and Leyte[34], O'Neil et all[35] and Bolewiski and Lubina[36] have reported that Zn^{2+}, Cd^{2+}, Mg^{2+} and Cu^{2+} also form stable complexes with PMA. Furthermore, it has been stated that the Cu-PMA chelate probably involves four carboxylate groups for every copper bound[33]. In order to contribute to the existing knowledge about PMA - cation interaction, the author has carried out a series of potentiometric titrations involving PMA, zinc and copper ions.

(a) Principle:

If cations are bound by a polyanion, their electrostatic fields alone will affect the acid base character of the titratable groups. This effect can be conveniently measured by determination of changes in titration curves.

Procedure:

A stock solution of PMA (0.01 base molar) was prepared and dilutions made as required. Generally 2.50×10^{-3} base molar PMA solutions were used throughout

the titrations. Potentiometric titrations were carried out at various degrees of ionization and various ionic strengths.

The general procedure in a typical experiment was as follows:

1.0 ml of 0.01 base molar PMA was pipetted into the titrating vessel. Enough KOH solution of known strength was added to give the desired degree of neutralization and also enough KNO_3 was added to give the desired concentration when the solution was diluted to 4.0 ml. The solution was then titrated with 12.0×10^{-4} M $Zn(NO_3)_2$ solution and the pH of the solution read from a Beckman pH Meter Model GS, after addition and after stirring for about three minutes. The volume added each time was also noted.

Generally, titrations with metal ions were carried out with the polymer pretitrated to varying degrees of neutralization (from α=0.1 to α=0.9). Pretitnation was carried out by adding known quantities of 25×10^{-3} M KOH. Four concentrations of added salt were used (0.01, ~~0.025~~ 1.0, 0.05, 0.10)M KNO_3. Also, for each titration, a blank titration was carried out to investigate the effect of dilution on metal-polymer interaction. All titrations were carried out at $24.5 \pm 0.1^{\circ}C$.

6.3 Results and Discussions

The potentiometric titration of polymethacrylic acid and polyacrylic acid has been studied by many investigators either from theoretical view point or experimentally[1-27]. In general, the experimental results for a single titration can be expressed by the modified form of Henderson-Hasselbalch equation

$$pH = pKa + n\log\frac{\alpha}{1-\alpha} \quad .....6-17$$

It appears in general from the published experimental evidence that the solution properties of PMA are somewhat peculiar.

It has also been shown by several workers that both polyacrylic and polymethacrylic acids form stable complexes with copper and zinc[31-36]. It has been stated that copper chelate probably involves four carboxylate groups for everybound copper ion[32-33]. Some authors[34,36] have proposed that the Cu-PMA complex involves two carboxylate groups to one metal ion bound. From the available results up to the present day, it has been difficult to decide what the co-ordination number of copper and zinc complexes with PMA is.

The potentiometric behaviour of PMA in the presence of copper and zinc has been investigated by the author.

Unlike the previous workers, pH behaviour of PMA pretitrated to various extents with a strong base and subsequently titrated with strong counterion binder: $Zn(NO_3)_2$ and $Cu(NO_3)_2$ has been reported here. These have been carried out in various constant ionic strength media.

6.3.1 Results:

The results reported here have been obtained by method of titration at constant ionic strength and constant polymer concentration. These titrations were carried out as outlined in sections 6.2.1.2 and 6.2.1.3. Figs 6.1 to 6.16 are various plots obtained from the potentiometric titrations of PMA in the absence and in the presence of divalent cations. Figs 6.1 and 6.2 are the plots obtained for potentiometric titrations of aqueous PMA solution at constant $[PMA]$ and at various constant ionic strengths at 25°C. Fig 6.1 is a plot of pH against $\log \frac{\alpha}{1-\alpha}$ while Fig 6.2 is a plot of $pKa = \left[pH - \log \frac{\alpha}{1-\alpha}\right]$ against α. These plots have been derived from equation 6-17 and are designed to monitor the solution properties of PMA.

Fig. 6.3 to 6.8 are the various plots obtained for potentiometric titration of pretitrated PMA with copper

nitrate solution at various experimental conditions while figures 6.9 to 6.12 are the various plots for titration of pretitrated PMA with zinc nitrate solutions. Fig. 6.13 and 6.14 compare the amount of COO^- bound by M^{2+} at $\alpha = 0.3$ and also the variation of COO_{bound} with α respectively. In figure 6.15 and figure 6.16 the ionic strengths effects on Cu-PMA and Zn-PMA complexes respectively, are compared at various degrees of ionization of the polymeric acid.

6.3.2... Discussion:

6.3.2.1. Potentiometric behaviour of aqueous solution of polymethacrylic acid (PMA).

According to Katchalsky and Sptinik[10], the plot of pH against log $\frac{\alpha}{1-\alpha}$ should yield for a polyacid for a large range of α values a straight line corresponding to equation 6-17 which is an extended form of Handerson-Hasselbach equation 6-18. MacLaren [38] and Gregor et al[31] obtained virtually straight line plots for pH against log $\frac{\alpha}{1-\alpha}$ while Mandel and Leyte[39] obtained two linear segments; one existing at $\alpha < 0.1$ and the other at $\alpha > 0.3$. In the present report, fig. 6.1 shows some striking differences from those of previous workers.

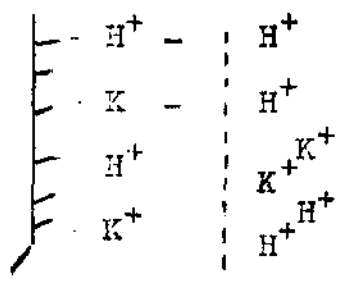
Each curve in figure 6.1 can be divided into three segments and these have been interpreted in terms of configurational changes. The depressed (concave upwards) region represents the region where configurational transition takes place. In figure 6.1, the value of n (from equation 6-17) which modifies log $\frac{\alpha}{1-\alpha}$ is not a constant and appears to vary along each curve.

Also for these titrations, values of pKa and the degree of ionization (α) have been calculated from pH values and polymer concentrations. However, the values obtained for (α) are not absolute values as will be seen shortly. Figure 6.2 shows the plot of pKa against α at various ionic strengths. This figure in particular reveals interesting properties of PMA. The figure shows that the apparent dissociation constant K_a of a polycarboxylic acid defined as

$$K_a = A_{H+}[COO^-]/[COOH] \quad .....6\text{-}38$$

is not a constant but is a function of the degree of ionization i.e. pKa is largely dependent on α. The shape of potentiometric titration curves of PMA in salt solutions may be interpreted by assuming a configurational transition in the region of low degrees of ionization[37,27]. Generally, fig. 6.2 shows, first, a decrease

in pKa which is followed by a rise to a plateau and eventually increases again at high charge densities of the polyion. This interesting but complicated behaviour seems to suggest a conformational transition in the region characterised by the plateau. It must be mentioned here that the complexities associated with the behaviour of PMA are largely caused by polyion configurational changes (which brings about expansion as COO^- are produced) and the distribution of the mobile ions in the vicinity of the charged chain. This will probably be understood if one considers a sort of double layer effect.



Polymer chain. Associated layer Bulk Solution

The picture presented above shows a polymer chain carrying negative charges. These charges are surrounded by H^+ and K^+ ions with some negatively charged byions so that one gets a sort of double layer. Now let a hypothetical situation exist where the double layer

(Associated layer) is separated by a membrane (shown in broken line) from the bulk solution. Now when the electrodes are dipped into the solution the $[H^+]$ in the bulk solution will be measured. Various situations can now be considered depending on the movement of ions across the hypothetical membrane.

As with Donnan effect mentioned in chapter 5, the number of ions in bulk solution will be less than in the double layer but in actual fact the distribution of these ions is determined by the ionic strength of the medium. One will probably find that at high ionic strength, the $[H^+]$ in the double layer will probably be the same as in bulk solution because the ions tends to distribute themselves evenly across the hypothetical membrane. However, at low ionic strength, because of maintance of equilibrium between the double layer and the polymer, more ions will tend to be found in the double layer. i.e. the distribution of ions is probably dissimilar and this may lead to measured pH not being a true representation of the degree of ionization of PMA.

It is noted that as the ionic strength increases, the transition region seems to spread over a larger

titration interval. In chapter 3, it was suggested that the increase in η_{sp} was due to repulsion caused by the fixed charges on COO^- groups. Thus the large dependence of pKa on α is generally attributed to the increase in electrostatic free energy of the ionized groups as the titration proceeds.

However, before considering the effect of KNO_3 on ΔG_{el}, one should first of all consider the effect of I on pKa. The variation of ionic strength with α has a long range effect on pKa than the short range. It has been suggested by Morawetz[40] that in a highly ionized polymethacrylic acid only one water molecule is believed to have space between two ionizable groups so that ionic strength effect is expected to have little influence on adjacent groups but will have a considerable effect on the long range groups. This probably accounts for the slopes of figure 6.1 having nearly the same value.

High concentration of KNO_3 has little effect on near neighbour COO^- groups but has a screening effect on the long range interactions with the result that the long-range electrostatic field of the polyion is minimized. In fact Katchalsky and Sptinik[10] have found that in many cases ΔG^i_{elec} is approximately proportional

to log $\frac{\alpha}{1-\alpha}$ over an extended range of the titration of polymeric acids ($0.1 < \alpha < 0.9$). With this in mind, equation (6-17) is now modified to give

$$pH = pKo + n' \log \frac{\alpha}{1-\alpha_i} \quad .....6 - 39$$

where deviation of n' from unity is a measure of the magnitude of the electrostatic effects. If $\Delta G'_{elec}$ is relatively small, then a plot of pH against log $\frac{\alpha_i}{1-\alpha_i}$ should be linear with slope = 1. Figure 6.1 is a revelation of the fact that ΔG^{i}_{elec} is quite large in these interactions.

The first initial decrease in pKa is associated with the compact structure of the PMA molecule. In this region, only the -COOH groups on the periphery are being titrated and this does not lead to expansion of the molecule. Chain expansion only starts when the solvent is able to penetrate the coiled molecule and ionize the buried -COOH groups.

6.3.2.2. Potentiometric behaviour of aqueous solutions of PMA in the presence of copper and zinc nitrate:

In this process, the hydrogen ion concentration of the solution was measured against the concentration

of the metal ion added and the pH reading was plotted as a function of the concentration of the metal ion used to titrate the preionized PMA solution. It was observed that when cations were added, the pH generally decreased. Thus it may be said that the pH changes produced by the addition of M^{2+} ions (M^{2+}=Cu^{2+} or Zn^{2+}) to a partially neutralized PMA solution in KNO_3 is associated with specific effects of these ions. A reaction of this nature may occur.

$$COO^- H^+ + M^{2+} \rightleftharpoons \underbrace{COO^- + M^{2+}}_{\text{Associated}} + \underbrace{H^+}_{\text{Measured.}}$$

The curves obtained from above procedure may therefore be used to estimate quantitatively cation affinities for polyions i.e. the magnitude of the displacement towards a lower pH is a measure of the degree of binding assuming hydrolysis is negligible.

Figures 6.3 and 6.4 and figures 6.9 and 6.10 are plots of pH + log $[COOH]$ against metal ion concentration for Cu-PMA and Zn-PMA systems respectively. These plots have been derived from plots of pH against concentration of metal ion added. It can be seen from these four plots that two types of equilibria exist i.e. corresponding to a double titration curve. This double

titration probably indicates a change from one mode of binding to another. This double equilibria can also be interpreted to monitor changes in co-ordination number. Each of these curves is characterised by a first rapid decrease in pH as M^{2+} ions are added. This region is then followed by another region of moderate pH change (hereafter called a plateau) and finally a last region of large decrease in pH as M^{2+} ions are added which finally levels off. This plateau is seen to occur in all the degrees of ionization studied but it is more pronounced at high α values. Another possible explanation of the plateau region is in terms of configurational transition. Because the polymer has been pretitrated to such high α values, one would expect it to exist in a fairly extended form and one would be titrating an extended chain with the metal ions. As M^{2+} ions are bound, the concentration of free COO^- groups will be reduced to such a number which permits transition from the extended state to a coiled state. If one draws a cross section as shown in fig. 6.3 one finds that irrespective of the degree of ionization and as long as the ionic strength is kept constant the amount of M^{2+} needed in each case for complete

transition (region a-b) is the same. This is established in all the figures.

In the present work, attention has been focussed on the concentration of hydrogen ions produced $\left[H^+\right]_p$ (and consequently the concentration of COO^- groups available for binding) by the counterion binding source M^{2+}. The quantity was calculated from pH values. Corrections for dilutions and other experimental artifacts have been taken into consideration. Since pH behaviour on addition of divalent cations is dependent on the degree of pretitration of the acid with a strong base, $\left[H^+\right]_p$ has been related to the degree of ionization and concentration of the polymer. The degree of dissociation is related to the number of COO^- groups in the following manner

$$\left[COO^-\right] = \alpha C$$

where C is the concentration of the $\left[COOH\right]$ groups originally present. Similarly the pH of the solution is related to αC by the relation

$$pH = pK'_a + \log \frac{\alpha C}{1-\alpha C} \quad \text{.....6-40}$$

$$= -\log(1-\alpha C) + \log \frac{\alpha C}{K'_a}$$

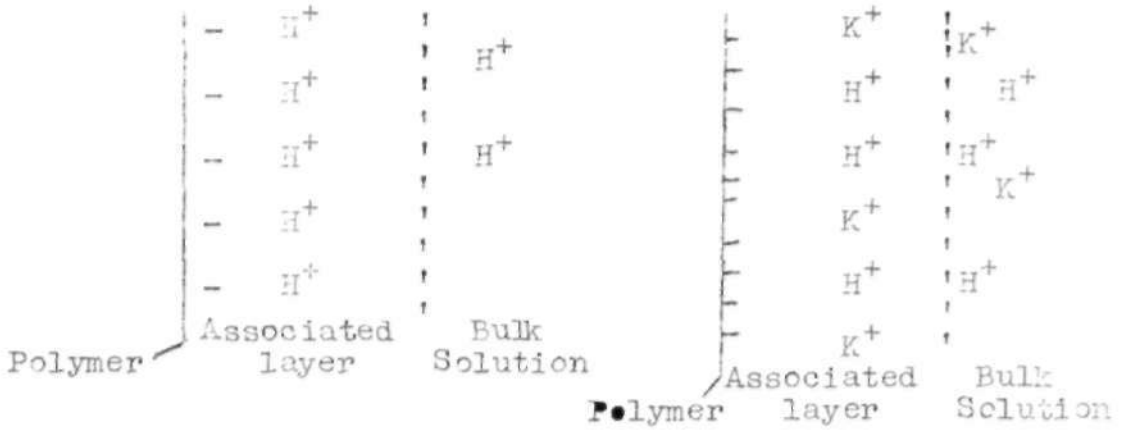
$$= Q + \log \frac{\alpha C}{K'_a}$$

where Q remains virtually constant and this comes from the original value of H^+ release.

$$\therefore \Delta pH \propto \Delta \log \frac{\alpha C}{K'_a} \quad \text{.....6-41}$$

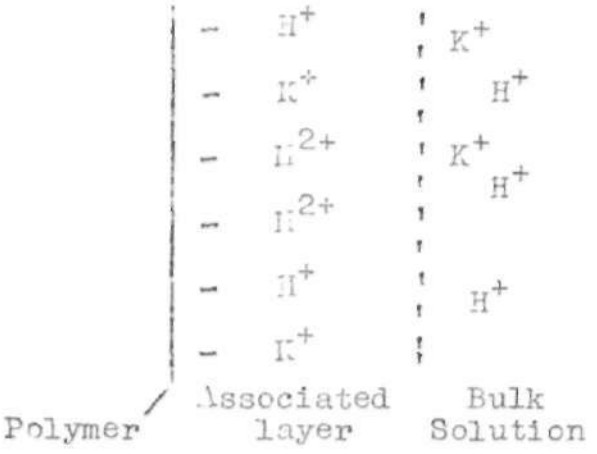
This equation is using the Handerson-Hasselbalch equation where all modifications are represented by the variable value of K'_a. This means therefore, that the observed changes in pH in figures 6.3 and 6.4 and figures 6.9 and 6.10 may be due to changes in $[COO^-]$ as cations are bound which causes the H^+ to be released into the bulk solution. This relationship affords one the opportunity of calculating the amount of bound COO^- as M^{2+} ions are added.

However, before proceeding to treat the experimental data in detail it is profitable to think of the way in which the polymer environment affects the measured pH. To do this one should take a look once more at the diagram presented for double layer on page (206) Let there be, in addition to the K^+ and H^+ ions in the associated layer, the binding ions under investigation, M^{2+}. One can now consider three situations depending on the movement of ions across the hypothetical membrance.



(i) $I = 0$, $M^{2+} = 0$.

(ii) $I = X$, $M^{2+} = 0$ Same α as in (i)



(iii) $I = X$, $M^{2+} = Y$ Same α as in (i) and (ii)

The binding mechanism may be pictured as a sort of competition between the H^+, K^+ and M^{2+} ions for the charged sites. Diagram (i) above represents the charged polymer chain surrounded by the H^+ ions maintained in

close proximity to it. This situation exists at $I = 0$ and $M^{2+} = 0$. Because of the strong attraction of H^+ for COO^-, very few H^+ ions will be released to the bulk solution. However entry of the potassium ions into the double layer will release H^+ ions to the bulk solution. This will lead to a decrease in the measured pH. This situation is illustrated in (ii) above. Also in (iii) entry of M^{2+} into the double layer will release K^+ and H^+ ions to the bulk and this will lead to a further decrease in measured pH. The binding equilibrium which exists between the ions in the double layer and the polymer depends on a number of factors. The number of M^{2+} ions in the double layer will be dependent on I i.e. the addition of K^+ ions will decrease the concentration of both H^+ and M^{2+} in the double layer, so that at higher ionic strengths, low $[M^{2+}]$ in the double layer will lead to a decrease in binding until excess M^{2+} is present. At excess $[M^{2+}]$ ions, and owing to stronger affinity of M^{2+} for COO^- than K^+ ions the M^{2+} ions will be able to penetrate the double layer to bind the charged sites, with the result that no decrease in binding will be observed at high ionic strength and excess $[M^{2+}]$. It should be

noted at this stage that not all the dissociated H^+ ions could be released to the bulk solution. Some H^+ ions will still be held in the double layer which means they can not be measured. Therefore in this type of titration it must be bourne in mind that the $[H^+]_p$ can not be strictly considered as equivalent to the amount of M^{2+} ions bound. It can only be a partial measure. In this respect, the amount of COO^- groups if measured will be a more reliable means of measuring the amount of M^{2+} bound. This has been treated in section 6.3.2.3. Thus one sees from the foregoing considerations that the movement of ions across the hypothetical membrane leads to the establishment of two equilibria.

(a) an equilibrium exist between the polymer and the double layer and this largely depends on the concentration of the ions in the double layer, and

(b) an equilibrium exists between the double layer and the bulk solution.

The concentration of the ions in the double layer will be affected by the concentration of ions in the bulk solution from point of view of Donnan equilibrium treated in chapter 5.

Generally, if $[H^+]$ in the double layer decreases, then further ionization of the near carboxyl groups will occur in order to maintain the equilibrium

$$COOH \rightleftharpoons COO^- + H^+$$

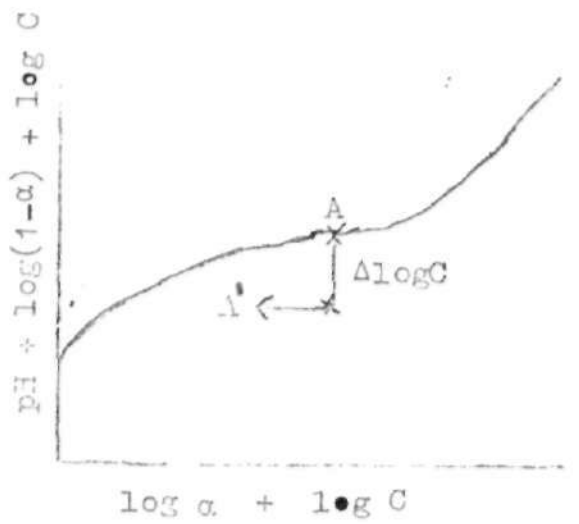
This will be expected at low degrees of ionization. The decrease of $[H^+]$ in the double layer may be caused by the presence of M^+ or M^{2+} and it may be said that once the M^{2+} ions are held in the vicinity of the COO^- groups, Coulombic attraction sets into action. Once M^{2+} ions are held near COO^- groups, ionization of the COOH groups may be made easier and the nearest COOH group enters into chelation.

6.3.2.2. Transformation of titration curves to complex formation curves:

Gregor and coworkers[31]; Mandel and Leyte[34] have all modified the method of Bjerrum for evaluating formation constants and co-ordination numbers of divalent metal ions associating with polyelectrolytes. The method of titrations employed in the present work is quite different from that used by other workers[31,34], and this necessitates a different approach towards calculation of formation curves. It was stated in the preceeding

section that the amount of COO^- groups rather than $[H^+]_p$ will give a better measure of the amount M^{2+} bound. It is therefore necessary to calculate the amount of bound COO^- groups.

In order to do this, a reference plot of pH + $\log[COOH] \equiv pK'_a + \log[COO^-]$ against $\log[COO^-]$ is constructed for $[PAA] = 2.5 \times 10^{-3}$M at various ionic strengths. The relationship between change in pH (and consequently pH + $\log[COOH]$) and αC has been stated in equation 6-41. After correcting for dilution, then pH + $\log[COOH]$ will correspond to a certain value of $\log[COO^-]$, since pK'_a is a function of α. This means that the amount of COO^-_{free} can be obtained. Also assuming that within the concentration range used, the pK_a does not vary appreciably, then a series of curves of varying log C could be obtained. Therefore by allowing for dilution, then one can obtain a graph of pH + log $(1-\alpha_1)$ + log C_1 against log α_1 + log C_1 lying on an equivalent curve to the previous one but displaced by an amount proportional to log C.



Here point A becomes point A^1 on a new curve displaced below the previous one by Δlog C.

However, it can be seen from fig. 6.2 that variation of pK_a is quite considerable and therefore allowance must be made for this. Therefore if the pH change as pK and α change the following relationship become valid.

$$pH + \log\left[COOH\right] = pK_a + \log\left[COO^-\right].$$

So that a plot of $pK_a + \log\left[COO^-\right]$ against $\log\left[COO^-\right]$ can be obtained. One is then in a position to obtain any value of $pH + \log\left[COOH\right] \equiv pH + \log(1-\alpha)C + \log \alpha$ $C_{original}$. Therefore if $\log C_{original}$ is known then one can obtain $\log COO^-_{bound}$ at every addition of M^{2+} ions.

When the procedure outlined above is now employed various plots are obtained. Figures 6.5 and 6.7 and fig. 6.11 are plots of $\log \Delta H^+$ against $\left[M^{2+}\right]$ for copper

and zinc respectively. These figures have been derived from figures 6.3 and 6.4 and from 6.9 respectively. The plots of log ΔH^+ against $\left[M^{2+}\right]$ are much more sensitive than the plots of pH + log$\left[COOH\right]$ against $\left[M^{2+}\right]$. It has been suggested earlier that a double titration is obtained. In figures 6.5 and 6.7 points of inflextion are obtained. These inflextion points have been associated with the end of one of the double titration while the second part of the titration curve is obtained beyond the inflextion points. If the titration is carried far enough, one obtains a more or less levelling off of the curves in the presence of excess Cu^{2+} ions. This is clearly seen from fig. 6.7. The same observation has been made in the case of Zn^{2+} in fig. 6.11. It should be mentioned that an absolute levelling off of log ΔH^+ is imposible because as the concentration of M^{2+} in the double layer is increase more and more H^+ will be displaced to the bulk solution and there can be no particular point when all H^+ in the double layer will be completely displaced.

When the procedure outlined for calculating the amount of bound COO^- groups is employed figs. 6.6. and 6.8 are obtained for copper and fig. 6.12 is obtained

for zinc. These curves are more reliable because they represent the true position of what happens in the polyion. They actually represent the formation curves of the complexes. The shapes of fig. 6.6 for Cu-PMA complex and of fig. 6.12 for Zn-PMA complex suggest two types of equilibria which probably indicate two types of complexes or simply a change in stereochemistry. The interpretation here is twofold. First, the inflection point may represent the end point of the first of the double titration earlier predicted. One clearly sees that the amount of $[COO^-]_{bound}$ at inflection point is about half of the total COO^- groups. Seconaly, the inflection point may be thought of as change in the mode of binding i.e. change in stereochemistry brought about by change in configuration. It could also mean that the inflection point reflect a break down of the complex to a new form of association.

However, at high ionic strength, this strange behaviour is absent. It would appear that the complex is stabilized in high ionic strength medium. In all cases, the graphs are seen to level off. The figures reveal that the amount of complex formed depends on the amount of M^{2+} and COO^- available up to maximum binding.

If the amount of COO^-_{bound} is taken as a measure of the complex formed, it is seen that amount of complex formed increases with increasing α. The final levelling off achieved in each case will mean the maximum binding capacity of the metal ions. In each case of the α studied and at low $\left[M^{2+}\right]$ the concentration of COO^- originally free is usually more than the $\left[M^{2+}\right]$ present. This means that the ratio $\left[COO^-_b\right]/\left[M^{2+}\right]_{Total}$ will be very large and will depend on the $\left[M^{2+}\right]$ i.e. at low metal ion concentration, the amount of complex formed depends on $\left[M^{2+}\right]$. On the other hand, at high $\left[M^{2+}\right]$ present, the amount of complex formed depends on $\left[COO^-\right]$.

It is worth noting that in figs. 6.6 and 6.7 and also in fig. 6.12, the amount of $\left[COO^-\right]_b$ reaches a stable state, when no more could be produced. This is evident from the good flattening out obtained in these curves. This is why this kind of plot is more reliable than those of log ΔH^+ against $\left[M^{2+}\right]$; where even at high $\left[M^{2+}\right]$ present H^+ ions are still being produced owing to the fact that they have been trapped in the double layer. Thus the plot in figs. 6.6, 6.7 and 6.12 are a better measure of the amount of the complex formed. Unfortunately, this type of plot does not give the amount metal required for maximum binding.

In fig. 6.13 the amounts of carboxylate groups bound for the same metal ion concentration are compared for copper and zinc at $\alpha = 0.3$ and ionic strength = 0.10. This figure shows generally, that copper is a stronger binder than zinc. At low metal ion concentration, the ratio $\left[COO^-\right]_b/\left[M^{2+}\right]_{Total}$ in the case of copper is twice that in the case of zinc. This means that the co-ordination sphere of copper is twice that of zinc. This revelation probably helps to explain why at low metal ion concentration, copper was able to accomodate four carboxylate groups and zinc only two in the conductance measurements. The ratio $\left[COO^-\right]_b/\left[M^{2+}\right]_{Total}$ tends to approach the same value at high metal ion concentration. This also means that at any $\left[M^{2+}\right]$, copper forms more complexes than zinc.

Fig. 6-14 shows a plot of maximum COO^-_{bound} against α for Cu^{2+} at I = 0,1; and 0.05, and for Zn^{2+} at I = 0.10. This figure shows that the amount of carboxylate groups bound (hence amount of complex formed) is directly proportional to α. At any α, more COO^- groups are bound in the case of copper than zinc when they are compared at the same ionic strength. This figure also shows that the maximum number of COO^- groups produced

is independent of the ionic strength in the case of copper.

6.3.2.4. Effect of ionic Strength:

Fig. 6.15 is a plot of $\left[COO^-\right]_b$ against $\left[Cu^{2+}\right]_{added}$ at $\alpha = 0.3$ and $\alpha = 0.5$, and at two different ionic strengths (0.05 and 0.10). Fig. 6.16 is also a similar plot for zinc at $\alpha = 0.3$ and $\alpha = 0.6$ and at ionic strength (0.01 and 0.10). In the case of copper, it is seen that at low $\left[Cu^{2+}\right]$ present the amount of complex formed depends on $\left[COO^-\right]$ and independent of the ionic strength. Also at high metal ions the amount of complex formed seems to be independent of the ionic strength and depends only on $\left[COO^-\right]$ i.e. curves of the same α and in different ionic strengths converge to same point. However, in the middle region, the concentrations of COO^- and Cu^{2+} are present in comparable quantities. Here the equilibrium constant is the determining factor on the amount of complex formed. It is also in this region where as can be seen, the ionic strength effect is playing a dominant role. This is probably due to the fact that the concentration of K^+ ions in the double layer controls the $\left[M^{2+}\right]$ in the double layer. This reaction understudy involves one in which there is a decrease in the number of free ionic charges i.e.

$$M^{n+} + L^- = ML^{n-1}.$$

This type of reaction is generally more enhanced in low ionic strength medium. As can be seen, the amount of COO^-_{bound} in 0.05 ionic strength is greater than in and ionic strength of 0.1. In high ionic strength medium, it appears that the binding efficiency of Cu^{2+} ions is greatly decreased in the middle region probably because of the great screening effect of the K^+ ions.

In the case of zinc i.e. fig. 6.16, the amount of complex formed depends on the ionic strength of the medium even at low metal ion concentration. However, at low metal ion concentration and in the same ionic strength medium the amount of complex formed depends only on $\left[COO^-\right]$. In the middle region of the curves, ionic strength effects are more pronounced in Zn-PMA than in Cu-PMA complexes probably because of the reasons outlined for copper above. This will also be associated with the binding power of the two ions, copper being a stronger binder than zinc. It is also quite noticable that at low α values and high M^{2+} the ionic strength effect is quite negligible. It also appears that the Zn curves at $\alpha = 0.6$ may eventually meet at high $\left[Zn^{2+}\right]$. The figures show that binding of divalent cations is much more favoured in low ionic strength medium than in high ionic strength medium.

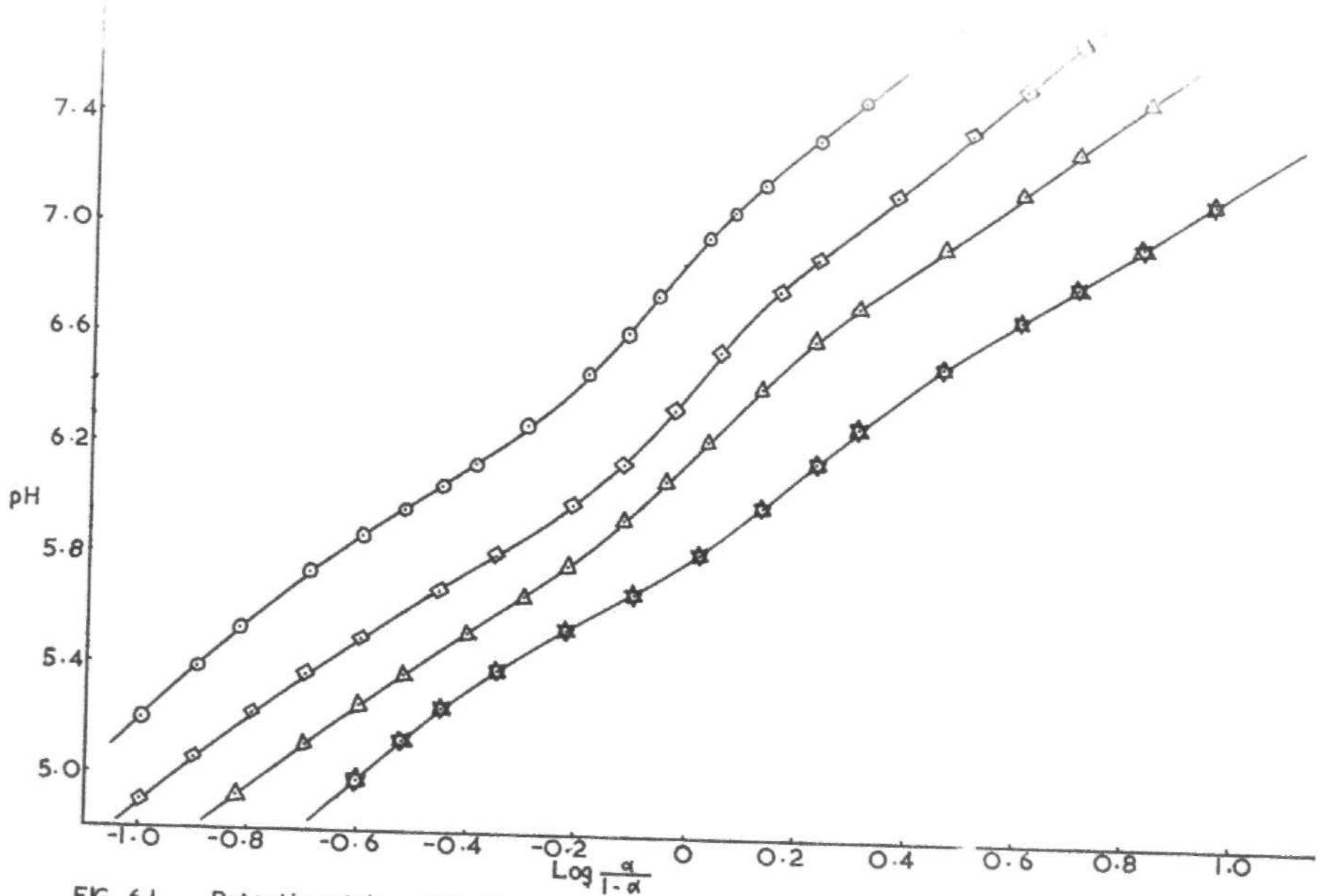


FIG 6.1 Potentiometric titration of PMA solutions with KOH at various constant ionic strengths and polymer concentration

I :- (⊙) 0.01 ; (⊡) 0.05 ; (△) 0.10 ; (★) 1.00 [PMA] 2.50 x10⁻³ M

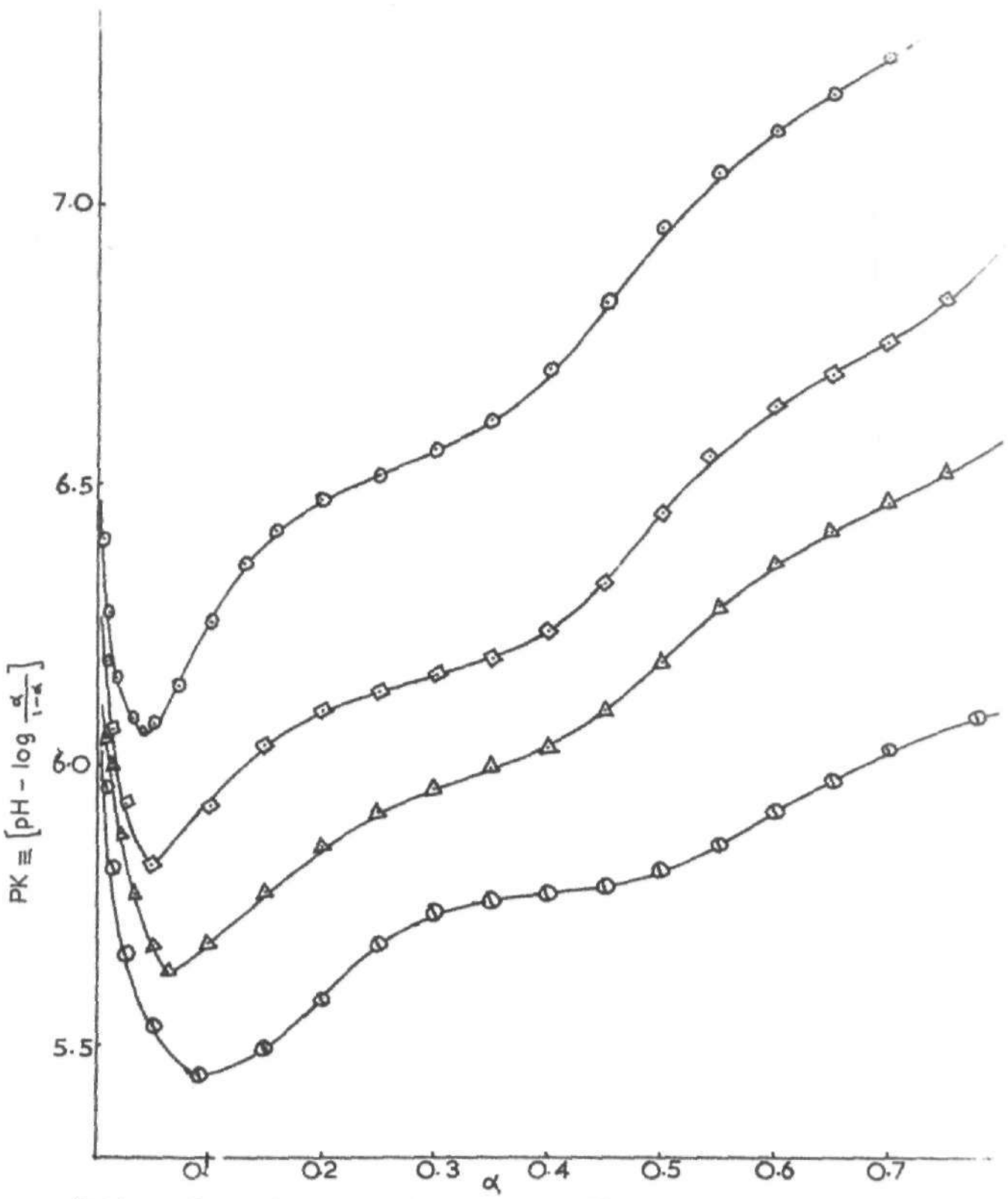


FIG 6·2. Potentiometric titration of PMA at constant ionic strengths and constant [PMA] at 25°C
o, $\bar{I}$ = 0·01; □, I = 0·05; △ I = 0·10; ⊙, I = 1·0; [PMA] = 2·5 X 10^{-3} M

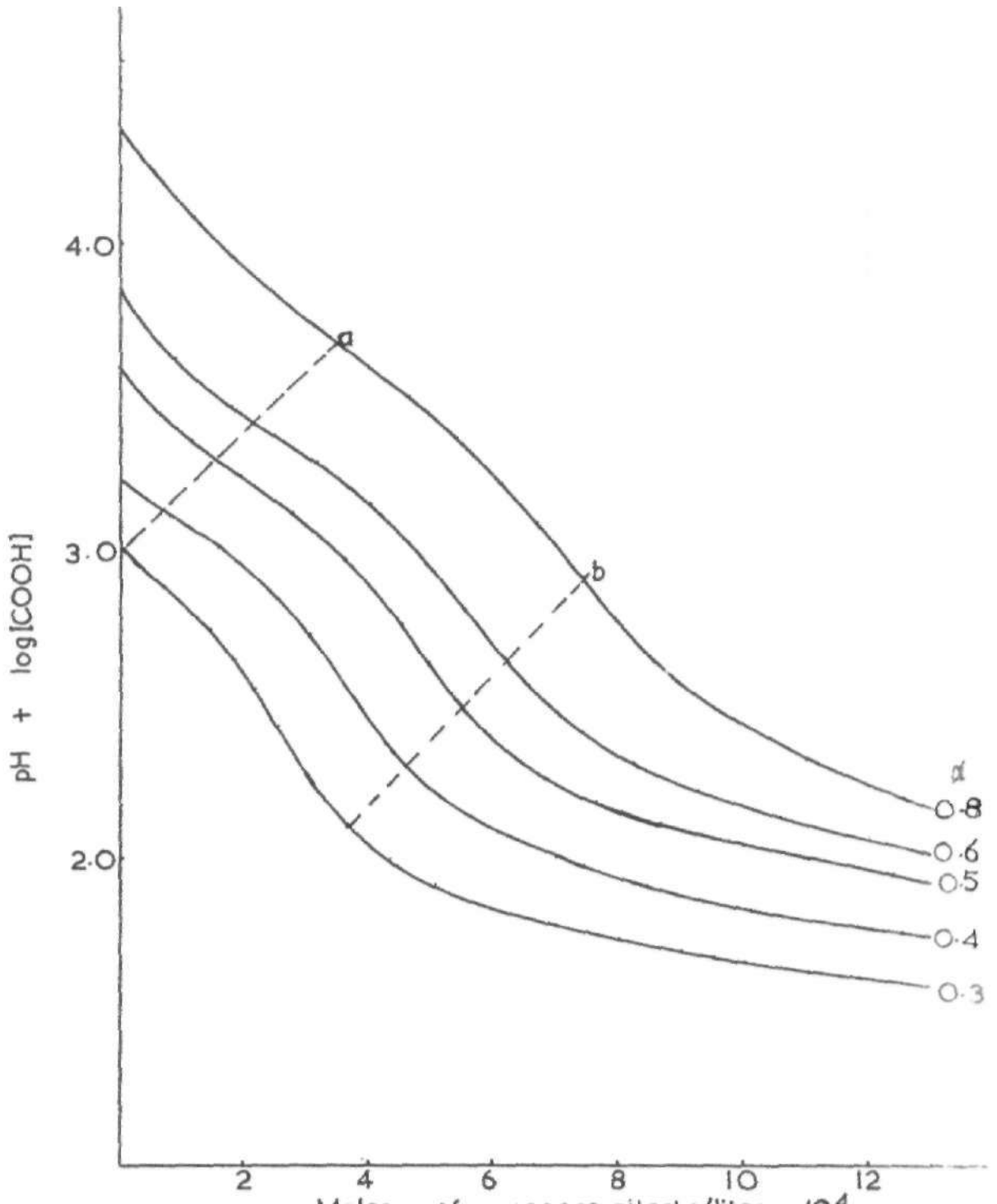


FIG 6·3 Potentiometric titration of partialy ionized PMA solutions with copper nitrate solution in the presence of constant ionic strength and various degrees of neutralization(α ; [PMA] = 2.50×10^{-3}M ; I = 0·05

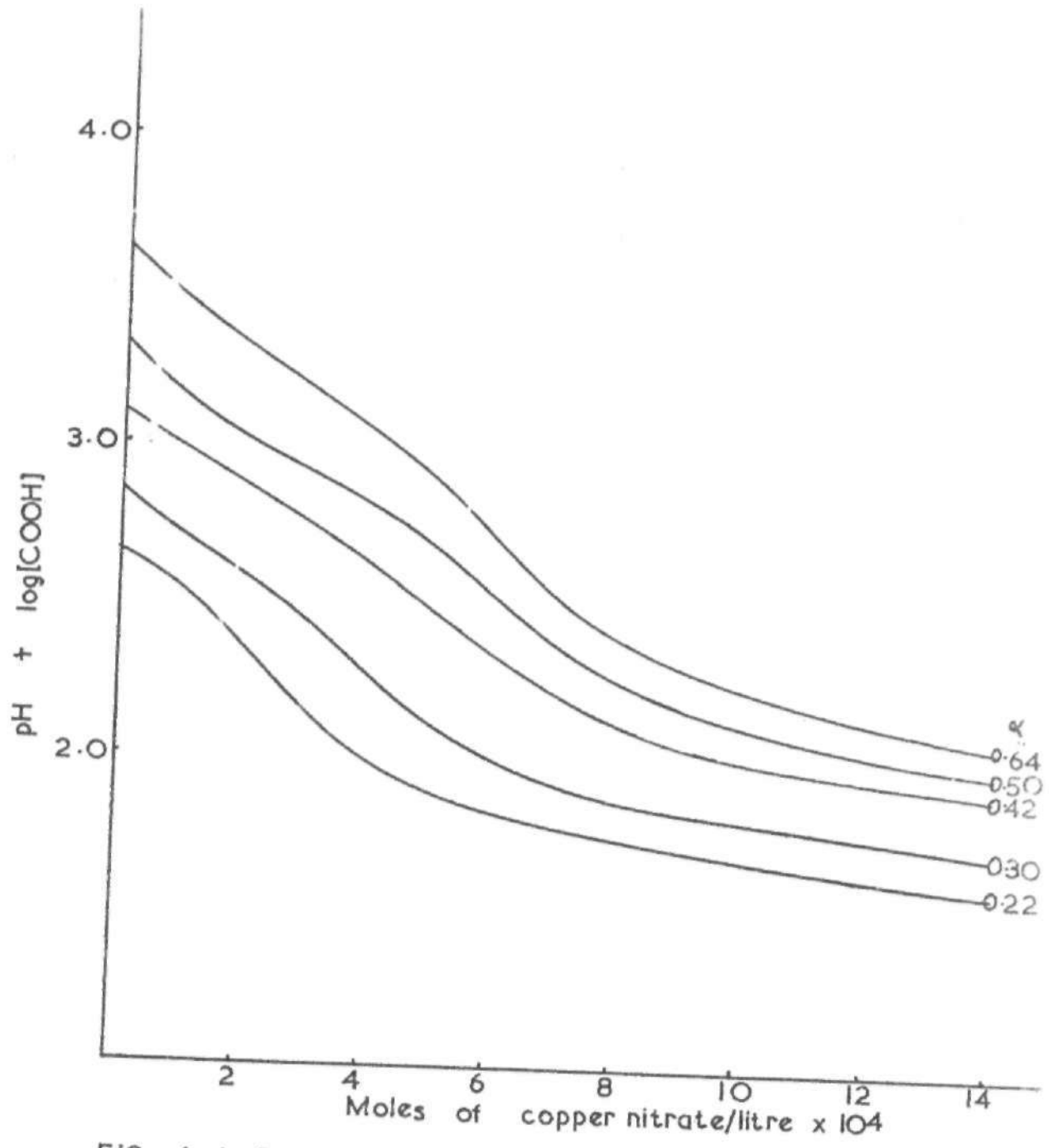


FIG 6.4 Potentiometric titration of partially ionized PMA solutions with copper nitrate solution in the presence of constant ionic stregth and various degrees of neutralization (α)
[PMA] = 2.50×10^{-3} M ; I = 0.10

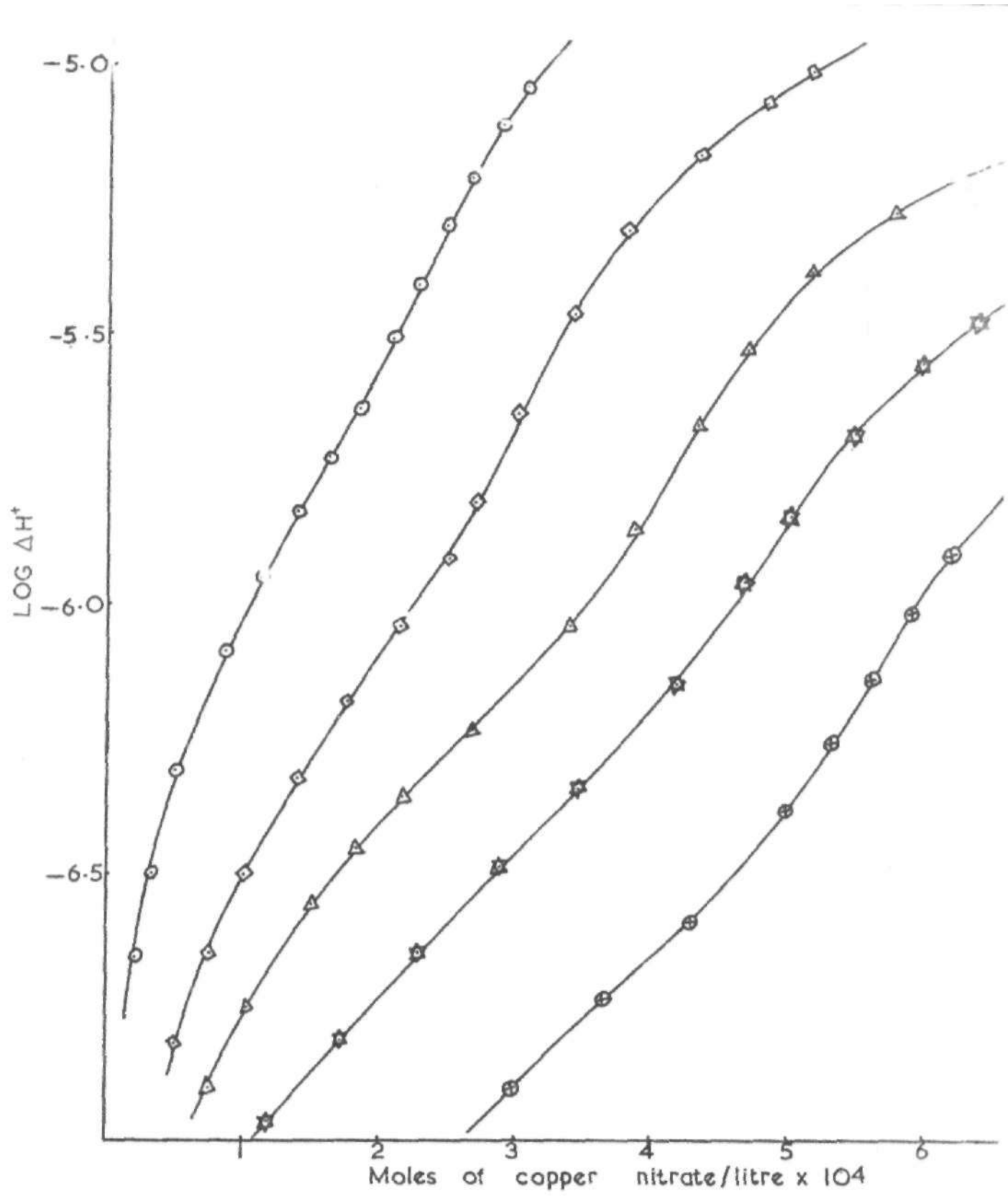


FIG 6.5 Formation curves of PMA – $Cu(NO_3)_2$ complexes at [PMA] = 2.50×10^{-3}M, I = 0.05 and varying values of α.
α :- (⊙) 0.30; (⊡) 0.40; (△) 0.50; (✡) 0.60; (⊗) 0.70 .

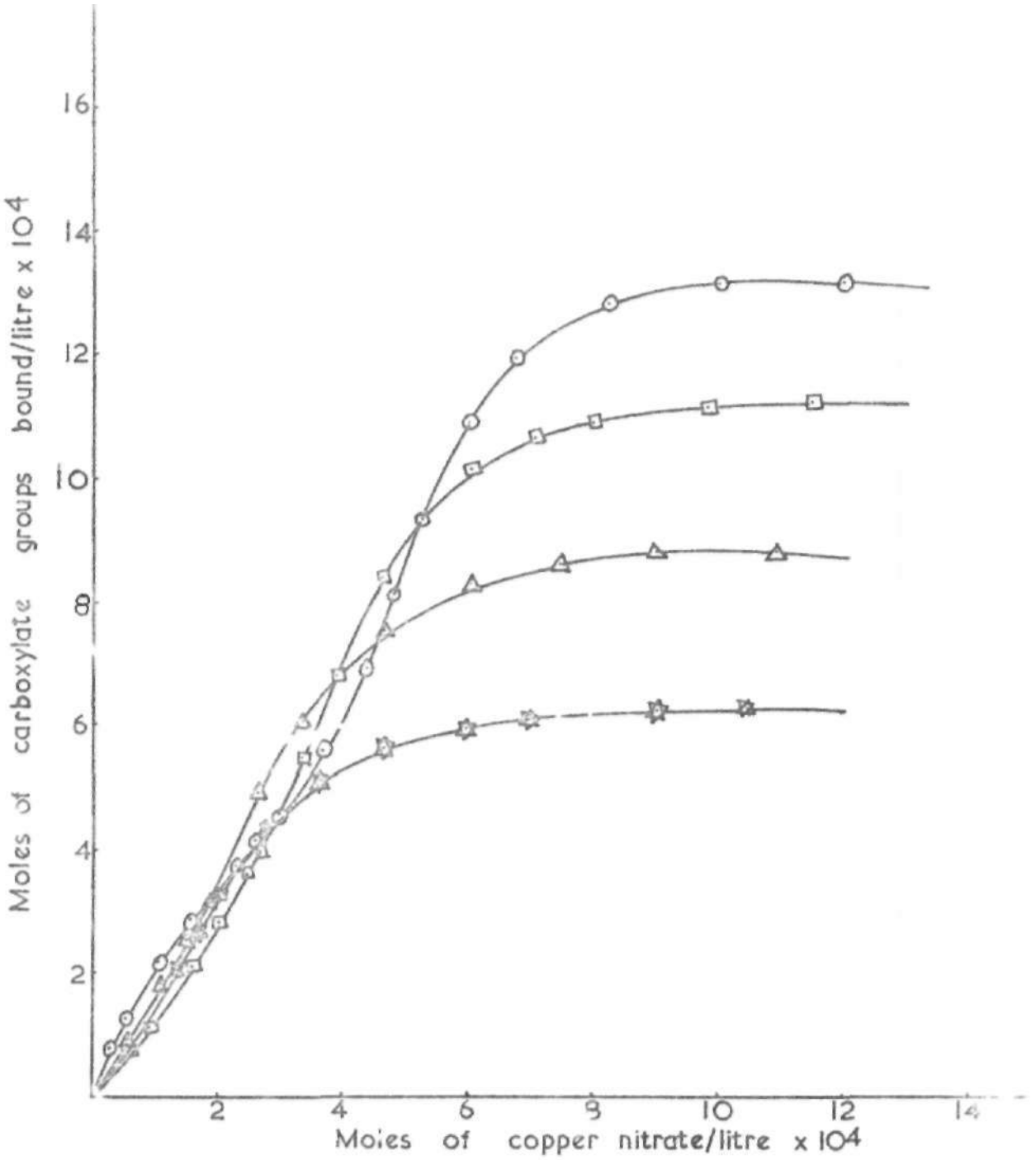


FIG 6.6 Complex formation curves of Cu- PMA at constant ionic strength and polymer concetration at various degrees of neutralization(α)

[PMA] = 2.50×10^{-3}M ; I = 0.05

α :- (⊙) 0.60 ; (⊡) 0.50 ; (△) 0.40 (✡) 0.30

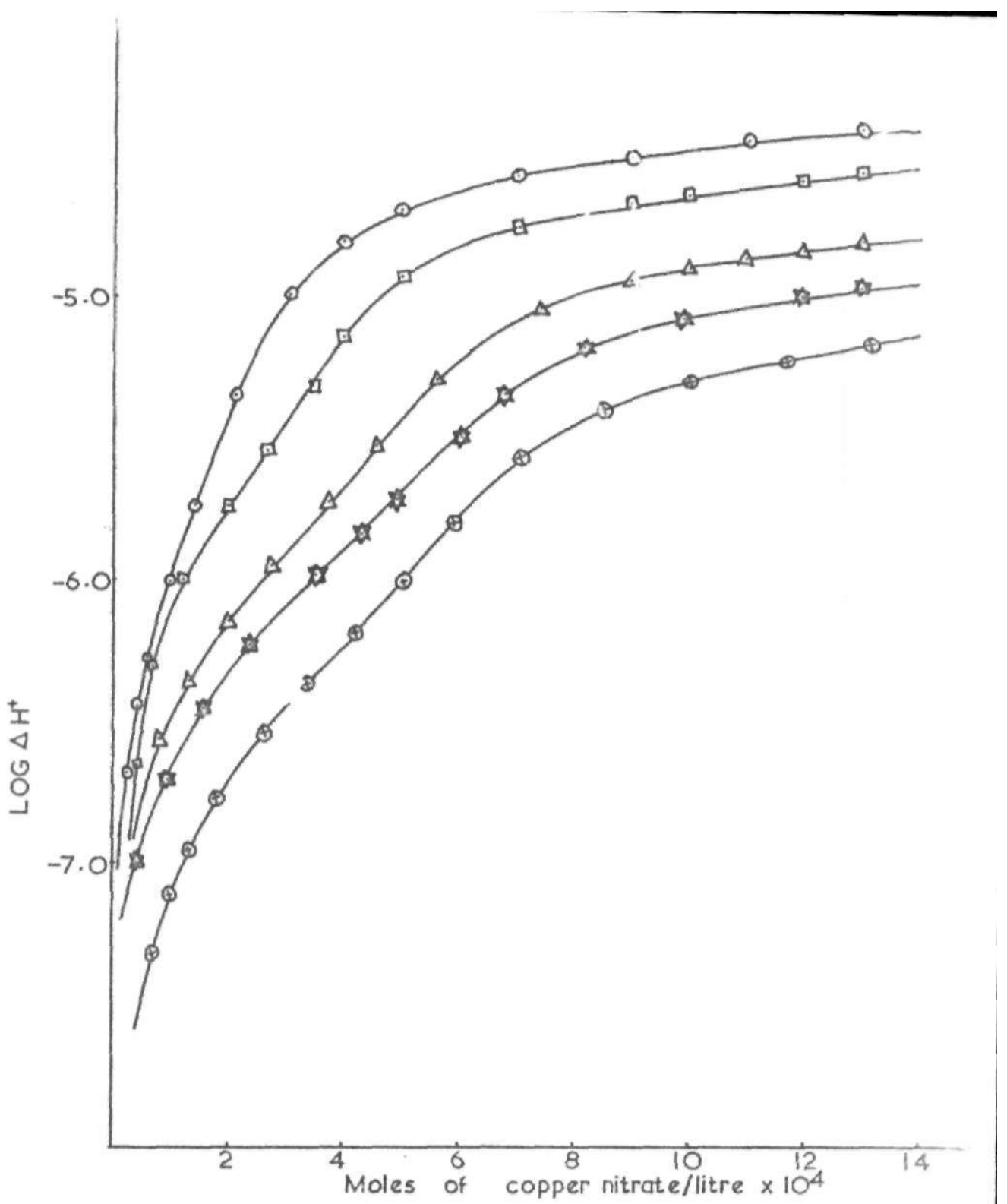


FIG 6.7 Formation curves of PMA—$Cu(NO_3)_2$ complexes at various values of α. [PMA]= 2.50 X 10^{-3}M ; I=0.10
α :- (○) 0.22 ; (□) 0.30 ; (△) 0.40 ; (☆) 0.50 ; (⊗) 0.64

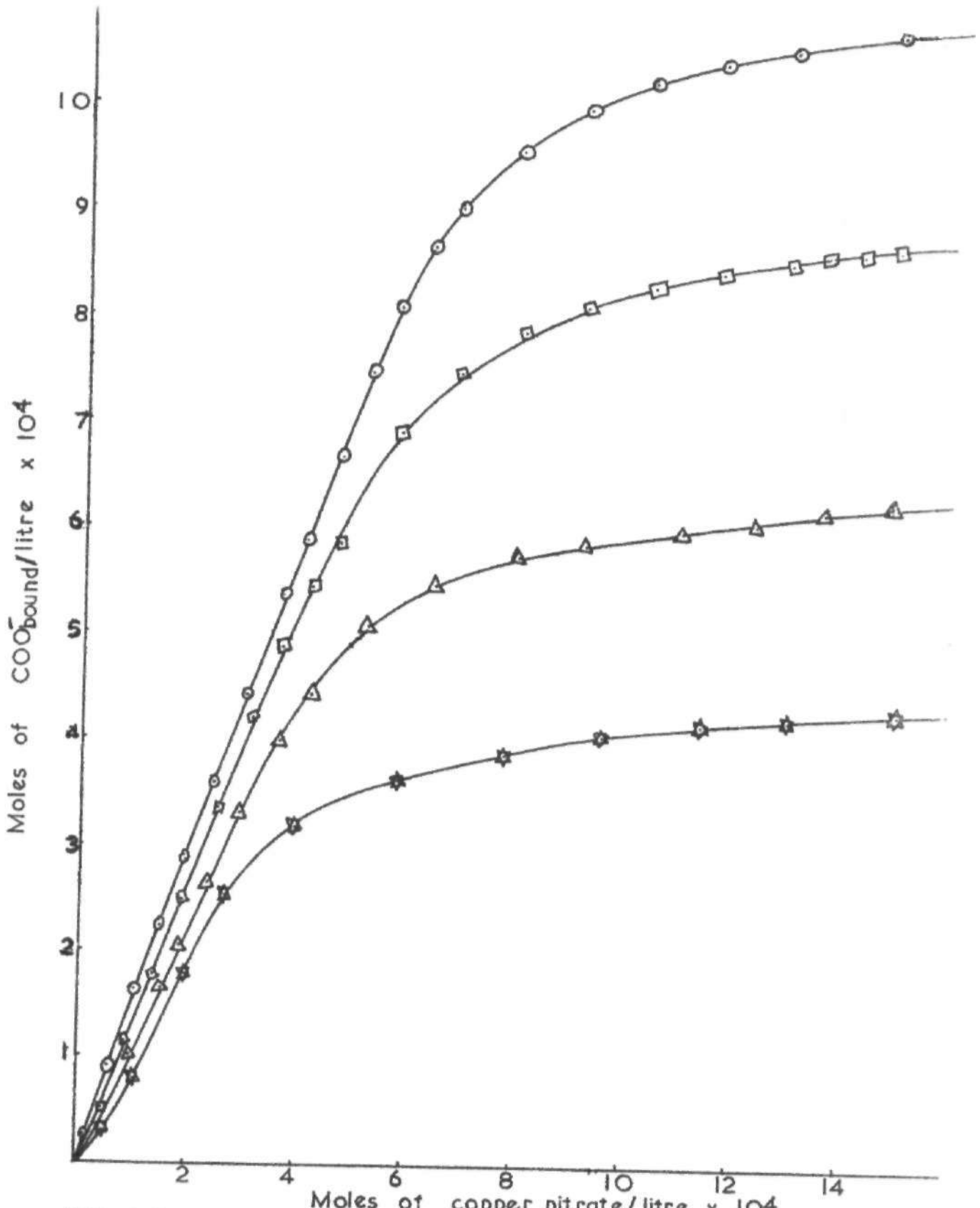


FIG 6.8 Complex formation curves of Cu PMA at constant ionic strength and polymer concentration at varying α [PMA] 2.5×10^{-3} M; I 0.10; α:- (⊙) 0.50; (⊡) 0.423; (△) 0.30; (✡) 0.22

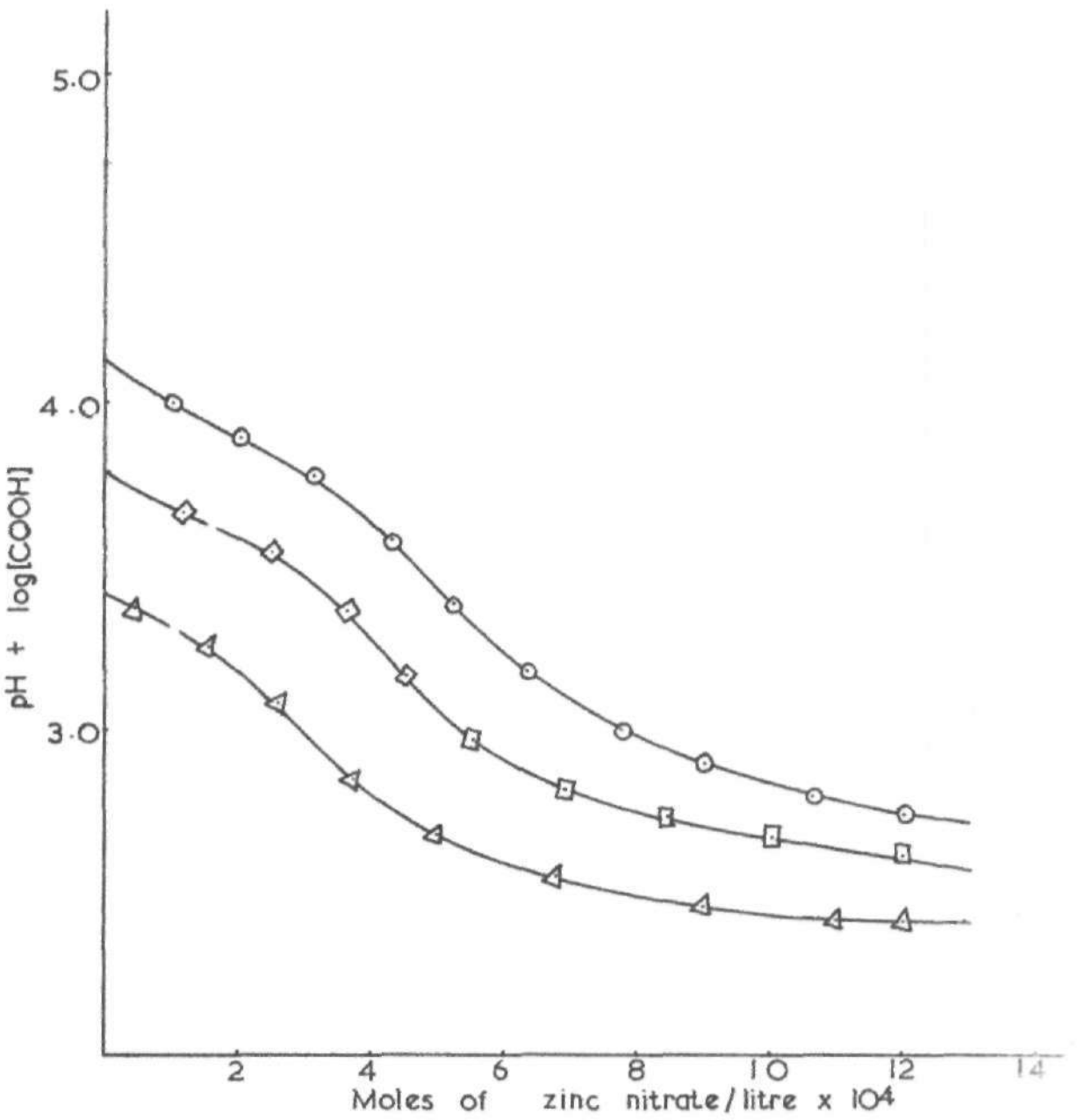


FIG 6.9 Potentiometric titration of partially ionized PMA solutions with zinc nitrate solution in the presence of constant ionic strength and various degrees of neutralization (α)

α :- (⊙) 0.60 ; (⊡) 0.45 ; (△) 0.30

[PMA] = 2.50×10^{-3} M ; I = 0.01

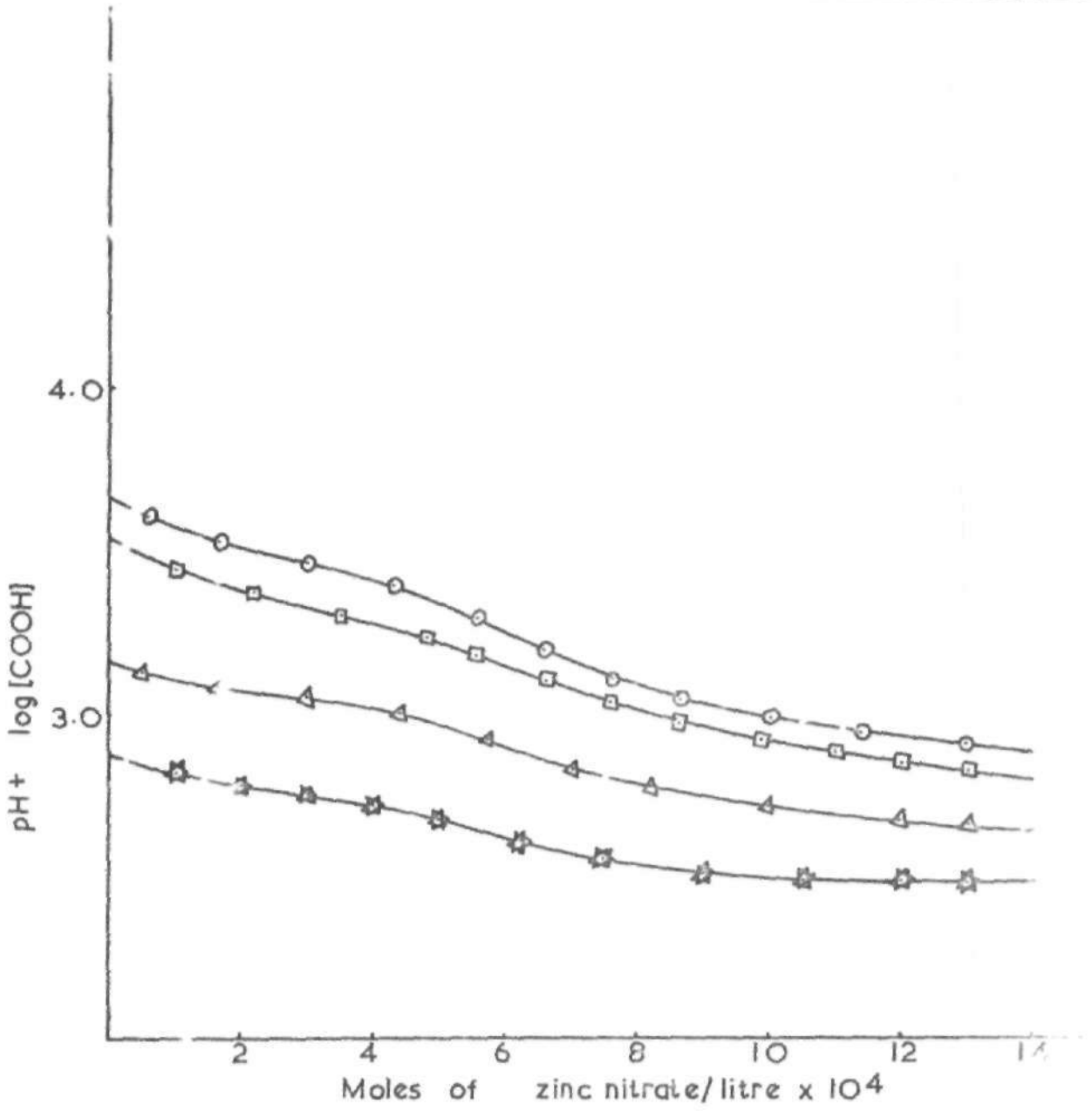


FIG 6 10 Potentiometric titration of partially ionized PMA solutions with zinc nitrate solution in the presence of constant ionic strength and various degrees of neutralization (α)

α :- (o) 0.75 ; (□) 0.60 ; (△) 0.45 ; (☆) 0.30

[PMA] = 2.50×10^{-3} M ; I = 0.10

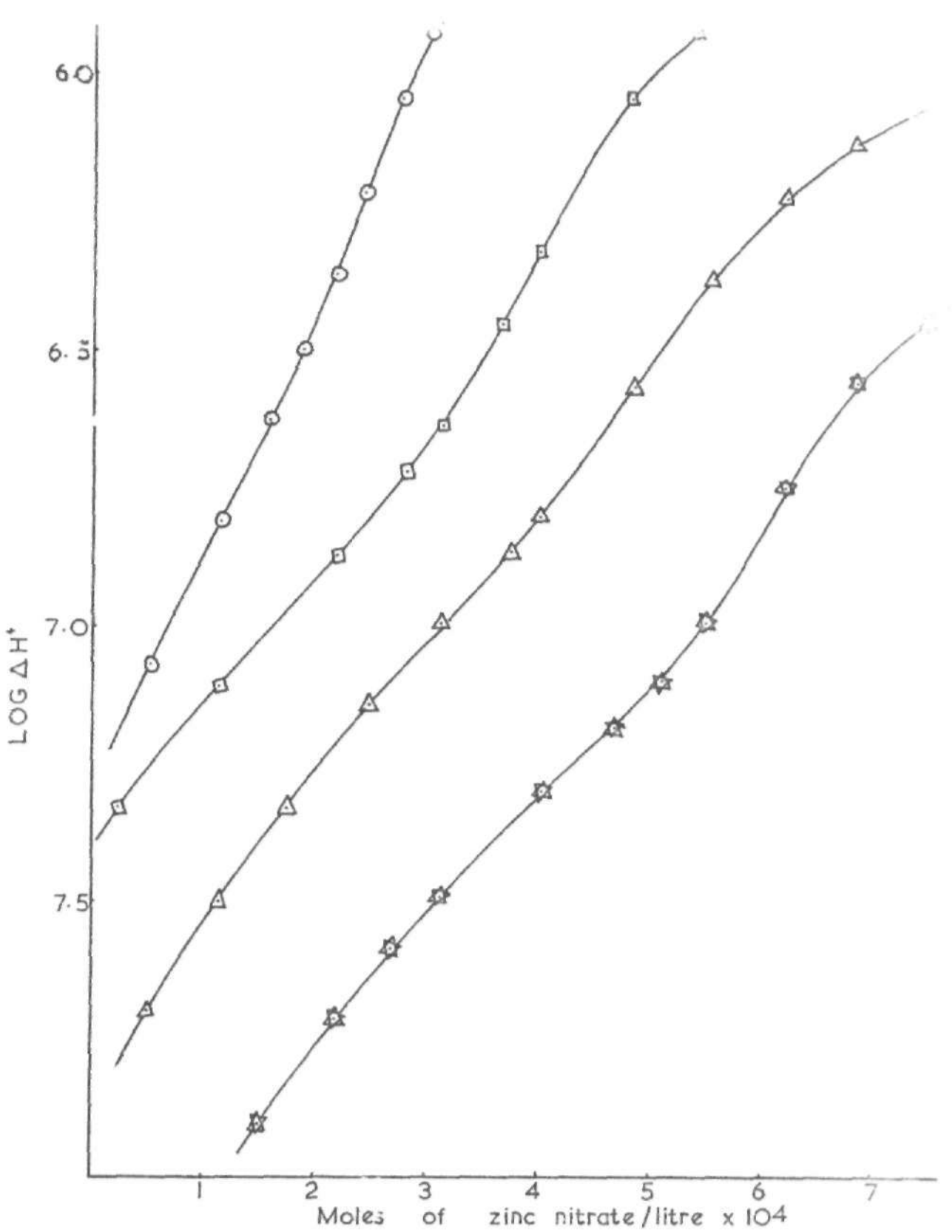


FIG 6.11 Formation curves of PMA – $Zn(NO_3)_2$ complexes at various values of α. [PMA] = 2.50×10^{-3}M, I = 0.01 α:-(⊙)0.30; (□)0.45; (△)0.60; (✡)0.75

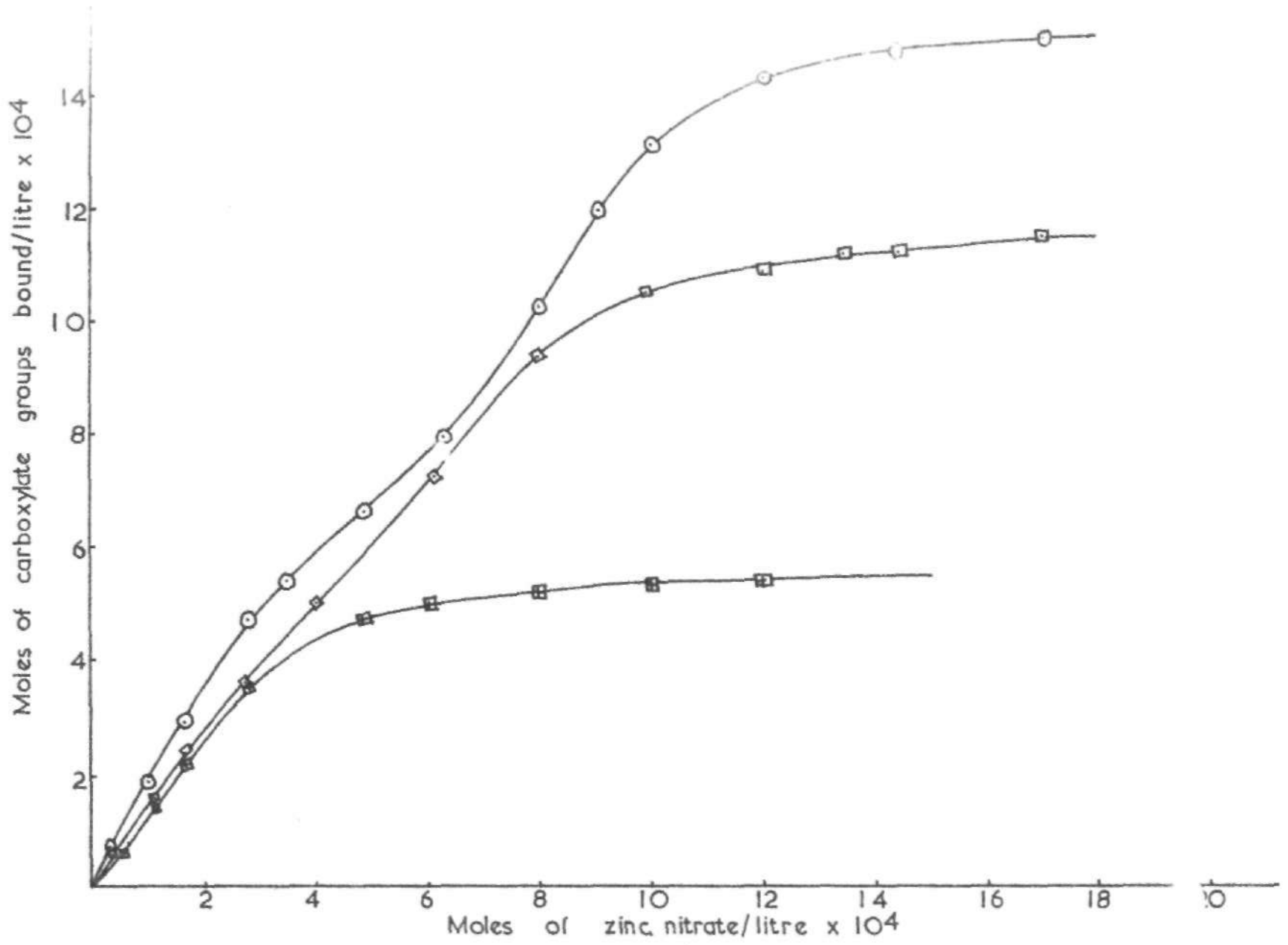


FIG 6.12 Complex formation curves of Zn–PMA at constant ionic strength and polymer concentration at various degrees of neutralization. [PMA]=2.50X10^{-3}M; I=0.01 α:- (⊙) 0.75 ; (⊡) 0.60 ; (⊞) 0.30

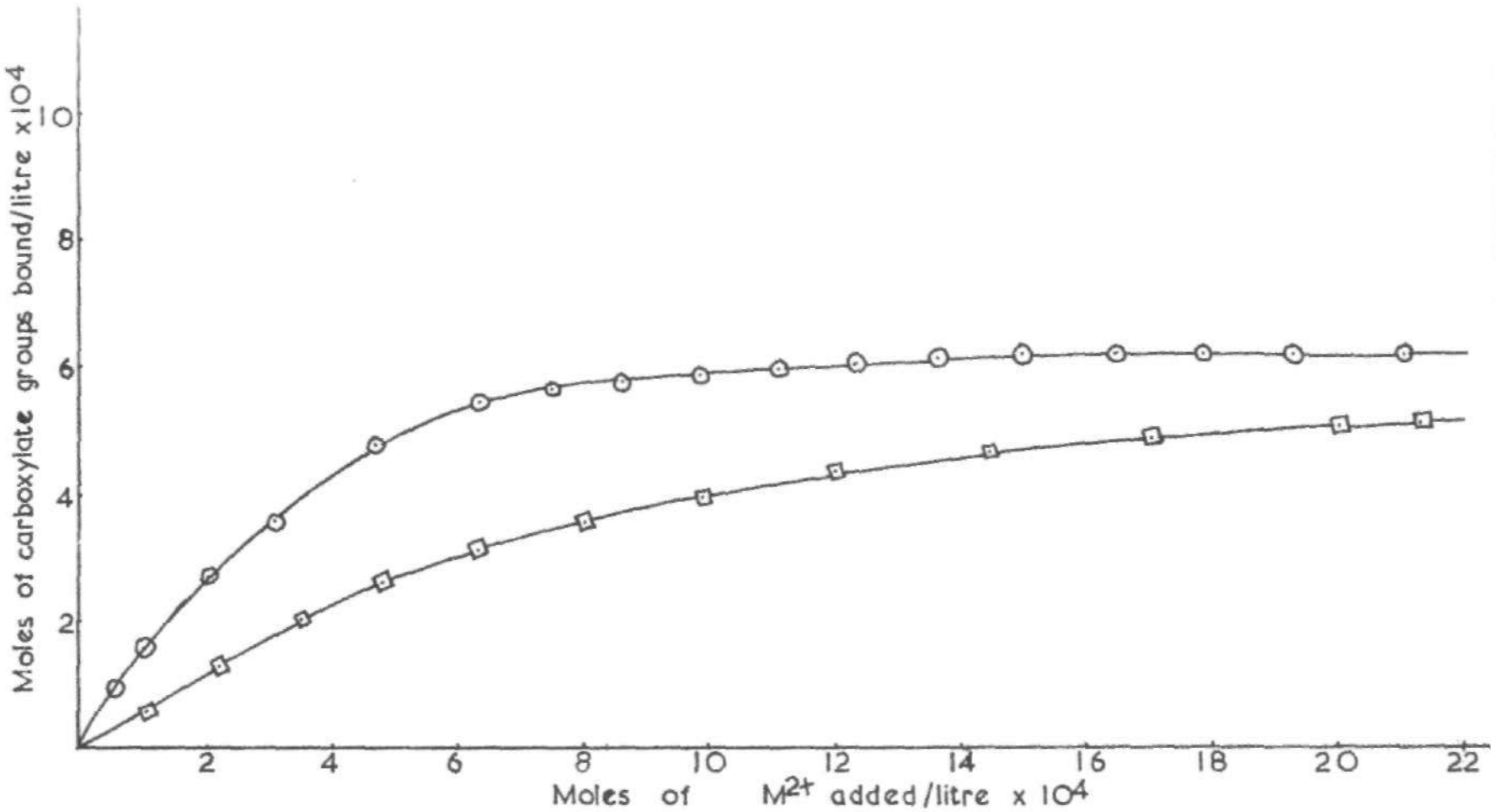


FIG 6·13 Comparison of the amounts of carboxylate groups bound for the same amount of copper or zinc nitrate added at $\alpha = 0.30$

[PMA] = 2.50×10^{-3}M ; I = 0·10 ; (⊙) Cu^{2+} ; (⊡) Zn^{2+}

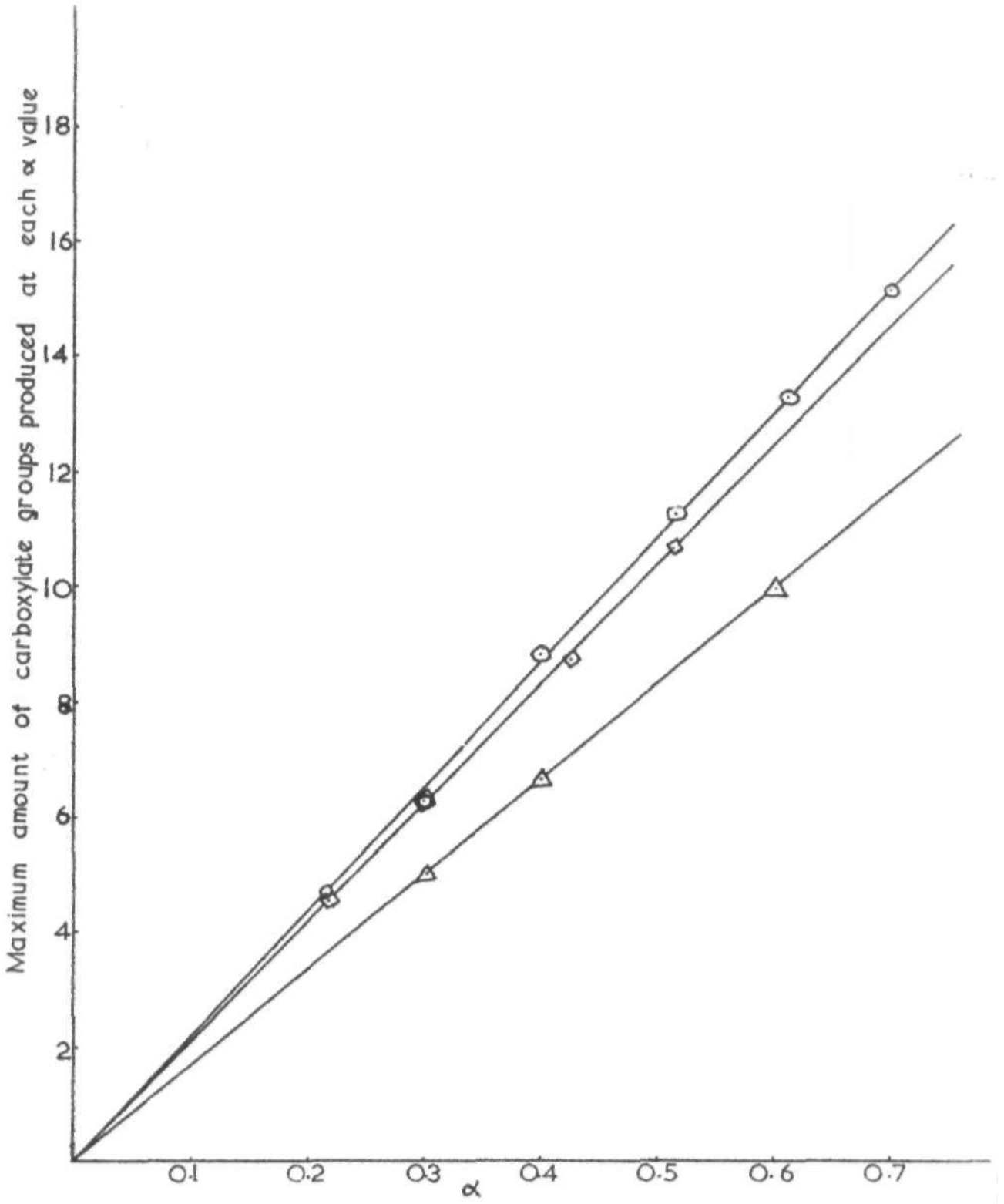


FIG 6.14 Comparison of maximum of carboxylate groups bound for Cu–PMA and Zn–PMA at varying α of PMA and in the presence of varying ionic strengths.
(⊙) Cu PMA at I = 0·05; (⊡) Cu–PMA at I = 0·10
(△) Zn – PMA at I = 0·10

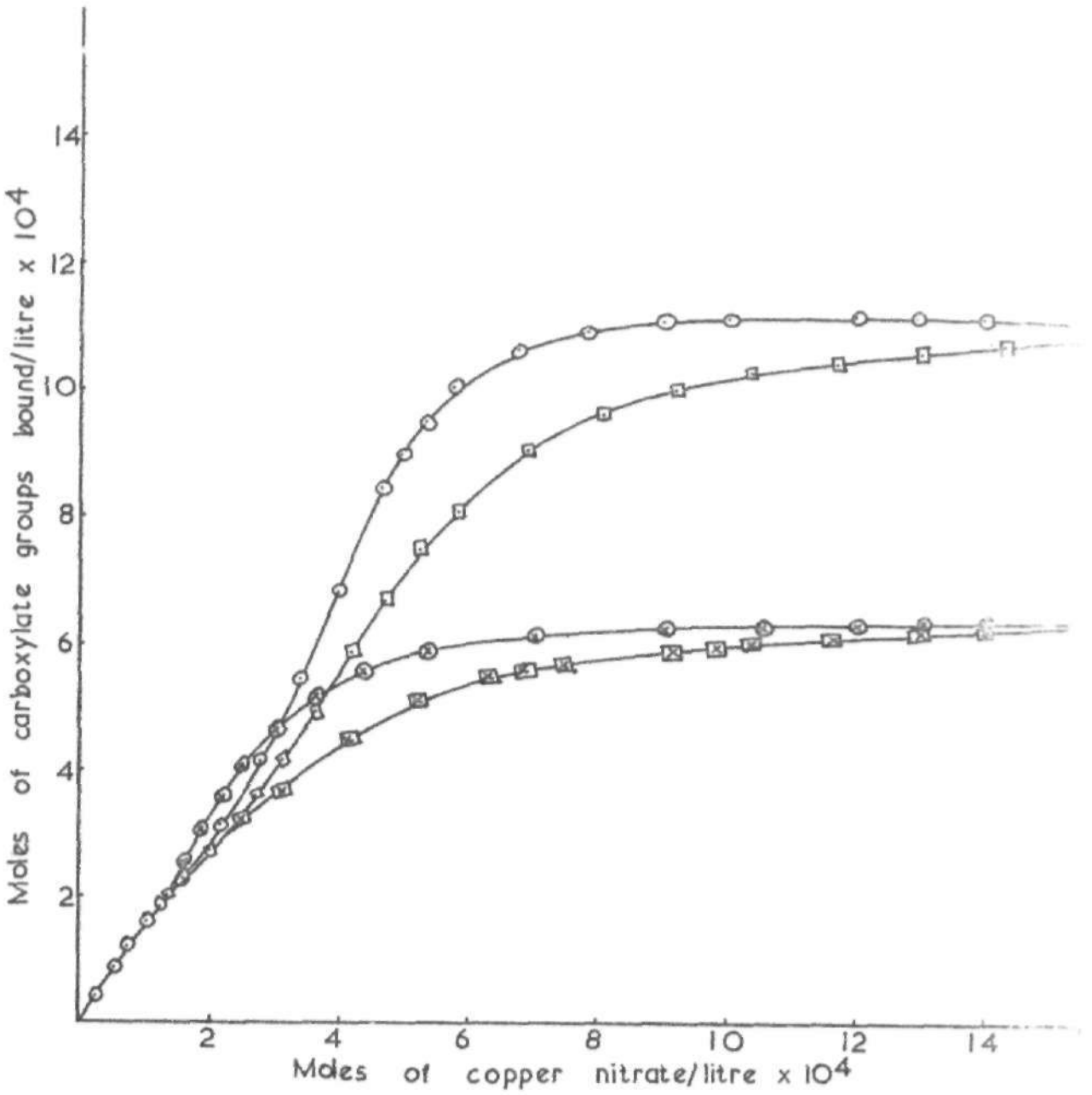


FIG 6.15 Effect of ionic strength on binding of copper to PMA at [PMA] = 2.50 X 10^{-3}M

(⊙) α = 0.50 ; I = 0.05 ; (⊡) α = 0.50 ; I = 0.10

(⊗) α = 0.30 ; I = 0.05 ; (⊠) α = 0.30 ; I = 0.10.

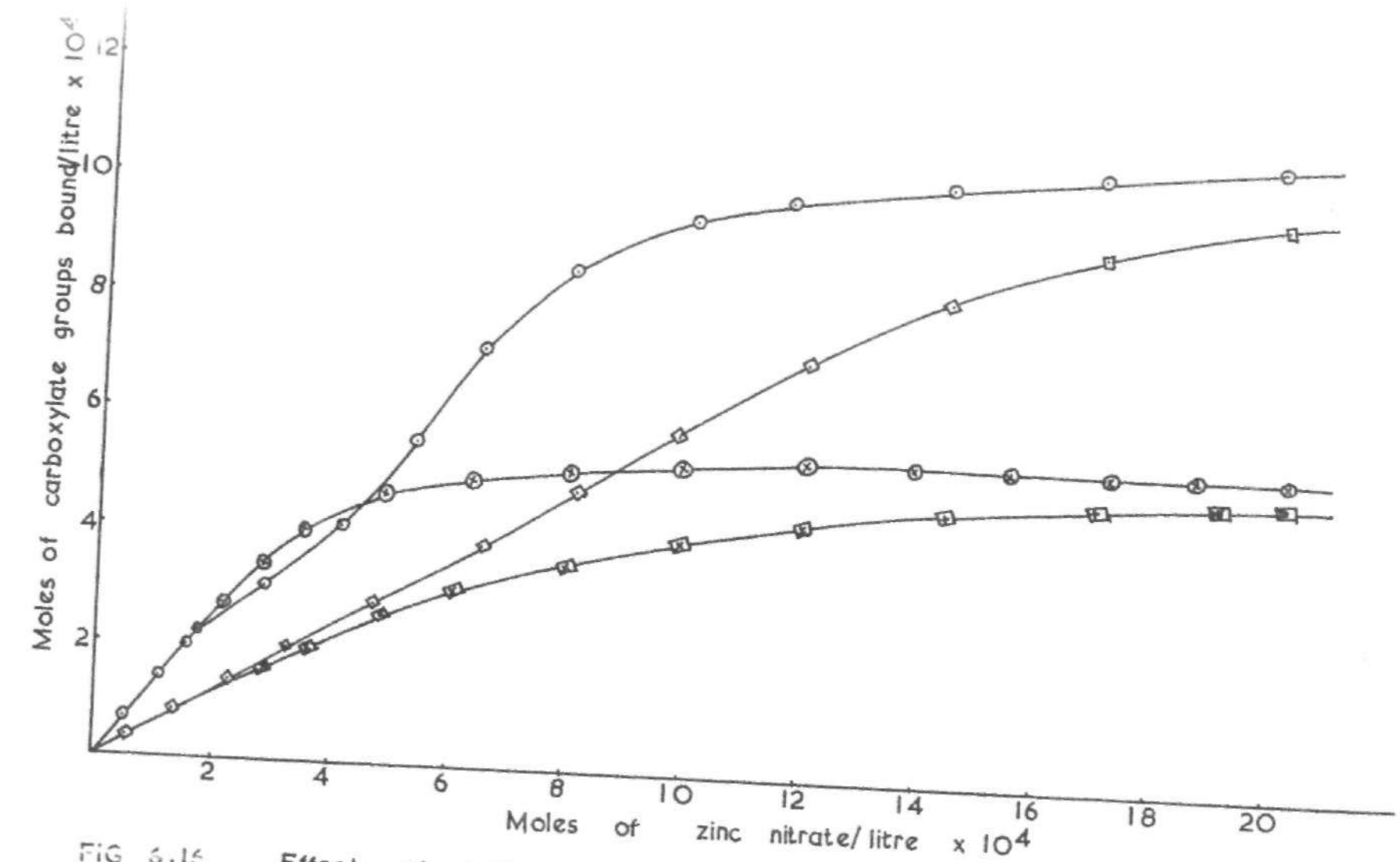


FIG 3.16 Effect of ionic strength on the binding of zinc to PMA at [PMA] = 2.50×10^{-3} M.

(⊙) $\alpha = 0.60$, $I = 0.01$; (⊡) $\alpha = 0.60$, $I = 0.10$;

(⊗) $\alpha = 0.30$, $I = 0.01$; (⊠) $\alpha = 0.30$, $I = 0.10$.

6.4 REFERENCES

1. McInnes D., Principles of Electrochemistry.
2. Kirkwood J. G. and Westhiemer F. H., J. Chem. Physics. 6, 506, (1938).
3. Eberson L., Acta. Chem. Scad. 13, 211, (1959).
4. Linderstrom-Lang K., Compt. Rend. Trav. 15, 17, (1924).
5. Bjerrum N., Z. Physik. Chem. 106, 214, (1923)
6. Von Mulrat A. L., J. Am. Chem. Soc. 52, 3518, (1930).
7. Cohn E. J., Cold Spring Habour Symposia Quant Biol. 6, 8, (1938).
8. Cohn E. J. et al, J. Am. Chem. Soc. 59, 509, (1937).
9. Kern W., Z. Physik Chem. 181, 249, (1938).
10. Katchalsky A. and Spitnik P., J. Poly. Sc. 2, 432, (1947).
11. Cannan R. K., Cold Spring Habour Symposia Quant Biol. 6, 1, (1938)
12. Cannan R. K., Kilbrick A. and Palmer A. H., Ann. N.Y. Acad. Sc. 41, 243, (1941).
13. Kagawa I. and Katsuura K., J. Poly Sc. 7, 89, (1951).
14. Katchalsky A., Shavit N. and Eisenberg H., J. Poly. Sc. 13, 69, (1954).
15. Spencer H. G., J. Poly. Sc. 56, S25, (1962).
16. Marcus R. A., J. Phys. Chem. 58, 621, (1954).

17. Katchalsky A., Mazur J., and Spitnik P., J. Poly. Sc. 23, 513, (1957)

18. Katchalsky A. and Gill J., Rev. Trav. Chim. 68, 879, (1949).

19. Arnold A. and Overbeek J.G., Rev. Trav. Chim. 69, 192, (1950)

20. Hermanns J.J. and Overbeek J.G., Rev. Trav. Chim. 67, 761, (1948).

21. Kuhn W., Kunzle O., and Katchalsky A., Helv. Chim. Acta. 31, 1994, (1948).

22. Fouss R. M., Katchalsky A., and Lifson S., Prod. Natl. Acad. Sc. U.S. 37, 57, (1952).

23. Kimbal G. E., Gutler N. and Samelson H., J. Phys. Chem. 56, 57, (1952)

24. Alfred T., Bery P. W. and Morawetz H., J. Poly. Sc. 7, 543, (1951)

25. Katchalsky A. and Lifson S., J. Poly. Sc. 13, 43, (1954).

26. Kuhn W. and Kuhn H., Helv. Chim. Acta. 26, 1394,(1943)

27. Katchalsky A., J. Poly. Sc. 7, 393, (1951).

28. Leyte J. C. and Mandel M., J. Poly. Sc. A2, 1899,(1964)

29. Mandel M., Leyte J. C. and Staudhouder M. G., J. Phys. Chem. 71, 603, (1967).

30. Zimm H. B., and Rise, S. A., Mol. Phys. 3, 391, (1960)

31. Gregor H. P., Lutinger L.B. and Loebl E. M., J. Phys. Chem. 59, 366, (1955).

32. Kotlair A. M. and Morawetz H. J. Am. Chem. Soc. 77, 3692, (1955).

33. Morawetz H. J., J. Poly. Sc. 17, 442, (1955)

34. Mandel M. and Leyte J. C., J. Poly. Sc. A2, 2883, (1964).

35. O'Neil J. J., Loeld E. M. and Kadania A. Y. and Morawetz H., J. Poly. Sc. 3, 4201, (1965).

36. Bolewiski C. and Lubira M., Dept. of Physical Chem. School of Medicine, Poznan (1970).

37. Arnold, R., J. Colloid Sc. 12, 549, (1957)

38. MacLaren, J. V., Doctoral Thesis, Nottingham Univ. (1956).

39. Mandel and Leyte, J. Poly. Sc. A2, 1879, (1964).

40. Morawetz, H., Polyelectrolytes Solutions pages 207-146.

Chapter 7

LIGHT SCATTERING STUDIES OF THE BINDING OF POTASSIUM, ZINC AND COPPER TO PMA

C O N T E N T S

		Page
7.1	**Theory**	229
7.1.1.	Introduction	229
7.1.2.	Lord Rayleigh's Treatment	230
7.1.3.	Light Scattering by Macromolecules	233
7.1.3.1.	Debye Equations	233
7.1.3.2.	Zimm Equations	235
7.1.3.3.	Particle Scattering Factor	238
7.1.4.	Average Molecular Weights	239
7.2.	The Practice of Light Scattering ..	240
7.2.1.	Treatment of Data	242
7.2.1.1.	Turbidity Method	242
7.2.1.2.	Rayleigh's Ratio Method	243
7.2.1.3.	Yang's Method..	245
7.3.	Experimental	248
7.3.1.	Introduction	248
7.3.2.	Apparatus Cleaning, Preparation and Clarification of Solvent and Experimental Solutions	248

		Page
7.3.3.	General procedure for preparation of solutions for light scattering measurements	250
7.3.4.	Light Scattering Measurements	251
7.3.4.1.	Turbidity Measurements	252
7.3.4.2.	Angular Dependence of Light Scattering	252
7.4.	Results and Discussion	253
7.4.1.	Results	253
7.4.2.	Discussion	256
7.4.3.	Number average and Weight average Molecular Weight and Polydispersity	261
7.5.	S u m m a r y	262
7.6.	R e f e r e n c e s	263

Chapter 7

LIGHT SCATTERING STUDIES OF THE BINDING OF POTASSIUM, ZINC AND COPPER TO POLYMETHACRYLIC ACID (PMA).

7.1. THEORY

7.1.1. Introduction:

Although the general phenomenon of light scattering has been well understood for several years, it is only within the last few years that its utility in the study of macromolecules has clearly been established[1]. As a consequence it is now possible to determine the shape, size and activity coeffiecients of macromolecules in solution by making relatively simple optical measurements. The method of light scattering is both supplementary and complementary to other physical methods (e.g. viscosity and sedimentation), of investigating the properties of macromolecules and therefore offers both a means of measuring and providing completely new and absolute information. Several papers and reviews of the theories of light scattering [1-15] have been published

but an attempt is made here to present only the theories relevant to the present study.

This presentation is concerned primarily with the application of the method of light scattering to the study of the binding of divalent cations to polymethacrylic acid in the presence of KNO_3 with a view to finding out the effect of binding on

(i) the structure of polymer

(ii) the extended length and radius of gyration of the ionized molecule

and (iii) the possible dimerization of the polymer.

7.1.2. Lord Rayleigh's Treatment[1]:

The scattered light arises from the interaction of the incident light with the electrons of the scattering molecule. The passage of light waves may be considered as creating an alternating electric field which induces corresponding oscillations of the electrons. If the characteristic frequency is far from those at which absorption occurs, these induced oscillations set up secondary light waves of the same frequency which are emitted in all directions. The intensity of the light absorbed and re-emitted in this way depends firstly, on

the intensity I_o and wavelength λ_o of the incident beam; secondly on the polarizability of the scattering particles, and thirdly on the number of molecules in a given volume, the concentration v. The theories which relate these are complex[1-15] and only final equations are given here.

The quantitative treatment of light scattering begins with the work of Lord Rayleigh[1] who investigated the scattering from a dilute gas composed of small, independent molecules. Rayleigh showed that the intensity i_θ scattered at an angle θ from the incident beam, relative to the incident intensity, I_o, is given by the expression

$$\frac{i_\theta}{I_o} = \frac{8\Pi^2 \alpha^2}{\lambda_o^4 r_s^2} (1 + \mathrm{Cos}^2\theta) \quad \ldots\ldots\ldots (7\text{-}1)$$

where α is the polarizability, I_o is the incident intensity, λ_o is the wavelength of light in vacuo, r_s is the distance between the illuminated volume and the point of observation. The polarizability is not experimentally determinable but Maxwell has related this to the refractive index of the medium and replacing v, the concentration, by Nc/M

$$\alpha = \frac{\left[n^2 - n_o^2\right]}{C} \frac{M}{4\Pi N n_o^2} \quad .....(7\text{-}2)$$

and equation 7-1 becomes

$$\frac{i_\theta r_o^2}{I_o} = \left[\frac{2\Pi}{N\lambda_o^4}\left(\frac{dn}{dc}\right)^2\right] Mc(1 + Cos^2\theta) \quad ..(7\text{-}3)$$

where n is the refractive index of the solute, n_o is the refractive index of the solvent, N is the Avogadros number, M is the molecular weight of the solute, C is the concentration in gm/ml and dn/dc is the refractive index increament.

In practice the quantity $\frac{i_\theta r_s^2}{I_o}$ is measured and not the individual terms. It has become usual to follow the suggestion of Zimm[16] and call this Rayleigh's ratio or reduced intensity R_θ so that equation 7-3 becomes

$$R_\theta = \left[\frac{2\Pi(dn/dc)^2}{N\lambda_o^4}\right] Mc(1 + Cos^2\theta) \quad ...(7\text{-}4)$$

For molecules whose size is small compared with the wavelength of light, R_θ is found to be independent of θ but when the particles have dimensions greater than 1/20 of the wavelength the molecules will incur a destructive interference from different parts of the

same molecule and the amount of destructive interference increases with increasing θ i.e. decreasing R_θ as θ increases[2, 7, 8].

The light scattering of a gas can be simply obtained by summing the contributions of all the molecules in the scattering volume. However, it is possible to calculate the light scattering of solutions, not by considering individual molecules, but by considering the system as a whole. Light scattering of solutions can be considered in terms of the fluctuation in concentration of the solute molecules by Brownian movement in small volume elements in addition to the density fluctuations of the solvent itself. Since these two properties can be related to measurable quantities, a theory of light scattering of polymer solutions has been formulated.

7.1.3. Light Scattering by Macromolecules:

7.1.3.1. Debye Equation[18]

Light scattering by macromolecules has been much investigated. The theory used was developed by Debye[18] who used a turbidity term $(\tau)cm^{-1}$, the fraction of incident light scattered in all directions by unit volume.

In arriving at an expression for τ, he made use of Eistein's fluctuation theory - the additional scattering from a solution as compared to that of the solvent is considered due to spontaneous fluctuations in concentration[19]. Debye related the intensity of scattering to the change in index of refraction connected with a change in concentration. The relationship can be expressed as for isotropic and non-interacting particles

$$\tau = HCRT(d\rho)dc) \quad .....(7-5)$$

where $H = (32\Pi^2 n_o^2 \, dn/dc)/ 3N\lambda_o^4$

where all the terms have the usual meanings, Debye has also shown that the equation for the scattering due to a solute at concentration c (gm/cc) can be written as

$$\frac{2\Pi n_o^2 (dn/dc)^2}{N\lambda_o^4} \cdot \frac{c}{R_{90}} = \frac{1}{M} + 2Bc \quad .....(7-6)$$

In the above expression, n_o, N, λ, M, c have the usual meanings and R_{90} is the reduced intensity at 90° angle of scattering and B is a constant. The optical constants are usually gathered together and equation 7-6 written as

$$\frac{Kc}{R_{90}} = \frac{1}{M} + 2Bc \quad .....(7-7)$$

or if turbidity is measured

$$\frac{Hc}{\tau} = \frac{1}{M} + 2Bc \quad .....(7-8)$$

where the constant B is a measure of the polymer-solvent interaction and therefore the value of B depends on the environment. In a good solvent B is large and positive, in a poor solven B can be zero or even negative[20-23]. Therefore from the measurements of Rayleigh's ratio at 90^{o} scattering and refractive index increament, plotting $\frac{Kc}{R_{90}}$ or $\frac{Hc}{\tau}$ against c, the molecular weight can be obtained from the reciprocal of the intercept on the ordinate i.e. $(\frac{Hc}{\tau})_{c=o}$ and the slope is 2B.

7.1.3.2. Zimm Equations[16]

The preceding treatment has been built upon the assumption that the particles are small compared with the wavelength of light, isotropic and that they do not strongly interact with one another. The theory has been extended by Zimm[16] to take account of these restrictions. When the light scatterers have dimensions greater than $\lambda/20$, then R_{θ} has been found to be dependent on θ. The interference between radiations from different parts of the same molecule is zero for scattering in the forward direction but increases with angle of observarion. Also, the amount of interference

depends upon the distribution in space of the macro-molecule.

The ratio of the amount of light scattered when internal interference occurs to that which would be scattered in the absence of this effect can be calculated from an equation first given by Debye for x-ray scattering and extended by him to light scattering[1]. This calculation involves summing the interference between all different segments of a molecule as functions of wavelength and the angle of observation. This requires that the extension in space of the molecule be known for certain models. This means that it is necessary to make some assumptions about the shape of the particle before its size can be determined from these factors. Debye also introduced a correction factor known as the particle scattering factor $P_{(\theta)}$[17, 24]. The molecular weight can be calculated using the equation

$$\frac{Kc}{R_{90}} = \frac{1}{MP_{(90)}} + 2Bcp(90) \quad ....(7\text{-}9)$$

This method was found not to be applicable to larger and more extended molecules and it becomes necessary to measure the full angular distribution of light scattering. At finite concentrations the intensity of the

scattered light is generally altered due to solute interaction as characterised by B as well as internal interference. These dual effect have been rigorously resolved by Zimm[16].

$$\frac{Kc}{R_\theta}(1 + Cos^2\theta) = \frac{1}{M_{(P_\theta)}} + 2Bc \quad ..(7\text{-}10)$$

By this means it is possible to extrapolate to zero angle R_θ where internal interference disappears and $P_{(\theta)}$ becomes unity. K, c, R_θ and B have the usual meanings in equation 7-10 and also $P^{-1}(\theta)$ appearing in equation 7-10 is given by

$$P^{-1}_{(\theta)} = 1 + \frac{16\Pi^2}{3}(\frac{P_g}{\lambda})^2 \sin^2\theta/2 \quad ..(7\text{-}11)$$

for linear coiling molecules, a model of greatest interest to the polymer chemist. Finally, equation 7-10 take the form

$$\frac{Kc}{R_\theta}(1 + Cos^2\theta) = \frac{1}{M}\left[1 + \frac{16\Pi^2}{3}(\frac{P_g}{\lambda})^2 \sin^2\theta/2\right] + 2Bc \quad (7\text{-}12)$$

where P_g = radius of gyration, $\lambda^1 = \frac{\lambda_o}{n_o}$ = wavelength of light in solution.

7.1.3.3. Particle Scattering Factor $P_{(\theta)}$

The factor by which the observed intensity at an angle θ must be multiplied to correct for interference is given by the reciprocal of the particle scattering factor appearing in equation 7-11. The expression provides a unique opportunity for measuring the radius of gyration of a molecule without ambiguity. The values obtained from such measurements are absolute, in that they do not depend on the knowledge of some other molecular parameters or some other physical constants. Expressions for $P^{-1}_{(\theta)}$ for the three models commonly encountered in the field of polymer chemistry have been derived by various workers[5, 17, 25, 26, 27]. These expression are

For a sphere of diameter D,

$$P(\theta) = \left[\frac{3}{x^3}(\sin x - x\cos x)\right]^2 \text{ where } x = \frac{KSD}{2} \quad \ldots(7\text{-}13)$$

For a rod of length L,

$$P_{(\theta)} = \frac{1}{x}\int_0^{2x} \frac{\sin w\, dw}{w} - \left(\frac{\sin x}{x}\right)^2, \text{ where } x = \frac{KSL}{2} \quad \ldots(7\text{-}14)$$

For a random coiling polymer for which the root mean square end-end length is h

$$P_{(\theta)} = \frac{2}{x^3}\left[e^{-x} - (1-x)\right] \text{ where } x = \frac{K^2 s^2 h^2}{6} \quad \ldots(7\text{-}15)$$

In the three preceding expressions $K = \frac{2\Pi}{\lambda^2}$ and the angle as $S = 2\sin\theta/2$. It is the last expression which is of the greatest interest to the present study and has appeared in equation 7-12.

7.1.4. Average Molecular Weights:

If a substance is not homogeneous with respect to its molecular weight, there are various ways of averaging molecular weights and each may be appropriate to what is needed. Three types of average molecular weights are encountered viz: the number average molecular weight $\bar{M}_n$, the weight average molecular weight $\bar{M}_w$ and the Z-average molecular weight $\bar{M}_z$. It was Zimm and Doty[28] who first demonstrated that the molecular weight obtained in light scattering is the weight average molecular weight given by

$$\bar{M}_w = \Sigma mi\ Mi^2 / \Sigma mi\ Mi$$

$$\text{or} \qquad = \Sigma ci\ Mi / \Sigma ci$$

where Mi is the molecular weight, ci denotes weight concentration and mi denotes molar concentration of its component. The dependence of light scattering on molecular weight average has the consequence that minute quantities of particles having quite high effective

molecular weights such as dust and other foreign, colloidal suspended matter will seriously affect the results obtained. Light scattering represents the only method besides sedimentation equilibrium of obtaining weight average molecular weights.

It is only if the material is completely homogeneous with respect to the molecular weight that all the averages would be exactly equal to each other. If the material is not homogeneous $\bar{M}_z > \bar{M}_w > M_n$. Indeed, the ratios of the various averages to each other gives some idea of the degree of heterogeneity.

7.2. THE PRACTICE OF LIGHT SCATTERING

Various forms of photoelectric apparatus for the measurement of the angular dependence of light scattering from polymer solutions have been described by various investigators[2, 29-33]. The model used for the present study is the Brice Phoenix 2000 Series Universal Light Scattering Photometer, a detail description of which is found in the manual of Phoenix Precision Instrument Company[15]. This equipment incorporates some important refinements over the previous types. All light

scattering photometers basically consist of a powerful source of monochromatic polarized or unpolarized light (5461A^{o} or 4360A^{o}), an arrangement of lenses and slits, a cell holding the experimental solutions and a rotable photomultiplier so that measurements can be made at varying angles.

In the present study the intensity of scattered light was measured at varying angles between 45^{o} and 135^{o} for studies involving angular dependence of light scattering and at 90^{o} for the turbidity measurement. Details of these measurements are found in reference[15]. The technical problems characteristic of light scattering are essentially the preparation of the solutions in such a state of optical clarity that light intensity actually measured is due only to the solvent and solutions. This means that the removal of dust and extraneous highly scattering particles is certainly a major source of error and poses a major problem facing many workers in this field. Various workers[34-42] have used centrifugation in conjuction with filtration through sintered filters to clarify the solution whilst millipore filters were used to clarify the solvent.

7.2.1. Treatment of Data:

In the present study, two methods can be used to give the information required.

(i) By measuring the turbidity at a fixed angle 90^{o} and at various concentrations of the solute, the molecular weight and polymer-solvent interaction can be obtained.

(ii) The measurement of Rayleigh's ratio at different angles of scattering, will give $\bar{M}_w$, ρ_g and B.

7.2.1.1. Turbidity Method:

Following from equation of Debye

$$Hc/\tau = 1/M + 2Bc \quad .....(7-8)$$

the ratio Hc/τ is plotted as a function of c, where c is expressed in gm per ml. The scattering at 90^{o} is measured and various values of R_{90} for different concentration would give the corresponding values of τ. The plot of Hc/τ against c is expected to be linear. The straight line can be extrapolated to the ordinate and the intercept $\left(\frac{Hc}{\tau}\right)_{c=0}$ is equal to the reciprocal of the molecular weight. The slope of the graph is 2B.

7.2.1.2. Rayleigh's Ratio (Double Extrapolation Method):

Firstly, R_θ has to be determined. A convenient method is to measure the intensity of scattering at various angles for the solvent and the solution. This is done by measuring a series of G_θ and G_w, (for solvent and then solution) where G_θ and G_w refer to scattering intensity at the zero angle and the angle concerned respectively. These values are then converted to R_θ by means of the equation given by Tomimatasu and Palmer[15]. The values of such R_θ obtained have been represented graphically in a Zimm plot[30] when $\frac{Kc}{R_\theta}(1+\cos^2\theta)$ is plotted as a function of $kc + \sin^2\theta/2$ where k is an arbitrary constant chosen to spread the abscissa scale. In the present work, values of R_θ have been calculated with the aid of a ICL 1901 computer. The compilation of $\frac{Kc}{R_\theta}(1 + \cos^2\theta)$ and $Kc + \sin^2\theta/2$ have been carried out by the computer. The program used for this analysis is presented in the appendix. The Zimm plot just mentioned makes double extrapolation possible. Smoothed lines are drawn through the experimental points at a constant angle and at a constant concentration, thereby forming a series of gridlines. Each of the lines is extrapolated to zero

angle or zero concentration. Lines are drawn through these extrapolated points, the two lines should meet at the same intercept and the reciprocal of the intercept is equal to the molecular weight if the incident light is vertically polarized, or is equal to twice the molecular weight if unpolarized light has been used[43]. The slope of the line of zero angle gives the value of B and the slope of the limiting line at zero concentration gives the radius of gyration ρ_g from the following relationships.

$$\rho_g^2 = \frac{3}{16\Pi^2}\left[\frac{\lambda'_o}{n_o}\right]^2 \frac{\text{Slope}}{\text{Intercept}}$$

$$\text{i.e. Limiting slope} = \frac{16\Pi^3}{3\bar{M}_w}\left(\frac{\rho_g^2}{\lambda'}\right) \quad \text{where } \lambda' = \frac{\lambda_o}{n} \quad ..(7\text{-}16)$$

In extrapolation, it is better to extrapolate the lines at constant concentration to zero angle before extrapolating the lines at constant angle to zero concentration. If the shape of the molecule is known especially from viscosity studies then the relations given below can be used to obtain the characteristic dimension from the radius of gyration.

For a sphere,[44] $\rho_g 2 = 3D|20$

For a rod of length L[44] $\rho_g 2 = L^2|12$

For a random coil of end to end distance h[44]

$$\rho_g 2 = h^2|6.$$

7.2.1.3. Yang's Method[45]

For particles having high molecular weights, double extrapolation of Zimm plot is frequently difficult and uncertain. With very assymetric molecules this extrapolation is difficult one owing to the extreme steepness of the Zimm plot. An alternative method of obtaining the same results was evolved by Yang[45] which obviates some difficulties and serves as a good check upon the accuracy of the extrapolation. Yang modified the original equation from which the Zimm plot was derived. Equation 7-12 can be rewritten as

$$\frac{Kc}{R_\theta}(1 + \cos^2\theta) = m\sin^2\theta|2 + 2Bc + \left(\frac{Kc}{R_\theta}\right)_{\substack{c=o \\ \theta=o}} \quad (7\text{-}17)$$

In the expression above, $m = 16\Pi^2\rho_g^2|3\bar{M}_w\lambda'^2$ from which the radius of gyration is determined and just as in Zimm's plot, if $\frac{Kc}{R_\theta}(1 + \cos^2\theta)$ is plotted against c a linear graph will be obtained having $(m\sin^2\theta|2 + \frac{1}{M_w})$

as the intercept and B as the slope and at $\theta = 0$, the intercept along $\left(\frac{Kc}{R_\theta}\right)_{\substack{c=o \\ \theta=o}}$ becomes $\frac{1}{M_w}$.

Now by dividing equation 7-17 all through by $\sin^2\theta/2$, Yang obtained

$$\frac{Kc(1 + \cos^2\theta)}{R_\theta \sin^2\theta/2} = m + \frac{2Bc}{\sin^2\theta/2} + {}^1/\bar{M}_w \sin^2\theta/2$$

$$= m + \frac{1}{\sin^2\theta/2}\left(2Bc + \frac{1}{M_w}\right) \quad \ldots\ldots (7\text{-}18)$$

Thus the plot of $Kc(1 + \cos^2\theta)/R_\theta \sin^2\theta/2$ against ${}^1/\sin^2\theta/2$ is expected to be linear and have an intercept of m and a slope of $(2Bc + 1/\bar{M}_w)$, becoming $1/\bar{M}_w$ for the c=o line. m has been identified with the limiting slope of the $Kc(1 + \cos^2\theta)/R_\theta$ against $\sin^2\theta/2$ in the Zimm plot. Now, by extrapolating to zero concentration, a zero concentration line can be drawn passing through m and having a slope of $1/\bar{M}_w$. Once $\bar{M}_w$ is obtained from the slope, ρ_g can be determined using equation 7-16.

There are several methods available for obtaining the zero concentration line and only two in common use will be mentioned here.

(i) Yang has shown that at any given value of $1/\sin^2\theta/2$

$$Kc(1 + \cos^2\theta)/R_\theta \sin^2\theta/2 = \left\{c_2\left[Kc(1+\cos^2\theta)/R_\theta \sin^2\theta/2\right]_{c_1} - c_1\left[Kc(1+\cos^2\theta)/R_\theta \sin^2\theta/2\right]_{c_2}\right\}/c_2 - c_1 \quad \ldots\ldots (7\text{-}19)$$

where c_1 and c_2 are any experimental points. This expression can be used to obtain $\left[Kc(1+\cos^2\theta)/R_\theta \sin^2\theta/2\right]_{c=o}$. For accurate extrapolation, more than one point is needed for three points in the following combination, c_1 and c_2, c_2 and c_3, c_3 and c_1 or six concentrations for four points in the following combination c_1 and c_2, c_2 and c_3, c_3 and c_4, c_1 and c_3, c_1 and c_4 and c_2 and c_4. In each case, the average of all the values is taken as $\left[Kc(1+\cos^2\theta)/R_\theta \sin^2\theta/2\right]_{c=o}$ for a chosen value of $1/\sin^2\theta/2$. Several values of $1/\sin^2\theta/2$ are chosen and the corresponding values of $\left[Kc(1+\cos^2\theta)/R_\theta \sin^2\theta/2\right]_{c=o}$ are calculated and plotted to define the c=o line.

(ii) A second method and one which has been applied in the present work consists of plotting a graph of $Kc(1+\cos^2\theta)/R_\theta \sin^2\theta/2$ against concentration c for chosen values of $1/\sin^2\theta/2$. The intercept on the ordinate $\left[Kc(1+\cos^2\theta)/R_\theta \sin^2\theta/2\right]_{c=o}$ is determined for each angle and plotted against the corresponding $1/\sin^2\theta/2$ to define the c=o line.

Yang applied this method successfully to the data of Benoit, Holtzer and Doty[46] on cellulose nitrate and obtained values consistent with the values obtained by the authors.

7.3. EXPERIMENTAL

7.3.1. Introduction:

With the great majority of Zimm plots reported in the literature, the set of angular measurements on each solution generally follows a systematic patern which allows ready extrapolation to zero angle. The corresponding extrapolation to zero concentration are much less certain. Thus whilst errors of calibration may be the cause of variations in the level of results between different workers[47] and faults of instrumental design would most probably give systematic errors[48], the major source of uncertainty within a given set of data results from the practical difficulties in preparing the solutions.

The removal of particles and extraneous scatterers from solvent and solutions required for scattered light intensity measurements is a formidable experimental problem peculiar to this technique.

7.3.2. Apparatus Cleaning, Preparation and Clarification of solvent and experimental solutions:

The avoidance of contamination, so far as possible, during solution preparation is desirable. All glassware was thoroughly cleaned with a cleaning mixture of

H_2SO_4 containing a little $NaNO_3$ and $NaClO_4$. The apparatus was later washed with all glass-distilled water and rinsed several times with ultrafiltered water. The ultrafiltered water was obtained by repeatedly passing the water through a 0.22μ millipore filter[49].

The optically polished cylindrical and square cells used in the light scattering apparatus were made scrupulously clean both inside and outside by first cleaning them with deacon 90 and later rinsing several times with ultrafiltered water. The cells were finally cleaned by flushing with a jet of redistilled acetone in an all glass closed apparatus[49]. Once cleaned, all glassware was kept in a desiccator which has been scrupulously cleaned as well.

All aqueous solutions other than the polymer solution were clarified by filtration under pressure using 0.22μ millipore filters[49].

The extraneous material found in solutions of polymers is made up of the dust, fibre and particles accumulated throughout its preparation. A variety of methods have been recommended for clarification of solutions[30,50-52]. In the present work centrifugation

in conjuction with filtration through sintered glass was used to clarify the polymer solution. Centrifugation at 17,000 rpm for 8 hours and at 25°C was found to give satisfactory results. The centrifuge tubes were quite large, easily accessible so that no shaking of solution occured when removing the seals. Only about half of the polymer solution in each centrifuge tube was removed with a clean pipette and this was used as the final stock solution. The final concentration of the polymer solution was determined spectrophotochemically at 213 millimicrons with the aid of a calibration curve previously prepared.

7.3.3. GENERAL PROCEDURE FOR PREPARATION OF SOLUTIONS FOR LIGHT SCATTERING MEASUREMENTS.

The interaction of PMA with divalent cations has been studied in KNO_3 and at a degree of neutralization $\alpha = 0.30$.

Dilutions were made from the stock solution to contain the required concentration of PMA and A.R. KNO_3 to give a strength equal to 0.05M was added.

Each solution was filtered slowly under low pressure of nitrogen through sintered glass (porosity 3)[53]; the filtrate being collected directly into the scrupulously clean scattering cell. An ultrafiltered solution of KOH was added from a micropipette in amounts equivalent to 0.30 of the total acid present. The total volume of the base added was in all cases about 1% of the volume of the solution. In studies involving divalent cations, the solutions were prepared as above except that divalent cations were added after filtration and addition of KOH.

As rightly pointed out by Arnold and Caplan[53] the use of sintered glass filter after centrifugation rather than ultrafiltration recommended by some authors for PMA solutions was necessitated by high viscosity of aqueous polymer solution.

7.3.4. Light Scattering Measurements:

Light scattering measurements were carried out at room temperature of 25 ± 1°C using unpolarized monochromatic light (green mercury line $\lambda = 5461\text{Å}$). The solvent used was ultrafiltered water. Two types of measurements were made. (i) Turbidity measurement at 90° scattering angle and (ii) Angular dependence of light scattering.

7.3.4.1. Turbidity Measurements:

The mean molecular weight of ionized polymethacrylic acid in 0.05M KNO_3 was determined at 90° scattering. Its value was also determined in the presence of copper and zinc ions. The turbidity of each solution was obtained by the relative degree of scattering of light at 90° and 0°. For each solution Hc/τ was calculated and plotted as a function of polymer concentration in gm/ml.

7.3.4.2. Angular Dependence of Light Scattering:

The scattered intensity was measured for each solution at angles ranging from 45° to 135° at 5° intervals. This was done to enable various values of R_θ at each angle to be calculated. These various values have been computed by ICL 1901 Computer. A cylindrical cell or the square cell was ued for all measurements. Systems containing ionized PMA, copper-PMA and zinc-PMA in presence of 0.05M KNO_3 were studied. The results obtained in (i) and (ii) have been presented graphically.

7.4. RESULTS AND DISCUSSION

7.4.1. Results:

Tables 1 - 3 below show the data obtained from light scattering measurements for the determination of molecular weight of PMA in KNO_3, $Cu(NO_3)_2$ and $Zn(NO_3)_2$ by Turbidity Method.

Table 7-I: PMA in 0.05M KNO_3 at $\alpha = 0.30$

Concentration of PMA x 10^4 gm/ml	Turbidity (τ) x 10^4 cm^{-1}	HC/τ x 10^6 gm cm
1.4930	3.7214	1.1157
2.2394	4.1420	1.5036
2.9859	4.9320	1.6837
3.7324	5.4530	1.9035
4.4789	6.2318	1.9988

Table 7-II: PMA in $Cu(NO_3)_2$ at $\alpha = 0.3$ and $\frac{[PMA]}{[Cu]} = 2.0$

Concentration of PMA x 10^4 gm/ml	Turbidity τ x 10^4 cm^{-1}	HC/τ x 10^6 gm cm
1.4930	5.9291	0.7000
2.2394	8.8797	0.7014
2.6127	9.3502	0.7771
2.9859	9.3379	0.8893
3.7324	10.0934	1.0284
4.4789	12.9941	0.9586

Table 7-III: PMA in $Zn(NO_3)_2$ at $\alpha = 0.3$ $\frac{[PMA]}{[Cu]} = 2.0$

Concentration of PMA x 10^4 gm/ml	Turbidity (τ) x 10^4 cm^{-1}	HC/τ x 10^6 gm cm
2.6127	10.2916	0.7100
2.9859	11.3877	0.7292
3.7324	11.8235	0.8779
4.4789	13.8687	0.8981
5.2254	16.0306	0.9065
6.0500	16.3350	1.0300

The Tables below show a summary of the results obtained from the study of the angular dependence of light scattering in determining the Molecular parameters ($\bar{M}_w$, ρ_g, and $\bar{h}$) of PMA molecule assuming the random coil model.

Table 7-IV:

System Studied	Fig. No.	Concentration of cation (M)	Mol. Wt. x 10^{-6}	$\rho_{g_{nm}}$	h_{nm}
PMA$^-$-K^+	1	0.05	0.500	-	-
	2	0.05	0.470	35.40	86.67
	3	0.05	0.481	34.77	85.17
Average Values			0.479	35.09	85.92

Table 7-V:

System Studied	Fig. No.	[PMA]/[Cation]	Mol. Wt x 10^{-6}	$\rho_{g_{nm}}$	h_{nm}
PMA$^-$-Zn^{++}	4	2.0	1.110	-	-
	5	2.0	1.125	29.96	73.38
	6	2.0	0.990	30.31	74.24
Average Values			1.075	30.14	73.81

Table 7-VI:

System Studied	Fig. No.	$\frac{[PMA^-]}{[Cation]}$	Mol. Wt x 10^{-6}	$\rho_{g_{nm}}$	h_{nm}
PMA—Cu^{++}	7	2.0	0.988	-	-
	8	2.0	1.023	28.52	69.88
	9	2.0	0.970	27.78	68.05
Average Values			0.994	28.15	68.97

7.4.2. Discussion:

Data from viscometric titrations, conductance titration and equilibrium dialysis indicate that two carboxylate groups bind one divalent metal ion. From viscometric and conductometric titrations there are strong indications that dimerization of ionized PMA molecules in the presence of divalent cations occur. It was therefore thought desirerable to carry out light scattering study on PMA and Cu^{2+} and Zn^{2+} ions with emphasis on the mode of binding of these cations to

polymeric chains, determination of molecular weight and molecular parameters.

In the present work, various attempts were made to study light scattering of PMA in aqueous solutions without added simple electrolyte. No reproducible results were obtained and it was impossible to draw a Zimm plot. From the data obtained, it was concluded that in the absence of simple electrolytes the intensity of scattered light is greatly reduced and makes it impossible to make any reasonable measurements. It has also been stated[39] that angular distribution is no longer a simple function of the molecular dimenssions in the absence of salt.

All the experiments were performed in presence of 0.05M KNO_3. Figures 7.1-3 show various plots obtained from light scattering of PMA in 0.05M KNO_3 and at $\alpha = 0.30$. The weight average molecular weight ($\bar{M}w$) obtained for the PMA sample was found to be 0.479×10^6. All plots; (Turbidity method, Yang's method and Zimm method) gave comparable results as seen from Table IV.

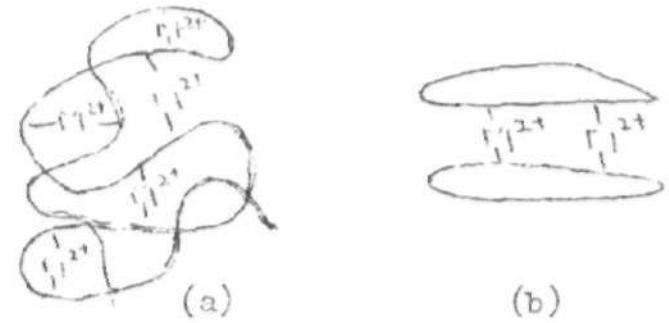
It has been stated in sections on viscosity, conductance and potentiometric titrations that K^+ does not interact to any appreciable extent with ionized PMA.

The presence of KNO_3 is to help stabilize the structure of the molecule in solution. One would therefore not expect the molecular weight to be affected by the presence of KNO_3, so that the molecular weight obtained by turbidity measurement is a true molecular weight of PMA. This observation is in agreement with Olayemi's[53] observation. He observed that the molecular weight of polyelectrolytes is independent of the presence and concentration of added simple electrolyte. The role of KNO_3 was therefore to enhance the intensity of scattered light through stabilization of molecular structure.

The above picture is quite different in the presence of copper and zinc ions. The weight average molecular weight has been found to be dependent on the concentration of divalent cations. Figures 7.4-6 and figures 7.7-9 show the various plots for PMA-Cu(II) complex and PMA-Zn(II) complex respectively. The data shown in Tables V and VI show that in the presence of these cations, the molecular weight is approximately doubled. This is yet another evidence in support of earlier suggestions that dimerization of PMA molecules in the presence of these divalent cations was feasible.

Dimerization here means association of two polyelectrolyte chains (through divalent cations).

These results can be used to predict the mode of association. Two structures are shown below:



(a) (b)

At low degrees of ionization, PMA molecules exist as random coils. As the degree of ionization increases, the coils unwind and tend. to stretch to a more rigid structure, the extent of stretching depends on degree of ionization. Structure (a) above, shows the coils with the divalent cations crosslinking the two chain segments. Because of the strong repulsive forces the molecules tend to obtain a more rigid rod-like structure (b) with divalent cations forming a bridge between two chains. However, a fully stretched molecule that will give the structure shown in (b) is difficult to obtain. It has been recorded[54] that PMA molecules rarely extend beyond half their contour

lengths even when $\alpha = 1.0$. The pictures presented here should therefore be seen as two extreme cases and the actual structure of the complex formed is between the coiled molecules and rod -like molecules. Any of these structures will lead to a shortening of the molecular chain when binding takes place. From Tables 7-V and 7-VI, it is seen that $\bar{h}_{KNO_3} > \bar{h}_{Cu} < \bar{h}_{Zn}$, but the actual difference in values is not enought to predict with certainty the prefered mode of association. Zinc is usually tetrahedrally co-ordinated while copper always forms square planar complexes. This way of binding may have a specific effect on the structure obtained and may well account for the observed differences.

It is also observed that in the presence of divalent cations, the value of B in Debye equation falls. In PMA-K^+, $B = 2.0 \times 10^{-3}$ whereas in PMA-Zn^{2+} $B = 1.0 \times 10^{-3}$ and in PMA-Cu^{2+}, $B = 0.95 \times 10^{-3}$ and the little differences probably account for the various shapes of Zimm plots. The second virial coefficient is not constant and as seen from above, depends on the molecular weight and probably on molecular weight distribution.

In calculating the various molecular parameters, the random coil model was assumed for partially ionized PAA. Fig.7.10 shows a plot of $P(\theta)^{-1}$ against $\sin^2\frac{\theta}{2}$ where $P(\theta)^{-1}$ is the particle scattering factor for a randomly coiling polymer [equation 7 - 11] In all the three cases, straight lines were obtained showing that the adoption of random coil model was suitable in the system studied.

7.4.3. Number Average and Weight Average Molecular Weight and Polydispersity:

The reciprocal of the slope of zero concentration line in Yang's plot gives the average molecular weight ($\bar{M}w$). Yang also suggested that the number average molecular weight ($\bar{M}n$) for very large particles could be obtained from a plot of $Kc(1 + \cos^2\theta)/R\sin^2\frac{\theta}{2}$ against $1/\sin^2\frac{\theta}{2}$. According to him, the intercept along the ordinate for low angles ($< 80^\circ$) gives $1/\bar{M}w$ while the assymptote at high angles (≥ 80) of the Zimm plot gives as the intercept on the ordinate $1/2\bar{M}_n$. In practice such estimation is very difficult and $\bar{M}_n$ values obtained could be very inaccurate.

In the present work, $\bar{M}_v$, viscosity average molecular weight has been obtained from viscosity measurements and $\bar{M}_w$ obtained light scattering. The value of $\bar{M}_v$ from viscosity is 0.516×10^6 which is comparable with the value of 0.479×10^6 obtained for weight average molecular weight from light scattering experiments.

7.5. Summary:

1. The end-to-end distance of PMA was found to depend on the divalent cation. The end-to-end distance was found to be of the order $\bar{h}_{Cu} < \bar{h}_{Zn} < \bar{h}_K$. The little differences in length could be due to prefered configuration.
2. The binding of copper and zinc to PMA leads to dimerization of PMA molecules. The molecular weight was approximately doubled in presence of divalent cation.
3. The value of the second virial coefficient B, which appeared in Debye equation decreases in presence of Cu^{2+}, Zn^{2+} and K^+ ions and in that order thus accounting for the various shapes of Zimm plots.
4. Partially ionized PMA molecules appear to exist as a random coil molecule.

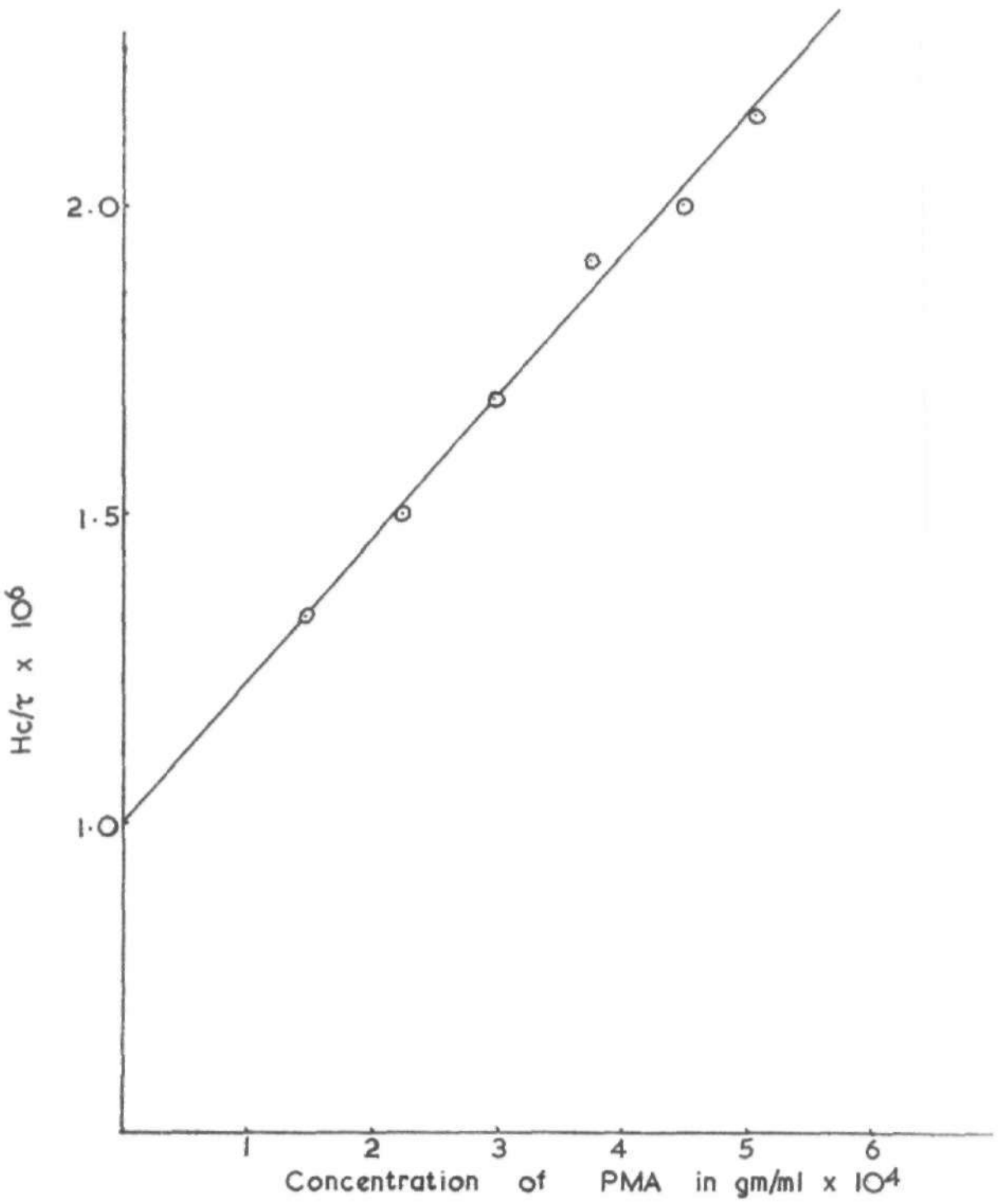


FIG 7.1 Determination of weight average molecular weight of PMA in KNO_3 solution at $\alpha = 0.30$; $I = 0.05$; $M_w = 0.5 \times 10^6$; $B = 2.3 \times 10^3$

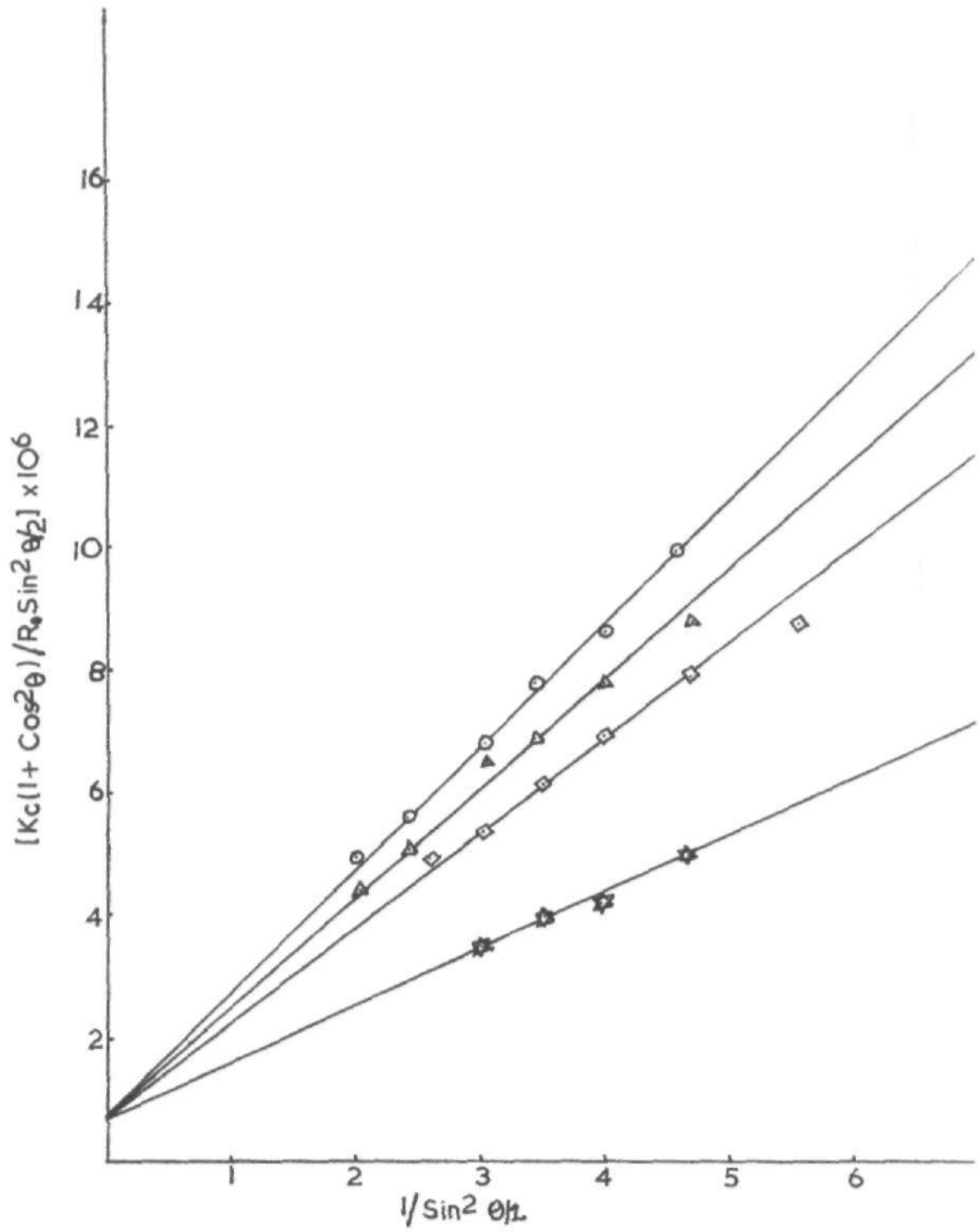


FIG 7.2 Yang's plot for PMA in KNO_3 at a=0.3 and I-0.05

Cocentration of PMA in gm/ml :-(✡ 0.00 ; ⊡ —2.450 ; △ —3.675 ; ⊙ —4.288) $\times 10^{-4}$

M_W=0.470x10^6 $\bar{h}$=86.67nm ρ_o =35.40nm

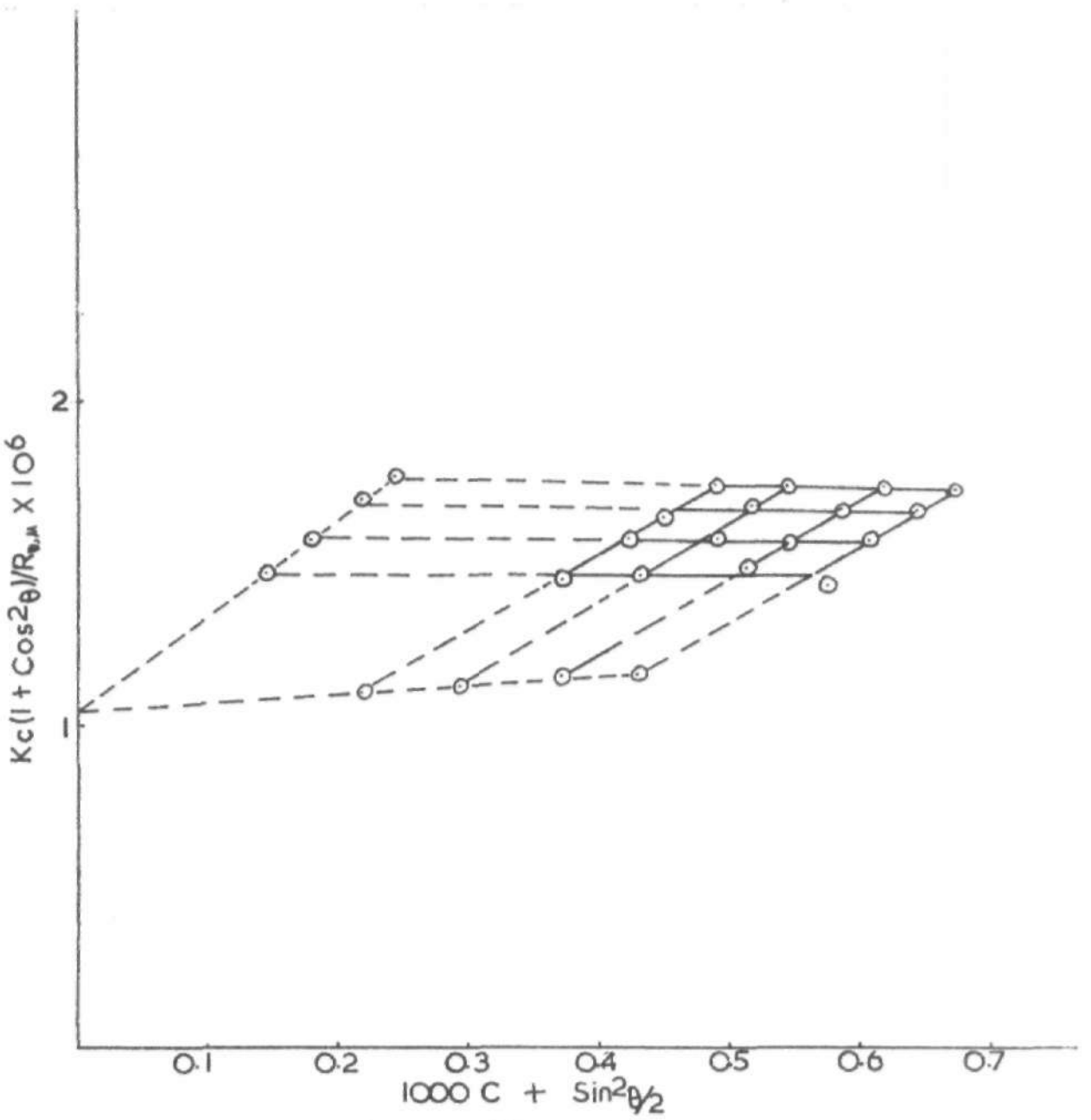


FIG 7.3 Zimm plot for PMA in KNO_3 at α = 0.3 ; I = 0.05

$\bar{M}_W = 0.481 \times 10^6$; $\bar{h} = 85.17$nm ; $\ell_g = 34.77$nm

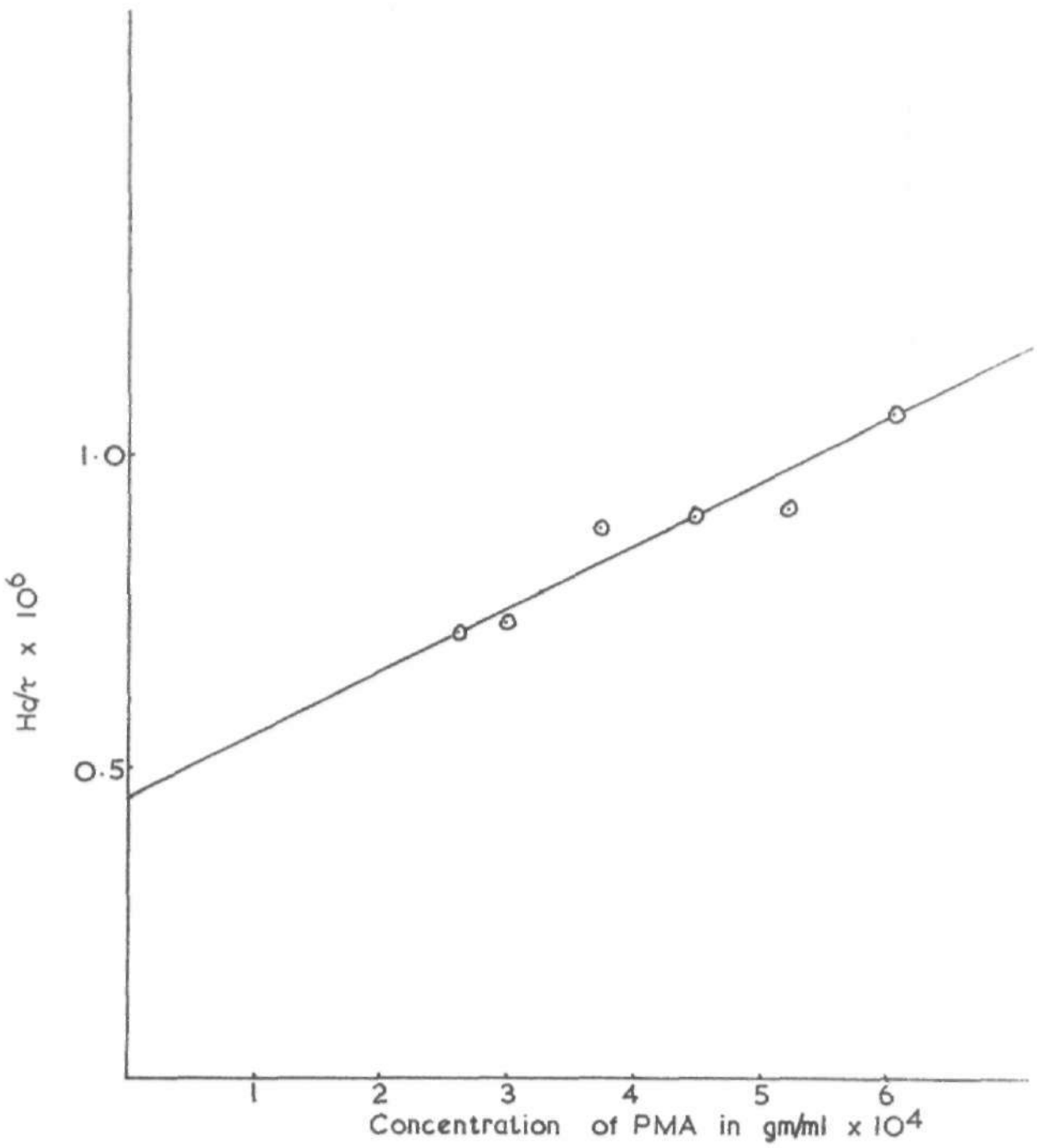


FIG 7.4 Determination of weight average molecular weight for PMA in $Zn(NO_3)_2$ solution at $\alpha = 0.3$; $I = 0.05$; $\frac{[PMA]}{[Cu(NO_3)_2]} = 2$

$M_w = 1.110 \times 10^6$; $B = 1.0 \times 10^{-3}$

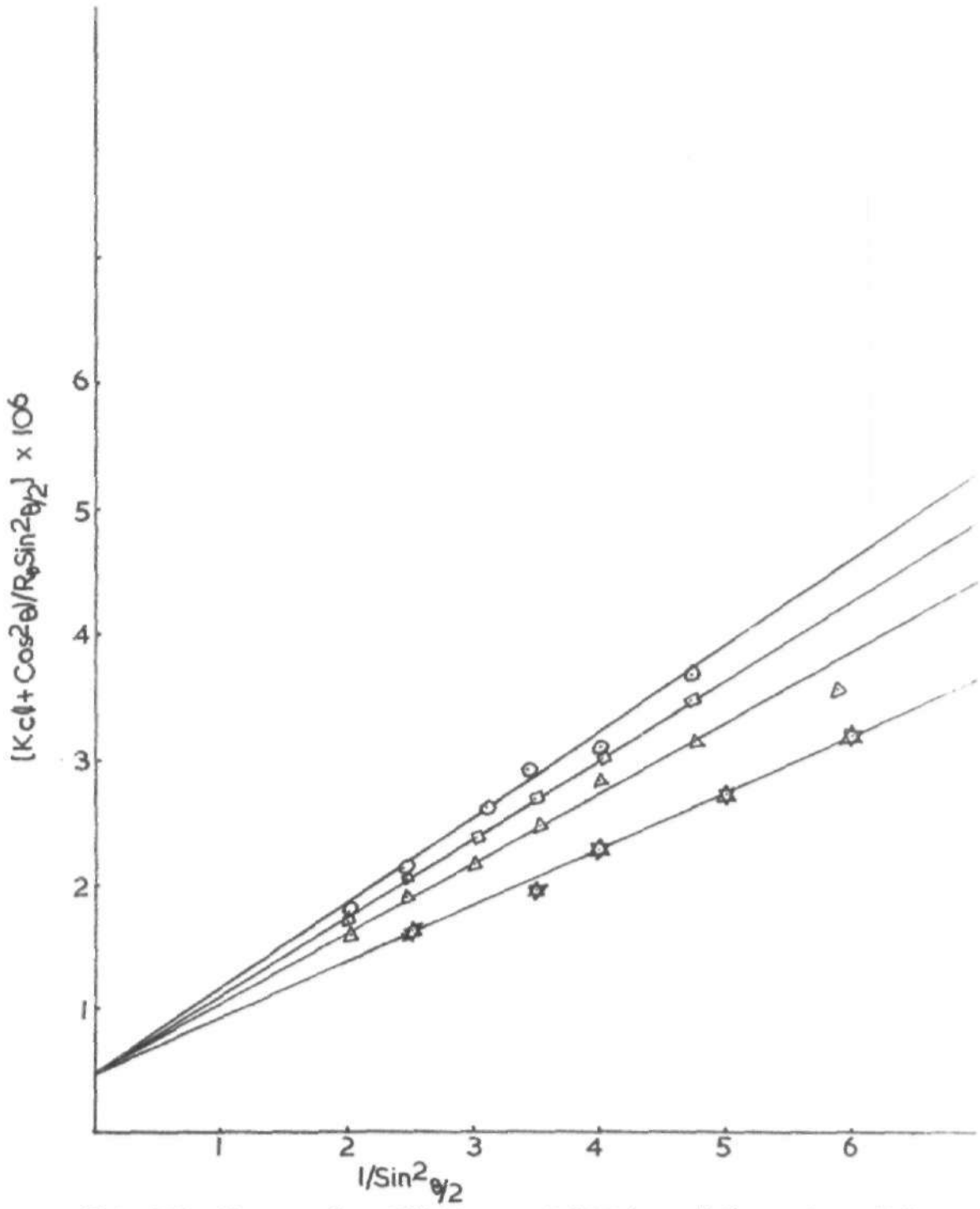


FIG 7.5 Yangs plot of PMA in $Zn(NO_3)_2$ solution at α=0.3;
I = 0.05 $\frac{[PMA]}{[Zn(NO_3)_2]} = 2$
Concentration of PMA in gm/ml :- (✡ — 0.000;
△ — 2.261 ; □ — 4.479 ; ⊙ — 5.225) x 10^{-4} .
$\bar{M}_w$ = 1.125x10^6 ; $\bar{h}$ = 73.38nm ; ℓ_o = 29.96nm.

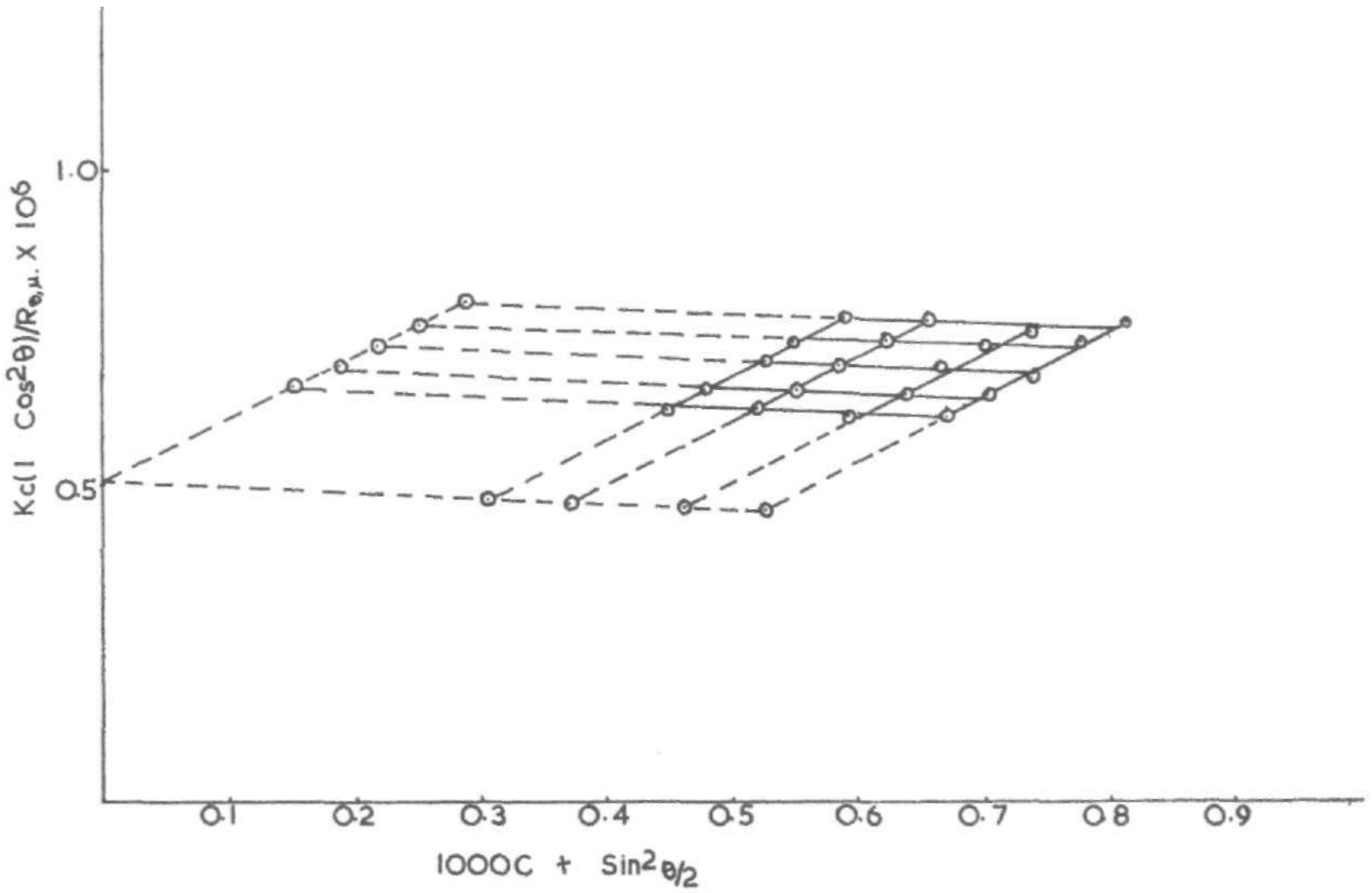


FIG 7.6 Zimm plot for PMA in $Zn(NO_3)_2$ solution at $\alpha = 0.03$; $I = 0.05$; $\frac{[PMA]}{[Zn(NO_3)_2]} = 2$. $\bar{M}_w = 0.99 \times 10^6$; $\bar{h} = 74.24$ nm ; $\rho_g = 30.31$nm .

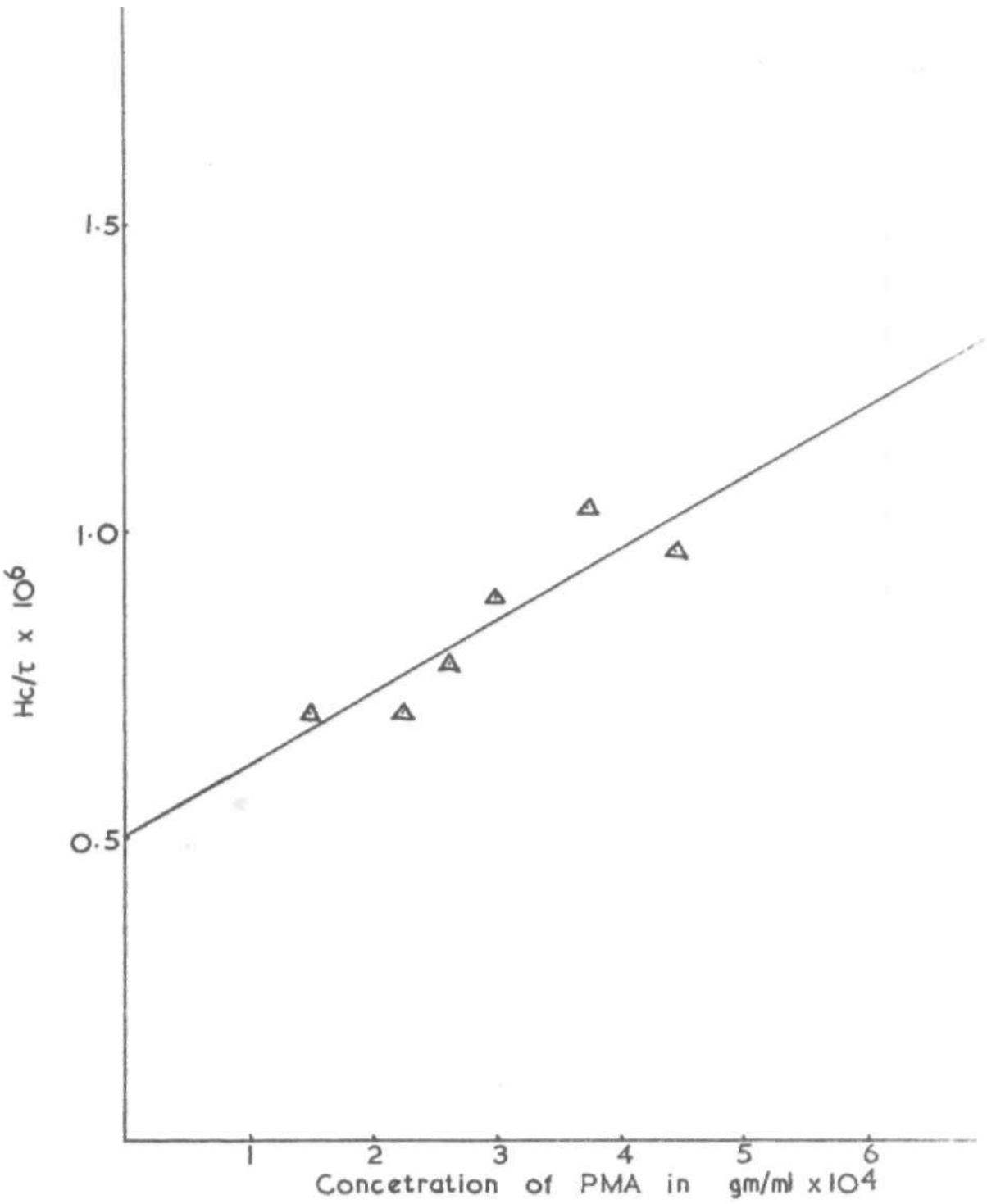


FIG 7.7 Determination of weight average molecular weight of PMA in $Cu(NO_3)_2$ solution at

$\alpha = 0.3$; $I = 0.05$; $\frac{[PMA]}{[Cu(NO_3)_2]} = 2$

$\bar{M}_w = 0.988 \times 10^6$; $B = 0.95 \times 10^{-3}$

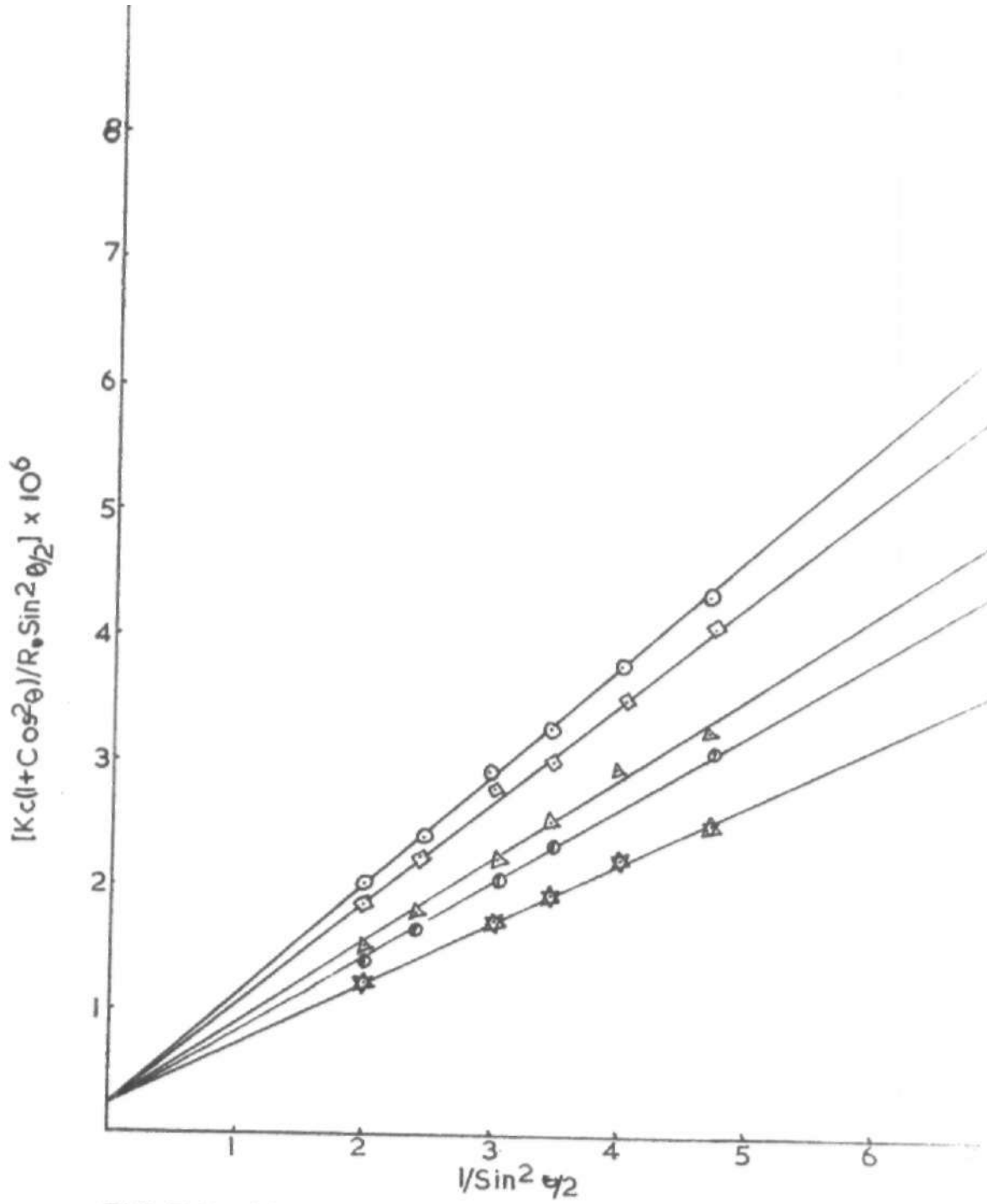


FIG 7.8 Yangs plot for PMA in $Cu(NO_3)_2$ solution at $\alpha = 0.3$; I=0.05 ; $\frac{[PMA]}{[Cu(NO_3)_2]} = 2$.

Concentration of PMA in gm/ml :- 1x 0.00

⊙— 2.239 ; △— 2.613 ; ⊡— 2.986 ; ⊙— 3.372) x 10^{-4}

$\bar{M}_w$ = 1.023 X 10^6 ; $\bar{h}$ = 69.88nm ; ρ_g = 28.52nm

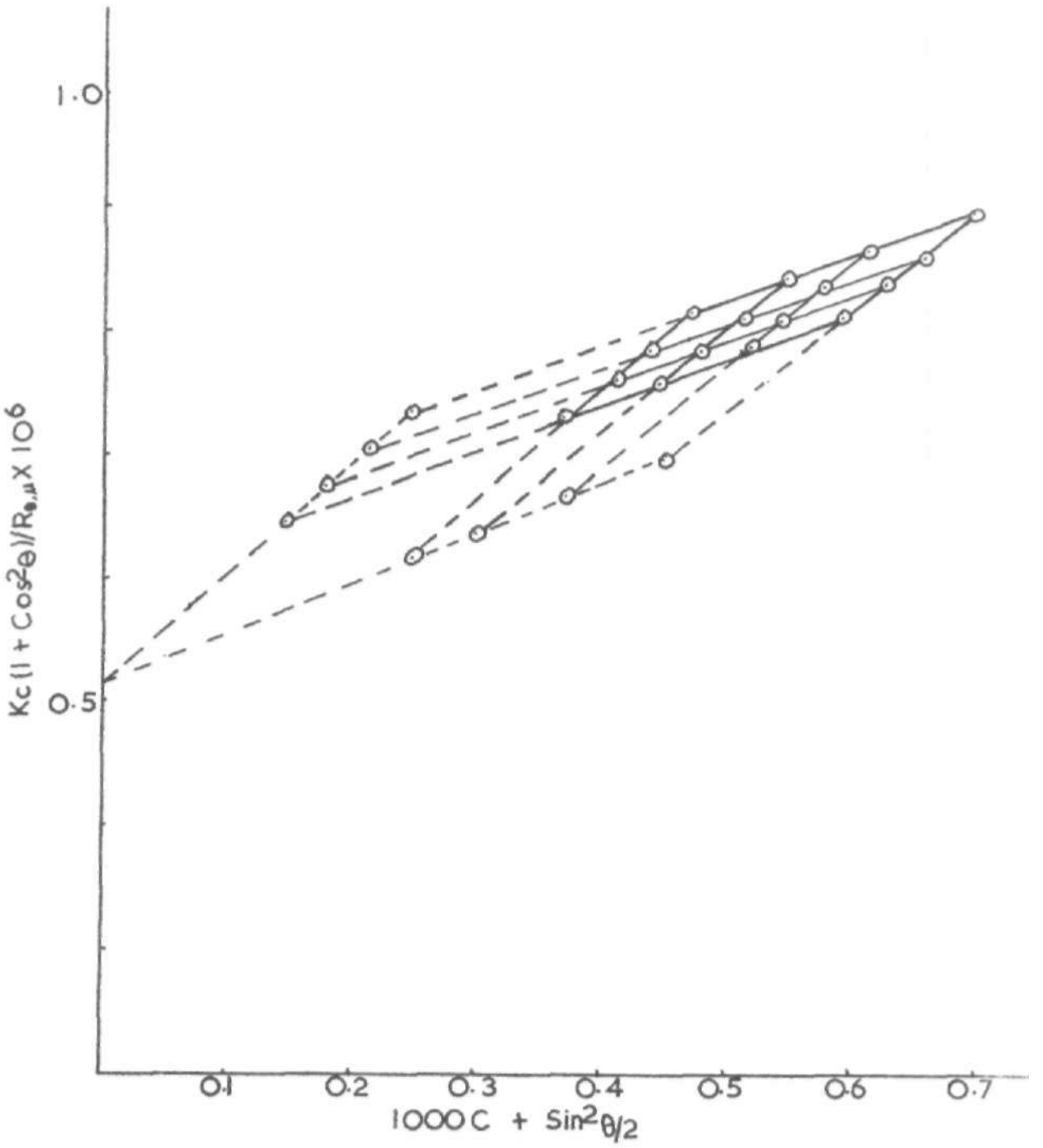


FIG 7.9 Zimm plot for PMA in $Cu(NO_3)_2$ solution at $a = 0.3$; $I = 0.05$; $\frac{[PMA]}{[Cu(NO_3)_2]} = 2$

$\bar{M}_w = 0.970 \times 10^6$; $\bar{h} = 68.05nm$; $\rho_g = 27.78nm$

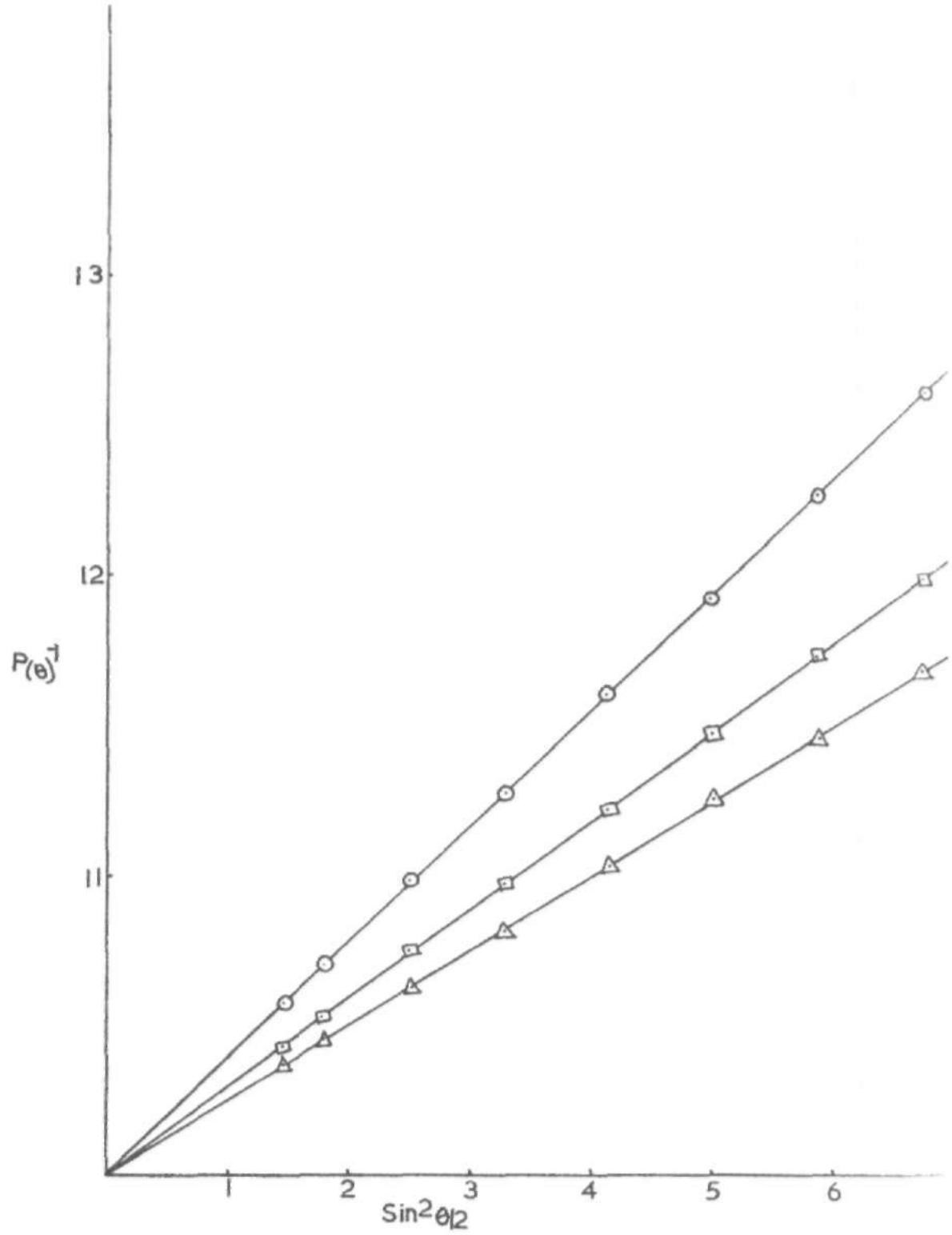


FIG 7.10 Variation of $P_{(\theta)}^{-1}$ with θ for PMA at $\alpha = 0.3$ $\bar{I} = 0.05$ and in the presence of KNO_3 ; $Cu(NO_3)_2$; $Zn(NO_3)_2$; $\frac{[PMA]}{[M^{++}]} = 2$

o – KNO_3 ; ⊡ – $Zn(NO_3)_2$; △ – $Cu(NO_3)_2$.

7.6. REFERENCES

1. Lord Rayleigh, Phil. Mag. 41, 447, (1871).
2. Stacey K. A. in Light Scattering in Physical Chemistry (1956).
3. Huglin, M. B. in Light Scattering from Polymer Solutions 1972.
4. Debye, P., J. App. Physics 15, 338, (1944).
5. Zimm, B. H.; Stein, R. S., and Doty, P., Polymer Bull. 1, 19, (1945).
6. Wilfriel, H.; Records of Chemical Progress 20, 209, (1959).
7. Kirkwood, J. G. and Guldberg, J.; J. Chem. Phys., 18, 54, (1950).
8. Partington, J. R., An Advanced Treatise on Physical Chemistry, 4, 242, (1953).
9. Stacey, K. A.; A Laboratory Manual of Analytical Methods in Protein Chemistry 245, (1961).
10. Doty, P. and Edsall, J. T.; Advances in Protein Chemistry, 6, 35, (1951).
11. Hulst, H. C. Vande, Recherches Astronomiques de L'observatoire D'utrech, 11, 1, (1946).
12. Doty, P.; J. Chem. Phys. 44, 76, (1947)
13. Oster, G.; Chem. Revs., 43, 319, (1948).
14. Oster, G.; Progress Biophys and Biophisical Chem., 1, 73, (1950).

15. Instruction Manual, Phoenix Precision Instrument Company, copyright (1963) Pages 1 - 63.

16. Zimm, H. B.; J. Chem. Phys. 16, 1093, (1948).

17. Debye, P.; J. Phys. Cheminstry, 51, 18, (1947).

18. Debye, P.; J. Phys. Colloid Chem. 51, 18, (1947).

19. Einstein, A.; Ann. Phys. Lipz. 33, 1275, (1910).

20. Flory, P. J.; J. Chem. Phys. 10, 51, (1952).

21. Huggins, M. L.; J. Phys. Chem. 46, 151, (1942).

22. Miller, A. R.; Proc. Cambridge Phil. Soc. 38, 109, (1942).

23. Miller, A. R.; Proc. Cambridge Phil. Soc. 39, 54, 131, (1943).

24. Doty, P. and Steiner, R. F.; J. Chem. Phys. 18, 1121, (1950).

25. Lord Rayleigh, Proc. Roy. Soc. London A84, 25,(1911).

26. Gans, R.; Ann. Physik, 76, 29, (1925).

27. Neugebaver, T.; Ann. Physik, 42, 509, (1943).

28. Zimm, H. B. and Doty, P.; J. Chem. Phys. 12, 203, (1944).

29. Debye, P.; J. Applied Physics, 17, 392, (1946).

30. Carr, C. I. and Zimm, H. B., J. Chem. Phys. 18, 1616, (1950).

31. Caplan, S. R., J. Sci. Instr., 31, 295, (1954).

32. Speiser, R. and Brice, B. A.; J. Opt. Soc. Am., 68, 364, (1946).

33. Gorring, D. A. I. and Johnson, P.; J. Chem. Soc., 33, (1952).

34. Debye, P. and Newman, R. V., J. Phys. Chem. 55, 1, (1951).

35. Debye, P. and Anaker, E.W.; J. Phys. Chem. 55, 644, (1951).

36. Lochet, R.; Acad. Sci. Paris 230, 437, (1950).

37. Martin, W.L., Proc. Roy. Soc. Can. 3, 151, (1923).

38. Alexander, P. and Stacey, K.A.; Trans Faraday Soc. 51, 299, (1955).

39. Alexander, P and Stacey, K.A.; Proc. Roy Soc. A212, 274, (1952).

40. Kushner, L.M. and Hubbard, W.D.; J. Phys. Chem. 58, 1163, (1954).

41. Schulz, G.V.; Cantow, H.J. and Meyerhoff, G.; J. Poly. Sc. 10, 79, (1952).

42. Bull, H.B.; An Introduction to Physical Biochemistry, Page 183, (1964).

43. Roess, L.C. and Shull, C.C.; J. Applied Physics, 18, 3031, (1947).

44. Yang, J.T.; J. Poly. Sc. 26, 305, (1957).

45. Benoit, H., Holtzer, A.M. and Doty, P.; J. Phys. Chem. 58, 635, (1954).

46. Kratohuil, J.P., Dezelic, Gj., Kerker, M. and Matijevic, E.; J. Poly. Sc. 57, 59, (1962).

47. Utiyama, H., Sugi, N., Kurata, M. and Tamura, M., Bull. Instr. Chem. Res. Kyoto Univ. 46, 77, (1968.

48. Manual of Microchemical and Instrumental Analysis - Millipore Coporation, Bedford, Massachussets, U.S.A.

49. Fendler, H.G. and Stuart, H.A., Makwmol. Chem. 21, 193, (1956).

50. Gornal, A.G., Bardawill, C.J. and David, A.M., J. Biol. Chem. 177, 751, (1949).

51. Harrinton, R.E. and Zimm, H.B.; J. Poly. Sc. A2, 294, (1968).

52. Arnold, R. and Caplan, S.R., Trans. Faraday Soc. 51, 864, (1955).

53. Olayemi, J. Y., Ph.D. Thesis, Ahmadu Bello University, Zaria, (1971).

54. Oth, A. and Doty, P.,J. Phy. Chem. 56, 43, (1952).

Chapter 8

COMPARISON OF DATA AND CONCLUSIONS

Figures 2.1-3 are plots of relative specific conductance against moles of copper nitrate added obtained from data in chapter 2. These show three end points and these have been associated with a change in the mode of binding. The results presented in table 2-I show among other things the various values of co-ordination numbers ranging from 4 to 2 to 1. Similarly, in the case of zinc, (fig. 2.7-12) two end points corresponding to different types of co-ordination have been obtained. The data presented in table 2-II show that zinc can form co-ordinate complexes involving two and one carboxylate groups per metal ion. These co-ordination numbers have been evaluated from the ratio of original carboxylate groups to the total amount of metal ion added to reach the end-points. These observations and how they affect the structure of the complex formed have been greatly discussed in chapter 2. It should be noted that the actual amount

of copper or zinc binding at the respective end-points in the curves could not be known by this method but as can be seen later, it has been possible to link these points with the similar observations made in chapters 5 and 6.

In chapter 5, figs. 5.1 and 5.2 are plots of M^{2+}_{added} for zinc and copper respectively at varying degrees of ionization of polymer at I = 0.1. It has been shown in section 5.5.2 that the shapes of the curves in fig. 5.2 suggest two types of equilibria which probably indicates two modes of binding: one existing at high charge density and low metal ion concentration and the other at high charge density and high metal ion concentration. It was suggested that the former probably corresponded to a four-co-ordinated complex while the latter was found to be a two-co-ordinated complex. However, in the case of zinc, there was no indication of the existence of four fold co-ordination but a stable complex having a co-ordination of two was found. The great importance of these curves in relation to other types of measurements lies in the fact that at any stage, the amount of M^{2+}_{bound} could be obtained for any amount of M^{2+}_{added}.

The values of M^{2+}_{bound} could then be related to M^{2+}_{added} in other experiments provided that the experiments are done at the same condition of ionic strength, polymer concentration and degree of ionization assuming that the Donnan equilibrium affects the reactions to the same extent. This type of relationship has been applied to the end points occuring in figs. 2.1, 2.2, 2.10 and 2.12.

The results presented in chapter 6 dealt with potentiometric titrations under various conditions already mentioned. In that chapter new methods of calculating the amounts carboxylate groups bound were developed (6.3.2.2) and these methods have been used to calculate the complex formation curves. As it has been stated in section 6.3.2.2., it was not possible to know the amount of M^{2+} which would be needed to saturate all the charged sites even when the actual amounts of COO^{-}_{bound} were known. However, if the amount of M^{2+}_{added} is known this could also be related to the values of M^{2+}_{bound} obtained from figs. 5.1 and 5.2 and by plotting graphs of M^{2+}_{bound} against COO^{-}_{bound} as series of graphs could be obtained. As a consequence of such

plots, figs. 8.1-3 have been obtained for copper-PMA systems and fig. 8.4 has been obtained for zinc-PMA systems.

In each of figs. 8.1-3, three linear segments have been obtained and these segments have been interpreted as indication of different modes of binding. In actual fact, the slope of each segment should give the co-ordination number $n\left\{\equiv \frac{[COO^-]_{bound}}{[M^{2+}]_{bound}}\right\}$ for each mode of binding. In figs. 8.1-3, the ratio has been found to follow the predicted order in chapters 2 to 5. The co-ordination number, n, for copper has been found to vary from 4 to 2 to 1 and these have been shown on the graphs as ML_4, ML_2 and ML_1 respectively. These results show convincingly that all the suggested stoichiometries in chapter 2 are in agreement with the recently obtained values. In the case of zinc-PMA systems presented in fig. 8.4, two segments have been found to give a co-ordination number of 1 and 2 and these have been marked on the graph as ML_1 and ML_2 respectively. In this case, ML_1 is first formed while ML_2 is building up. ML_2 is formed last probably

because it is the most stable complex formed as suggested in chapters 3 to 5. This is also in agreement with the results presented in chapter 2. It is also interesting to note that the present results have been obtained as a result of combination of data obtained from two different experimental techniques. The fascination of these results concerning the values of n is that it is an embodiment of the previous suggestions[1-4]. These results also probably clear the previous contradictions. Previous interpretations have always been in isolation.

It has been stated earlier that one could obtain the amount of M^{2+} which would be bound by PMA at the end-points in figs. 2.1 and 2.2 for copper if the amount of M^{2+}_{bound} taken from fig. 5.2 for an added amount of M^{2+} and this is related to a corresponding amount of added M^{2+} in figs. 2.1 and 2.2. If this is done, it can be seen that the breaks occuring in figs. 2.1 and 2.2 and in figs. 8.1-3 occur at the same amount of M^{2+}_{added}. This means that equal amounts of Cu^{2+} were required to give the same ratio of $COO^{-}_{b}/M^{2+}_{bound}$. A similarly interesting agreement has been reached in

the case of PMA-Zn complexes in fig. 8.4 and fig. 2.8. Thus it is satisfying to note that by comparing the data obtained from three different experimental techniques it is found that there is good agreement between the overall results and the deductions obtained from individual methods. The agreement obtained between these methods point to the fact that copper is able to form a complex involving four, two and one carboxylate groups to one metal ion. These results also confirm that it would be difficult if not impossible for zinc to form a four co-ordinated complex with PMA but very capable of forming complexes involving two and one carboxylate groups to one zinc ion.

It has been suggested in chapters 2 to 5 that whenever copper forms a four co-ordinated complex, such a complex may not be very stable for various reasons given earlier in those chapters. In addition, increase in M_f/L_f ratio will tend to decrease the co-ordination number of any complex formed. It was also suggested that this complex probably breaks down in favour of another form of binding. In chapters 4 and 5 where it was suggested that a four co-ordinated

complex first formed, it was only the most stable state of two co-ordinated complex that could be detected. In order to confirm that the four co-ordinated complex breaks down, attempts have been made to calculate the amounts of complex formed at every stage of the reaction. In this respect, data from dialysis experiments have been combined with data from potentiometric titrations. The results of such calculations have been presented in tables 8.1-VII. It was also suggested in chapter 2 that the two co-ordinated complex formed between PMA and zinc and between PMA and copper probably breaks down in favour of a one co-ordinated complex. Calculations have also been made to verify this suggestion.

Tables 8.1-VII below show the amounts of complex formed at various stages of the reaction between PMA and $M^{2+}\left[\underline{\equiv} Cu^{2+} \text{ or } Zn^{2+}\right]$ at the degree of ionization shown and at I = 0.10.

Table 8-I:

α	$COO^-_b \times 10^4$	$Cu^{2+}_b \times 10^4$	$ML_4 \times 10^4$	$ML_2 \times 10^4$
0.30	4.00	1.35	0.65	0.70
	4.50	1.84	0.41	1.43
	4.65	2.00	0.33	1.68
	5.00	2.35	0.15	2.20

Table 8-II:

α	COO_b^- x 10^4	Cu_b^{2+} x 10^4	ML_1 x 10^4	ML_2 x 10^4
0.30	5.30	2.75	0.20	2.55
"	5.50	3.05	0.60	2.45
	5.80	3.50	1.20	2.30
	6.00	3.85	1.70	2.15
	6.10	4.00	1.90	2.10

Table 8-III:

α	COO_b^- x 10^4	Cu_b^{2+} x 10^4	ML_4 x 10^4	ML_2 x 10^4
0.40	4.00	1.10	0.90	0.20
	4.50	1.45	0.80	0.65
	5.00	1.80	0.70	1.10
	5.50	2.13	0.62	1.91
	6.00	2.50	0.50	2.00
	6.50	2.83	0.42	2.41

Table 8-IV:

α	COO_b^- x 10^4	Cu_b^{2+} x 10^4	ML_1 x 10^4	ML_2 x 10^4
0.40	7.50	3.75	0.00	3.75
	7.87	4.25	0.63	3.62
	8.00	4.40	0.83	3.60
	8.25	4.75	1.25	3.50
	8.50	5.05	1.60	3.45

Table 8-V:

α	$COO^-_b \times 10^4$	$Cu^{2+}_b \times 10^4$	$ML_4 \times 10^4$	$ML_2 \times 10^4$
0.50	4.25	1.25	0.875	0.375
	5.00	1.70	0.80	0.90
	6.00	2.30	0.70	1.60
	6.50	2.60	0.65	1.95
	7.00	2.90	0.60	2.30
	8.00	3.50	0.50	3.00
	8.50	3.80	0.45	3.35

Table 8-VI:

α	$COO^-_b \times 10^4$	$Cu^{2+}_b \times 10^4$	$ML_1 \times 10^4$	$ML_2 \times 10^4$
0.50	9.25	4.53	0.00	4.53
	9.50	4.83	0.13	4.67
	10.00	5.43	0.86	4.57
	10.50	6.05	2.60	4.45

Table 8-VII:

α	$COO^-_b \times 10^4$	$Zn^{2+}_b \times 10^4$	$ML_2 \times 10^4$	$ML_1 \times 10^4$
0.60	1.20	1.00	0.20	0.80
	1.85	1.50	0.35	1.15
	2.35	2.00	0.35	1.65
	2.95	2.50	0.45	2.05
	3.50	2.93	0.57	2.36
	4.00	3.30	0.70	2.60
	4.65	3.65	1.00	2.65
	5.27	3.95	1.32	2.63
	5.85	4.25	1.60	2.65
	6.50	4.55	1.95	2.60
	7.10	4.82	2.27	2.55
	7.65	5.10	2.45	2.65
	8.15	5.33	2.82	2.51

The above calculations are based on the existence of only two types of complexes at any one time. In the segment labelled ML_4 in figs. 8.1-3, it is assumed that a four co-ordinated complex is obtained and this is likely to be the case in view of the small amounts of Cu^{2+} present in a large excess of COO^-. In the segment labelled ML_2 it is assumed that a mixture of ML_4 and ML_2 probably exist in the mixture while in the segment labelled ML_1 a mixture of ML_2 and ML_1 probably exist. Now taking tables 8-I and 8-II as

a specific case, then what happens to the complexes
formed can be explained. From table 8-I it can be
seen that ML_4 decreases as ML_2 increases. The decrease
in ML_4 probably means that the complex is disintegrating.
time. At the same time ML_2 remains practically
In table 8-II it can be seen that as $[ML_4]$ increases
increases while the amount of ML_1 gradually building up.
In general, it may be said that as $[ML_4]$ increases
constant. In general, it increases, also as $[ML_2]$ constant value. The same
decreases $[ML_2]$ reaches a virtually constant value for other α values
observation has been established. This has been interpreted
as can be seen in the tables. This has been co-ordinated
predicted in terms of breakdown of four complexes.
complex. Further, since the value of ML_2 reaches a
virtually constant value, it means that break down of
this complex is highly unlikely. This may probably
mean that ML_2 is the most stable complex formed
between copper and PHA.
In the case of zinc, values of ML_1 and ML_2 have
been presented in table 8-VII. The data shows that
ML_1 remains virtually constant while ML_2 increases.
This means ML_1 is a very stable complex. The results
from viscometric titrations support this idea.

of zinc n = 1.56. On one hand, if it assumed that n must be a whole number then the co-ordination number for these ions is 2. On the other hand, the fractional nature of these values may be interpreted that the true co-ordination number is a mixture of 1 and 2.

Fig. 8.7 shows curves comparing spectrophotometric and viscometric titration curves. Two metal ion concentrations have been used [10.0×10^{-4} and 5.0×10^{-4}M $Cu(NO_3)_2$] at an ionic strength of 0.02. The spectrophotometric titrations have been carried out in the visible range. These results have been discussed in great details in chapters 3 and 4, nevertheless, it will be profitable to think of correlating these results. In chapter 3, in fig. 3.4, the minimum points were associated with the points of equivalence of metal ion and ligands i.e. the minimum point on each curve represents a point where an amount of COO^- groups equal to the copper ions present is bound to the copper ions. It was found that at these points the ratio $COO^-_{original}/Cu^{2+}_{Total} = 2$.

In chapter 4, by the method of spectroscopy, the ratio $COO^-_{original}/Cu^{2+}_{Total}$ at the end of the linear

portion in fig. 4.7, was found to be equal to 2. The end of the linear portion was associated with the point of equivalence of copper and ligands.

The fascination of the foregoing explanations is that the end of the said linear portion in the preceeding paragraph coincides exactly with the minimum points on the viscosity curves as is evident in fig. 8.7. At these points the same value is obtained for the ratio $COO^{-}_{original}/Cu^{2+}_{Total}$. In the spectra curves, the maximum points give a value of approximately 4 for the ratio $COO^{-}_{original}/Cu^{2+}_{Total}$. Beyond the maximum point, the fall in percentage absorption as seen in fig. 8.7 has been attributed to a partial break-down of a four co-ordinated complex. This suggestion is in agreement with the suggestion made earlier when potentiometric titrations and dialysis equilibrium techniques were compared i.e. this suggestion is in agreement with the fall in $\left[ML_4\right]$ recorded in tables 8.I-VI; so that it appears possible to co-ordinate all the experimental methods to monitor similar facts.

On the stability of the complex, attempts have been made to calculate the cumulative or gross constant β_n for the various species present in the reaction

mixture. In doing this, β_n is given by

$$M + nL = MLn.$$

$$\beta_n = \frac{[MLn]}{[M][L]^n}$$

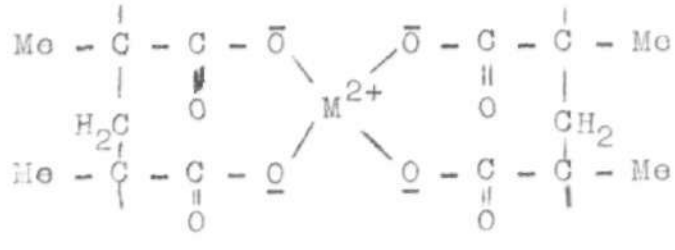
where in this case M $\equiv Cu^{2+}$ or Zn^{2+} and L = COO^-. In calculating the cumulative constants two possible modes of complex formation must be considered:- dimerization and chelation.

To obtain values of β_4 the following equilibrium should be considered

$$M^{2+} + 2(COO^-)_2 = \frac{M(COO)_4}{[M^{2+}][(COO^-)_2]^2}$$

$$\beta_4 = \frac{M(COO)_4}{[M^{2+}][(COO)_2]^2} \quad \text{.....8-1}$$

This expression assumes chelation as the mode of binding. This is quite possible if two carboxylate groups are regarded as contributing one bond in a four co-ordinated complex and the following will be a typical structure



If the mode of complex formation is assumed to be a dimerization involving four carboxylate groups then equation 8-1 becomes

$$\beta_4 = \frac{\left[M(COO)_4\right]}{\left[M\right]\left[COO\right]^4} \quad \ldots\ldots\ldots\ldots 8\text{-}2$$

The structure given above is still applicable but the carboxylate groups would be assumed to arise from different regions of the polymer. To obtain values of β_2 the following equilibrium has been considered.

$$M^{2+} + 2COO^- = M(COO^-)_2.$$

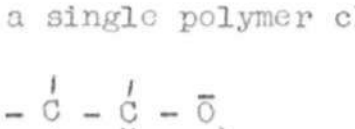
$$\beta_2 = \frac{\left[M(COO)_2\right]}{\left[M^{2+}\right]\left[COO^-\right]^2} \quad \ldots\ldots\ldots 8\text{-}3$$

Equation 8-3 assumes the complex formed to be a dimer resulting in a two co-ordinated complex, as a consequence of dimerization. If the complex formed is

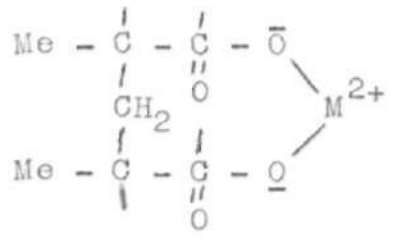
a chelate . Then equation 8-3 becomes

$$\beta_2 = \frac{\left[M(COO)_2\right]}{\left[M\right]\left[(COO^-)_2\right]} \quad \ldots\ldots\ldots 8\text{-}4$$

The type of structures envisaged are (i) for a dimer where the carboxylate groups is assumed to arise from different chains.



or (ii) as a chelate where the COO^- groups come from near sites on a single polymer chain



To calculate β_1 the equilibrium obtained is

$$M + COO^- = MCOO^-$$

so that $\beta_1 = \dfrac{\left[MCOO^-\right]}{\left[M\right]\left[(COO^-)\right]}$ $\quad \ldots\ldots\ldots 8 - 5$

The various β values obtained are presented below.

Table 8-VIII:

α	M^{2+}	$\beta_4 \times 10^{-6}$	$\beta_2 \times 10^{-6}$ (dimer)	$\beta_2 \times 10^{-6}$ Chelate	$\beta_1 \times 10^{-2}$
0.3	Cu	1.37±0.1	9.4-29.1	10.0-43	-
0.4	Cu	1.06±0.05	1.0-45.0	0.25-13.0	8.91±1.5
0.5	Cu	0.824±0.3	1.7-34.7	1.2-47.2	1.26±0.5
0.6	Zn	-	0.58±0.2	2.32±0.2	1-5

As can be seen from table 8-VIII, reasonably constant values of β were obtained for ML_4 and ML_1 where as for ML_2, a range of value of β were obtained. In calculating β_4 equation 8-1 has been used where chelation was assumed to be the mode of binding. In calculating β_2, both chelation and dimerization have been considered. In actual fact, the values of β_2 obtained for both possibilities rather justify that there is the likelyhood for both types of complexes to be co-existing. In chapter 5 it was not possible to obtain any value of β for copper but in the case of zinc, a single value of 1.844×10^3 was obtained when the reaction $M^{2+} + (COO^-)_2 = M(COO)_2$ was considered.

In all the chapters in this thesis, there are various suggestions as to the actual mode of binding

and the structure of the complex formed. It was suggested in chapters 2 to 5 that for a four co-ordinated complex to be able to exist, dimerization would probably have to result. It was suggested in chapter 5 that the mode of binding could be intramolecularly or intermolecularly depending on the ionic strength, charge density and divalent ion concentration. Now, combining the results presented in this chapter with those of chapters 4 and 5, it may be said that when a two co-ordinate complex is formed it may involve a single interwinding polymer molecule or two separate molecules forming a dimer. However, co-ordination involving interwinding chain may be unlikely owing to the electrostatic effects. It has been concluded from light scattering studies that the binding of copper and zinc to PMA at $\alpha = 0.3$ leads to dimerization of PMA molecules because the molecular weight was approximately doubled in the presence of these cations. Since it has just been concluded that the most stable structure of M^{2+}-PMA complex is one involving two carboxylate groups binding per metal ion

and since the molecular weight was approximately doubled in presence of M^{2+} [≡ Cu or Zn] then one one may tentatively conclude that dimerization leading to doubling of molecular weights will probably involve two separate polymer chains.

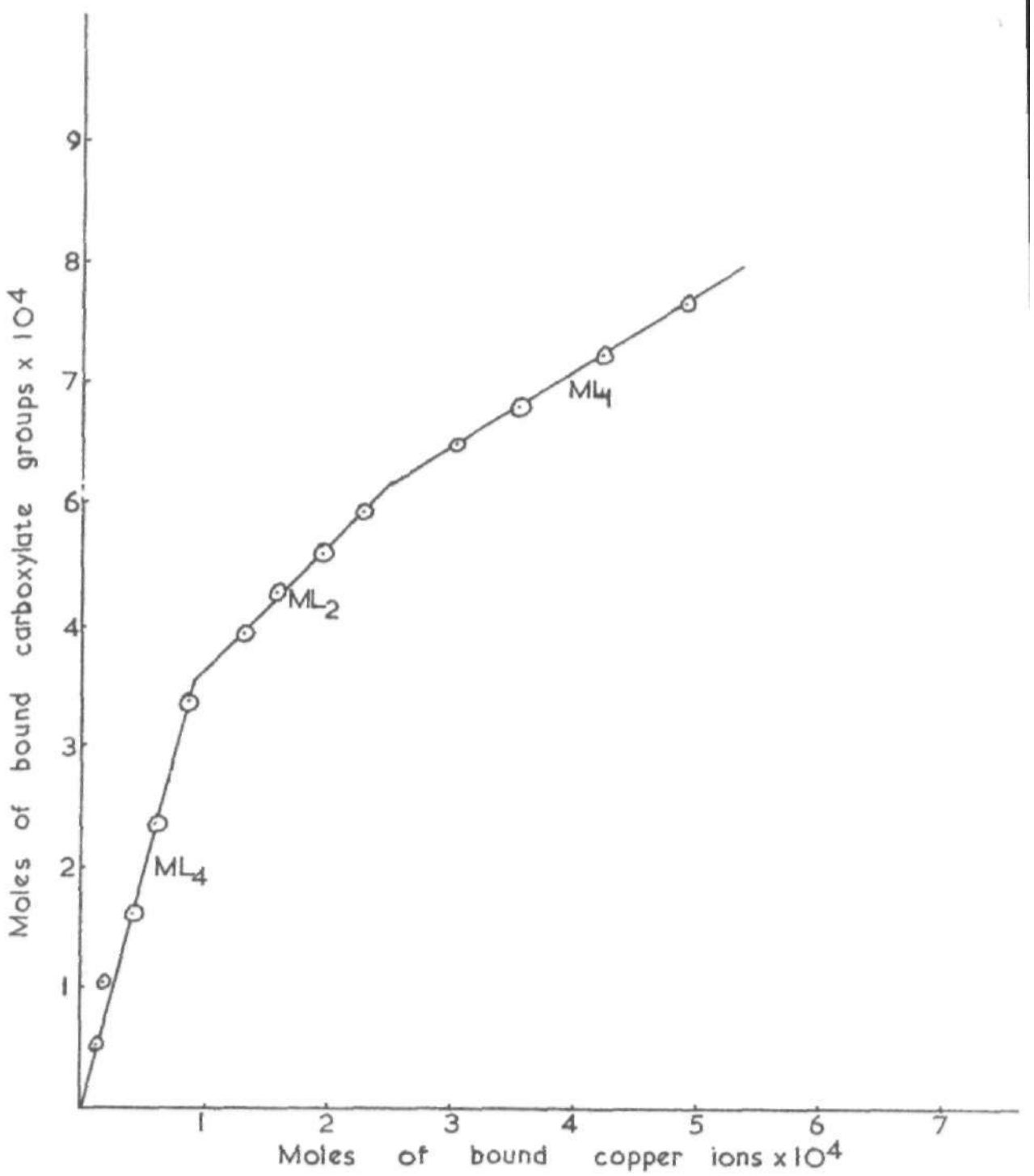


FIG 8.1 Combination of data from potentiometric titrations and dialysis equilibrium at $\alpha = 0.30$; $I = 0.10$; [PMA] = 2.50×10^{-3}M

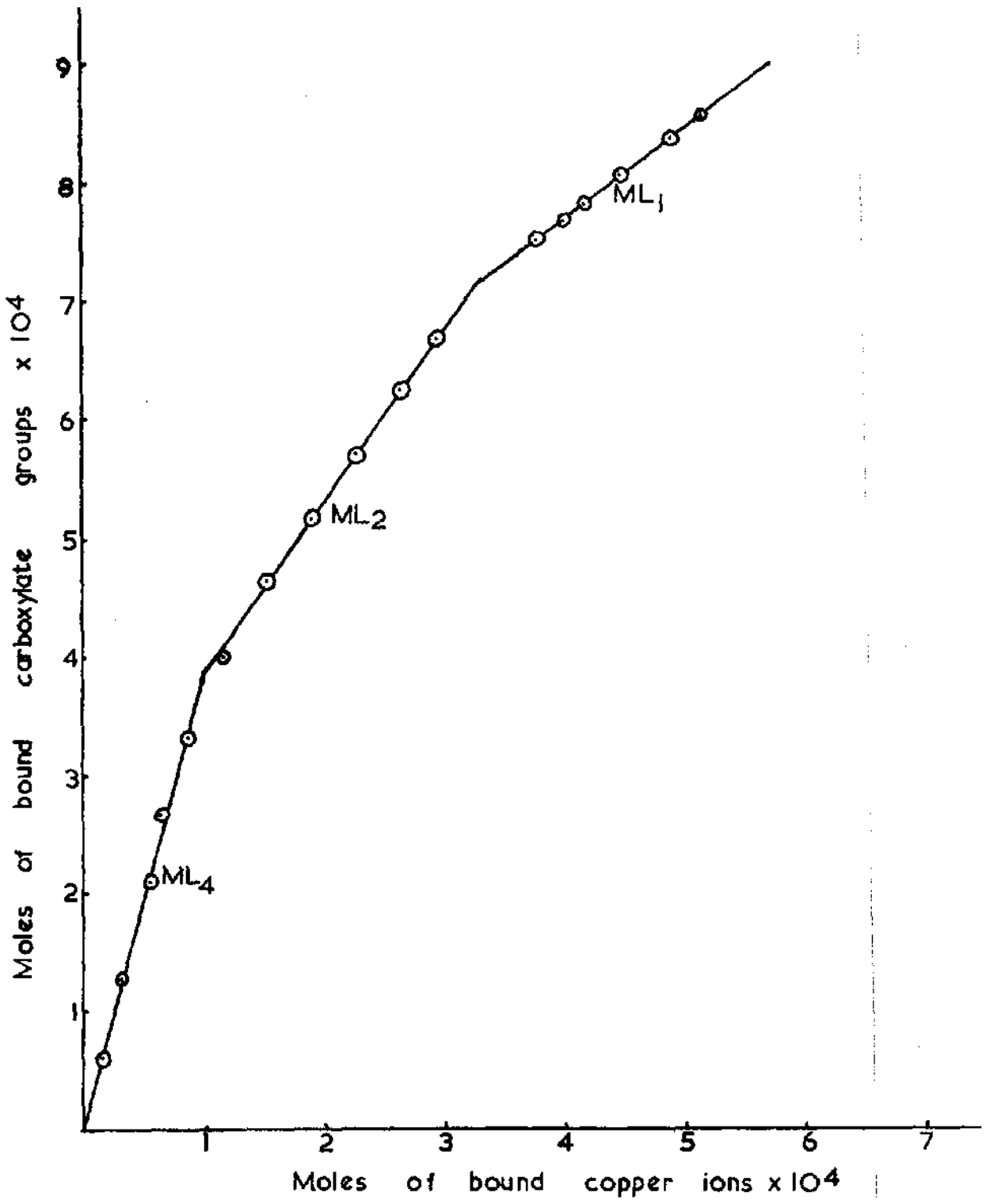


FIG 8·2 Combination of data from potentiometric titrations and dialysis equilibrium at $\alpha = 0.4$; $I = 0.10$; $[PMA] = 2.50 \times 10^{-3} M$.

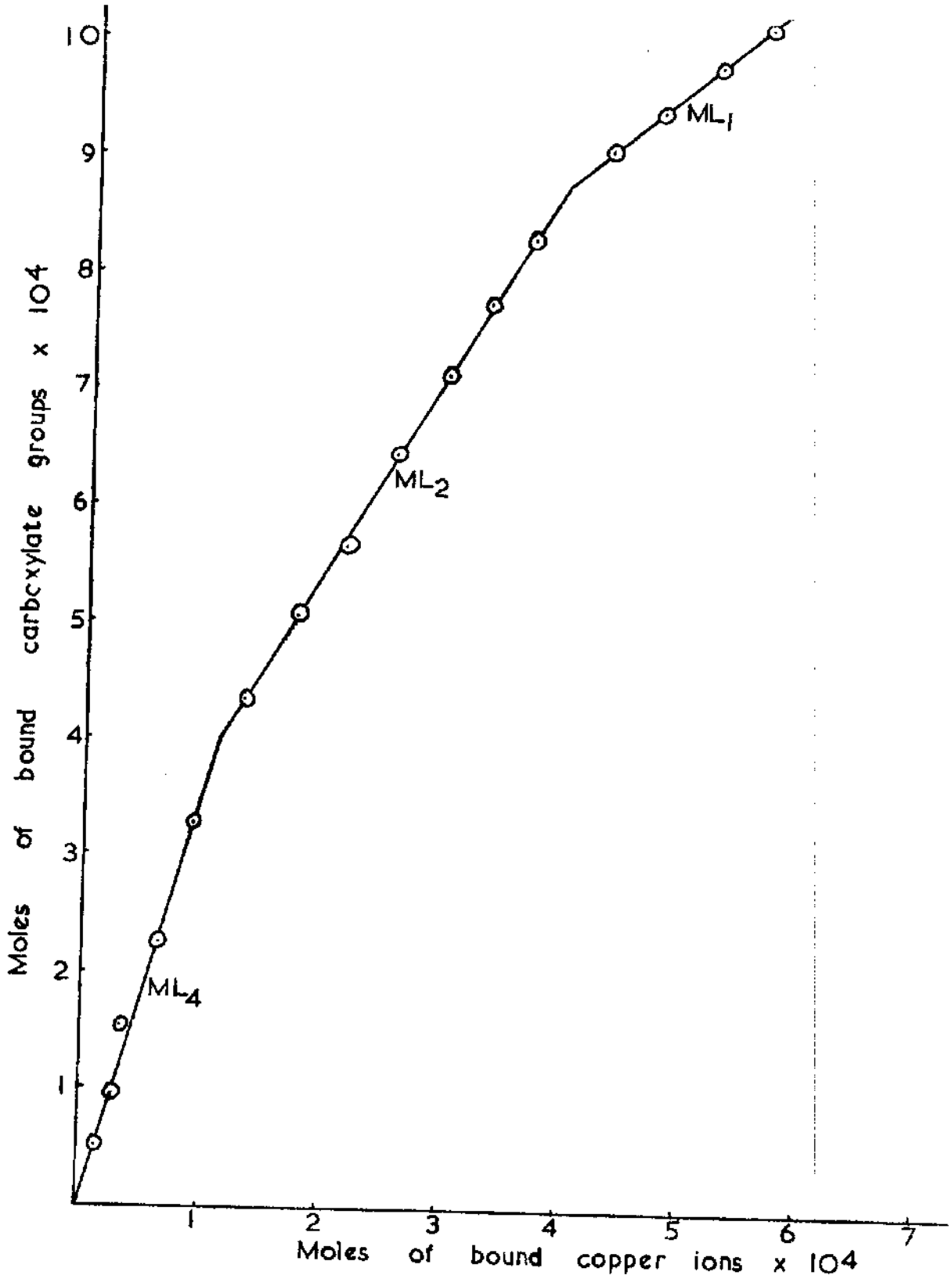


FIG 8.3 Combination of data from potentiometric titrations and dialysis equilibrium at $\alpha = 0.50$; $I = 0.10$; [PMA] = 2.50×10^{-3} M .

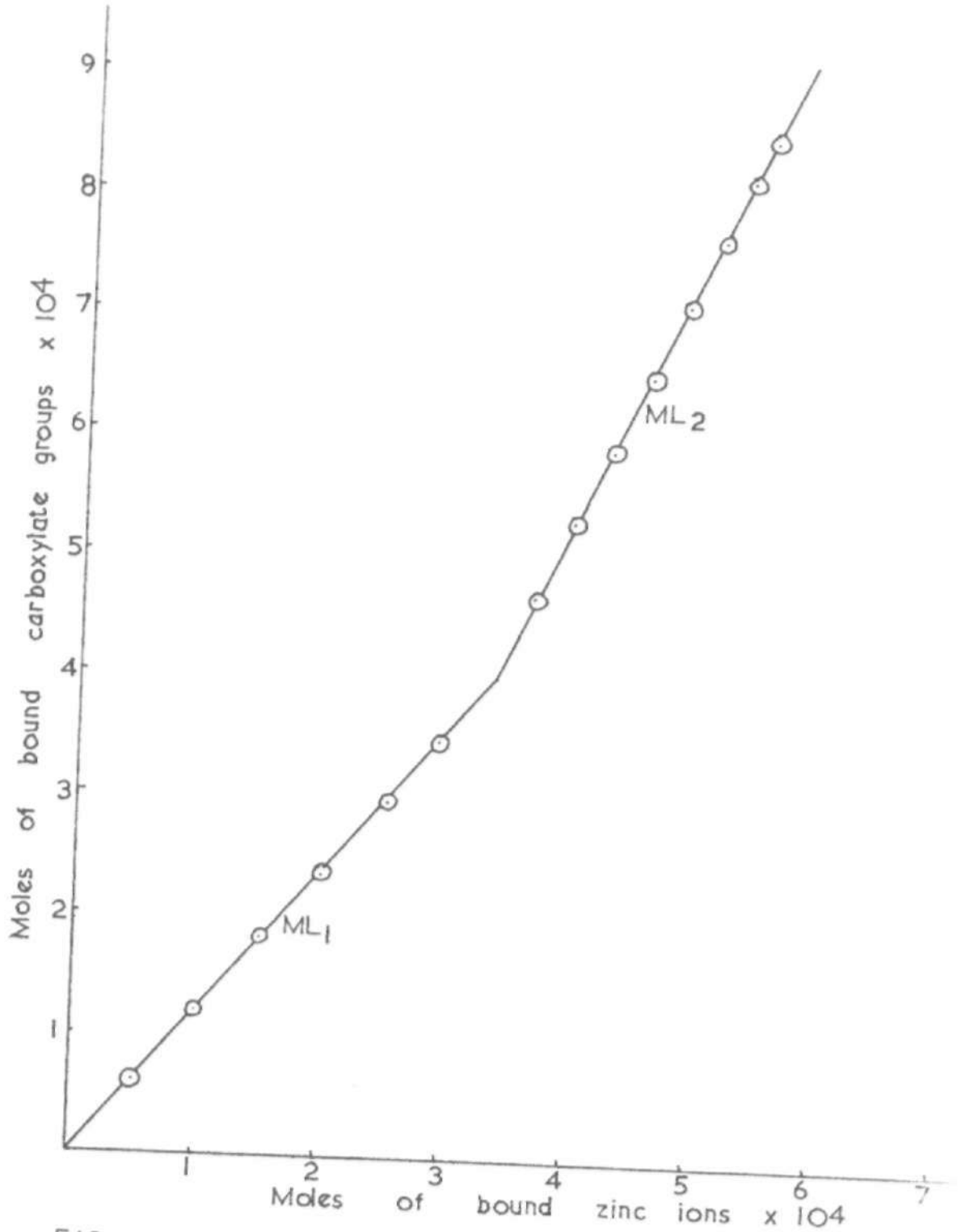


FIG 8-4 Combination of data from potentiometric titrations and dialysis equilibrium at $\alpha = 0.60$; $I = 0.10$; $[PMA] = 2.50 \times 10^{-3}$ M

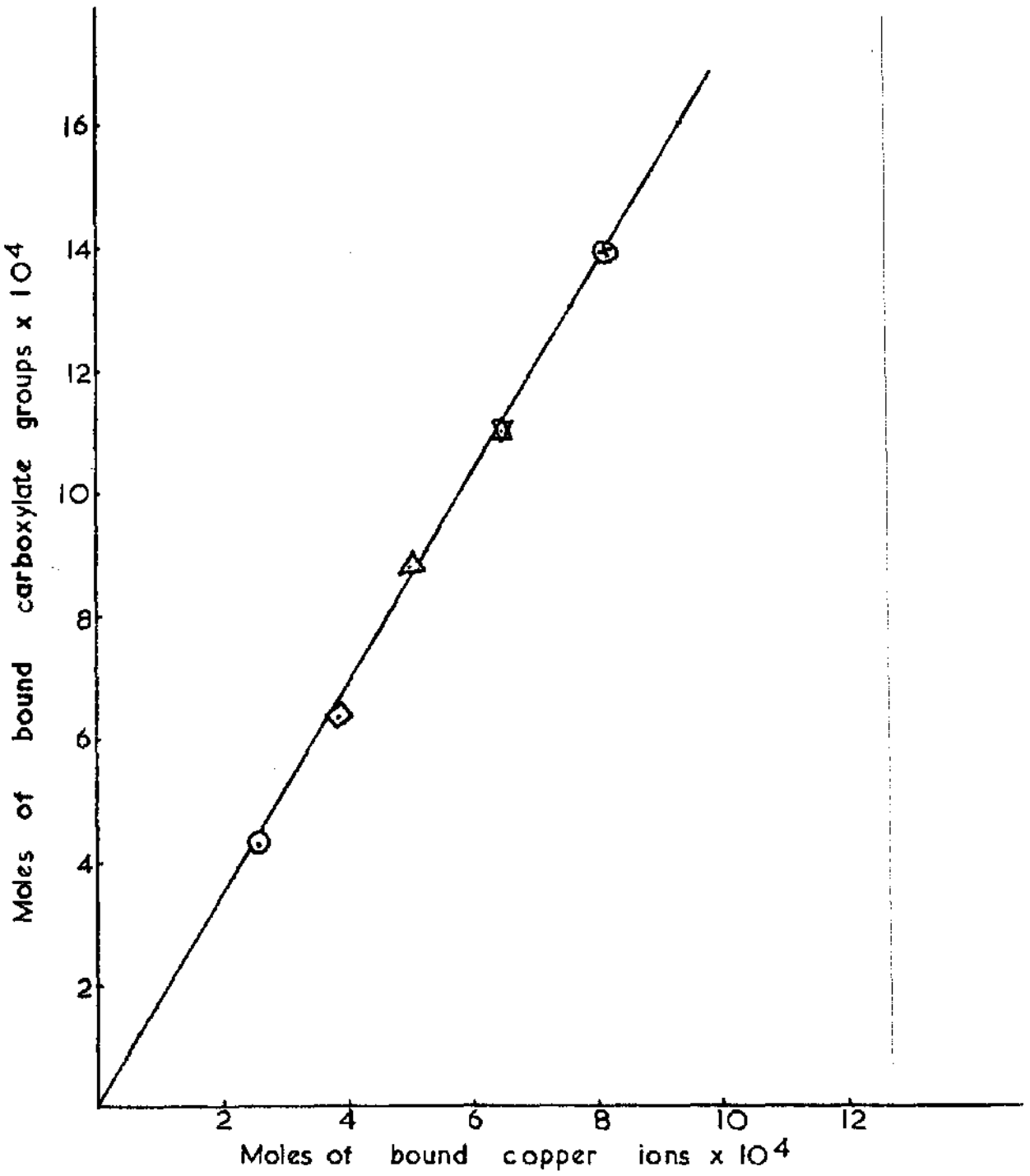


FIG 8.5 Combination of maximum amount of bound carboxylate groups and maximum amount of bound copper ions at various α values

$I = 0.10$; [PMA] = 2.50×10^{-3} M

α :- (⊙) 0.22 ; (□) 0.30 ; (△) 0.40 ; (☒) 0.50 ; (⊕) 0.60 .

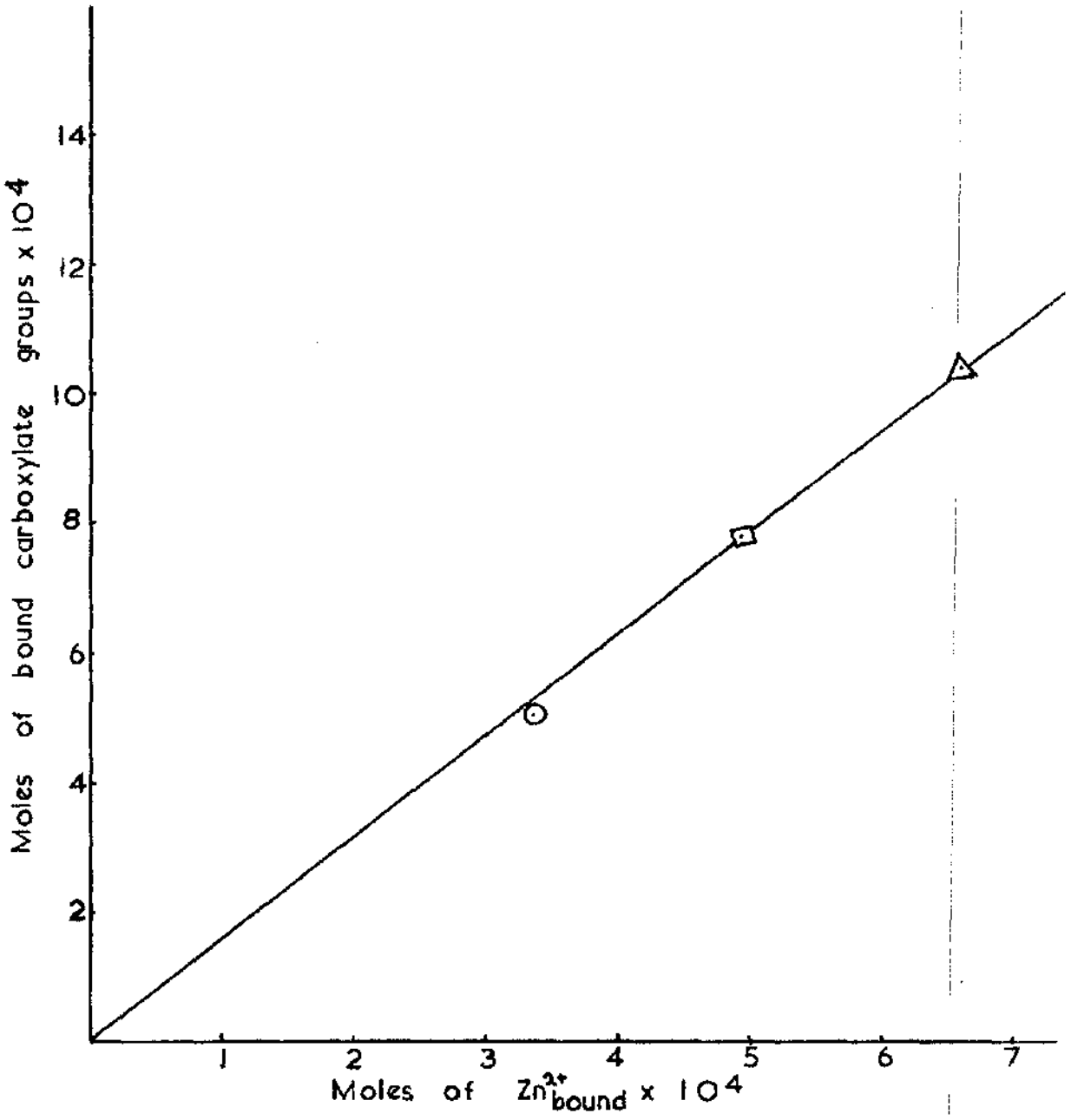


FIG 8.6 Combination of maximum amount of bound carboxylate groups and maximum amount of bound zinc ions at various α values
$I = 0.10$; $[PMA] = 2.50 \times 10^{-3}$ M .
α :- (⊙) 0.30 ; (⊡) 0.45 ; (△) 0.60

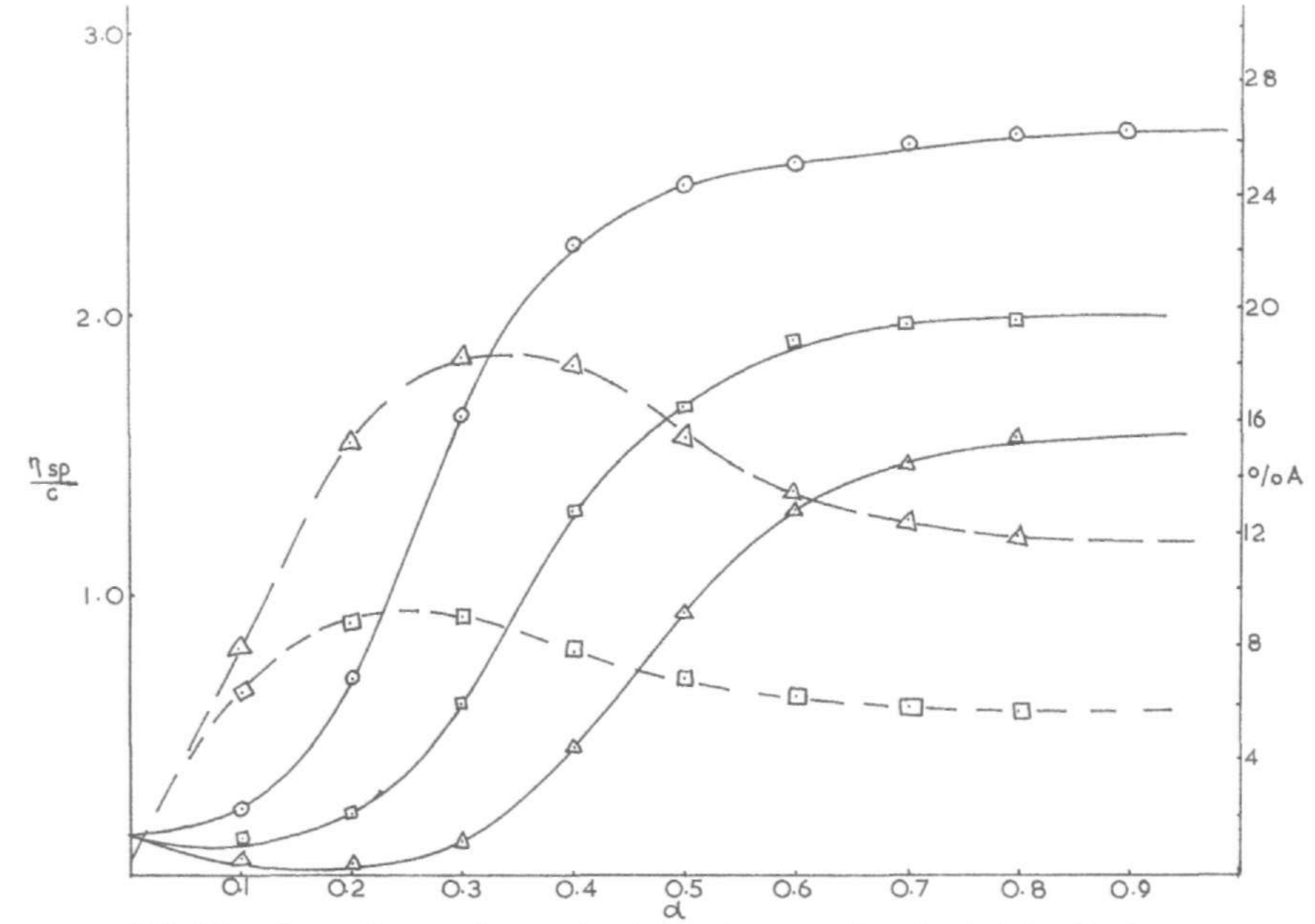


FIG 8.7 Comparison of spectrophotometric and viscometric titration curves
I = 0.02 ; [PMA] = 0.01M ; - - - - - Specta curves ; ——— viscosity curves ·
(⊙) No metal ions ; (□) 5.0×10^{-4}M (△) 10.0×10^{-4}M $Cu(NO_3)_2$

REFERENCES

1. Kotlair, M. and Morawetz, H., J. Am. Chem. Soc. 77, 3692, (1955).

2. Morawetz, H., J. Poly. Sc. 17, 442, (1955).

3. Bolewski, C. and Libina, M., Roczniki Chemi, Ann. Soc. Chim, 44, 647, (1970).

4. Mandel, M. and Leyte, J. C., J. Poly. Sc. A2, 1879, (1964).

A P P E N D I X

THE FOLLOWING PROGRAMMES WAS USED IN COMPUTER ANALYSIS OF THE RESULTS OBTAINED FROM LIGHT SCATTERING STUDIES

FORTRAN COMPILATION BY F/XFAM MK 4E

```
   LIST
   PROGRAM(COMP)
   INPUT  1 = CRO
   OUTPUT 2 = LPO
   COMPRESS INTEGER AND LOGICAL
   TRACE 2
   END
```

```
 MASTER  COMP
C
C    PROGRAM TO DO CALCULATIONS FOR BRICE PHOENIX
C            LIGHT SCATTERING PHOTOMETER
C    SEE OPERATION MANUAL OM-2000 PAGE 32
C    DEPARTMENT OF CHEMISTRY, A.B.U.
C    INPUT: FIRST CART  INITIAL CONSTANT TD*A...R.SMALLK,BIGK,C
C           NEXT CARDS IN PAIRS  (1)  SOLVENT
C                                (2)  SOLUTION
C           T=THETA
C           (1) T GT GW F G180-T GW F
C           (2)   GT GW F G180-T GW F R/R'
C    NUMBERS SEPARATED BY AT LEAST ONE SPACE
C    FOR F 4 NUMBERS MUST BE PUNCHED - ZEROS USED TO MAKE UP 4
C           LAST CARD     PUCH ****  IN COLUMNS 1-4
C E.G. OMITTING C IN COLUMN 1 - CHANGING C TO * FOR LAST CARD
C
C 0.007773 0.0381 1000 0.0000001661 0.000245
C 45 93.0 98.5 1 2 3 4 98.5 96.0 1 2 3 4
C ***
C           ANY NUMBER OF DATA PACKS MAY BE RUN AT ONE TIME,
C           THE LAST BEING TERMINATED BY AN ADDITIONAL CARD WITH
C           *** IN COLUMNS 1-4
C
     CALL REALMASTER
     END

END  OF  SEGMENT, LENGTH  6, NAME  COMP
```

```
      SUBROUTINE REALMASTER
      INTEGER EOF
      COMMON SMALLK,BIGK,C,
     1       TT,T(20),ONEPLUSC2T(20),SIN2HALFT(20),RTU(20),EOF
      DIMENSION IF1(4),IF180MT1(4),IF2(4),IF180MT2(4)
      EXTERNAL ENDOK
1     TT=0
      CALL ETRAP(ENDOK)
      READ(1, 2)FC,R,SMALLK,BIGD,C
2     FORMAT(10F0.0)
      WRITE(2,3)FC,R,SMALLK,BIGK,C
3     FORMAT(1H1,8HTD*A...=,F12.8,3H R=,F12.8,8H SMALLK=,F12.1,
     1       6H BIGK=,F12.10,3H C=,F12.9)
      WRITE(2,4)
4     FORMAT(1H ,7X,44H - - - - - - SOLVENT - - - - - -  ,
     1              44H   - - - - -SOLUTION - - - - - -  /
     2 121H      0     GO    GW   F   G180-0   GW  F     GO
     3 GW     F     G180-0 GW   F    R/R'      R 0,U    /
     4 121H+      -      -                -            -
     5                   -                -            )
      EOF=0
      FR=1.0/( (1.0-R) **2 * (1.0-4.0*R**2) )
      DTR=3.14159265359/180.0
7     TT=TT+
      READ(1,14)T(IT),GT1,GW1,IF1,G180MT1,GW180MT1,IF180MT1,
     1                GT2,GW2,IF2,G180MT2,GW180MT2,IF180MT2,RDRP
      IF(EOF.EQ.1) GO TO 1
14    FORMAT(F0.0,4(2F0.0,4I0),F0.0)
      C2T=COS(DTR*T(IT))**2
      ST=SQRT(1.0-C2T)
      ONEPLUSC2T(IT)=1.0+C2T
      TT=ST/ONEPLUSC2T(IT)
      SIN2HALFT(IT)=SIN(DTR*T(IT)*0.5)**2
      W=GT2*F(TF2)/GW2
      X=GT1*F(IF1)/GW1
      Y=G180MT2*F(IF180MT2)/GW180MT2
      Z=G180MT1*F(IF180MT1)/GW180MT1
      RTU(IT)=FC*RDRP*TT*FR*( (W-X)-2.0*R*(Y-Z) )
      WRITE(2,23)T(IT),GT1,GW1,IF1,C180MT1,GW180MT1,IF180MT1,
     1                 GT2,GW2,IF2,G180MT2,GW180MT2,IF180MT2,RDRP,RTU(IT
     2)
23    FORMAT(1HO,F7.1,4(2F7.1,4I2),F8.4,F16.10)
      GO TO 7
      END

END  OF  SEGMENT,  LENGTH  287, NAME  REALMASTER
```

```
      FUNCTION F(IF)
      DIMENSION TF(4),IF(4)
      DATA TF/0.491,0.261,0.122,0.0551/
      V=1.0
      DO 1 I=1,4
      IF(IF(I).EQ.0)GO TO 2
    1 V=V*TF(IF(I))
    2 F=V
      RETURN
      END
```

END OF SEGMENT, LENGTH 65, NAME F

```
      SUBROUTINE ENDOK(IE)
      IF(IE.GT.0)GO TO 5
      IF=67008-IE
      WRITE(0,100)IE
  100 FORMAT(17H1EXECUTION ERROR ,A4,1H')
      RETURN
    5 IF(IE.EQ.105)GO TO 102
      WRITE(0,101)IF
  101 FORMAT(17H1EXECUTION ERROR ,I3)
      RETURN
  102 CALL FINISHOFF
      RETURN
      END
```

END OF SEGMENT, LENGTH 71, NAME ENDOK

```
      SUBROUTINE FINISHOFF
      INTEGER EOF
      COMMON SMALLK,BIGK,C,
     1       IT,T(20),ONEPLUSC2T(20),SIN2HALFT(20),RTU(20),EOF
      IF(EOF.EQ.1)STOP
      EOF=1
      WRITE(2,1)
    1 FORMAT(    1H ,38H          2                 2          /
     1           1H ,38H    0  SIN 0/2 + KC(1+COS 0)/R 0,U /
     2           1H+,38H    -      -                  -    -   /)
      SMALLKC=SMALLK*C
      BIGKC=BIGK*C
      DO 2 I=1,IT-1
        A=SIN2HALFT(I)+SMALLKC
        B=BIGKC*ONEPLUSC2I(I)/RTU(I)
    2   WRITE(2,3)T(I),A,B
    3   FORMAT(1HO,F7.1,F13.4,F18.10)
      RETURN
      END
```

END OF SEGMENT, LENGTH 102, NAME FINISHOFF

```
    FINISH
PROGRAM NAME #COMP, CORE  5068,LOWER AREA  603,PROGRAM 3725
END  OF  COMPILATION - NO ERRORS
```